RADON IN ARIZONA

edited by

Jon E. Spencer

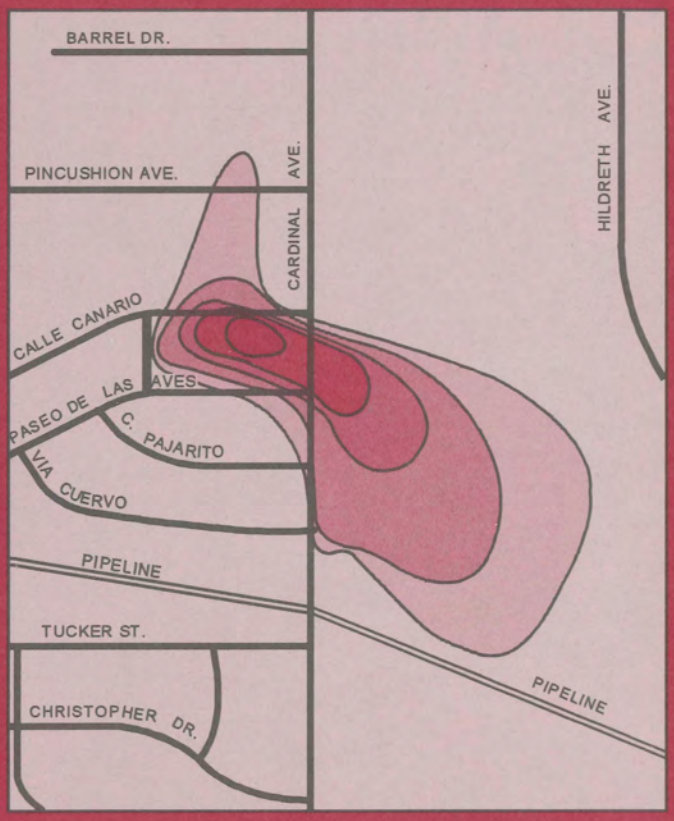

ARIZONA GEOLOGICAL SURVEY

Bulletin 199

1993

ARIZONA GEOLOGICAL SURVEY STAFF

April 1993

Larry D. Fellows
Director and State Geologist

Geology and Mineral Resources Program
Thomas G. McGarvin, Geologist I
Philip A. Pearthree, Research Geologist
Stephen M. Richard, Research Geologist
Jon E. Spencer, Research Geologist
Richard A. Trapp, Geologist II
Contracted Employees
Raymond C. Harris, Project Geologist*
P. Kyle House, Project Geologist*
Gary A. Huckleberry, Project Geologist*
Michael H. Ort, Project Geologist*
Steven J. Skotnicki, Project Geologist*
Steven Slaff, Project Geologist*

Oil and Gas Regulation Program
Steven L. Rauzi, Oil and Gas Program Administrator
Pamela J. Lott, Secretary

Publications and Administration Program
Rose Ellen McDonnell, Administrative Services Officer
Laurette E. Colton, Publication Sales Manager
Peter F. Corrao, Graphics Supervisor
Emily C. Creigh, Editorial Assistant
Denise M. Ingram, Accounting Technician II
Marjorie Tiznado, Clerical Assistant*
Evelyn M. VandenDolder, Geological Editor
Contracted Employee
Diane Murray, Librarian*

*Not paid from General Fund

RADON
IN ARIZONA

edited by

Jon E. Spencer

ARIZONA GEOLOGICAL SURVEY

Bulletin 199
1993

Copyright © 1993 Arizona Geological Survey

Permission is granted for individuals to make single copies for their personal use in research, study, or teaching and to use short quotes, figures, or tables from this bulletin for publication in scientific books and journals, provided that the source of the information is appropriately cited. This consent does not extend to other kinds of copying for general distribution, for advertising or promotional purposes, for creating new collective works, or for resale. The reproduction of multiple copies and the use of articles or extracts for commercial purposes require specific permission from the Arizona Geological Survey.

Published by
Arizona Geological Survey
845 N. Park Ave., Suite 100
Tucson, AZ 85719-4816
(602) 882-4795

400AL693AZGS5604

Preface

In 1984, a resident of eastern Pennsylvania repeatedly set off radiation alarms when he entered the nuclear power plant where he worked. The alarm system had been installed to determine whether employees were exposed to radiation while at work. Investigators discovered that his home had such high levels of radon that his clothing and hair had become radioactive. Radon soon became a front-page issue and a focus of national hysteria.

This incident indicated that indoor-radon concentrations throughout the country could also be elevated and should be investigated. Radon is radioactive and is considered to be a cause of lung cancer for persons who are exposed to high concentrations for long periods.

Studies of radon in Arizona began in 1987 when the Arizona Legislature appropriated funds to the Arizona Radiation Regulatory Agency and the Arizona Geological Survey. Studies since then have been done by State and Federal agencies and university faculty and students. Results of many of these studies are presented in this bulletin.

Indoor-radon levels in Arizona are among the lowest in the Nation. In several areas, however, uranium concentrations in rock and soil are elevated, as is the potential for elevated levels of indoor radon. (Radon is derived from uranium.) Radon levels in Arizona ground water are highly variable and are not well correlated with surface geology. In some areas radon levels are elevated, but guideline levels for radon in water have not been formally established.

The purpose of this report is to present detailed information about radon levels in ground water and about the geology of areas with elevated concentrations of uranium in soil, rock, and ground water. Some information about indoor-radon levels is also included. This report will be useful to anyone who is interested in the geology, geography, and hydrology of radon in Arizona. There is still much that we do not know about this subject, especially about radon in ground water. This bulletin, however, should provide a foundation for future studies.

Larry D. Fellows
Director and State Geologist

Acknowledgments

Many of the studies in this report were supported by a grant from the U.S. Environmental Protection Agency to the Arizona Radiation Regulatory Agency (ARRA), which in turn provided funds to the Arizona Geological Survey (EPA State Indoor Radon Grant Program K1-009544-01-0). I thank Paul Weeden and John Lamb of the ARRA for their interest and support and for providing information regarding radon levels in Arizona. John Duncan and Larry Fellows of the Arizona Geological Survey and John Lamb of the ARRA are gratefully acknowledged for many helpful discussions that influenced the focus of studies presented herein. This bulletin also benefited from careful editing by Evelyn VandenDolder and Emily Creigh, creative design and layout by Emily Creigh, and original illustrations by Peter Corrao.

Jon E. Spencer

Contents

Geology of radon in Arizona: Introduction and overview 1
Jon E. Spencer

Geology, radioactivity, and radon at the Cardinal Avenue uranium anomaly, southwestern Tucson 10
Jon E. Spencer, Dudley F. Emer, and Jonathan D. Shenk

^{222}Rn distribution in the ground water of the north-central Tucson Basin and its relationship to the hydrogeology 17
Bruce D. Smith

Uranium and radon in southeastern Arizona 40
John T. Duncan and Jon E. Spencer

Investigations of uranium and radon in the Phoenix metropolitan area 43
John T. Duncan and Jon E. Spencer

Uranium-bearing rocks in Verde Valley, Yavapai County, and implications for indoor-radon gas 51
John T. Duncan and Jon E. Spencer

Uranium and radon in the Prescott area, Yavapai County 57
John T. Duncan and Jon E. Spencer

Radiometric and petrochemical characteristics of the Dells Granite, Yavapai County 61
Paul D. Proctor, Kenneth S. Fleck, and Ahmed N. Shahin

Radon on the Navajo Nation Indian Reservation, Arizona, New Mexico, and Utah 82
Michael A. Taylor and John T. Duncan

A reconnaissance study of radon and other radionuclides in Arizona well water 86
John T. Duncan, Jon E. Spencer, Pejman Eshraghi, and Steven M. Emrick

A survey of uranium concentrations in rocks and soils in populated areas of Arizona: Methods 93
John T. Duncan and Jon E. Spencer

Plate 1: Areas in Arizona with elevated concentrations of uranium ..... in pocket
Jon E. Spencer, Jonathan D. Shenk, and John T. Duncan

Plate 2: Geology and uranium concentrations in Verde Valley, Yavapai County, Arizona ..... in pocket
John T. Duncan and Jon E. Spencer

Geology of radon in Arizona: Introduction and overview[1]

JON E. SPENCER *Arizona Geological Survey, 845 N. Park Ave., #100, Tucson, Arizona 85719*

INTRODUCTION

Radon is a colorless, odorless, radioactive gas produced by the decay of uranium, which is present in virtually all rocks and soils, typically at concentrations of 1 to 4 parts per million (ppm). Radon can accumulate inside homes and other buildings at concentrations that are commonly tens of times greater than in outdoor air and, in some cases, may be hundreds or even thousands of times greater. Most indoor radon is derived from uranium in underlying soil and rock and gradually seeps into buildings through cracks or other openings in the ground floor. Houses with unusually high concentrations of indoor radon are typically built on rock and soil that contain unusually high uranium concentrations.

Exposure to elevated levels of radon is thought to cause lung cancer. In the late 1980's, public health concerns regarding radon led to government funding for studies of the distribution and significance of radon. The U.S. Environmental Protection Agency (EPA), U.S. Geological Survey (USGS), and virtually all States initiated programs to study radon or to educate the public about the dangers of radon and about radon detection and mitigation. Many of the studies in this bulletin were supported by the EPA or the State of Arizona.

Radon concentration in air is commonly measured in picocuries per liter (pCi/l), a measure of the number of nuclear decays in a liter of air within a specific period. One picocurie corresponds to about two decays per minute. The EPA has established 4 pCi/l as a general guideline for maximum acceptable, long-term, indoor-radon concentration.

The amount of uranium in underlying rock and soil is a major factor influencing indoor-radon concentrations. Knowledge of the distribution and nature of uranium-rich rocks is therefore helpful in locating areas where radon is more likely to be a health hazard than in normal geologic environments. The terms "uranium-rich" and "anomalous," as used in this publication, refer to soil or rocks that contain more than 6 ppm uranium, or about two to three times the average concentration in the Earth's upper crust. Uranium ore, in contrast, usually contains more than 1,000 ppm.

Many studies in this bulletin were directed at determining the location of uranium-rich rocks in populated areas or in areas that are likely to become populated in the near future. Uranium-rich rocks are present at numerous localities in Arizona, five of which are in populated areas: (1) limestone in southwestern Tucson that contains up to 20 ppm uranium (Spencer and others, this volume, p. 10-16); (2) volcanic rocks in a small area of the Phoenix Mountains that contain up to 8 ppm uranium (Duncan and Spencer, this volume, p. 43-50); (3) sedimentary rocks in the Cave Creek area that contain up to 33 ppm uranium (Duncan and Spencer, this volume, p. 43-50); (4) sedimentary rocks in Verde Valley that contain up to 43 ppm uranium (Duncan and Spencer, this volume, p. 51-56; Plate 2); and (5) the Dells Granite near Prescott, which contains up to 40 ppm uranium (Duncan and Spencer, this volume, p. 57-60; Proctor and others, this volume, p. 61-81). Taylor and Duncan (this volume, p. 82-85) present the results of radon surveys in homes on the Navajo Nation Indian Reservation. Average indoor-radon levels in some of these areas are higher than in other parts of Arizona. Many other areas of the State that contain uranium-rich rocks are either largely or entirely uninhabited or are small and only weakly anomalous, i.e., they contain only slightly more than 6 ppm uranium (Plate 1).

Radon in tap water can also cause elevated indoor-radon levels. Radon is derived from aquifer minerals, transported to homes in water-distribution systems, and released as soon as water is exposed to air, typically in a sink or shower. Tap-water levels may be much lower than well-water levels because radon decays during water transport and escapes if water is exposed to air before reaching homes. Geologic and hydrologic factors that control radon content in water are not well understood. Aquifer rocks that are prodigious radon producers may not have elevated uranium

[1] This article is a modified version of the following report: Spencer, J.E., 1992, Radon gas: A geologic hazard in Arizona: Arizona Geological Survey Down-to-Earth Series 2, 17 p.

in Spencer, J.E., ed., 1993, Radon in Arizona: Arizona Geological Survey Bulletin 199, p. 1-9.

concentrations except in thin mineral crusts lining pore spaces. Analyses of such rocks may not reveal high uranium concentrations.

Studies of radon in water in this bulletin are primarily surveys of radon levels in well water that include some assessment of geologic and hydrologic factors that may influence radon concentrations. Smith (this volume, p. 17-39) presents data on radon levels in well water in the Tucson Basin and discusses their relationship to basin geology and hydrology. Duncan and Spencer (this volume, p. 43-50) review well-water radon data from the Cave Creek-Carefree area and assess the relationship of radon levels to aquifer geology. A regional survey of radon in well water in eight populated areas of Arizona (Duncan and others, this volume, p. 86-92) establishes typical Arizona well-water radon levels.

OVERVIEW OF RADON

Origin of Radon

Most of the rock in the Earth's crust, as well as soil and alluvium derived from it, contains uranium. About 99.3% of this uranium is the isotope uranium-238 (^{238}U), which has a half-life of about 4.5 billion years (approximately the age of the Earth). Decay of a ^{238}U atom marks the beginning of a series of 14 decays that end at the stable isotope lead-206 (^{206}Pb; Fig. 1; Table 1). The decay product of an individual parent isotope is called its daughter product. Unstable daughter isotopes are referred to as intermediate daughter products. Radium-226 (^{226}Ra) and radon-222 (^{222}Rn) are intermediate daughter products in the decay of ^{238}U to ^{206}Pb. ^{226}Ra, with a half-life of 1,600 years, is the immediate parent of ^{222}Rn.

When ^{226}Ra decays to ^{222}Rn, it releases a high-energy alpha particle that is like a bullet shot from a gun. Obeying the laws of physics, the newly formed radon atom undergoes recoil in the same manner that a gun is propelled backward when a bullet is fired. If the radon atom is near the surface of a mineral grain, it can be knocked out of the grain by recoil. In some materials, such as clay, radon that is not dislodged by recoil is loosely trapped in the mineral's molecular structure and can escape without the assistance of recoil. This more gradual process of migration is known as diffusion. Radon atoms are liberated from geologic materials by both recoil and diffusion.

Migration of Radon Into Homes

Radon gas is present in the pore spaces in soil and rock after it is liberated from geologic materials. Radon is an inert gas and, unlike all other uranium-series decay products, does not form chemical bonds. As a result, a radon atom can move freely through the pore spaces of a porous and permeable geologic material without bonding to other mineral grains or substances. The mixture of air, radon, and other gases in underground pore spaces is known as soil gas.

Soil gas moves through soil or fractured rock by two mechanisms: (1) diffusion in all directions due to the random movements of gas atoms and molecules, and (2) flow in one direction due to pressure gradients. Diffusion and flow result in the transport of radon to above-surface environments or into underground mines. The ability of radon to migrate through soil is highly dependent upon the physical prop-

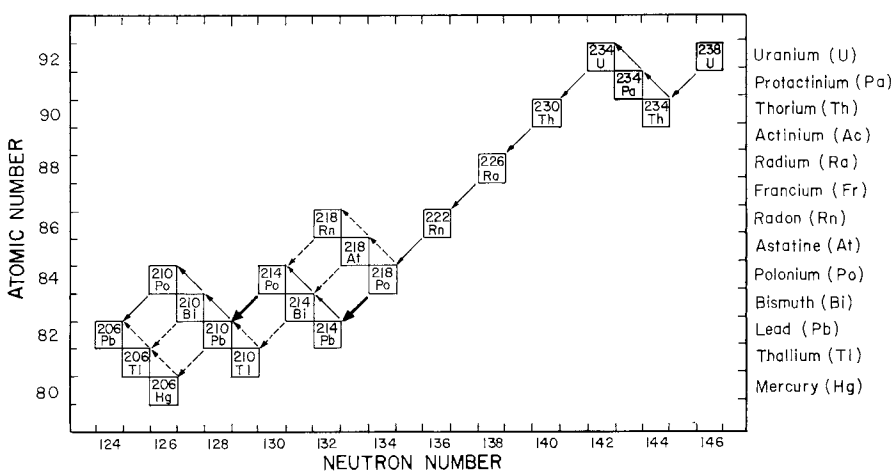

Figure 1. Decay path of ^{238}U to stable ^{206}Pb. Each box represents an isotope produced in the ^{238}U decay series. The atomic number plotted on the vertical axis corresponds to the number of protons in the nucleus; the neutron number plotted on the horizontal axis corresponds to the number of neutrons in the nucleus. The isotope number in each box is the sum of the atomic number (proton number) and the neutron number. Arrows that point down to the left represent alpha decays; arrows that point up to the left indicate beta decays. The heavy solid arrows are the two alpha decays that, by far, cause the greatest damage to lung tissue due to inhalation of airborne radon-decay products. The dashed arrows are the decay paths that are followed by a small fraction of atoms (<1%). Modified from Faure (1977).

erties of the soil. Well-fractured rock and coarse, well-drained soils are likely to be highly permeable to radon, whereas clays and muds, particularly if wet, permit little or no radon movement (Tanner, 1986).

Radon originating from depths greater than a few meters in the Earth generally does not reach the Earth's surface because it decays so quickly (3.8 days). As a result, the uranium concentration of only the top few meters of the Earth's surface is important when evaluating possible indoor-radon levels. Because radon enters the atmosphere at the ground surface and has a short half-life and a high density, it is not well mixed with the Earth's atmosphere and tends to be concentrated at low altitudes near the land surface. Radon levels may be significantly elevated in valleys or other topographic depressions during periods of atmospheric inversion (Texas Instruments, 1975).

High indoor-radon levels are almost always the result of upward transport of soil gas from underlying soil and rock. Radon typically diffuses and flows out of underlying soil and into basements, crawl spaces, and lower levels of homes or buildings, eventually reaching upper levels. Cracks in concrete floors, open spaces around pipes that enter homes from below ground, joints where floor meets wall, and drainage outlets or sumps can all provide conduits for entry of radon-bearing soil gas into houses. Even microscopic cracks in concrete can significantly increase permeability to soil gas, although concrete-slab floors that are not cracked are generally good barriers. In a few areas where local water supplies are derived from wells in uranium-rich rock and the water is used within a week or two from the time it is pumped from the ground, significant amounts of radon can enter a home when the water is exposed to air within the house, such as in a shower or sink.

Probably the most significant factor affecting radon infiltration into homes is the difference in air pressure between indoor air at ground level and outdoor air. If indoor air pressure is lower, soil gas flows up and out of underlying soil and into homes while outdoor air is drawn downward into surrounding soil to replace the soil gas that flows into homes. Even if outdoor air travels through soil for only 2 or 3 days before it is sucked into a home, it can acquire a high concentration of radon. Reduced air pressure in basements and the lowest levels of homes results from heating indoor air. Warm indoor air rises to the upper levels of a house, where it builds up positive air pressure that pushes the heated indoor air through cracks and other openings to the outside. At lower levels in the same house, air is drawn in through cracks and other openings as a result of lower indoor air pressures. Some homes are remarkably efficient at sucking up soil gas because of air-pressure differences. In contrast, use of evaporative coolers increases air pressure in a home, forcing indoor air downward through cracks and openings and reducing or preventing the influx of soil gas.

Table 1. Half-lives, alpha-decay energies, and maximum beta-decay energies of uranium-238 decay series. Gamma-ray energies are generally less than the maximum beta-decay energies and are significant only for the decay of lead-214 and bismuth-214. MeV = million electron volts.

Radio-nuclide	Half-Life	Alpha Energy (MeV)	Maximum Beta Energy (MeV)
^{238}U	4.5 billion years	4.1 - 4.2	—
^{234}Th	24 days	—	0.06 - 0.2
^{234m}Pa	1.2 minutes	—	2.3
^{234}U	250,000 years	4.7 - 4.8	—
^{230}Th	80,000 years	4.6 - 4.7	—
^{226}Ra	1,600 years	4.6 - 4.8	—
^{222}Rn	3.82 days	5.5	—
^{218}Po	3.05 minutes	6.0	—
^{214}Pb	26.8 minutes	—	0.7 - 1.0
^{214}Bi	19.7 minutes	—	0.4 - 3.3
^{214}Po	16 milliseconds	7.7	—
^{210}Pb	22 years	—	<0.1
^{210}Bi	5 days	—	1.2
^{210}Po	138 days	5.3	—
^{206}Pb	stable	—	—

Radiation Exposure Due to Radon

Alpha particles produced by alpha decay are each composed of two protons and two neutrons and, because of their large size and positive charge (+2), have less penetrating ability than gamma rays and beta particles, the other types of radiation associated with radioactive decay. Alpha particles produced by typical alpha decay will travel only a few centimeters through air before being stopped by collisions with air molecules and will travel only a few hundredths of a millimeter in rocks or within the human body. Alpha radiation from outside the human body is an insignificant source of radiation; when it occurs within the human body, however, alpha decay can be a major cause of radiation exposure.

Approximately 7,000 to 12,000 liters (1,750 to 3,000 gallons) of air are inhaled and exhaled by the average adult every 24 hours. The spontaneous decay of radon in the lungs is not a major source of radiation because almost all radon is expelled after each inhalation. The decay of polonium-218

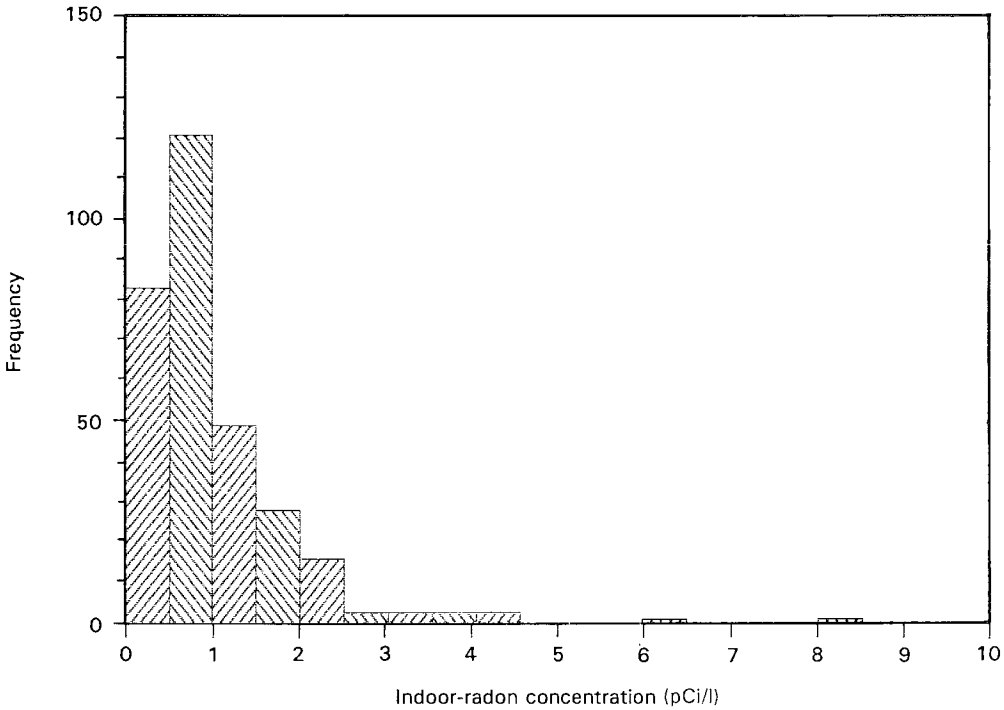

Figure 2. Histogram of randomly sampled, residential radon levels in Arizona determined using alpha-track detectors for 1-year exposure periods. The data are from the Phase 1 survey conducted by the ARRA during 1987 and 1988.

(^{218}Po), however, can cause radiation damage to lung tissue. The immediate daughter product of ^{222}Rn, ^{218}Po begins a sequence of four decays with a total half-life of about 50 minutes before reaching lead-210 (^{210}Pb), which has a half-life of 22 years (Fig. 1; Table 1). Polonium and its short-lived daughter products are chemically reactive and typically are highly charged immediately after decay. Newly formed ^{218}Po and its daughter products tend to adhere to the first solid with which they come in contact, including lung tissue and airborne dust particles that may be temporarily trapped by the lungs. The residence time of individual radon-daughter atoms and dust particles in the lungs is usually longer than the half-lives of the immediate daughter products of radon. Two of the four decay steps between ^{218}Po and ^{210}Pb are alpha decays that can cause significant molecular disruption in adjacent lung cells because of the large mass and high energy of ejected alpha particles (Fig. 1; Table 1).

For the average person, inhalation of radon decay products causes the lungs to receive more radiation than any other body organ and causes more total human radiation exposure than all other sources combined (National Council on Radiation Protection and Measurements [NCRP], 1984b). High radon levels in underground mines are a known cause of lung cancer in miners (NCRP, 1984a). Based on surveys of indoor-radon levels in homes and estimates of the cancer-causing ability of radon from studies of underground miners, the EPA estimated in 1986 that 5,000 to 20,000 persons in the United States die of lung cancer each year from inhaling radioactive radon-decay products in homes and buildings (EPA, 1986a). Radon has no other perceptible effects on the human body; it does not cause symptoms of radiation exposure, nor does it cause asthma, headache, dizziness, or nausea.

The NCRP reviewed all available data on lung cancer and radon-daughter exposure from studies of underground miners and laboratory animals. The NCRP study determined that radon-related lung cancer rarely occurs before 5 to 7 years after exposure and that the period between exposure and cancer appearance decreases with increasing age. Radon-related lung cancer rarely appears before age 40; the median age of appearance in miners is about 60 in nonsmokers and a few years younger in smokers (NCRP, 1984a). The EPA estimated that the risk of contracting lung cancer from living in a home with an indoor-radon level of 4 pCi/l is equivalent to smoking a fourth to a half pack of cigarettes per day or receiving more than 200 chest X rays per year (EPA, 1986a, undated).

Radon Measurement

Two types of commercially available radon monitors are commonly used in homes and other buildings. One type is the charcoal canister, a small charcoal-filled can that is opened in the home, closed after several days, and sent to a laboratory for analysis. Though excellent for a quick "spot check," this type of detector does not determine average radon levels over longer periods. Seasonal radon-level variations, for example, may be substantial; thus, a quick spot check will not necessarily determine a radon level that represents the long-term average concentration. It is the best method, how-

ever, for quickly determining the approximate radon concentration in a home or building.

The other type of radon monitor, an alpha-track detector, consists of a plastic film that records the tracks of alpha particles emitted by atmospheric radon and its daughter products. The detector may be placed in the home for months or even a year, thus recording the long-term, average radon concentration that more accurately reflects the potential health hazard. Both types of detectors may be purchased at some hardware stores.

RADON IN ARIZONA HOMES

The EPA provided funds to the Arizona Radiation Regulatory Agency (ARRA) to conduct statewide surveys of radon in homes in Arizona. The first survey, referred to as Phase 1, was conducted in 1987 and 1988. More than 2,000 homes were surveyed, mostly with charcoal-canister detectors. Alpha-track detectors were used in 170 randomly distributed homes for 1-year periods. The alpha-track data indicated that the median of the yearly average radon concentration was 0.8 pCi/l and that only about 1.6% of homes had yearly average levels above 4 pCi/l (Fig. 2; Table 2). The highest yearly average level measured by the alpha-track detectors was 8.4 pCi/l.

Phase 1 charcoal-canister testing was primarily done during the cooler months, when indoor-radon levels are typically higher. Homeowners were instructed to place the canisters in areas that inhabitants occupied frequently and to close windows and doors to the outside. Higher radon levels were usually recorded by the canisters than by the alpha-track detectors. The median level was 1 pCi/l, and 5.4% of homes had levels above 4 pCi/l (Fig. 3; Table 2).

Phase 2 charcoal-canister testing in 1988 and 1989 was also primarily done during the cooler months. Canisters were distributed by county health departments using various criteria. Combined Phase 1 and Phase 2 data from homes on the Colorado Plateau (mainly the Flagstaff area) indicated that indoor-radon levels were slightly higher than statewide levels, with a median of 1.2 pCi/l and 9.5% of homes above 4 pCi/l. Combined Phase 1 and Phase 2 data from areas where a significant number of homes are on granite or related (crystalline) rocks, primarily in the Prescott and Payson areas, indicated that the median indoor-radon level for these homes was 1.3 pCi/l, with 14% of homes above 4 pCi/l (Table 2). Higher radon levels in these areas are attributed to slightly higher uranium concentrations in underlying rocks and to the greater permeability of weathered granitic rocks, which allows more rapid radon movement (see also Kearfott, 1989).

METHOD	AREA	NO. OF MEASUREMENTS	MEDIAN VALUE (pCi/l)	PERCENT >4 pCi/l	PERCENT >10 pCi/l
Alpha-Track Phase 1	statewide	311	0.8	1.6	0
Charcoal Canister Phase 1	statewide	2,037	1.0	5.4	0.3
	Maricopa County	986	1.1	7.0	0.4
	Pima County	437	1.0	4.1	0.2
Charcoal Canister Phase 1 and 2	Plateau counties (Coconino, Navajo, Apache)	368	1.2	9.5	1.6
	Crystalline rock (mostly Prescott and Payson)	125	1.3	14.0	0.8
	Camp Verde area	40	1.4	10.0	7.5

Table 2. Indoor-radon measurements from the ARRA Phase 1 and Phase 2 surveys (1987-89). The 311 alpha-track detector measurements recorded radon levels from 170 homes that typically had two detectors each, placed in different areas in each house.

Similar studies of indoor-radon levels in other States revealed that Arizona radon levels were generally lower than most. Northern States tended to have higher radon levels because of heating and ventilation practices in colder climates and because glacial deposits and derivative soils are commonly permeable.

GEOLOGY OF RADON IN ARIZONA

Knowledge of uranium concentrations in geologic materials is probably the most accurate basis for identifying areas that are at greatest risk of having unacceptably high indoor-radon concentrations. Most crustal rocks have uranium concentrations of 1 to 4 ppm (Table 3), whereas uranium ore typically contains more than 1,000 ppm. Most uranium ore deposits in Arizona are in largely uninhabited areas on the Colorado Plateau (Wenrich and others, 1989). Many areas in Arizona contain uranium in concentrations that are far lower than those in uranium ore but significantly higher than those typical for crustal rocks. Some of these areas are within or near population centers and are known to be associated with high indoor-radon levels. These areas with moderate uranium concentrations (6 to 50 ppm) have significant potential for producing elevated indoor-radon levels (Fig. 4; Emer and others, 1988).

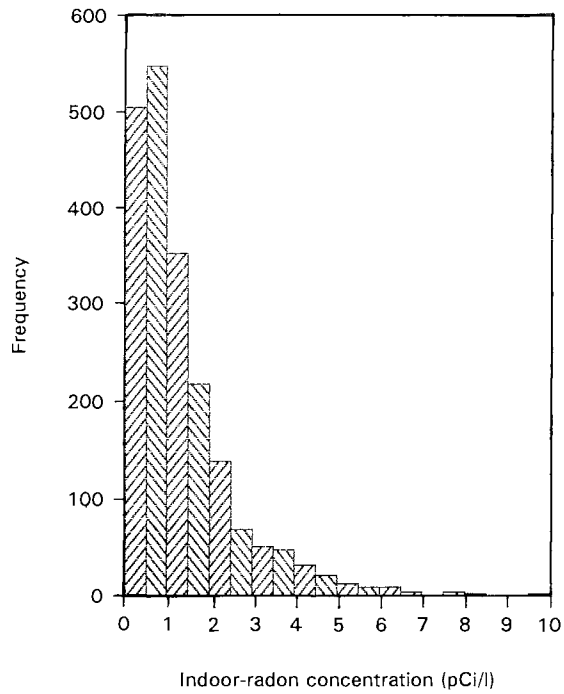

Figure 3. Histogram of randomly sampled, residential radon levels in Arizona determined using charcoal-canister detectors. The data are from the Phase 1 survey conducted by the ARRA during 1987 and 1988 and were primarily acquired during the winter months under low-ventilation conditions.

Most homes in the Tucson and Phoenix metropolitan areas, as well as many other parts of southern and western Arizona, are built on young, unconsolidated to poorly consolidated sand, gravel, and soil. These sediments are not known to contain unusually high uranium levels, probably because most uranium has been leached from the sediments during weathering and transport. Limestones that were originally deposited in lakes are exposed in many small areas in Arizona and are the most common type of rock with elevated uranium levels in or near population centers. Some granites also have elevated uranium levels. High indoor-radon levels have been associated with both of these rock types. Homes built on granite and decomposed granite seem to be at greater risk for elevated radon levels, even if underlying rocks contain average uranium concentrations. This is probably because of the greater permeability of fractured and weathered granitic rocks (compared to other rock types), which allows a large proportion of the radon in the rock to escape.

Radon levels inArizona well water are commonly above the EPA proposed guideline of 300 pCi/l (Duncan and others, this volume, p. 86-92; Fig. 5). One study of the Cave Creek and Carefree area (Duncan and Spencer, this volume, p. 43-50) revealed that aquifers composed of sand and gravel derived from nonanoma-lous rocks transmit radon to water in pore spaces more effectively than limestones containing much higher uranium concentrations. This is probably because uranium is present in thin mineral coatings within the pore spaces. Radon produced in such coatings is more readily transmitted to pore-space water than is radon produced well with-in mineral grains. This study indicates that developing predictive geologic criteria for radon levels in ground water will be difficult because the lithology and uranium content of aquifer materials do not correlate well with radon levels in pore-space water.

In one unusual situation, a house built over a water well had extremely high indoor-radon levels because of radon transmission through the air space between the well casing and host rock. This house was above a 240-foot-deep water well within the Dells Granite near Prescott. The well casing (a 6-inch-diameter pipe) extended upward through the floor of the house, turned 90°, and exited through a wall to the outside. A 1-inch gap between the casing and the floor allowed radon from outside the well casing to enter the home. A charcoal canister placed near the well casing in the house yielded a radon level of 11,000 pCi/l (a world record for indoor-radon levels!). Sealing the gap between the well casing and floor and venting

ROCK TYPE	AVERAGE (ppm)	HIGH VALUE (ppm)
Basalt (crustal average)	0.5 - 1	—
Granite (crustal average)	3.0	—
Wilderness granite, Santa Catalina Mountains (19 analyses from Reynolds and others, 1980)	1.17	2.9
Oracle Granite and gneissic derivatives, Santa Catalina Mountains (9 analyses from Reynolds and others, 1980)	3.5	8.1
Granitic rocks in Prescott 15' quadrangle, including Dells Granite (13 analyses from May and others, 1982)	8.2	26.3
Lawler Peak Granite near Bagdad, Yavapai County (19 analyses total, highest 3 not included; from May and others, 1982)	14.6	51
Lawler Peak Granite (only highest 3 of 19 analyses included; from May and others, 1982)	269	551

Table 3. Uranium content of typical basalt and granite, as well as several types of granitic rocks in Arizona, in parts per million (ppm).

the subfloor space to the outside with a 1.25-inch pipe reduced indoor-radon levels to less than 5 pCi/l (Kearfott, 1989).

REDUCING INDOOR-RADON LEVELS

Most studies of radon-reduction methods are directed at houses with basements or crawl spaces. Radon-reduction methods include ventilating the basement or crawl space, using fans to draw air from the basement or crawl space to the outside, and placing pipes under the home to remove radon before it flows upward into the home. Homes that are elevated from the ground so that outdoor air can flow freely underneath should have no radon problems (EPA, 1986b; NCRP, 1989).

Some homes in Arizona have underground return-flow air ducts that carry air back to air conditioners from various rooms in the house. Many of these ducts allow soil gas to be transported into the home. One study (Kearfott and others, 1992a) of eight of these homes in the Phoenix area showed that most had higher indoor-radon levels when air conditioners were in use and that levels in one home increased by a factor of more than 10 when the air conditioner was on. Homes with this type of duct construction should probably be tested for radon, especially in areas where uranium levels in underlying soil or rock are known or suspected to be high. Testing should be done when heaters or air conditioners are on and air is flowing through the ducts. Kearfott and others (1992b) also describe duct modifications that will decrease radon intake. The EPA has recommended that sub-slab ducts be avoided in new homes (Osborne, 1988).

In general, any procedure that increases the air pressure in a home so that, at ground-floor level, it is greater than the outdoor air pressure will prevent radon entry. Under such conditions, indoor air is gently pushed down through cracks in the floor and, in turn, pushes radon into the ground and away from the home. Use of evaporative coolers makes the air pressure inside higher than outside and should decrease radon levels in the home. Indoor-radon levels are likely to be higher in the winter when evaporative coolers are not in use and ventilation to the outside is reduced.

Most homes in Arizona have concrete-slab floors. A common method of reducing indoor-radon levels is to seal cracks in the floor so that radon cannot easily seep into the home. It is not clear, however, how effective this method is because new cracks can develop with time. Radon may even pass through some concrete slabs that have no cracks.

Methods for preventing or reducing radon entry are still being developed for buildings with

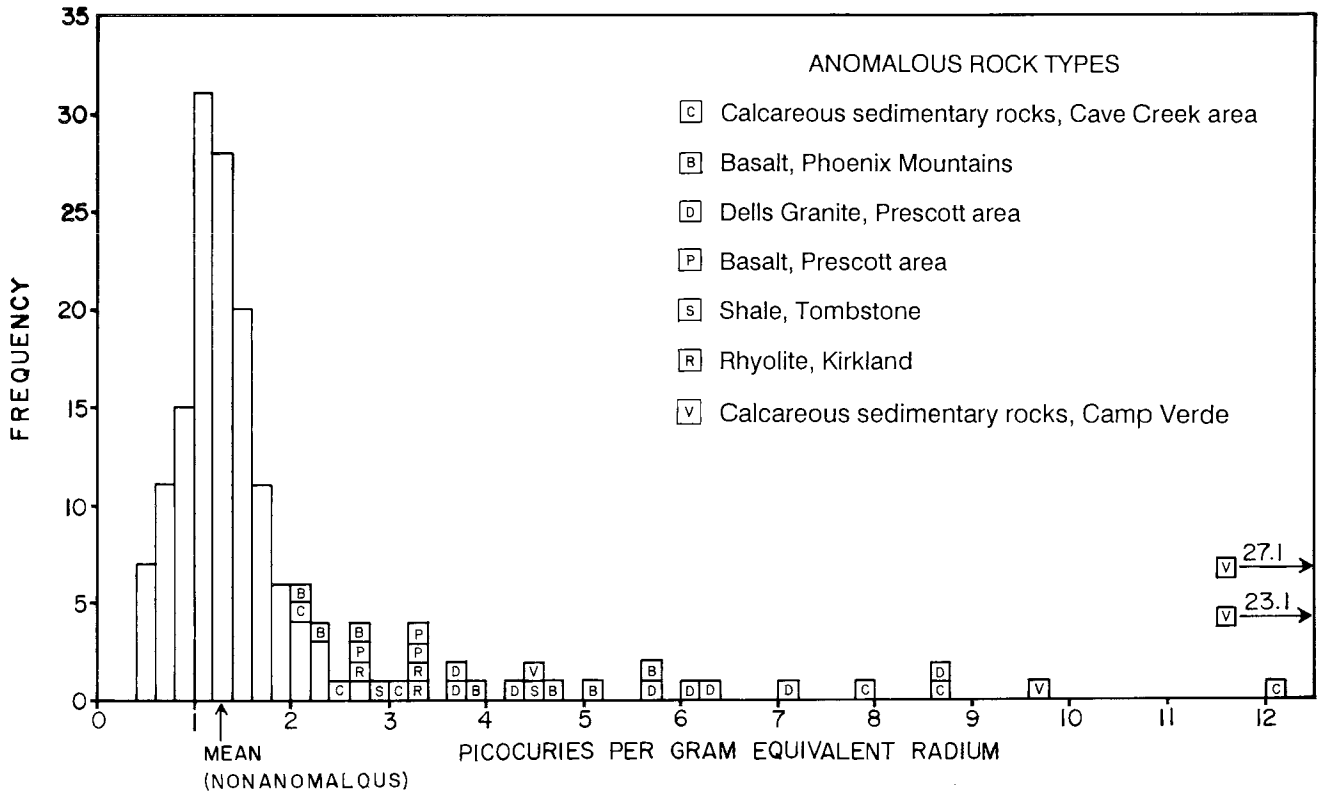

Figure 4. Histogram of measurements of background radiation from bismuth-214, a radon-decay product, given in picocuries per gram of equivalent radium. Multiply the radium content by three to determine the approximate uranium content in parts per million. All measurements reported by Emer and others (1988), except strip-chart records, are included. The data presented in this graph represent the results of the first statewide survey of uranium daughter isotopes in populated areas in Arizona. The reports in this bulletin generally improve upon this survey, which was funded by the Arizona Legislature in Fiscal Year 1987-88 with an $8,000 appropriation to the Arizona Geological Survey.

concrete-slab floors. In the late 1980's, a church (Santa Cruz Lutheran Church, 6809 S. Cardinal Ave.) was built in southwestern Tucson on an area with elevated uranium levels. To prevent radon entry, the concrete-slab floor was constructed above a sheet of impermeable plastic that, in turn, overlay a layer of gravel. Perforated pipe was placed in the gravel and connected to a pipe that vented above ground, outside the building. This appears to be an effective method of preventing indoor-radon accumulation.

CONCLUSION

Uranium is present in virtually all geologic materials. Radon gas, which is produced during the chain of radioactive decays that begin with uranium, is constantly being generated underground. The rate of radon production by geologic materials is directly related to their uranium content. Geologists can locate areas with unusually high uranium concentrations; homeowners and public-health officials can take actions to reduce radon exposure to residents in these areas.

Recent surveys reveal that Arizona has lower average radon levels than most States. This is probably the result of several factors, including indoor heating, cooling, and ventilation practices associated with Arizona's relatively warm climate, as well as the absence of large areas with unusually high uranium concentrations. Several small populated areas in Arizona, however, do have unusually high uranium concentrations. The average radon level in homes in some of these areas is greater than the statewide average. Residents of these areas should take appropriate measures to test for radon in their homes and reduce levels if necessary.

Radon levels in well water in Arizona are highly variable and not well known. Tap-water levels are typically much lower than well-water levels because of radon decay and escape in water-distribution systems. Small water-distribution systems where well water is used in homes soon after subsurface extraction are at greater risk for high radon levels.

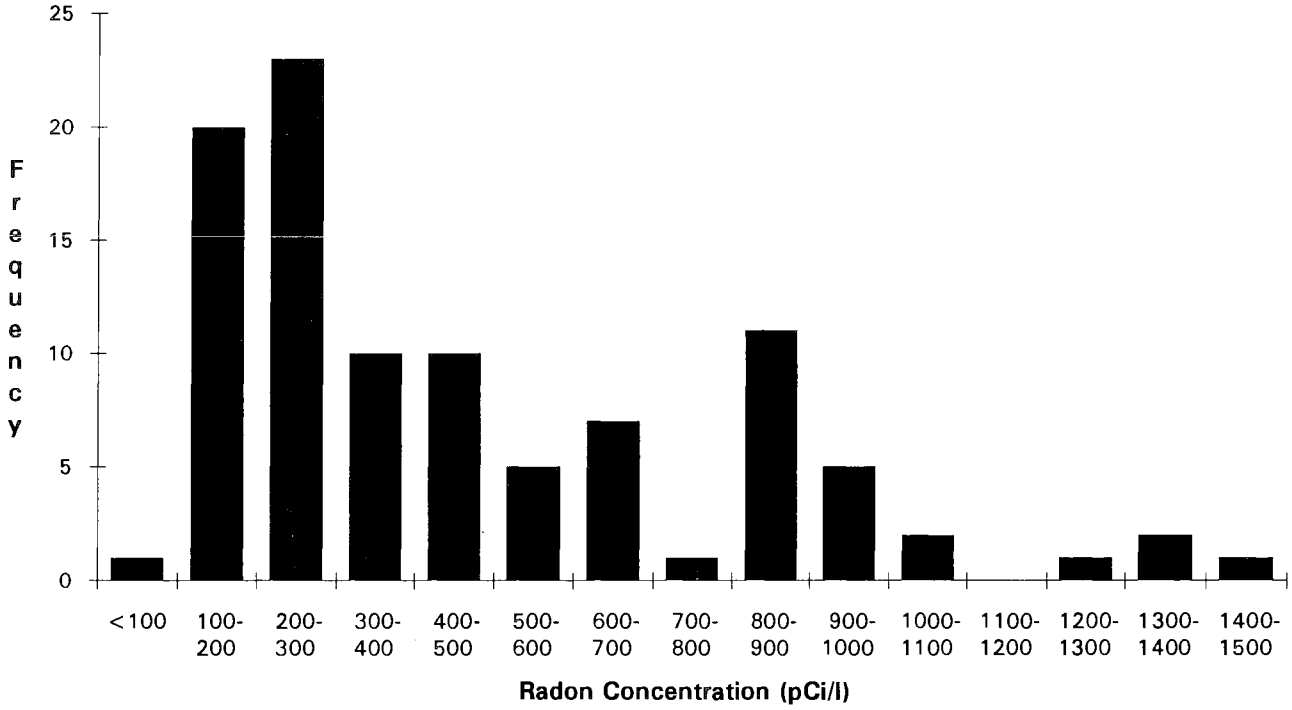

Figure 5. Histogram of ^{222}Rn concentrations in Tucson Basin well water (data from Smith, this volume, p. 17-39).

REFERENCES

Emer, D.F., Shenk, J.D., and Spencer, J.E., 1988, Reconnaissance gamma-ray survey of radon-decay products in selected populated areas of Arizona: Arizona Geological Survey Open-File Report 88-12, 88 p.

Environmental Protection Agency (EPA), 1986a, A citizen's guide to radon: 14 p.

_____ 1986b, Radon reduction methods: 24 p.

_____ undated, The radon detection kit: Pamphlet.

Faure, Gunter, 1977, Principles of isotope geology: New York, John Wiley and Sons, 464 p.

Kearfott, K.J., 1989, Preliminary experiences with ^{222}Rn gas in Arizona homes: Health Physics, v. 56, p. 169-179.

Kearfott, K.J., Metzger, R.L., and Holbert, K.E., 1992a, Underground air returns as active transportation pathways for radon gas entry into homes: Health Physics, v. 63, p. 665-673.

Kearfott, K.J., Metzger, R.L., Kraft, K.R., and Holbert, K.E., 1992b, Mitigation of elevated indoor radon gas resulting from underground air return usage: Health Physics, v. 63, p. 674-680.

May, R.T., White, D.L., and Nystrom, R.J., 1982, National uranium resource evaluation, Prescott quadrangle, Arizona: U.S. Department of Energy Open-File Report GJQ-015 (82), 62 p.

National Council on Radiation Protection and Measurements (NCRP), 1984a, Evaluation of occupational and environmental exposures to radon and radon daughters in the United States: Report 78, 204 p.

_____ 1984b, Exposures from the uranium series with emphasis on radon and its daughters: Report 77, 131 p.

_____ 1989, Control of radon in houses: Report 103, 90 p.

Osborne, M.C., 1988, Radon-resistant residential new construction: U.S. Environmental Protection Agency Report 600/8-88/087.

Reynolds, S.J., Keith, S.B., and DuBois, J.F., 1980, Locations, lithologic descriptions, petrographic information, and analytical data for geochemical samples, *in* Coney, P.J., and Reynolds, S.J., eds., Cordilleran metamorphic core complexes and their uranium favorability (appendix E): U.S. Department of Energy Open-File Report GJBX-258 (80), p. 187-245.

Tanner, A.B., 1986, Indoor radon and its sources in the ground: U.S. Geological Survey Open-File Report 86-222, 5 p.

Texas Instruments, Inc., 1975, Airborne geophysical survey, southeastern Arizona: U.S. Department of Energy Open-File Report GJO-1643, 44 p.

Wenrich, K.J., Chenoweth, W.L., Finch, W.I., and Scarborough, R.B., 1989, Uranium in Arizona, *in* Jenney, J.P., and Reynolds, S.J., eds., Geologic evolution of Arizona: Arizona Geological Society Digest 17, p. 759-794.

Geology, radioactivity, and radon at the Cardinal Avenue uranium anomaly, southwestern Tucson[1]

JON E. SPENCER — *Arizona Geological Survey, 845 N. Park Ave., #100, Tucson, Arizona 85719*
DUDLEY F. EMER[2] — *West Tech Geophysics, 6931 E. Hawthorne St., Tucson, Arizona 85710*
JONATHAN D. SHENK[3] — *Arizona Geological Survey, 845 N. Park Ave., #100, Tucson, Arizona 85719*

INTRODUCTION

Tertiary limestone near Cardinal Avenue and Valencia Road in southwestern Tucson contains visible uranium minerals; in fact, the area was prospected for uranium in the 1950's. Background-radiation levels above the limestone were measured during the 1970's and were below the level considered to be a health risk. Homes were subsequently built on the limestone. Radon gas is produced during the decay of uranium to stable lead, and indoor-radon levels correlate statistically with uranium concentrations in underlying soil and rock. Recognition during the 1980's of indoor radon as a health hazard in a small percentage of U.S. homes led to renewed interest in the Cardinal Avenue limestone.

To aid Pima County health officials in surveying homes for radon, the Arizona Geological Survey (AZGS) conducted a detailed gamma-ray-spectrometer survey of the Cardinal Avenue uranium anomaly. Data points were contoured in multiples of average gamma radiation from the uranium (and radon) decay product bismuth-214 (^{214}Bi) in surrounding neighborhoods to determine the background level. The center of the Cardinal Avenue uranium anomaly had a radioactivity level due to ^{214}Bi that was approximately 15 times the regional background level. Results of this survey were used to direct a radon-measuring program by the Pima County Health Department. The department discovered that radon levels were higher than 4 picocuries per liter (pCi/l) in about half of the 40 homes within the 2-times-background contour. (The EPA recommends keeping average indoor-radon levels below 4 pCi/l.) Details of the spectrometer survey are presented below, along with a review of the geology of the area and a brief history of human interest in this area.

GEOLOGY

Brown (1939) was the first geologist to publish information about the Tertiary lake beds at the southeastern end of the Tucson Mountains. He described them as 1-ft-thick lake beds of limestone with interbedded calcareous shales and minor beds of white pumiceous ash and gypsum. Ostracods and concentric algal structures are associated with the shales and limestones, respectively. Brown recognized that the beds were folded into a syncline with a maximum bed dip of 20°. He was unable to determine the dip of the western contact with adjacent andesite because of cover and low relief, but he interpreted the contact as a fault. At the time of Brown's study, a vertical shaft was present near the center of the limestone. Brown did not enter the shaft, but observed andesite on the dump and inferred that the andesite underlay the limestone. He was unable to confirm the nature of the underlying contact, but offered two alternatives: (1) the contact is depositional on eroded volcanic rocks; or (2) the contact is a thrust fault. The nature of the northern contact was also in question, but Brown assumed that the beds were resting unconformably on adjacent rhyolite.

Kinnison (1958) described the lake beds in his thesis on the geology and ore deposits of the Amole mining district. He determined a minimum thickness of more than 30 ft for the lake beds. Kinnison observed that the andesite fragments near the shaft appeared weathered, with rounded edges, and suggested that the volcanic rocks at the contact beneath the limestone formed a weathered soil surface. In contrast to Brown (1939), Kinnison mapped the northern contact with the rhyolite as a fault.

Grimm (1978) studied the lake beds as part of her thesis on Cenozoic pisolitic limestones of

---

[1]This article supersedes the following report: Spencer, J.E., Emer, D.F., and Shenk, J.D., 1987, Geology, radioactivity, and radon at the Cardinal Avenue uranium occurrence, southwestern Tucson: Arizona Bureau of Geology and Mineral Technology Open-File Report 87-3, 16 p.

[2]Present address: Reynolds Electrical and Engineering Co., M.S. 738, P.O. Box 98521, Las Vegas, NV 89193.

[3]Present address: P.O. Box 1036, Mammoth, AZ 85618.

in Spencer, J.E., ed., 1993, Radon in Arizona: Arizona Geological Survey Bulletin 199, p. 10-16.

southeastern Arizona. The following description is taken from her work:

> The beds at the surface consist of finely crystalline limestone, light olive gray to dark yellowish brown, weathering to yellowish gray and light olive gray, with locally abundant pisolitic structures (0.5 mm to 4 cm in diameter), limited amounts of slightly coated angular carbonate grains (0.2-1 mm), and rare stem(?) fragments. Moderate to extreme silicification occurs, with the greatest degree of replacement being in areas with the largest and most abundant pisolites. The strata are thin- to medium-bedded, with a thickness of approximately 7 feet presently observable. A shallow syncline with a maximum dip of 22 degrees on the beds is present along the northern side of the exposure.

Grimm differed with Brown in her interpretation of the northern contact, but agreed with Kinnison in suggesting that the lake beds and the rhyolite appear to be in fault contact. From discussions with J.S. Vuich of the Arizona Bureau of Mines, who observed the contact in utility-line trenches, Grimm concluded that the lake beds are in depositional contact with the andesite. (Vuich described the underlying volcanic rocks as weathered at the contact and stated that the overlying carbonate rocks graded downward into siltier, sandier, and more brownish limestone near the contact.) Grimm stated the following concerning the organic content of the beds:

> Palynological examination, of samples from the limestone of the lake beds, yielded Miocene pollen assemblages.... Organic recovery included as much as 30-40% recycled carbonized woody material. The carbonization levels of the pollen are primarily in the early hydrocarbon generation state. The larger fragments of organic material are sheet-like with no cellular structure, and may be algal in character.

AZGS geologists compiled a map of the Cardinal Avenue area (Fig. 1), which is located on the lake beds, from aerial photographs, field reconnaissance, and maps prepared by Grimm (1978), Kinnison (1958), and Vuich (1978). The nature of the contacts with the volcanic rocks (i.e., whether they are faulted or depositional) is still unclear.

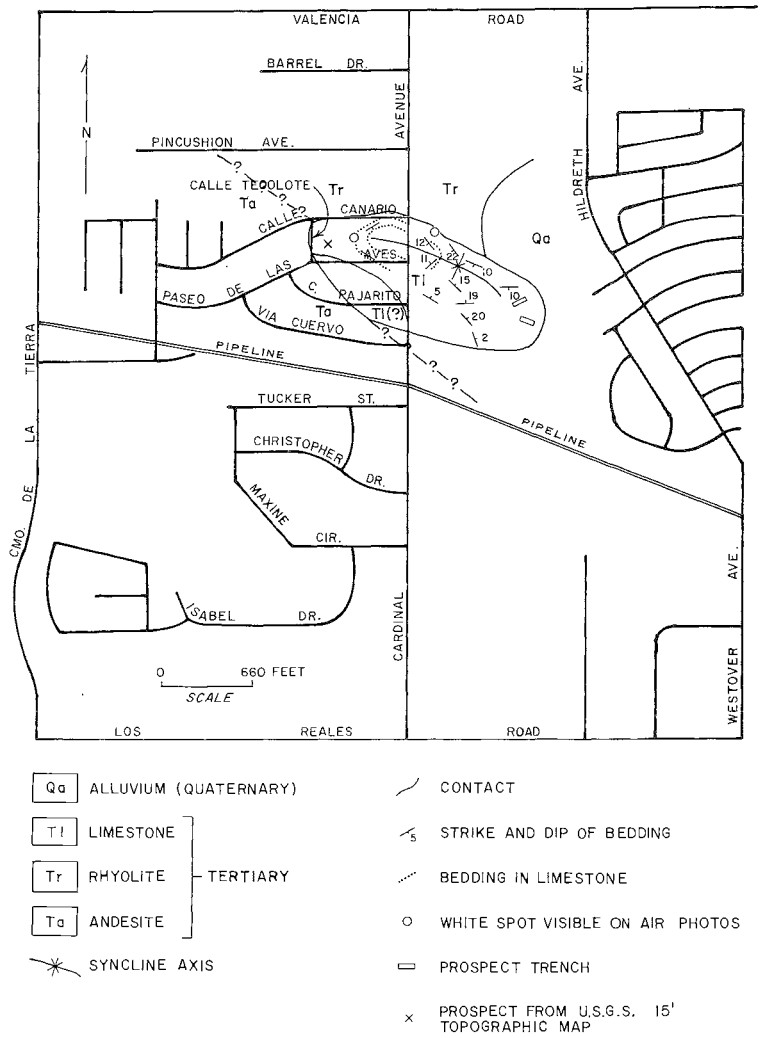

Figure 1. Simplified geologic map of the uraniferous Tertiary limestone and adjacent rock types near Cardinal Avenue and Valencia Road, southwestern Tucson.

The aerial photographs and U.S. Geological Survey (USGS) topographic maps were used to determine geologic contacts and the locations of early shafts and prospect pits. Figure 2 was compiled by projecting the locations of the following four items onto a 7.5' topographic base: (1) a prospect symbol from the 1957 San Xavier Mission USGS 15' topographic map; (2) disturbed areas appearing as white spots on 1971 aerial photographs; (3) streets and houses from 1983 aerial photographs; and (4) the location of the highest radiation reading from this study. The eastern white spot was readily located in the field, situated on the contact between the rhyolite and the limestone. The western white spot, however, was not located in the field. We believe it is likely that the

prospect symbol represents the western white spot, but because of distortions inherent in projections, the symbol and white spot do not correspond exactly on the map.

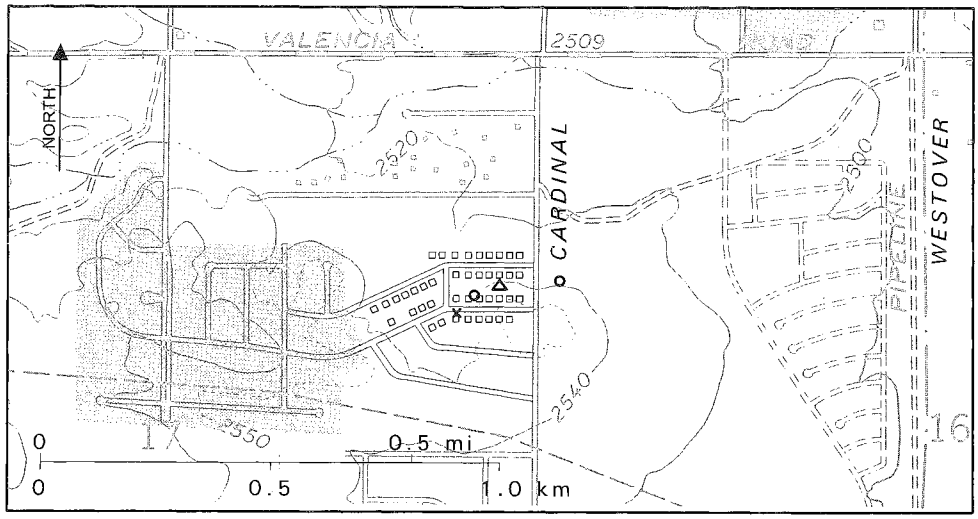

□ HOUSE

△ LOCATION OF HIGHEST MEASURED BACKGROUND RADIOACTIVITY

× APPROXIMATE LOCATION OF PROSPECT FROM USGS 15' TOPOGRAPHIC MAP

○ WHITE SPOT VISIBLE ON OLD AERIAL PHOTOGRAPHS

Figure 2. Topographic map of the area in and around the Cardinal Avenue uranium anomaly, showing homes and other features on or near the Tertiary limestone. Topographic base map from USGS Cat Mountain 7.5' topographic quadrangle map (1968).

URANIUM MINERALIZATION

Miller (1955) examined the Cardinal Avenue limestone for the U.S. Atomic Energy Commission during a preliminary reconnaissance for potential uranium sources. At the time, the area was known as the Dutchess Claims, held by Ward and Richard Kinnan of Tucson. Miller noted five claims and discovery pits. Two of his samples contained 0.06% and 0.05% equivalent U_3O_8. Miller recorded a background radiation of 0.02 milliroentgens per hour (MR/hr) and a maximum radiation of 0.60 MR/hr. He found uranophane in a 1- to 2-ft-thick zone within a pit.

Peirce and others (1970) also recorded the presence of uranophane, but undertook no new investigations. In late 1975 and early 1976, while working for the Arizona Bureau of Mines on an urban land-use-planning project, Vuich (1978) noted the presence of uranium in the Cardinal Avenue limestone. Texas Instruments, Inc. (1978) carried out an aerial radiometric reconnaissance survey of the Tucson 1° x 2° quadrangle. The data did not reveal a radiation anomaly over the Cardinal Avenue area, however, because the area was between flight lines. The Pima County Planning and Zoning Department (1978) showed the anomaly in a southwest-area plan. Scarborough and Wilt (1979) recorded 5 to 7 times the background radioactivity in the Cardinal Avenue area and noticed carnotite fracture coatings on many parts of the limestone.

RADIATION STUDIES

A preliminary scintillometer survey of the Cardinal Avenue area (Vuich, 1978) indicated that average radioactivity levels were 2 times the background level. The Arizona Atomic Energy Commission (AAEC), after being notified by Vuich, carried out a detailed radiation survey of the Chastain housing development property (Ochoa and others, 1976; Vuich, 1978). The AAEC concluded that the "Chastain property yearly total was calculated to be 0.22380 rem. AAEC permissible yearly total is 0.5 rem. No remedial action is recommended by the AAEC."

Krieski (1979), a graduate student at the University of Arizona, did a radiometric study similar to Vuich's preliminary survey and recorded up to 4 times the background level in the alley just north of Paseo de las Aves and in four lots west of Cardinal Avenue. The areas of greatest radioactivity seemed to correspond to the axis of a northwest-plunging syncline. Krieski determined that the limestone in the alley contained an average of 6.7 parts per million (ppm) total uranium. (The average in Arizona is 2 to 3 ppm.)

In response to citizen concern, the Arizona Radiation Regulatory Agency, formerly the AAEC, carried out a brief survey in the alley north of Paseo de las Aves and on the east side of Cardinal Avenue at a recent excavation (Henckel, 1984). The agency reported that "Using data from a minimal

number of sites, calculations indicate radiation levels of approximately 0.24 R/yr (roentgens per year) on the west side of Cardinal Ave. in the alley north of Paseo de las Aves behind lots four (4) and five (5) and 0.11 R/yr on the east side of Cardinal Ave. in the undeveloped area where three backhoe pits have been developed."

Because of increased awareness of the potential health hazard of radon gas, AZGS geologists began to study geologic and other aspects of radon in 1986. This effort included preparing a map that identified areas in Arizona where the uranium content of rock and soil is known to be significantly greater than average (Spencer, 1986; Spencer and Shenk, 1986). Attention by the press and subsequent concern by citizens about radon in the Cardinal Avenue area led the AZGS to conduct a detailed radiation study there to locate areas of unusually high background radiation, so that radon-testing devices could be placed in homes that may have been at risk (Emer and Shenk, 1987).

Dudley Emer, of West Tech Geophysics, volunteered his time and equipment for a detailed gamma-radiation survey of the Cardinal Avenue uranium anomaly. With assistance from Jon Shenk, a former graduate research assistant at the AZGS, Emer surveyed the area in March and April of 1987. They used a four-channel spectrometer, one channel of which measured gamma rays at the energy of gamma emissions from ^{214}Bi. (See Appendix A for technical details.) ^{214}Bi is an intermediate daughter product in the uranium-238 (^{238}U) decay series. The concentration of ^{214}Bi in the top few inches of soil and rock, as approximately determined by gamma-radiation surveys of this type, is considered to be an accurate indicator of the amount of uranium in the soil and rock and is consequently used as an exploration tool for uranium. Radium-226 (^{226}Ra), also an intermediate daughter product of ^{238}U, decays into radon-222 (^{222}Rn), which in turn decays rapidly (in about 1 hour) through several isotopes, including ^{214}Bi. Thus, measurement of gamma radiation from ^{214}Bi is actually a more sensitive indicator of ^{222}Rn levels than of ^{238}U levels.

Figure 3. Location map of gamma-radiation (from ^{214}Bi) measurement points, showing measurements in counts per minute (cpm). Stations with readings considered anomalous and therefore not used in Figure 4 are shown with parentheses.

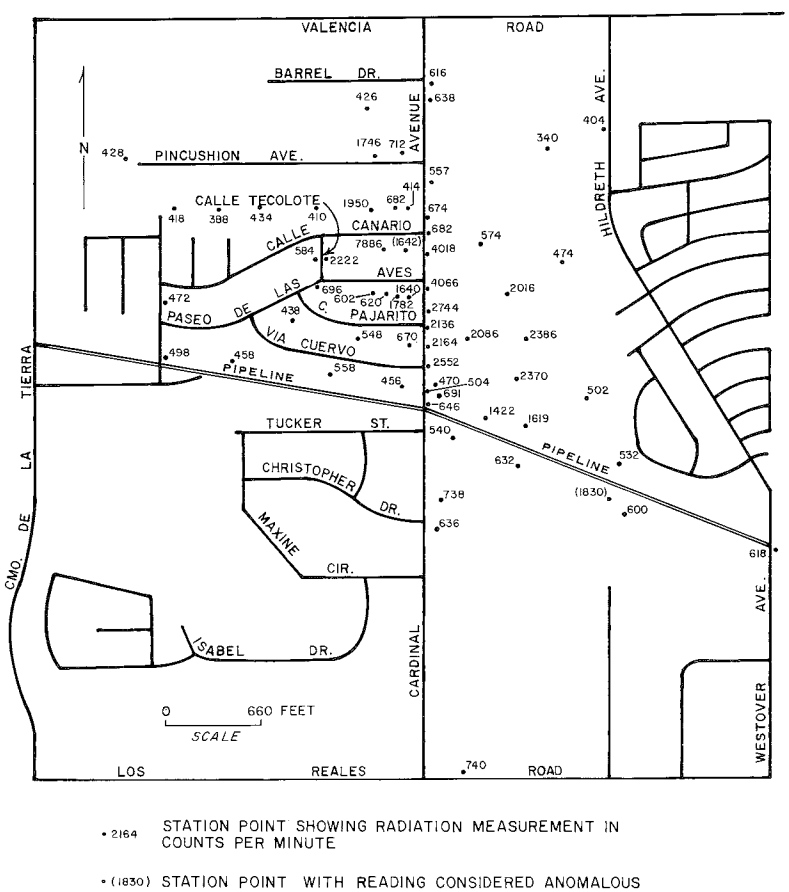

The survey was run in two parts: traverse (reconnaissance) and point mapping. In the traverse portion of the survey, the spectrometer continuously recorded four channels of data using a 1-second count time while it was moved at approximately 3 to 5 miles per hour. The researchers' objective was to cover a large area of ground rapidly while delineating lithologic contacts and ensuring that localized areas of either high or low radiation levels were included in the point mapping.

The point mapping was accomplished by using a long count time (30 seconds) while the spectrometer remained stationary at preselected or random stations. The long count time enhances the count statistics and allows a much better resolution of the distribution of low levels of uranium. Long count-time measurements were taken where significant changes were observed in radiation levels during a traverse. The result was a traverse of continuous data, using a 1-second sample time, with specific features detailed at high resolution. The data from point mapping (Fig. 3) were used to draw a contour map of the data points (Fig. 4).

In April 1987, the Pima County Health Department used the results of the radiation survey to select homes for indoor-radon measurement. Homes within the approximate 2-times-back-

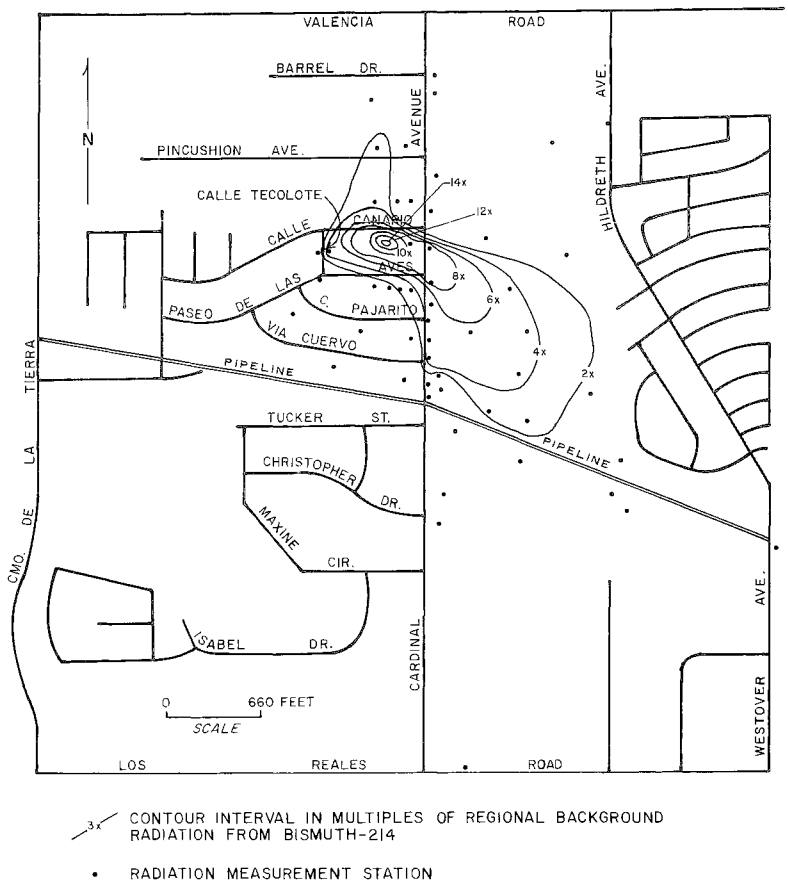

Figure 4. Contour map of gamma-radiation levels derived from data presented in Figure 3. Contours are in multiples of average background radiation (500 cpm) from surrounding areas that are not anomalously radioactive.

ground-radiation contour were tested. Radon levels in about half the homes tested were higher than the maximum average level considered acceptable by the EPA (Nolan, 1987). Additional tests outside the 2-times contour revealed generally low indoor-radon levels.

To determine the degree of correlation between background radioactivity and indoor-radon level, a background level was estimated for each home in the study area for which radon data were available. The data in Figure 4 were used to estimate radiation levels using a linear extrapolation between contours. A plot of indoor-radon level vs. estimated background radioactivity for each tested home (Fig. 5) clearly shows a positive correlation.

CONCLUSION

Tertiary limestone in southwestern Tucson contains visible uranium minerals. A gamma-ray spectrometer survey of the limestone and surrounding areas revealed that anomalous levels of radioactivity are restricted to the limestone and are not characteristic of surrounding areas. A positive correlation between measured indoor-radon levels and background gamma radiation indicates that gamma-ray surveys are useful in delineating areas at elevated risk for high indoor-radon levels.

REFERENCES

Brown, W.H., 1939, Tucson Mountains, an Arizona Basin Range type: Geological Society of America Bulletin, v. 50, p. 697-760.

Emer, D.F., and Shenk, J.D., 1987, Preliminary map of gamma radiation due to surface uranium mineralization, Cardinal Ave., Tucson, AZ: Arizona Bureau of Geology and Mineral Technology press release, April 9, 1 p.

Grimm, J.P., 1978, Cenozoic pisolitic limestones of Pima and Cochise Counties, Arizona: Tucson, University of Arizona, M.S. thesis, 71 p.

Henckel, George, 1984, Chastain housing development located near Valencia Road and Cardinal Ave., Tucson, Arizona: Arizona Radiation Regulatory Agency memorandum to John Lutton, April 24, 2 p.

Kinnison, J.E., 1958, Geology and ore deposits of the southern section of the Amole mining district, Tucson Mountains, Pima County, Arizona: Tucson, University of Arizona, M.S thesis, 126 p.

Krieski, Mark, 1979, Radiation safety study of Chastain housing development near Valencia Road and Cardinal Avenue: Unpublished manuscript, 6 p.

Miller, R.A., 1955, Dutchess claims, Amole mining district, Pima County, Arizona: U.S. Atomic Energy Commission Preliminary Reconnaissance Report PRR A65, 1 p.

Nolan, P.A., 1987, Preliminary investigation of radon levels in homes in southwest Tucson: Pima County Health Department news release, May 1, 2 p.

Ochoa, R.B., Coleman, Mattie, Moore, R.T., and Vuich, J.S., 1976, A radiation survey of Chastain housing development property near Valencia Road and Cardinal Avenue, Tucson, Arizona: Arizona Atomic Energy Commission, unpublished file data.

Peirce, H.W., Keith, S.B., and Wilt, J.C., 1970, Coal, oil, natural gas, helium, and uranium in Arizona: Arizona Bureau of Mines Bulletin 182, p. 103-146, plus appendix, table K, p. 250-260.

Pima County Planning and Zoning Department, 1978, Southwest area plan (Co13-76-1), phase III: 45 p., 2 plates, scale 1:50,000.

Scarborough, Robert, and Wilt, J.C., 1979, A study of uranium favorability of Cenozoic sedimentary rocks, Basin and Range Province, Arizona; part I, general geology and chronology of pre-late Miocene Cenozoic sedimentary rocks: Arizona Bureau of Geology and Mineral Technology Open-File Report 79-1, 101 p.

Spencer, J.E., 1986, Radon gas, a geologic hazard: Arizona Bureau of Geology and Mineral Technology Fieldnotes, v. 16, no. 4, p. 1-6.

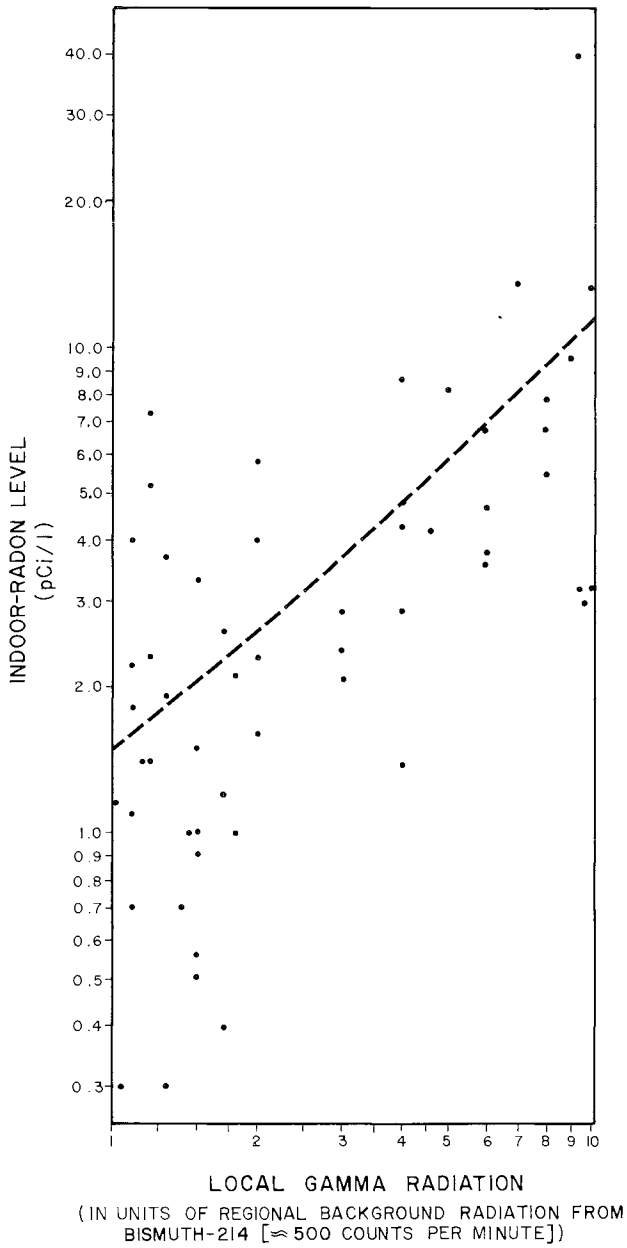

Figure 5. Plot of indoor-radon levels versus background radioactivity for homes near the Cardinal Avenue uranium anomaly. Indoor-radon levels were measured with charcoal canisters during April and May 1987. Radon data were provided by the Pima County Health Department. Background gamma radiation from ^{214}Bi for each home was estimated from Figure 4. The dashed line is a linear regression of the data points and represents the equation y = 1.094x - .373, where y is the indoor-radon level in pCi/l and x is the background-radiation level in multiples of the regional-background level (approximately 500 cpm; x = 1 for 500 cpm, x = 2 for 1,000 cpm, etc.). The line is curved because a log-log scale was used.

Spencer, J.E., and Shenk, J.D., 1986, Map showing areas in Arizona with elevated concentrations of uranium: Arizona Bureau of Geology and Mineral Technology Open-File Report 86-11, scale 1:1,000,000.

Texas Instruments Inc., 1978, Aerial radiometric and magnetic reconnaissance survey of portions of Arizona-New Mexico, Tucson quadrangle, v. 2-C: U.S. Department of Energy Open-File Report GJBX-23-79, 203 p.

Vuich, J.S., 1978, Geologic considerations in land utilization (a study near Tucson, Arizona): Arizona Bureau of Geology and Mineral Technology, unpublished manuscript.

APPENDIX A
by Dudley Emer

The equipment used to delineate the uranium anomaly at Cardinal Avenue was a Scintrex GAD-6 four-channel gamma-ray spectrometer containing three 1.6-liter thallium-activated sodium iodide crystals mounted 3 ft aboveground in a fixed geometry and attached to the back of a jeep. This equipment, designed specifically for airborne and mobile mineral prospecting, measures broad-band gamma radiation as well as gamma radiation due to potassium, uranium, and thorium.

The operating principle is the same as for a handheld scintillometer: when a gamma ray is absorbed by the sodium iodide crystal, it produces a small flash of light called a scintillation. This scintillation is detected by a photomultiplier tube and converted into an electrical pulse, which is counted over a specified period. The count rate is proportional to the amount of gamma radiation present. A gamma-ray spectrometer takes this process one step further and measures the amplitude of the electrical pulse. Because the energy of the gamma ray is proportional to the brightness of the scintillation, it is also proportional to the amplitude (pulse height) of the electrical pulse produced by the photomultiplier tube.

Naturally occurring gamma-ray sources of potassium, uranium, and thorium emit a characteristic energy spectrum. By analyzing the spectrum of an unknown radiation source and its characteristic energy peaks, researchers can identify the radioisotopes present. The gamma-ray spectrometer, also called a pulse-height analyzer, counts only those pulses whose amplitude corresponds to the energy peak of interest. This count rate is proportional to the amount of radioisotope present. The counting times selected for a survey depend on the survey requirements and the background-radiation levels. In general, the count time for a moving survey is set to 1 second, whereas stationary measurements may use a 30-second or greater count time, which offers greater accuracy because of improved count statistics. The GAD-6 digitally measures four channels (energy peaks) simultaneously. The specification for each channel

and preset windows are as follows:

Channel 1 — Total Count: Measures changes in gamma radiation of all energies in the range 0.15 to 2.77 MeV. This channel provides the most sensitivity to overall changes in gamma radiation and will also detect manmade gamma-radiation sources within its energy band (e.g., cesium-137 and cobalt-60).

Channel 2 — Potassium: Measures the potassium-40 peak at 1.461 MeV with the counting window extending from 1.380 to 1.560 MeV.

Channel 3 — Uranium: Measures the bismuth-214 peak at 1.764 MeV with the counting window extending from 1.660 to 1.900 MeV.

Channel 4 — Thorium: Measures the thallium-208 peak at 2.615 MeV with the counting window extending from 2.440 to 2.770 MeV.

The system is calibrated each day and checked periodically throughout the day. The calibration of the spectrometer relies on a fifth channel that is centered on the thorium peak at 2.615 MeV but uses a window width of only 2.580 to 2.650 MeV. The calibration is accomplished by using a thorium-oxide calibration source in a fixed geometry with detector #1 and adjusting the gain of the spectrometer's pulse-height analyzer to shift the 2.615-MeV thallium-208 peak from the detector into the calibration window. Once the thorium peak from detector #1 is properly aligned in the calibration window, the respective energy peaks representing potassium, uranium, and thorium will fall into their preset windows within the spectrometer. When the pulse-height analyzer has been calibrated to detector #1 (the standard), detector #1 is turned off and the thorium-oxide calibration source is used to calibrate detector #2. The gain of detector #2 is then adjusted to shift its thorium peak to match that of detector #1. Detector #3 is calibrated in a similar manner so that the thorium peak from each detector is properly aligned for the pulse-height analyzer and each channel is properly centered.

Although the spectrometer is very sensitive because of the large crystal volume, it will respond only to very near surface radiation sources because of the attenuation effects of various materials on gamma radiation. As an example, penetration through about 4 in. of rock or 8 in. of soil will reduce 2-MeV gamma radiation by about a factor of two. About 3 ft of water or 1.5 ft of rock will almost completely shield out potassium, uranium, or thorium radiation. Attenuation in air is negligible at distances less than about 15 ft. Gamma radiation is reduced by about one-half through 400 ft of air. To be most effective, therefore, this type of survey requires either (1) outcrops or near-surface soils with anomalously high concentrations of uranium; or (2) upwardly migrating radon gas that deposits daughter products in the very near surface material.

During the survey, the output from the spectrometer was continuously displayed on a six-channel strip-chart recorder as total, potassium, uranium, and thorium counts. The strip-chart recorder allowed the operator to monitor individual radiation levels as the survey progressed and ensured that no areas of elevated radiation were missed. Digital data from all four channels were simultaneously recorded in a computer that displayed the total, potassium, uranium, and thorium counts, as well as the Compton stripped data and the amount of potassium, uranium, and thorium in parts per million.

Bibliography for Appendix A

Briener, S., Lindon, J.T., and Kalenbach, R.J., 1976, Gamma ray measurements and data reduction considerations for airborne radiometric surveys: International Symposium on Exploration of Uranium Ore Deposits, Vienna, Austria, Paper #34.

Fleischer, R.L., and Turner, L.G., 1984, Correlation of radon and carbon isotopic measurements with petroleum and natural gas at Cement, Oklahoma: Geophysics, v. 49, p. 810-817.

geoMetrics, 1977a, Field surveys using a portable gamma ray scintillometer: Sunnyvale, California, Technical Report 12, 12 p.

——— 1977b, Survey guidelines for using a gamma ray spectrometer in uranium exploration: Sunnyvale, California, Technical Report 13, 12 p.

George, A.C., 1984, Passive integrated measurements of indoor radon using activated carbon: Health Physics, v. 46, p. 867-872.

Grasty, R.L., Glynn, J.E., and Grant, J.A., 1985, The analysis of multichannel airborne gamma ray spectra: Geophysics, v. 50, p. 2611-2650.

LeGrand, H.E., 1987, Radon and radium emanations from fractured crystalline rocks — A conceptual hydrologic model: Ground Water, v. 25, p. 59-69.

Lovborg, L., and Mose, E., 1987, Counting statistics in radioelement assaying with a portable spectrometer: Geophysics, v. 52, p. 555-563.

Rock, R.L., and Beckman, R.T., 1979, Radiation monitoring: U.S. Department of Labor, Mine Safety, and Health Administration.

Scintrex Ltd., 1979, GAD-6 four channel stabilized gamma ray spectrometer operation manual: Ontario, Canada, Scintrex Ltd.

^{222}Rn distribution in the ground water of the north-central Tucson Basin and its relationship to the hydrogeology[1]

BRUCE D. SMITH[2] *Department of Hydrology and Water Resources, University of Arizona, Tucson, Arizona 85721*

INTRODUCTION

Radon-222 (^{222}Rn) is a chemically inert, radioactive gas that decays by alpha emission and has a half-life of 3.82 days. ^{222}Rn originates from the disintegration of radium-226 (^{226}Ra), and both elements are part of the uranium-238 (^{238}U) decay series. ^{222}Rn is ubiquitous in soil and rock and varies in concentration, depending on the ^{226}Ra concentration as well as other factors. Because ^{222}Rn is soluble in water, it can enter and travel in ground water.

Numerous studies of ^{222}Rn in ground water have been conducted to evaluate it as a health hazard in potable water (Hess and others, 1978); as a precursor to earthquakes (Smith and others, 1980); as an indicator of effluent stream reaches (Rogers, 1958; Lee and Hollyday, 1987); as a tool for uranium, geothermal, and oil and gas exploration (Cadigan and Felmlee, 1977; Kruger and others, 1977; Whitehead, 1980); as an estimate of aquifer porosity (Semprini, 1987); and as an aid to research on hydrogeochemical (dis)equilibrium (Asikainen, 1981; King and others, 1982).

^{222}Rn in public water supplies has recently become a topic of concern because it can contribute significantly to ^{222}Rn concentrations in air within buildings. As of January 1992, the U.S. Environmental Protection Agency (EPA) had not established a health standard for ^{222}Rn in public water supplies, but was considering levels of 300 picocuries per liter (pCi/l). The average ^{222}Rn concentration in public water supplies in the United States poses an estimated lifetime risk of 1 death in 10,000 persons, the highest risk level allowed for any contaminant under the Safe Drinking Water Act (Cothern, 1987).

The relationship between ^{222}Rn concentrations in ground water and hydrogeology has been well documented in suspect crystalline terrain, such as the New England region (Hall and others, 1987). In Maine, ^{222}Rn concentrations in ground water are as high as 300,000 pCi/l in granitic rocks (Brutsaert and others, 1982). Sandstones in consolidated sedimentary aquifers have concentrations as high as 1,000 and 3,300 pCi/l (Gilkeson and Cowart, 1987; Cech and others, 1987; respectively). In the Newark Basin of New Jersey, ground water in black mudstones contains ^{222}Rn concentrations as high as 15,900 pCi/l (Szabo and Zapecza, 1987). The average ^{222}Rn concentration in all ground-water systems is estimated to range from 200 to 600 pCi/l (Cothern, 1987). Research into the relationship between aquifer rock type and ^{222}Rn concentration in unconsolidated aquifers has been less intense, probably because researchers believed that these waters contained relatively small amounts of ^{222}Rn. Projects designed to investigate the health hazards were, therefore, less numerous.

A recent study (Semprini, 1987), however, focused on the relationships between ^{222}Rn emanation and hydrogeology in a shallow alluvial aquifer in California. Semprini reported levels in alluvial aquifers that ranged from 100 to 1,100 pCi/l and an average concentration of about 250 picocuries per kilogram (pCi/kg). He concluded that ^{222}Rn emanation from the aquifer solids was the main source of ^{222}Rn in the ground water, and that the emanation coefficient increased with a decrease in the particle size of the aquifer material.

Tanner (1964a), in a thorough and often-referenced paper, investigated both ^{222}Rn and ^{226}Ra within the ground water of an unconsolidated artesian aquifer in the Great Salt Lake area. He examined the relationships between the well discharges and the ^{222}Rn and chemical parameters, and investigated the sources of ^{222}Rn and the physical controls on its distribution. Tanner's investigations of the possible influence of distant

---

[1]This article is based on the following report: Smith, B.D., 1988, The distribution of radon-222 in the ground water of the north-central Tucson Basin and its relationship to the hydrogeology: Tucson, University of Arizona, M.S. thesis, 100 p., scale 1:126,720.

[2]Present address: 129 Alcove Ct., Grand Junction, CO 81503.

in Spencer, J.E., ed., 1993, Radon in Arizona: Arizona Geological Survey Bulletin 199, p. 17-39.

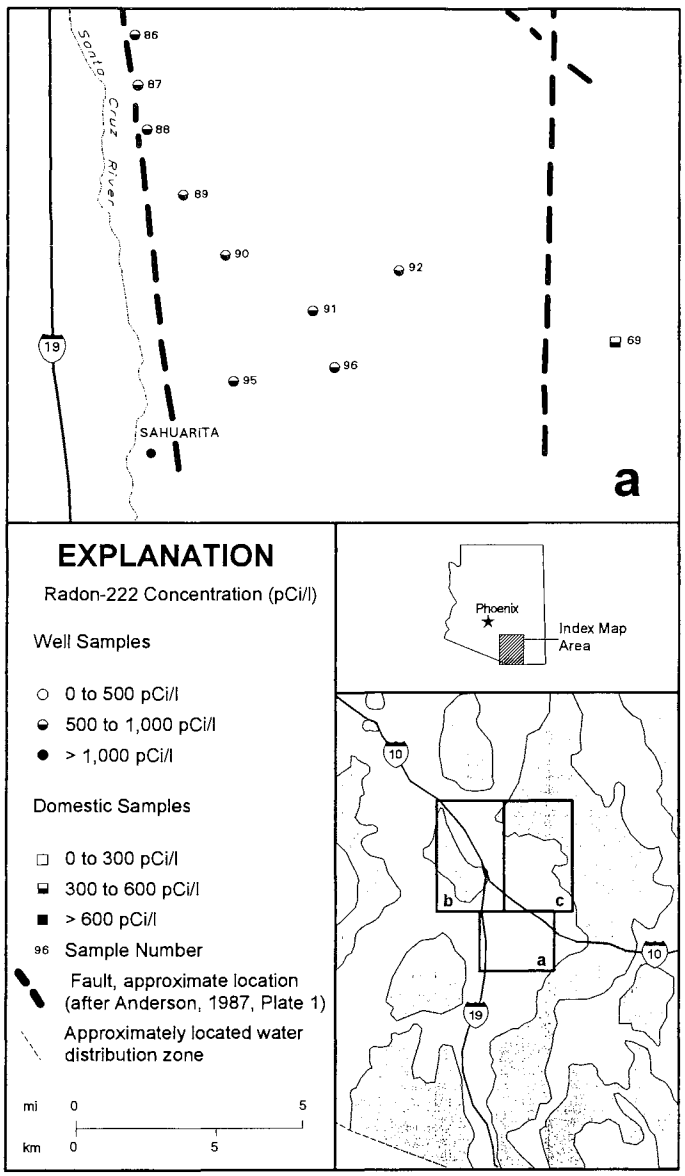

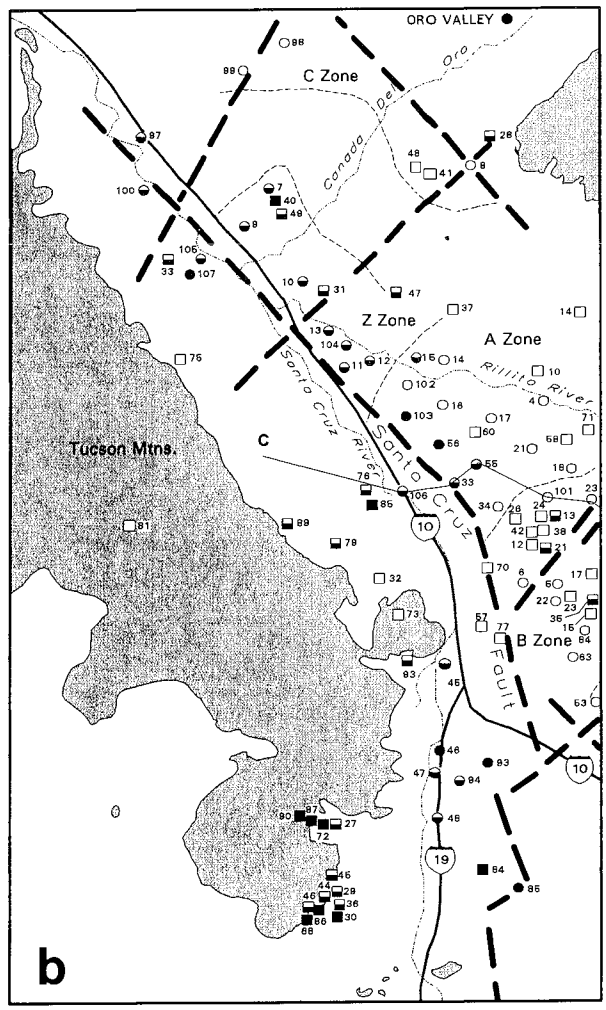

Figure 1(a,b,c). Map of ^{222}Rn concentrations in well and domestic water samples in north-central Tucson Basin.

sources on ^{222}Rn well concentrations led him to conclude that the source of ^{222}Rn was near each well. The physical controls on ^{222}Rn emanation and concentration and how these amounts are affected by faulted sediments and porosity were more difficult to assess. Tanner concluded that ^{222}Rn distribution in the ground water must be determined by ^{226}Ra distribution in the sediments.

Several studies have concentrated on the relationship between ground-water ^{222}Rn anomalies and faults or other geologic structures (Lorenz and others, 1961; King, 1978; Smith and others, 1980; Wei and Yi-Yao, 1984). Another study (Harvey, 1981) examined ^{222}Rn anomalies in soil gas and ground water near earth fissures in the Picacho Basin of Arizona.

My study is the first in-depth research on ^{222}Rn in the ground water of the Tucson Basin. The main objectives of this study were to (1) determine the distribution of ^{222}Rn in city and private well waters of the north-central Tucson Basin, and (2) attempt to identify the hydrogeologic controls on ^{222}Rn concentrations in ground water. Domestic waters in the city of Tucson were also sampled for ^{222}Rn to check for significant differences between ^{222}Rn concentrations in the well heads and in home taps.

PHYSIOGRAPHY AND CLIMATE

The Tucson Basin is a broad, northwest-trending valley in southeastern Arizona bounded by mountain ranges on the eastern, northern, and western sides. The basin is approximately 2,590 km^2 (1,000 mi^2) in area.

The study area is the north-central Tucson Basin, which is defined in this report as the area encompassing the city of Tucson and extending

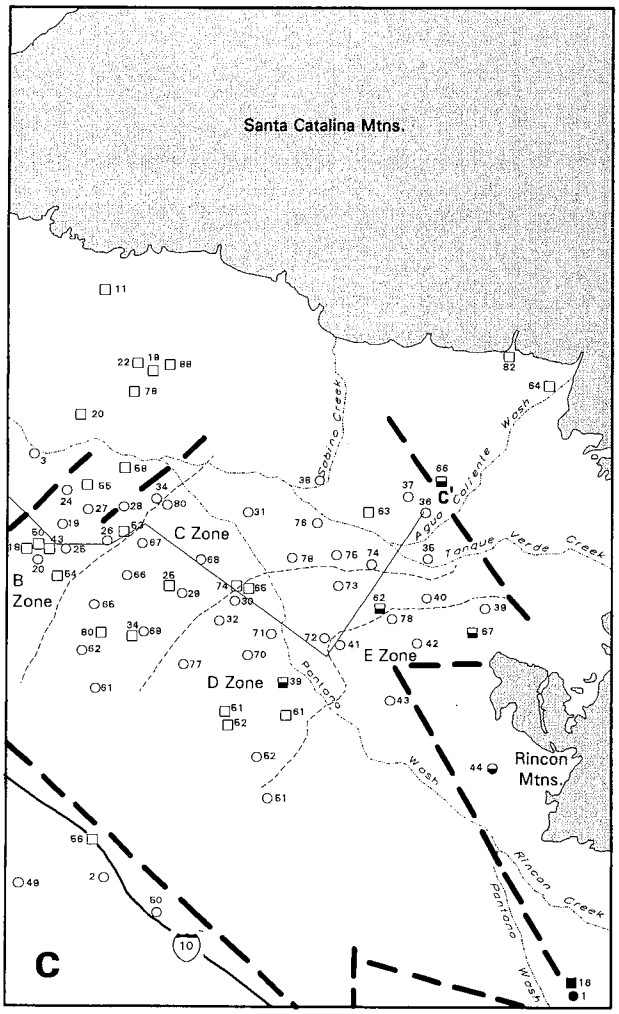

northward to the town of Rillito and southward to Sahuarita (Fig. 1). This region will be referred to as the Tucson area and is about 1,114 km^2 (430 mi^2) in area. The Tucson area is bounded on the northeast, east, southeast, southwest, and west by the Tortolita and Santa Catalina, Tanque Verde and Rincon, Santa Rita, Sierrita, and Black and Tucson Mountains, respectively. The elevations of the eastern mountains range from 1,890 to 2,895 m (6,200 to 9,500 ft); the elevations of the western mountains range from 914 to 1,829 m (3,000 to 6,000 ft).

The principal drainage in the Tucson area is the ephemeral north- to northwest-trending Santa Cruz River. The surface of the Tucson area slopes northwestward from an elevation of about 914 m (3,000 ft) at the southern edge to an elevation of about 608 m (2,000 ft) at the northern edge. The Tucson area is flat to gently rolling terrain covered with typical Sonoran Desert vegetation, such as creosote and palo verde. The ground water stored in the aquifer that underlies the basin has been a major source of water in the Tucson area.

The climate in southeastern Arizona, including the Tucson area, is classified as desert or semi-desert. The mean monthly temperature is 20.3°C (68.6°F), with a mean daily minimum and maximum of 11.5°C (52.8°F) and 29°C (84.3°F), respectively. The mean annual precipitation is about 305 mm (12 in.) in the basin and about 635 mm (25 in.) or more in the mountains (Davidson, 1973). About half of this falls during the summer, commonly during intense thunderstorms. During the winter, the basin receives gentle widespread rains and an occasional light snowfall that originate from cold Pacific storms (Sellers and Hill, 1974).

HYDROGEOLOGY

Geologic History

From the decline of the Laramide orogeny (53 m.y. ago) to the late Oligocene (28 m.y. ago), southwestern Arizona was largely quiescent with regard to magmatic and tectonic activity (Eberly and Stanley, 1978; Dickinson, 1991). Normal faulting began late during this time and was associated with deposition of the subareal fanglomerates and lacustrine sediments of the Pantano Formation. Deposition of the Pantano Formation marked the beginning of the first of two major tectonic events that would affect this area — the mid-Tertiary orogeny, which lasted until the early Miocene. Rocks formed before and during this event were faulted, steeply tilted, and locally folded (Dickinson, 1991). The orogeny produced significant quantities of rhyolitic to andesitic tuffs, breccias, and flows, which were intercalated with red sands, gravels, and fanglomerates. Local algal limestone, mudstone, and associated beds of water-laid tuff were also deposited. From 28 to 24 m.y. ago, during the mid-Tertiary orogeny, low- to moderate-angle normal faulting occurred, and gneissic domes and arches, as well as the Catalina-Rincon, Tortolita, and Tanque Verde metamorphic core complexes, were uplifted (Spencer and Reynolds, 1989; Dickinson, 1991). The mid-Tertiary orogeny began to wane 20 to 17 m.y. ago, and a distinct unconformable surface developed (Eberly and Stanley, 1978).

The second major tectonic event — the Basin and Range disturbance — started at about 13 to 12 m.y. ago. The resulting development of the horst-graben terrain and new interior drainage facilitated the deposition of local detritus and thick bodies of evaporites. The Basin and Range disturbance may have renewed uplift of the metamorphic core complexes (Anderson, 1987a; Dickinson, 1991). Late Pliocene erosion and exterior drainage development led to the modern landscape.

Stratigraphy

The Santa Catalina, Tanque Verde, Rincon, and Tortolita Mountains are mainly composed of mylonitic gneiss and granite, as well as a variety of structurally deformed Precambrian to Tertiary crystalline rocks and sediments. The Tucson and Sierrita Mountains are composed of andesitic to rhyolitic flows, tuff, and agglomerate and minor amounts of interbedded conglomerate and sandstone. The Black Mountains are composed of basaltic andesite (Anderson, 1987a). The Santa Rita Mountains are composed of Mesozoic and Paleozoic sedimentary and igneous rocks (Davidson, 1973).

The sediments underlying the north-central Tucson Basin consist of three Cenozoic stratigraphic units: the Oligocene Pantano Formation, Miocene Tinaja beds, and Pleistocene Fort Lowell Formation. The total thickness of these units may be as much as 6,096 m (20,000 ft; Anderson, 1987a).

The Pantano Formation unconformably overlies Precambrian and Tertiary rocks. The formation may be as thick as thousands of feet and consists of reddish mudstone, siltstone, sandstone, and moderately to tightly cemented gravel. Sediments are locally interbedded with volcanic flows and tuffs (Anderson, 1987a). These rocks have been radiometrically dated at 26 to 38 m.y. (Oligocene; Dickinson and Shafiqullah, 1989). In the western part of the basin, the Pantano Formation is primarily composed of volcanic detritus; even near the Santa Catalina and Rincon Mountains, gneissic detritus is not always present in this unit. The Pantano Formation is generally composed of sedimentary, volcanic, and granitic particles in an arkosic to clay-rich matrix (Davidson, 1973).

The Tinaja beds unconformably overlie the Pantano Formation and are unconformably overlain by the Fort Lowell Formation. The Tinaja beds are separated into three unconformable units, the lower, middle, and upper, which are late Oligocene to Miocene, Miocene, and Miocene to Pliocene in age, respectively. The upper beds crop out at the basin margins. Most deposits of the Tinaja beds are 0 to 610 m (0 to 2,000 ft) thick, but some are as much as 1,524 m (5,000 ft) thick (Davidson, 1973).

The lower Tinaja beds are composed of silty gravel and conglomerate and probably contain interbedded volcanic flows and tuffs (Eberly and Stanley, 1978). The middle Tinaja beds are mainly confined to the central subsurface of the basin. These sediments were deposited in a complex graben that formed east of the Santa Cruz Fault as a result of Basin and Range block faulting. Within the north- to northwest-trending graben, gypsiferous and anhydritic clay, silt, and mudstone were deposited. The upper Tinaja beds mostly consist of sand and clayey silt in the central parts of the basin, and gravel and sand near the mountains (Anderson, 1987a).

The sources of the detritus that make up the Tinaja beds were apparently the nearby mountain ranges. An increase in the amount and size of gneissic fragments from the lower to the upper beds is probably due to a highland that rose while the beds were being deposited. The northern and eastern parts of the basin contain abundant granitic detritus in a feldspathic to arkosic sand matrix. Well B-10 (Fig. 1b, sample 101), for example, contains almost 100% gneissic gravel, and mostly quartz, feldspar, and gneiss in the sand matrix. Sedimentary and volcanic rock fragments are more common to the southeast (Davidson, 1973). In the western part of the basin, near the Santa Cruz Fault, wells B-085 and Z-013 (Fig. 1b, samples 94 and 9, respectively) contain abundant (>50%) volcanic gravel and coarse-grained material. Davidson (1973) reported that the fine-grained facies within the central part of the basin contains only 5 to 25% material coarser than silt and commonly contains disseminated gypsum nodules in the upper beds, and nodules to thin beds of fine- to coarse-grained crystalline anhydrite in the lower beds. Anderson (1987a, Plate 2) produced contour maps of the percentage of fines in the upper Tinaja beds and the Fort Lowell Formation.

The Fort Lowell Formation unconformably overlies the Tinaja beds and is unconformably

Table 1. Hydrological properties of sediments of Tucson Basin. From Davidson (1973) and S. Rogers (Tucson Water, personal commun., 1988).

Formation	Porosity (%)	Transmissivity (10^3 m^2/d)	Well Yield (10^3 m^3/d)	Specific Capacity (Y/m_d)*
Pantano Fm.	20 - 27	< 0.12	0.5 - 27.0	0.36 - 0.7
Tinaja beds	24 - 35	0.12 - 1.9	2.7 - 8.2	0.02 - 0.7
Fort Lowell Fm.	26 - 34	0.25 - 12.4	2.7 - 8.2	0.18 - 1.8

*Y = well yield (10^3 m^3/d); m_d = well drawdown in meters; d = day

overlain by a thin veneer of younger sediments. The Fort Lowell Formation forms most of the basin's surface and has been assigned an age of early to middle Pleistocene on the basis of local stratigraphic correlations. The formation is 91 to 122 m (300 to 400 ft) thick. Sediments typically consist of pebbly sand, medium to coarse sand, and silty sand with some clayey silt near the center of the basin. The coarse-grained material mainly consists of Catalina Gneiss with traces of volcanic rocks derived from local sources (Davidson, 1973).

Structure

One of the most recent structural interpretations of the Tucson Basin (Anderson, 1987a, Plate 1) modified earlier work (Davidson, 1973). The following summary, including fault locations (Fig. 1), is based on this recent study (Anderson, 1987a).

The Santa Cruz Fault, which trends northwest along the western side of the Tucson Basin, parallel to the Santa Cruz River, is a block fault resulting from the Basin and Range disturbance. From the area near well SS-24 (Fig. 1b, sample 46) toward the northwest, this fault has juxtaposed Tertiary volcanic rocks to the west with Tinaja beds to the east. The southern part of the Santa Cruz Fault has juxtaposed sediments of the lower Tinaja beds with those of the middle to upper Tinaja beds. As much as 1,830 m (6,000 ft) of differential offset may have occurred. A secondary and subsequent, oblique and northeast-trending fault system developed while the upper Tinaja beds were being deposited and the mountain highlands were being uplifted during the late Miocene and Pliocene (Anderson, 1987a).

The north- to northeast-trending fault that crosses the western side of the Tucson area is the Pirate fault, a block fault of the Basin and Range disturbance. The so-named I-10 fault trends northwest and parallels Interstate Highway 10 south of Tucson. Although some faults may have become active during the Quaternary (Anderson, 1987a), the Fort Lowell Formation is not offset.

The most recent structural movement occurred in the late Pliocene to middle Pleistocene. A prominent through-flowing drainage developed as the basin was uplifted with respect to the Santa Cruz River (Davidson, 1973; Anderson, 1987a).

Hydrology

The Tucson Basin aquifer consists of the Pantano Formation, Tinaja beds, and Fort Lowell Formation. The hydrological properties of these formations are listed in Table 1. Unconfined-aquifer conditions prevail, but some local perched-water and confined-aquifer conditions exist.

The Pantano Formation yields small to moderate amounts of water to wells. Relatively few wells have penetrated as deep as the Pantano Formation, but aquifer tests reveal that this unit is characterized by leaky, confined conditions where it is composed of or overlain by fine-grained sediments (Davidson, 1973).

Of the Tinaja beds, only the upper unit is a good aquifer. Very few production wells extend far into the middle unit. S. Rogers (Tucson Water, personal commun., 1988) has divided the upper Tinaja beds into two units, an upper unconsolidated unit and a lower consolidated unit. The two units are separated by the "Rillito surface" — an erosional surface that commonly coincides with the unconformity between the Tinaja beds and the Fort Lowell Formation. The upper unconsolidated unit is the better water producer and yields small to large amounts of water to wells.

The Fort Lowell Formation is the thickest of the highly permeable units in the basin and has supplied most of the water used in the basin (Davidson, 1973). Coarse-grained facies of the upper Tinaja beds and Fort Lowell Formation may yield more than 5,450 m^3/day (1,000 gal/min) of water to properly constructed wells (Anderson, 1987b).

CHARACTERISTICS OF ^{222}Rn

Properties of ^{222}Rn

^{222}Rn is the heaviest of the noble gases. It evolves from the radioactive decay of ^{226}Ra within the decay series of ^{238}U (Spencer, this volume, p. 2, Fig. 1). ^{222}Rn decays by alpha emission and has a 3.82-day half-life. The other isotopes of radon, ^{220}Rn (thoron) and ^{219}Rn (actinon), have short half-lives of 55 and 4 seconds, respectively. Because of their short half-lives, thoron and actinon are usually not present in measurable concentrations. The radioactive nature, gaseous (mobile) state, and chemical inertness of the ^{222}Rn isotope allow it to be easily measured.

^{222}Rn is more soluble than any other noble gas (Cook, 1961). The solubility of ^{222}Rn in water may be expressed in several ways. The water/air concentration ratio or partition coefficient for ^{222}Rn is about 0.23 at 25°C (77°F) and 760-mm pressure (UNSCEAR, 1982); alternatively, at 25°C (77°F), 22.4 cm^3 of ^{222}Rn will dissolve in 100 cm^3 of water (Weast and Astle, 1980). The Henry's Law constant for ^{222}Rn is 3.97×10^{-6}, making it a moderately soluble gas compared to weakly soluble oxygen and highly soluble hydrogen sulfide, for which Henry's Law constants are 30.4×10^{-6} and 0.37×10^{-6}, respectively (Prichard, 1987).

Table 2. Diffusion coefficients of ^{222}Rn for different media. From UNSCEAR (1982).

Medium	Diffusion Coefficient (cm^2/s)
Air	10^{-1}
Water	10^{-5}
Soil	10^{-2}
Ionic Crystals	10^{-20}

Emanation Power and Factors Affecting ^{222}Rn Concentrations in Ground Water

The sources of ^{222}Rn in ground water are the uranium- and radium-bearing rocks, minerals, and their weathering products that compose the aquifer. The average uranium concentration in crustal rocks is 2.7 parts per million (ppm). The uranium abundance varies by rock type, with averages of 4.8 ppm in granite, 4 ppm in rhyolite, 0.6 ppm in basalt, 3.2 ppm in shale, and 1 to 2 ppm in sandstone and carbonates (P.E. Damon, University of Arizona, personal commun., 1988; Hall, 1988). The Catalina and Oracle Granites, which make up a good portion of the mountains to the north and east of the Tucson area, contain 1 to 1.5 and 3 to 4 ppm uranium, respectively (Reynolds and others, 1980). The Turkey Track Andesite of the Tucson Mountains contains an unusually high amount of uranium at 3.3 ppm (Mielke, 1965; P.E. Damon, University of Arizona, personal commun., 1988). Sediments underlying the Tucson area and derived from the Santa Catalina, Tanque Verde, and Rincon Mountains are estimated to contain 60% Catalina Granite, 30% Oracle Granite, and 10% other rock types (S.J. Reynolds, Arizona State University, personal commun., 1988). Based on this information, it seems reasonable to assume that about 1 ppm uranium is in the sediments derived from these mountains. It is, however, difficult to say how much of this uranium contributes to ^{226}Ra that, in turn, contributes to the ^{222}Rn concentration in the ground water. (For an areal distribution of these sediments, see Anderson, 1987a, Plate 3.)

^{222}Rn in ground water originates from its parent nuclide, ^{226}Ra, either within the water itself (supported radon) or from immobile ^{226}Ra within or on the surface of the surrounding mineral grains of the aquifer (nonsupported radon). ^{226}Ra commonly exists in very small amounts in ground water, less than 1 pCi/l (Longtin, 1988); therefore, the concentrations of radon derived from dissolved ^{226}Ra are usually insignificant. With a dry specific gravity of 2.0 g/cm^3 and an available pore space of 20% by volume, a material containing 0.7 pCi/l of emanating ^{226}Ra (the amount that would be in equilibrium with a ^{238}U concentration of 1 ppm) would produce a ^{222}Rn concentration of 3,500 pCi/l in pore-space water (Smith and others, 1980). Although the ^{226}Ra concentration in the aquifer material is of major importance, several other factors related to the mechanisms of ^{222}Rn emanation affect the ^{222}Rn concentration in ground water.

The four processes by which ^{222}Rn enters ground water are direct radioactive recoil, indirect recoil, diffusion, and weathering. The combined result of these mechanisms is referred to as the emanating power of the solid ^{226}Ra-containing material. Tanner (1964b) defined emanation power as the fraction of ^{222}Rn atoms formed in a solid that escape from the solid under steady-state conditions.

During alpha decay of a ^{226}Ra atom, an alpha particle is emitted in one direction and the recoiling ^{222}Rn atom in the other, releasing 85 kilovolts (keV) of energy. The ^{222}Rn atom travels distances ranging from 20 to 30 nanometers (nm, or 10^{-9} m) in minerals of normal rock density, about 60 micrometers (μm, or 10^{-6} m) in air, or about 0.1 μm in water (Tanner, 1964b).

The first process that contributes to emanating power is direct recoil. The direct-recoil fraction is the fraction of ^{222}Rn atoms that recoil from rock into an open pore space. The presence of water in the pore is a vital factor in the emanating power of a medium. If the water-filled pore is larger than the recoil range, a ^{222}Rn atom recoiling into the pore loses kinetic energy to the water, and the recoil path ends short of the adjacent grain. The width of this saturated pore need be only about 0.1 μm for recoiling ^{222}Rn atoms to concentrate in the pore water. For materials with equal emanation rates, those with lower porosity will have a greater ^{222}Rn concentration (Tanner, 1964a). In a dry soil, ^{222}Rn release is reduced by readsorption onto solid surfaces.

Andrews and Wood (1972) demonstrated that 23.5% of ^{222}Rn atoms within the recoiling distance of the mineral surface will escape. They also showed that ^{222}Rn release (in pCi/g) is proportional to $1/d^{1/2}$, where d is the particle or grain diameter in micrometers, and that the recoil escape percentage was 4.9/d. A particle of 100 μm would, therefore, release only 0.049% of the ^{222}Rn generated. These authors concluded that for mineral grains, the direct-recoil mechanism contributes a very small amount to the total emanating power and is less than 1% in dry compact materials.

The indirect-recoil fraction, from the second process that contributes to emanating power, involves an enhanced diffusion rate. When a recoiling atom collides with a mineral grain or rock particle after passing through a pore, it forms a crater or pocket. This crater may measure 10 nm

x 1 to 10 nm in size. The recoil process momentarily vaporizes the rock, causing the thermal conductivity of about 10^{-1} cm^2/s to approach the diffusion coefficient. This condition allows more rapid diffusion of the recoil atom back through the crater pore; however, because this process requires diffusion and not recoil into a pore, the indirect-recoil fraction is probably no larger than that of direct recoil (Tanner, 1964b).

The third process that contributes to emanating power is diffusion. Diffusion coefficients for ^{222}Rn vary according to medium (Table 2). The diffusion coefficient for a solid crystal is very small, whereas for air it is relatively large. Amirkhanoff and others (1961) inferred that diffusion coefficients are characteristic of the minerals rather than of the diffusing gases. Nicolaysen (1957) reported values of 10^{-21} to 10^{-23} cm^2/s for the diffusion of lead in zircon and monazite. Because of the short half-life of ^{222}Rn and the extremely slow process of diffusion of inert gases in solids, this process probably releases only a small percentage of ^{222}Rn atoms (Andrews and Wood, 1972). For these same reasons, the contribution of ^{222}Rn to ground water due to the fourth process — weathering — is also insignificant.

Mineralogical characteristics of aquifer materials are perhaps the primary controlling factors in radon emanation power. The bulk of ^{222}Rn release is from radium isotopes within secondary crusts, films, or cements (Tanner, 1964b) or from within grains that have a large internal surface area, such as a mineral grain perforated by less than 1 μm pores (Rama and Moore, 1984).

The increase in emanation power with decrease in grain size is apparently related to the increased surface area of the smaller grains (which, in turn, provide greater area for crusts and films), as well as a thinner matrix through which direct recoil may occur. In some aquifer materials, decreasing particle size is correlated with increasing iron content (from cementing material) and increasing radon-emanation power (Tanner, 1964a; Andrews and Wood, 1972). This is because of the strong adsorption of ^{226}Ra to iron and manganese hydroxides (Szabo and Zapecza, 1987). The concentration of ^{226}Ra in soil particles also increases as particle size decreases below 100 μm (Megumi and Mamuro, 1977).

Although several studies support the particle-size/emanation-power relationship, other research (Starik and Melikova, 1957; Tanner, 1964a) indicates that the amount of ^{222}Rn released to passing fluids may be the same or even less after a rock is crushed than before. If corrosion films, crusts, and secondary cements, as well as nanopores due to weathering of mineral grains, are major contributing factors to ^{222}Rn emanation in ground water, this research may not accurately simulate aquifer conditions.

In summary, ^{226}Ra concentration in the solid phase (including secondary crusts, films, and cements), particle size, and saturated porosity are crucial parameters that affect the ^{222}Rn-emanating power of a homogeneous sediment.

^{222}Rn Migration in Ground Water

Once ^{222}Rn has become a solute in the pore fluid, it is subject to movement by diffusion and convection, providing the pore is open to flow. A transport velocity of only 10^{-5} cm/sec^{-1} is more effective than diffusion in causing the movement of ^{222}Rn in ground water (Andrews and Wood, 1972). Numerical analysis of one-dimensional diffusion indicates that the ^{222}Rn concentration in ground water will decrease 100-fold 10.7 cm (4.3 in.) from saturated rock and soil (Tanner, 1964a). Diffusion, therefore, is not a significant process for transporting ^{222}Rn in ground water.

The short half-life of ^{222}Rn and the slow migration of ground water allow ^{222}Rn to be in secular equilibrium with ^{226}Ra in the local rock (Brutsaert and others, 1982). Tanner (1964a) examined the transport of ^{222}Rn in ground water using the time restriction of one mean life of a ^{222}Rn atom. This is 1/l, or 5.5 days, where l is the decay constant for ^{222}Rn. For one-dimensional gravitational flow, the mean migration distances are proportional to the ground-water flow rates. Normal ground-water flow rates are 2 m (6.6 ft)/year to 2 m (6.6 ft)/day (Todd, 1980). In a homogeneous aquifer with a uniform distribution of ^{226}Ra, one would expect a well to produce constant ^{222}Rn levels when the flow to a well is steady, radial, and horizontal. Under these conditions, the migration distance is proportional only to the square root of the flow rate and reciprocal of the porosity (Tanner, 1964a). This distance for well A-32 (Fig. 1b, sample 56), for example, may be estimated using the flow rate of 3.14 m^3/min (830 gpm), the screened interval of 166 m (545 ft), an estimated effective porosity of 25%, and the mean life of a ^{222}Rn atom. The volume and radius of a cylinder that is as high as the well screen is thick may be calculated using the known flow rate. A geometrical volume of 99,524 m^3 (3.5 x 10^6 ft^3) would hold the amount of water discharged during one mean life of ^{222}Rn. The corresponding radius is about 14 m (45 ft). As Tanner (1964a) stated, this simple calculation does not take into account the disproportionate amounts of water being supplied by aquifer materials; even so, the error in the radius is proportional to the square root of the error in the thickness estimate. This calculation indicates that most of the ^{222}Rn measured in well water comes from immobile ^{226}Ra close to the well bore.

Harvey (1981) observed that ^{222}Rn concentrations increased during the first few hours after a pump was turned on, but then stabilized at a lower concentration. He attributed this fluctuation to compressional stresses in the aquifer due to pumping. Dixon and Lee (1987) noted a similar trend and attributed the decrease in ^{222}Rn concentration to the expansion of the cone of depression into water-bearing, lower ^{222}Rn concentrations, a site-specific phenomenon. Flow of ^{222}Rn-containing water to a well through a fracture has not been extensively studied for alluvial aquifers. If the source of ^{222}Rn is within the walls of the fracture itself, the ^{222}Rn concentration would be limited by the small surface-area/water ratio. In general, flow rates would have to be high to transport ^{222}Rn long distances to a pumping well.

^{222}Rn ANALYSIS

Methodology

^{222}Rn was measured by degassing a water sample into a Lucas-type alpha-scintillator cell and counting the disintegrations with an EDA Instrument RDA 200 Radon Detector. The degassing method extracts the dissolved ^{222}Rn gas with a carrier gas, such as helium, or in this case, nitrogen.

One advantage of the degassing alpha-scintillation-cell method is its ability to measure, quickly and accurately, ^{222}Rn in water. The method is also field compatible and minimizes sample preparation and ^{222}Rn loss during the sampling procedure and analysis. Detection limits for this method are reportedly as low as the sub-picocurie/liter level (EDA Instruments, 1988).

A widely used alternative method is direct-scintillation counting. This method lacks specificity because any alpha-particle or hard-beta emitters (not just ^{222}Rn and its daughters) that are soluble in toluene will contribute to the count rate (Yang, 1987). ^{222}Rn may be lost while the sample is being transported and stored because of permeable or leaky caps or stopcocks. The detection limit for this method is about 10 to 70 pCi/l (^{222}Rn only) (Yang, 1987; K.J. Herwehe, Tucson Water, personal commun., 1988).

Gamma spectroscopy and extraction-concentration/liquid-scintillation counting are two other methods for measuring ^{222}Rn (Yang, 1987). The detection limits for the gamma-spectroscopy and extraction-concentration methods are 10 pCi/l for a 1-l sample and 0.2 pCi/l for a 500-ml sample, respectively.

Instrument Description

I designed and constructed the degassing instrument to be fieldworthy and compatible with the scintillator cells of EDA Instruments. Through the use of a hand pump, the degassing system was placed in a partial vacuum of 685 torr and then raised to atmospheric pressure (about 720 torr) by drawing in nitrogen through a silica diffuser and allowing it to bubble through the water sample. The purged gases passed through a drierite (anhydrous calcium sulfate) trap, which absorbed moisture, and were collected in a scintillator vacuum cell.

A more detailed description of the degassing system follows. The inlet of the degassing system consisted of Tygon tubing, through which the carrier gas nitrogen was introduced. The flow of nitrogen was regulated by a glass and plastic Rotoflo valve (valve 1). The nitrogen passed through Tygon tubing and a fine, fritted, gas-diffuser tube into a 125-ml Erlenmeyer flask. (The diffuser and flask together are referred to as the bubbler.) The diffuser was fitted to the top of the flask through a drilled-out, no. 5, rubber stopper and situated close to the bottom of the flask. ^{222}Rn extracted from the water sample escaped through the nipple port of the flask, through Tygon tubing, and into stainless-steel tubing that led to a brass valve (valve 2). After exiting this valve, gases entered a glass drierite tube (1.9 cm outside diameter x 21.3 cm). The exiting end of the drierite tube was connected to stainless-steel tubing that, in turn, was connected to a brass valve (valve 3). On the exiting side of this valve, a vacuum gauge was attached via a T-shaped connecting fixture. Stainless-steel tubing connected this fixture to Tygon tubing with a male Swagelok connector on the end. The male connector was connected to its female counterpart on an alpha-scintillation cell.

To prevent premature aeration of the water sample, a sampling adapter was constructed from a rubber sleeve, Tygon tubing, and glass tubing through a rubber stopper. The glass tubing, through which the water sample entered the flask, was situated so that it almost touched the bottom when the stopper was placed on the flask. Most of the water sample entered the flask slowly, under the water-sample surface, and was not free-falling or subject to aeration.

The RDA 200 was specifically designed for ^{222}Rn detection. It measures the alpha-particle activity of ^{222}Rn and its daughters. The alpha particles strike the silver-activated, zinc-sulfide, phosphor coating of the scintillator-cell interior, resulting in emission of several photons of ultraviolet light. Each photon registers on the high-gain photomultiplier tube and is transformed into an electrical impulse. The impulses are counted and

digitally displayed after a preset time (EDA Instruments, 1988).

Before the cell is counted in the alpha detector, the ^{222}Rn is allowed to reach secular equilibrium with its two short-lived, alpha-emitting daughters: polonium-218 (^{218}Po) and lead-214 (^{214}Pb). When this equilibrium is established in 3 to 4 hours, the cell is counted for 30 minutes, and the counts per minute (cpm) are recorded. To minimize buildup of a high cell background, after the cell is counted it is flushed with filtered outdoor air for 15 to 30 minutes and then evacuated to about 300 torr. Initial testing of the degassing unit showed an optimum degassing time of about 2 minutes. Repeated tests of the same sample showed that about 85% of the ^{222}Rn was extracted during the first degassing period.

Calibration

The efficiency of each of eight cells was calibrated at UNC Geotech, Grand Junction, Colorado. The cells were flushed with ^{222}Rn gas of a known concentration (313 pCi/l) for 45 minutes. The cells were then counted in the RDA 200 detector after reaching secular equilibrium. Counting was done twice after equilibration periods of about 4 and 6 hours. The counts per minute divided by the ^{222}Rn concentration (pCi/l) is the cell's yield, or efficiency, factor. An average yield factor was calculated for each cell. Cell 5 had the median factor after the first count and was used as a normalizing cell. All other cell yield factors were divided into cell 5's yield factor to normalize the data to cell 5, thus eliminating the need to construct a calibration curve for each cell.

A National Bureau of Standards traceable ^{226}Ra solution, provided by the University of Arizona Radiation Control Office, was used to prepare standards. Six 100-ml ^{226}Ra solutions were prepared in degassing flasks with approximately the same volume as the sampling bubbler. Errors in preparing the standards were insignificant compared to the $\pm$2.7% overall error of the quoted radioactive concentration of the original ^{226}Ra solution.

The ^{226}Ra-solution flasks were constructed entirely of glass — a 100-ml flask with stopcock valves on both a gas-diffuser inlet tube and a glass outlet tube. The diffusers were the same type used in the degassing instrument; however, the size and quantity of bubbles varied during normal degassing procedures. The head-space volume in the ^{226}Ra flasks was similar to that of the sampling flask.

The solutions were degassed into the cells only after a week of ^{222}Rn ingrowth. (Complete ingrowth of ^{222}Rn occurs in about 38 days.) This was done consecutively for 8 weeks so that each of the eight cells would collect a different ^{222}Rn concentration and the results would yield a more accurate cpm/pCi/l ratio. The concentrations of the solutions, including compensations for the age of the original solution and the incomplete ingrowth time, were calculated at about 72, 180, 360, 540, 719, and 3,597 pCi/l. The counts per minute for each cell for each concentration were normalized to the counts per minute for cell 5 and then plotted against the corresponding ^{222}Rn concentration (Fig. 2).

Once a water sample was degassed and the counts per minute recorded, the net value was multiplied by the cell's normalizing factor (cell 5 cpm/cell # cpm, where # equals the number of the cell [1 through 8]). The equation of the best-fit line ($y = 0.34x - 3.9$; Fig. 2) was then used to calculate ^{222}Rn concentrations in water values. This line indicates a detection limit of about 12 pCi/l in water at 0 cpm. Background levels in the cells ranged from about 0.5 to 2.5 cpm; most were less than 2 cpm. The calculated ^{222}Rn concentration for this background range is 13 to 19 pCi/l.

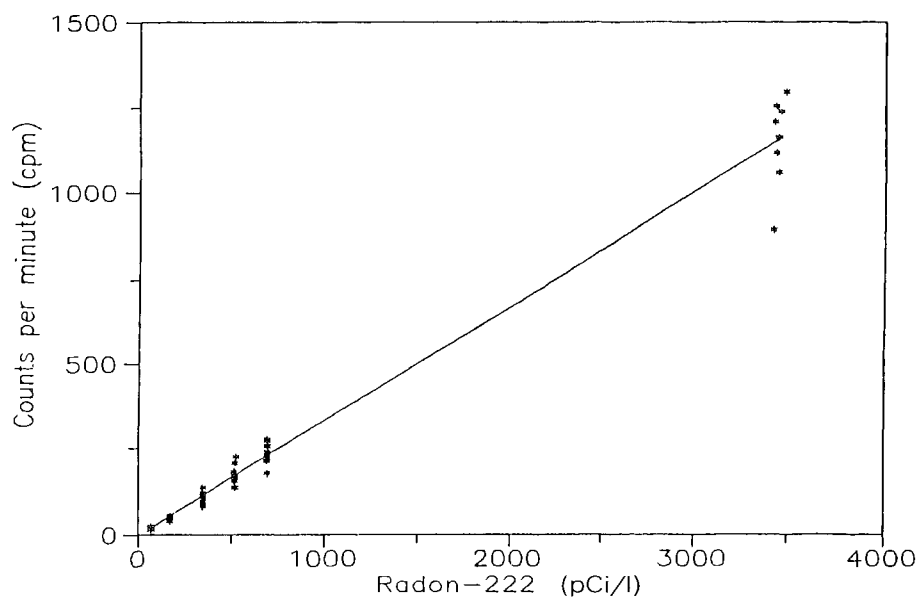

Figure 2. Calibration line (best fit, y = 0.33x - 3.92) resulting from degassing of standard ^{226}Ra solutions and normalized to cell 5.

Field Sampling

Sample wells were first selected among Tucson Water wells along several basinwide northeastern traverses and one northwestern traverse. (Tucson Water is a department of the city of Tucson.) Sampling private wells was not a priority because of the wide distribution of Tucson Water wells and the limited information on private wells. After the traverses were completed, the remaining unsampled areas were sampled so that the overall sample density was about one well per square mile. A total of 99 wells were sampled in the Tucson area: 86 Tucson Water wells and 13 wells owned privately or by other water companies or institutions. Most of the wells were sampled from early April through August 1988, between 9 a.m. and 1 p.m. Most of the Tucson Water wells had been pumping for several hours, if not more than 24 hours, before sampling. At each well, two samples were taken at the sample port between the well head and the pressure tank and assigned sample numbers.

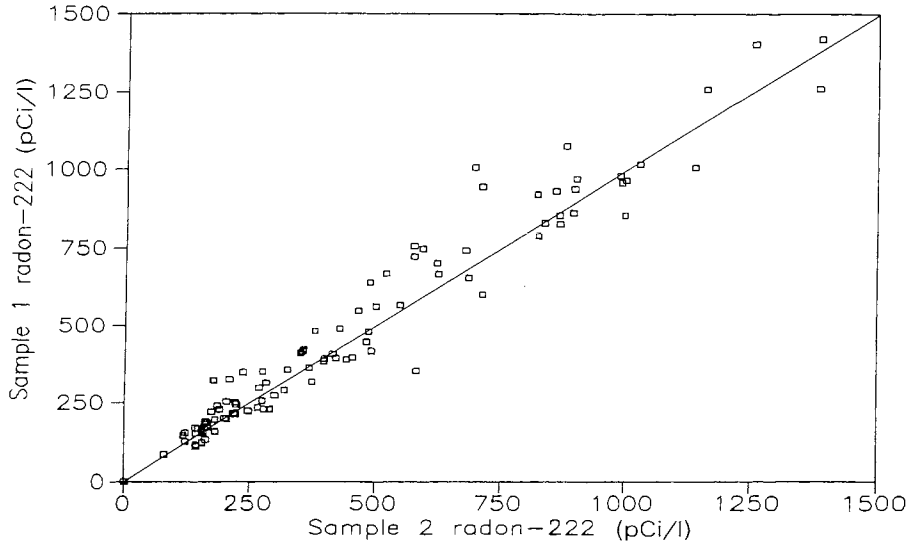

Figure 3. Instrument variation of replicate samples. The line represents the 1:1 relationship.

The sampling procedure included assembling the degassing equipment. All valves of the degasser were kept closed until use. The sampling adapter was connected to the sample port, which was then opened. Water was allowed to flow for 5 to 10 minutes into a Nalgene bottle, where the temperature was measured and recorded. A scintillator cell, for which background counts per minute had been measured, was connected to the degassing instrument.

Valve 1, the valve controlling the nitrogen flow, was kept closed, and the main nitrogen-tank valve and diaphragm were opened, allowing nitrogen to flow through the gas filter to valve 1. Valve 3 between the cell and drierite was opened. The hand pump was connected to the other Swagelok valve on the cell, and a vacuum of approximately 685 torr was produced in the cell and drierite tube. (Valve 2 was closed.) The hand pump was disconnected, and a water sample was taken. The flow at the sample port was decreased to minimize agitation in the 125-ml Erlenmeyer vacuum flask, but kept high enough to prevent drawing air into the adapter at the sleeve-spigot interface. While the water was flowing, the flask was tightly connected to the adapter.

The water was turned off when the level reached the 100-ml mark. The nipple air port on the flask was covered tightly with a finger, and the stopper of the adapter was quickly replaced with a rubber stopper. The sampling time was noted. The flask was then quickly connected to the degassing unit, the Tygon tubing firmly pushed on the nipple, and the stopper with the diffuser pushed on the top opening. The vacuum gauge was checked to make sure no leaks had occurred in the degassing instrument.

Valve 2 was slowly opened, allowing the air and nitrogen that were in front of the diffuser to be pulled through the diffuser, bubbled through the water sample, and pushed into the evacuated portion of the system. This caused an initial degassing of about 15 seconds and a drop in the vacuum from about 685 to 585 torr. As this bubbling began to subside, valve 1, the nitrogen-control valve, was slowly opened and periodically adjusted, providing a continuous degassing over a total of about 2 minutes. The sample flask was swirled as the sample was degassed to increase agitation and mixture of the carrier gas with the water sample. When the pressure gauge read atmospheric, valves 1 and 3 were closed, and the cell was disconnected. The system was then backflushed with nitrogen for 1 to 2 minutes, and the water temperature was checked again.

The duplicate sample was treated in the same way. The sample flask and adapter were rinsed with deionized water after being used at each well.

Three to 4 hours after a sample was collected in a cell, the cell was placed in the RDA 200 detector and counted for 30 minutes. The background counts per minute were subtracted from the counts per

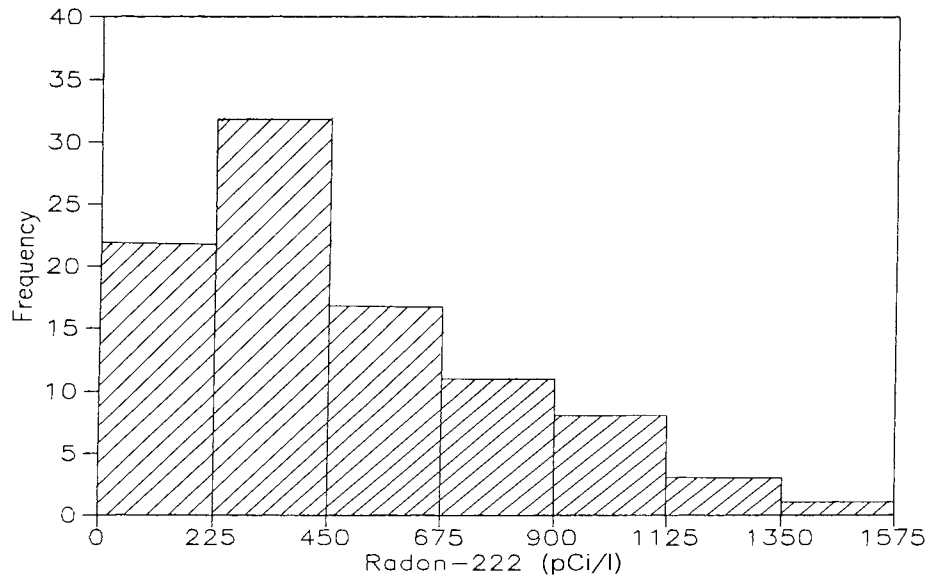

Figure 4. Frequency distribution of ^{222}Rn concentration in Tucson-area wells.

minute calculated from the 30-minute counting period to give the net count for that cell sample. This value was converted to pCi/l by use of the calibration line, as previously discussed.

Eighty homes in the Tucson area were sampled for ^{222}Rn in the drinking water from mid-November 1987 to June 1988. Seventy of the 80 samples were collected by the end of March 1988. Test homes were initially selected among those owned by faculty and staff members of the Hydrology and Geosciences Departments at the University of Arizona. Other homes were tested as a result of publicity, word of mouth, and cooperation with the Pima County Health Department and the Respiratory Sciences Division at the university. Water samples from homes were treated in the same manner as the well samples, with the adapter connected to the kitchen tap or outdoor spigot. No duplicate samples were taken at the homes. The domestic water samples were assigned sample numbers from 10 to 90.

Instrument Variation

The precision of the degassing scintillation-cell method was checked by plotting the results of the first well sample versus that of the duplicate sample for all wells tested (Fig. 3). The average precision or percent difference was calculated at about ±13%. Sample measurements repeated at four wells at a later date showed a reproducibility of ±3 to ±25% and an average of ±10%. A standard solution was prepared by degassing deionized water and storing it in glass containers. Repeated analysis of 100-ml samples of this solution showed a mean standard deviation of 14.6%.

RESULTS

Well Water

The range of ^{222}Rn concentrations for wells sampled in the Tucson area is 83 to 1,404 pCi/l (Fig. 1). The average and median values are 470 and 384 pCi/l, respectively (Fig. 4).

The wells in the central part of Tucson (those of the B, C, and D zones, excluding anomalous well samples 93 and 94) have an average ^{222}Rn concentration of 254 pCi/l and range from 125 to 483 pCi/l. The highest ^{222}Rn concentrations are in wells near the Santa Cruz River, which closely parallels the Santa Cruz Fault (Fig. 1a,b). This zone, defined within the limits of the data, is approximately 3.7 to 4.6 km (2 to 2.5 mi) wide at the northern end, up to 9.3 km (5 mi) wide at the southern end, and up to 59 km (32 mi) long, and includes 30 wells with ^{222}Rn levels between 500 and 1,404 pCi/l. (Figure 5 shows the ground-water concentrations of ^{222}Rn in wells along an east-trending geohydrologic cross section [Fig. 1b,c].) ^{222}Rn in the 400-pCi/l range was measured in some wells associated with other faults in the basin. Of the 13 samples with ^{222}Rn concentrations between the median value (384 pCi/l) and 500 pCi/l, 10 are from wells within 1.8 km (1 mi) of a fault, and 5 lie within 0.92 km (0.5 mi). Samples 28, 24, 23, 6, and 5 all lie within 0.5 km (0.25 mi) of the northeast-trending faults near the middle of the study area, but their ^{222}Rn concentrations are lower than about 250 pCi/l. Samples 2 and 50 were taken within about 0.92 km (0.5 mi) of the postulated I-10 fault, but showed no evidence of thermal or ^{222}Rn anomalies. The high-^{222}Rn-containing waters in the Santa Cruz well field, about 22 km (12 mi) south of Tucson and bounded on the west by the Santa Cruz Fault, are included as the southern end of the Santa Cruz ^{222}Rn trend.

The relationships between ^{222}Rn concentrations and temperature, pumping (bowl) depth, well discharge, average lower- and upper-perforation depths, and pumping water level were investigated (Figs. 6a through 6f, respectively).

^{222}Rn concentrations are not obviously dependent on temperature ($r = 0.14$); however, a positive correlation is apparent for wells with greater than 500 pCi/l of ^{222}Rn (Fig. 6a). The average temperature of all the wells tested was 25.7°C (78.3°F). The

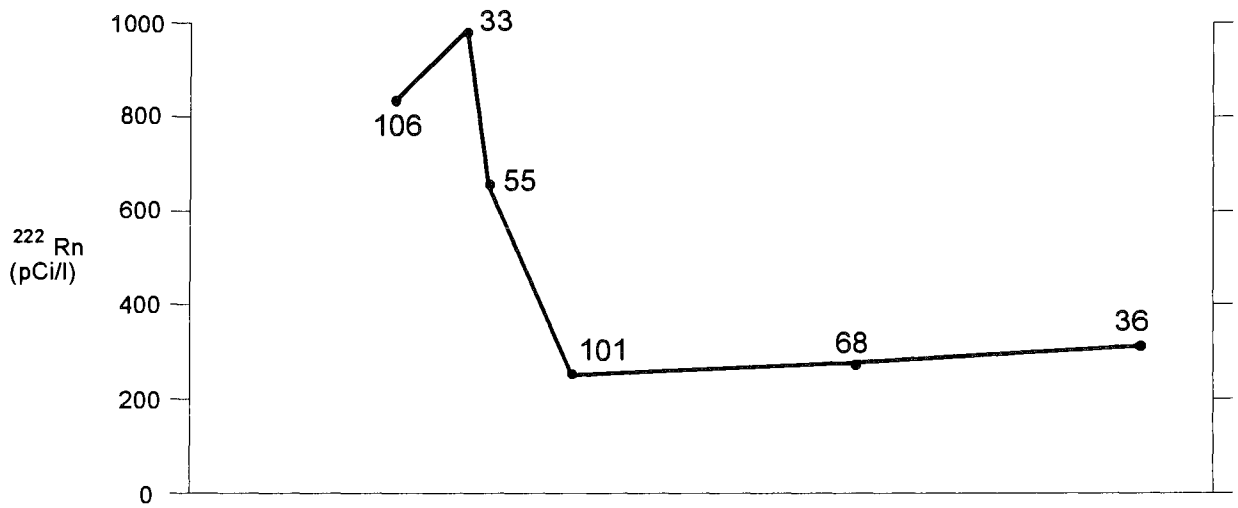

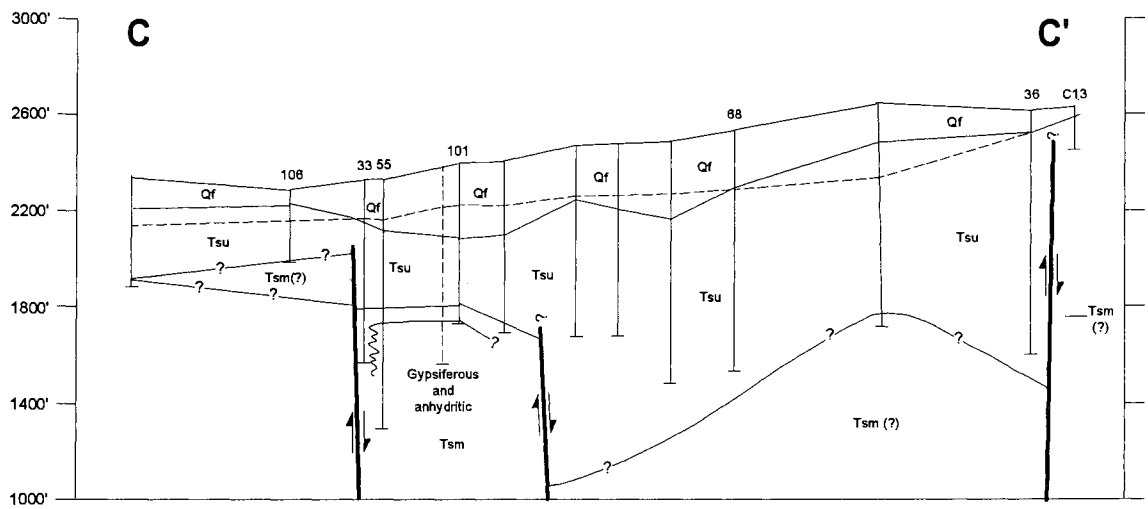

EXPLANATION

Qf	FORT LOWELL FORMATION
Tsu	UPPER TINAJA BEDS
Tsm	MIDDLE TINAJA BEDS
Gypsiferous and anhydritic	GYPSIFEROUS AND ANHYDRITIC CLAYEY SILT AND MUDSTONE UNIT - Approximately located. Queried where uncertain.
?	CONTACT - Approximately located. Queried where uncertain.
?	FAULT - Approximately located. Queried where uncertain. Arrows show relative movement.
	WATER LEVEL - Measured or approximate in 1981.
101	WELL - Number is ^{222}Rn concentration in water sample analyzed in this study. Dashed where projected to sections.

highest temperature (34.1°C, or 93.4°F) was associated with the highest ^{222}Rn concentration (1,404 pCi/l), yet wells with a temperature of about 30°C (86°F) showed a range of ^{222}Rn concentrations from 150 to 1,200 pCi/l. If the average temperatures for ^{222}Rn concentrations are categorized in 100-pCi/l ranges, wells with ^{222}Rn concentrations greater than 1,000 pCi/l have an average temperature that is 4°C (7°F) higher than that of wells with any other range of concentrations. The 900, 800, and 700 pCi/l categories all fall at or below the overall mean temperature of 25.7°C (78.3°F). No anomalously high ^{222}Rn concentrations were associated with low-temperature waters.

This study showed a slight negative correlation (r = -0.35) between ^{222}Rn concentration and pumping bowl depth (Fig. 6b) and virtually no correlation between ^{222}Rn concentration and well discharge (Fig. 6c).

The perforation depth (Figs. 6d and 6e) is the average depth of the interval; for wells with multiple well screens, the upper and lower intervals were examined separately. The scatter-plot of ^{222}Rn concentration versus the average depth of the lower-perforation interval shows a poor correlation (Fig. 6d). ^{222}Rn concentrations greater than 500 pCi/l may originate at depths of less than 30 m (100 ft) to more than 213 m (700 ft). Fourteen of 19 samples above 700 pCi/l are associated with perforation depths between 107 and 213 m (350 and 700 ft). The correlation of ^{222}Rn concentration with the average depth of the upper-perforation interval was slightly negative (r = -0.25; Fig. 6e). This plot shows 26 samples that have ^{222}Rn concentrations greater than 500 pCi/l and well-perforation average depths between 30 and 122 m (100 and 400 ft).

The pumping water level is a parameter that suggests the minimum depth of the aquifer that could contribute significant amounts of ^{222}Rn to the well. Even though some water flows vertically to the well, the amount of ^{222}Rn contributed from drainage above the cone of depression, as well as shallower depths within the cone of depression, should be small because of the longer travel time. ^{222}Rn concentration and pumping water level show a weak negative correlation (r = -0.35; Fig. 6f). Pumping water depths of less than about 79 m (260 ft) contribute the highest ^{222}Rn levels (>700 pCi/l), whereas depths greater than this contribute ^{222}Rn levels below 700 pCi/l. Gamma-ray logs of a few wells showed inconclusive tendencies.

Figure 5 (left). Geohydrologic section C-C' (Fig. 1b,c), showing wells of Anderson (1987a, Plate 1) and corresponding ^{222}Rn concentrations in ground water of wells sampled in this study.

Domestic Water

The range of ^{222}Rn concentrations in the domestic water samples was about 67 to 1,263 pCi/l (Fig. 1). The average and median values were 314 and 206 pCi/l, respectively. Approximately 55% of the domestic water tested had greater than 200 pCi/l of ^{222}Rn (Fig. 7).

The most obvious area with high ^{222}Rn concentrations in domestic water was in the densely sampled area of southwestern Tucson. The average ^{222}Rn concentration in the water of these 12 homes was 669 pCi/l; two of the homes had values near 1,250 pCi/l. Other areas that had ^{222}Rn concentrations between 300 and 599 pCi/l were in eastern and west-central Tucson, as well as several scattered points in northern Tucson within 2 to 4 perpendicular miles of the Santa Cruz ^{222}Rn trend for well samples. Two other homes with similar but anomalous ^{222}Rn levels were in the northern foothills of Tucson. One home in the southeastern foothills that has its own well contained 733 pCi/l of ^{222}Rn.

INTERPRETATION

^{222}Rn in Domestic Water

Average and median ^{222}Rn concentrations in well water are significantly different from concentrations in domestic water. The potential for ^{222}Rn degradation by decay or degassing varies considerably depending on the design of and demands on the distribution system. The demands on the distribution system, in turn, vary seasonally and determine which wells or well fields operate at any particular time. During the winter, for example, when most of the homes were sampled, Tucson Water was not operating the well system at full capacity. R. Lowrie (Tucson Water, personal commun., 1988) stated that even though there are typical flow patterns in most areas of Tucson, it is impossible to determine from which well or well region a particular home is receiving its water at a given time. This is because the distribution system is automated; water essentially flows to points of low pressure while traveling to or from booster stations or reservoirs. Isolated areas, such as those in extreme northwestern and eastern Tucson, receive water from nearby wells. Wells within a lettered zone generally supply homes within that zone (Fig. 1b,c).

The source of the domestic high ^{222}Rn concentrations in southwestern Tucson (samples in the area, plus samples 27, 44, and 84) is water from wells in Avra Valley, which lies outside the study area, 16 km (10 mi) to the west of these homes. Several wells in Avra Valley tested high in ^{222}Rn,

Figure 6a. ^{222}Rn concentration vs. temperature in Tucson-area wells.

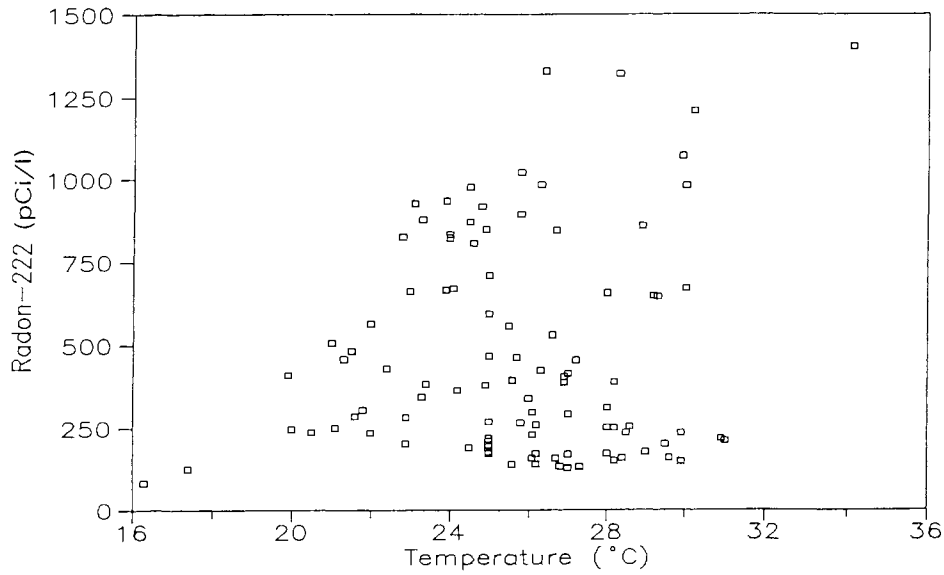

Figure 6b. ^{222}Rn concentration vs. pumping bowl depth in Tucson-area wells.

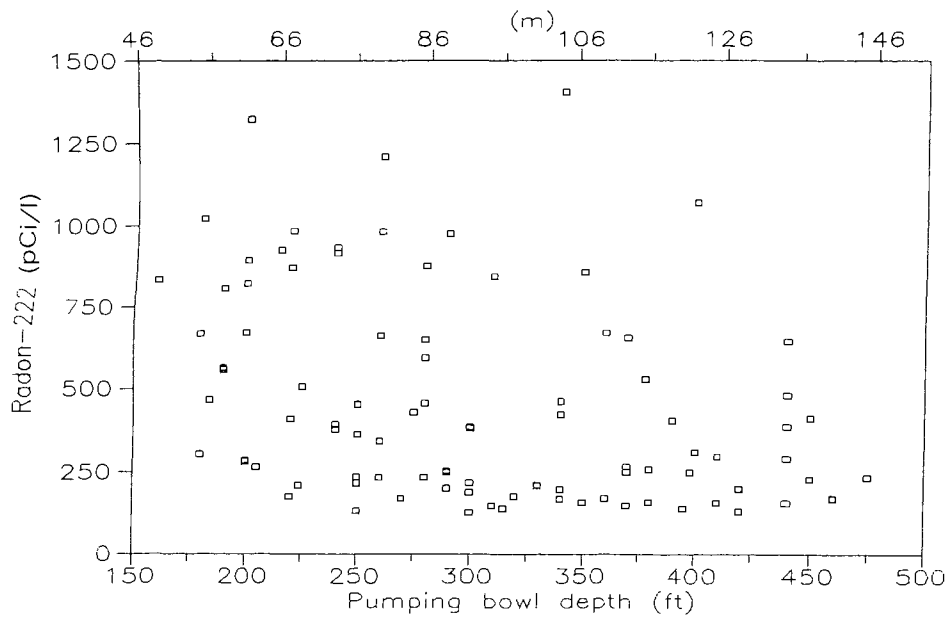

Figure 6c. ^{222}Rn concentration vs. well discharge in Tucson-area wells.

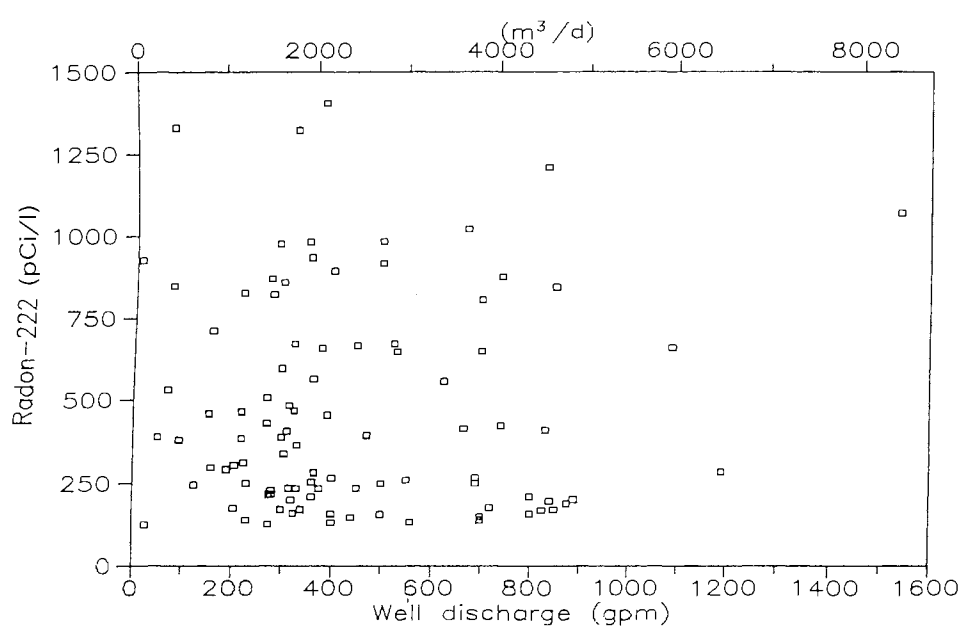

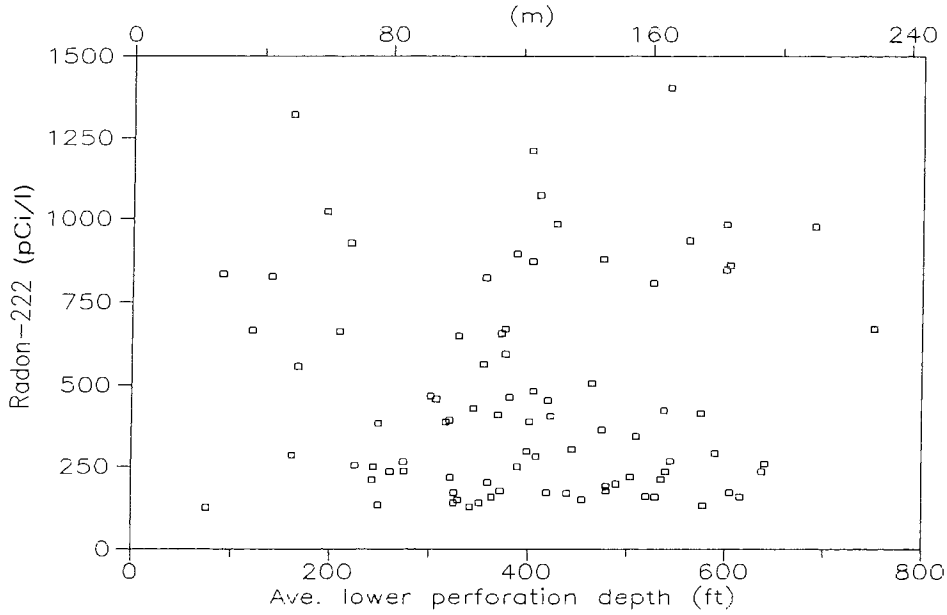

Figure 6d. ^{222}**Rn concentration vs. average lower-perforation depth in Tucson-area wells.**

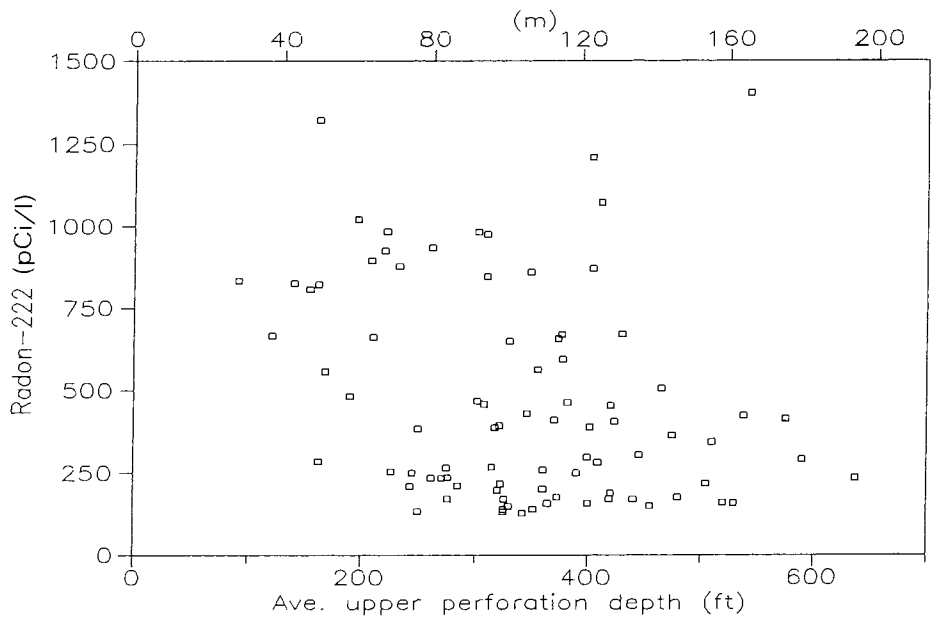

Figure 6e. ^{222}**Rn concentration vs. average upper-perforation depth in Tucson-area wells.**

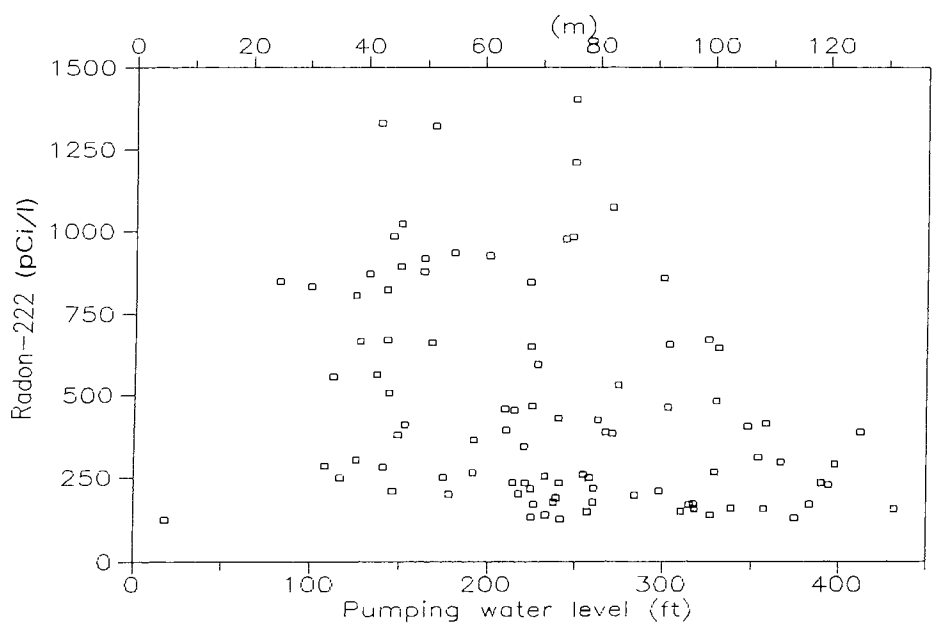

Figure 6f. ^{222}**Rn concentration vs. pumping water level in Tucson-area wells.**

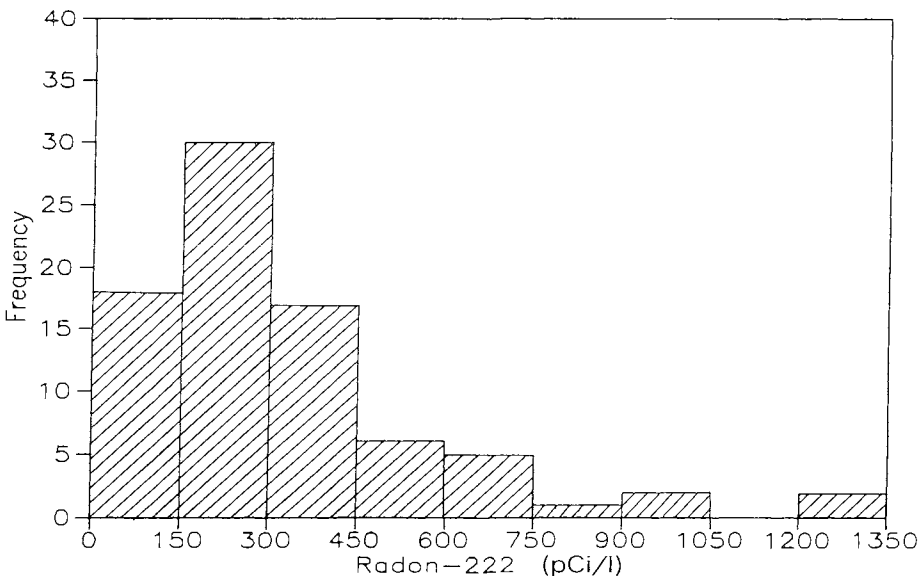

Figure 7. Frequency distribution of ^{222}Rn concentrations in Tucson-area domestic waters.

which is consistent with this relationship, but researching ^{222}Rn in the ground water of Avra Valley is beyond the scope of this study.

In this study, "degradation of ^{222}Rn" refers to the decay and degassing of the element. "Percent degradation" is defined as the percentage of ^{222}Rn that has decayed or degassed from the concentration in a well to that in a distribution point, such as a home. Because the homes and wells were not sampled within a short time interval, the degradation can only be estimated.

The percentage of degradation for homes in southwestern Tucson is calculated by taking a nonweighted average of ^{222}Rn concentrations in Avra Valley wells and comparing it to the average ^{222}Rn concentration in homes in the southwestern area. The result is about 49%. The Avra Valley water is piped to a booster station near southside (SS) well 18 (sample 85), where it is distributed into the C zone (area of C-lettered wells); surplus water goes to the B zone. Water from the Santa Cruz well field (well samples 86 to 92, 95, and 96) also follows this path, feeding B, C, and D zones. During the winter, the Santa Cruz well-field water probably supplies central and eastern areas of Tucson (R. Lowrie, Tucson Water, personal commun., 1988). If the Santa Cruz well field is the only supplier to the C zone, the degradation of ^{222}Rn is about 42%.

All southside wells, except for well SS-24 (sample 46), supply a reservoir near domestic sample 57 that, in turn, supplies the A zone and the western part of Tucson. The SS-24 well supplies the B zone. The ^{222}Rn concentrations in domestic samples 13, 21, and 35 in the B zone could have resulted from a single well or from any mixture of well water from SS-24, B-83, and B-85 (samples 46, 93, and 94, respectively), Avra Valley, and the Santa Cruz well field. Western Tucson may also receive water from a main on the northern end of the A zone, including wells Z-1 (sample 11), Z-2, and Z-3 (sample 12). The domestic waters with greater than 300 pCi/l of ^{222}Rn in western Tucson are probably from the SS wells or A- or Z-zone wells.

Northwestern Tucson is somewhat hydraulically isolated. The domestic water samples 40 and 49 probably originated from waters in nearby wells Z-13 and Z-17 (samples 9 and 7, respectively). The degradation of ^{222}Rn between these wells and homes, on the average, is about 28%, but for well Z-17 and home 40 the degradation is only 8%. Anomalous domestic sample 33 (579 pCi/l) is directly related to the high well samples 105 (850 pCi/l) and 107 (1,331 pCi/l) because these three samples were taken within the distribution system of a small, local water company. The degradation between the average ^{222}Rn value of the wells and the home value is 47%. Domestic water samples 31 and 47 probably obtained their ^{222}Rn from nearby anomalous wells, but this area is within another water company's district, and no well samples were taken there. Well C-97 (sample 8) contained water with a ^{222}Rn concentration of 483 pCi/l and supplies water to domestic sample 28, which contained 495 pCi/l (R. Lowrie, Tucson Water, personal commun., 1988). The difference between the home and well ^{222}Rn values is probably due to instrument variation and different sampling times. Nevertheless, if pumping and distribution conditions were representative when these samples were taken, virtually no degradation occurred. Water from C-97 may flow to the C-zone reservoir, which is about 2.4 km (1.5 mi) west-northwest of domestic sample 88. The origin of the water in sample 88 (444 pCi/l) is probably water in well C-97 or water from the Santa Cruz well that feeds the C-zone reservoir.

Domestic samples 39, 62, 66, and 67 in eastern Tucson had ^{222}Rn values that ranged from 300 to 350 pCi/l. Wells within 2 km (1 mi) of these homes (except for home 39) contained ^{222}Rn values greater than this range and were most likely the cause of

the domestic values. Domestic sample 39 may have received water from the Santa Cruz well field.

^{222}Rn in Well Water

The correlations between ^{222}Rn well-water concentrations and water temperature, well-discharge rate, pumping depth, perforation depths, and pumping water level were not straightforward but showed some tendencies.

The correlation between ^{222}Rn concentration and water temperature shows two trends: wells with the higher concentrations (>500 pCi/l) show a slight positive correlation, whereas those with the lower concentrations show no correlation. This difference does not appear to be caused by the geothermal gradient in deep wells. Wells along the Santa Cruz Fault, on average, are not deeper than wells elsewhere in the Tucson area. This fault, therefore, may influence ^{222}Rn concentrations. The area around the Santa Cruz Fault may be more thermally conductive than other parts of the Tucson area.

Theoretically, a relationship may exist between discharge rate of a well and the ^{222}Rn concentration in water flowing from it. In fractured crystalline rock, the correlation between discharge rate and ^{222}Rn concentration is commonly negative. This occurs when fractures hydraulically connected to a well draw in distal waters deficient in ^{222}Rn, and the ^{222}Rn concentration in the water of the fracture increases because of emanation from the fracture surfaces. The ^{222}Rn concentration varies according to residence time in the fracture (Chen and Wilson, 1987). In a homogeneous sedimentary aquifer with uniform ^{222}Rn-emanating power, the ^{222}Rn concentration would not be expected to change as it enters the well. As the discharge increases, the relative proportion of transmitted water from specific strata probably changes, but this change may affect the ^{222}Rn concentration either negatively or positively. Fine-grained, higher ^{222}Rn-emanating sediments may decrease their relative water contribution to the well because of lower transmissivities. Tanner (1964a) did not find a correlation between discharge rate and ^{222}Rn concentration in the well water from an unconsolidated artesian aquifer. The relationship between ^{222}Rn concentration and discharge rate is probably site specific.

No linear correlation was observed between ^{222}Rn concentration and pumping depth. This is probably because many wells have large or multiple screen intervals, so pumping depth was not indicative of the depth of water entering the well. To refine this correlation, perforation intervals were also examined. The slight negative tendency of the plot of upper-perforation depth versus ^{222}Rn concentration (Fig. 6e) indicates that the higher concentrations are from a shallow source, from 30 to 129 m (100 to 425 ft) deep. Twenty-five of 35 wells with ^{222}Rn concentrations greater than 500 pCi/l are in this category. The weak correlation between pumping water level and ^{222}Rn concentration (Fig. 6f) shows a similar trend: 27 of 35 wells with ^{222}Rn concentrations higher than 500 pCi/l fall between pumping water levels of 30 and 91 m (100 and 300 ft). The negative tendency of the scatter plot indicates that as the pumping water level deepens, ^{222}Rn concentrations decrease, which supports the hypothesis that the ^{222}Rn source is shallow.

^{222}Rn and Hydrogeology

Wells in the main part of Tucson, i.e., those in the B, C, and D zones (excluding anomalous well samples 93 and 94), have an average ^{222}Rn concentration of 254 pCi/l. The Fort Lowell Formation and upper Tinaja beds underlying this area are primarily composed of granitic and gneissic sediments derived from the Santa Catalina, Tanque Verde, and Rincon Mountains. This region seems to reflect background concentrations of ^{222}Rn in ground water, but further research could also prove it to be a zone of anomalously low ^{222}Rn concentrations. Certainly, it is a region with its own hydrogeochemical ^{222}Rn signature, which probably indicates that the uranium and ^{226}Ra concentrations and the physical nature of the granitic and gneissic rocks from which the sediments were derived are not conducive to emanating large amounts of ^{222}Rn.

Three hypotheses might explain the presence of high ^{222}Rn concentrations in the ground water underlying the Santa Cruz River area. High ^{222}Rn concentrations may be related to the following: (1) water movement along the Santa Cruz Fault; (2) lithology; and (3) aquifer compaction.

The Santa Cruz ^{222}Rn trend closely follows the Santa Cruz Fault trace (Fig. 1). The association of anomalous ^{222}Rn concentrations in soil gas and ground water with faults has long been known (Williams and Lorenz, 1957; Lorenz and others, 1961; Smith and others, 1980), but the mechanisms causing this relationship are speculative. An initial hypothesis is that the Santa Cruz Fault and associated fractures act as high-capacity conduits, providing a pathway for deep-seated, high-^{222}Rn-containing water to move upward to a pumping well. The enhanced transport may be due to increased thermal convection or to induced circulation caused by pumping wells. Some evidence suggests that these mechanisms are not the cause of the Santa Cruz ^{222}Rn trend.

As mentioned previously, wells with ^{222}Rn concentrations greater than 1,000 pCi/l had an average temperature that is 4°C (7°F) higher than

any other well producing water in the 100-pCi/l range. Of the six wells that had greater than or equal to 1,000 pCi/l of ^{222}Rn, three lie within 1 km (0.5 mi), two lie within 2 km (1 mi), and one lies 3.7 km (2 mi) away from the Santa Cruz Fault (Fig. 1). One of these wells had temperature values that are about equal to or below the mean temperature for all wells tested; the remaining five wells had temperatures above the mean. If the Santa Cruz Fault were the sole source of the anomalous ^{222}Rn concentrations in the ground water, how may the inconsistencies in well proximity and temperature be explained?

Perhaps yet-undetected splays of the fault system exist. The inconsistent temperatures could be caused by mixing with colder waters, without dilution of ^{222}Rn concentrations. Starik and Melikova (1957) found that ^{222}Rn emanation from uranium ore, at temperatures around 20°C (68°F), increased approximately 1%/°C (about 1%/2°F; Tanner, 1964a). The possibility that local warm waters enhance ^{222}Rn emanation from sediments containing background concentrations of ^{226}Ra may be discounted if this relationship applies along the Santa Cruz ^{222}Rn trend. Tanner (1964a) showed that, for small thermal anomalies in the ground water near the Great Salt Lake, the effect of increased diffusion rate should be negligible.

The depth to bedrock in the Tucson area may be as great as 6,100 m (approximately 20,000 ft; Anderson, 1987a). Transporting ^{222}Rn-bearing water from this depth seems unreasonable. Even if a high-^{222}Rn-containing source of ground water existed at a depth of 500 m (approximately 1,600 ft), the concentrated ^{222}Rn-bearing water would probably not reach the well in significant concentrations. If an assumed ^{222}Rn concentration at this depth were an order of magnitude greater than the highly anomalous wells (10,000 pCi/l), water would have to be transported from the deep source area to the bottom of the wells within 13 days. This is a transport velocity of 38 m (124 ft)/day. Groundwater velocities a magnitude lower than this are considered uncommonly high (Tanner, 1964a). It is therefore unlikely that the ^{222}Rn anomalies originated from a deep-seated, concentrated source.

This study found no convincing evidence that supports the association of higher ^{222}Rn concentrations with other faults in the Tucson area. Of the 13 well samples with ^{222}Rn concentrations between the median value (384 pCi/l) and 500 pCi/l, 10 samples were from wells that lie within 2 km (1 mi) of a fault, and 5 were from wells that lie within 1 km (0.5 mi) of a fault. Well samples 28, 24, 23, 6, and 5, however, all lie within 0.5 km (0.25 mi) of the northeast-trending faults near the middle of the study area, and their ^{222}Rn concentrations were less than about 250 pCi/l. Well samples 1 and 44, in the southeastern and eastern Tucson area, could be associated with the eastern block fault that is associated with basin formation or with a detachment fault in the region, but their temperatures were low. Well samples 2 and 50 were taken within about 1 km (0.5 mi) of the postulated I-10 fault; no thermal or ^{222}Rn anomalies were evident in the samples. It is unlikely that all faults are associated with ^{222}Rn anomalies because their geologic history and physical characteristics vary considerably.

The physical disturbance of geologic materials near a fault, as evident in crushed rocks and microfractures, may enhance the ^{222}Rn-emanation power of the material by exposing a greater surface area. Fault gouge is commonly poorly sorted material with a lower porosity. The decreased porosity would enable higher concentrations of ^{222}Rn to accumulate, but the gouge would have to be transmissive and significantly abundant to act as a source of ^{222}Rn.

Because the wells within the Santa Cruz trend lie within a 3.5- to 5.5-km- (2- to 3-mi-) wide tract, it is unlikely that the material within a single fault plane is responsible for the ^{222}Rn anomalies. Geologically long-term, ground-water flow along the fault could preferentially deposit, by ion exchange, greater amounts of ^{226}Ra within the gouge zone, but could not account for the breadth of the Santa Cruz trend. ^{226}Ra deposition over a broad area and the mixing of chemically different, "incoming" water with basin water, however, might explain the elevated ^{222}Rn concentrations in the Santa Cruz River area. The source of the ^{226}Ra-bearing waters may be deep waters emanating from the fault or recharge waters from the Tucson Mountains to the west.

Wollenberg (1974) found that deep hot water transported ^{226}Ra to the surface, where it was preferentially associated with $CaCO_3$ hot-spring deposits. The ground water of the Tucson Mountains is commonly high in total dissolved solids (TDS), conditions that would favor ^{226}Ra mobility. When recharge waters are mixed with "normal" basin waters, hy-drogeochemical conditions might cause ^{226}Ra to precipitate with $CaCO_3$ or adsorb to iron and manganese hydroxides or clays, which are prevalent in the area. Higher TDS in the ground water underlying the Santa Cruz River area may be an indication of this mixing zone. Tanner (1964a) concluded that ^{226}Ra coprecipitation with iron hydroxide could occur when oxygen-poor ground water containing ^{226}Ra and iron was mixed with oxygen-rich ground water. An in-depth hydrogeochemical study of the aquifer of the Tucson area is needed to investigate whether this mechanism contributed to elevated ^{222}Rn concentrations in the Santa Cruz River area.

Numerous lithologic conditions could also account for the Santa Cruz ^{222}Rn trend. For ex-

ample, the gypsiferous, anhydritic evaporite beds in the middle Tinaja beds may contain a greater concentration of ^{226}Ra, which could have coprecipitated with the $CaSO_4$, and this could be the source of the elevated ^{222}Rn in the Santa Cruz River trend. The arguments against this hypothesis are as follows: (1) the middle Tinaja beds are not penetrated by many producing wells and generally are poorly transmissive (S. Rogers, Tucson Water, personal commun., 1988); (2) several wells tested in this study and included in Anderson's (1987a) report did not show an obvious correlation between ^{222}Rn concentration and proximity to the middle Tinaja beds; and (3) the hydrogeochemical conditions favorable for coprecipitation of ^{226}Ra and $CaSO_4$ (or $BaSO_4$) probably did not exist. Much higher concentrations of ^{226}Ra than those of current ground waters would be required for this reaction, and large concentrations of barium are not available for coprecipitation of ^{226}Ra and $BaSO_4$ (Humphreys, 1987).

Along the southern two-thirds of the Santa Cruz ^{222}Rn trend, the Fort Lowell Formation and upper Tinaja beds contain a higher percentage of fine-grained materials. Whether the correlation between fine-grained sediment and the Santa Cruz ^{222}Rn trend is meaningful is still unknown, but this lithologic relationship cannot be ruled out.

The composition of an aquifer obviously affects its ability to emanate ^{222}Rn. Anderson (1987a, Plate 3) mapped the sources of the late Tertiary and Quaternary sediments in the Tucson Basin. North of well Z-5 (sample 104), the Santa Cruz ^{222}Rn trend falls along the interface between sediments derived from the Santa Catalina, Tanque Verde, Rincon, and Tortolita Mountains and those derived from the Tucson and Black Mountains. Farther south, the interface lies just east of the ^{222}Rn anomalies but curves west just before reaching the Santa Cruz well-field area, which is composed of sediments derived from the Santa Rita and Sierrita Mountains. A single source of sediment, as mapped by Anderson, cannot account for the Santa Cruz ^{222}Rn trend. Well logs of the interior well field in central Tucson agree with Anderson's study, confirming the abundant gneissic material derived from the Santa Catalina, Tanque Verde, and Rincon Mountains. Because of physical or chemical reasons, this material does not emanate anomalous amounts of ^{222}Rn into the ground water. Several wells near the Santa Cruz Fault contain abundant, coarse-grained, andesitic or rhyolitic material derived from the Tucson Mountains. This type of rock is normally deficient in uranium and would not be expected to emanate anomalous amounts of ^{222}Rn. P.E. Damon (University of Arizona, personal commun., 1988), however, noted that the Turkey Track Andesite (actually a calcic latite) exposure in the Tucson Mountains contained an above-average amount of uranium (3.3 ppm) for a rock of this type. Unusual concentrations of uranium and ^{226}Ra within sediments derived from the Tucson Mountains may be related to the Santa Cruz ^{222}Rn trend, but further studies are needed to verify this hypothesis.

Another mechanism to consider is the existence of a "hidden" tectostratigraphic unit within the Fort Lowell Formation or upper Tinaja beds, characterized by a richer concentration in ^{226}Ra or an enhanced ability to emanate ^{222}Rn. Such a unit or time-rock zone could have been deposited as sediments in the alluvial plain of the ancestral Santa Cruz drainage during its development in late Pliocene to Pleistocene time. The ancient river probably meandered naturally but was bounded on the west by the Santa Cruz Fault scarp. This could account for the broad distribution of the Santa Cruz ^{222}Rn trend. The origin of the ^{222}Rn-emanating sediments was probably the southern part of the Tucson Basin, possibly as close as the Santa Rita Mountains, because the ^{222}Rn anomalies extend the full 8-km (5-mi) width of the Santa Cruz well field. Additional measurements in the southern and southwestern part of the basin, however, could reveal similar concentrations of ^{222}Rn in the ground water, indicating a more ubiquitous source of ^{222}Rn.

A final hypothesis relates ^{222}Rn emanation to aquifer compaction. Stress can influence ^{222}Rn emanation and transport (Smith and others, 1976; Harvey, 1981). Local or regional aquifer compaction or compression associated with water-level declines may result in microfracturing of mineral grains, as well as a squeezing effect, which can transport pore water. Harvey (1981), who studied ^{222}Rn concentrations in soil gas and ground water in the Picacho Basin just north of the Tucson Basin, did not find a good correlation between ^{222}Rn concentrations in ground water and the magnitude of subsidence in the area. Also, the spatial relationship between ^{222}Rn concentrations and subsidence faults was inconsistent. Anderson (1987b) concluded that in the Tucson Basin, the potential for differential land subsidence and earth fissures is greatest in areas where saturated, fine-grained deposits of the Fort Lowell Formation and upper Tinaja beds overlie shallowly buried faults or convex irregularities. The region underlying the Santa Cruz Fault fits this criterion well, particularly in the area south of well A-32 (sample 56), where 40 to 80% of the upper Tinaja beds and Fort Lowell Formation consists of fine-grained material (Anderson, 1987a, Plate 2). The U.S. Geological Survey showed that aquifer compaction has occurred in this area, but only by 2.4 cm (0.08 ft) during the last 8 years (Babcock and others, 1988).

The region north of well A-32 (sample 56), on the other hand, contains only 20 to 40% clay and silt but includes many high-^{222}Rn ground-water anomalies. Strain from aquifer compaction and subsidence, under Anderson's definition, does not appear to account for the Santa Cruz ^{222}Rn trend.

SUMMARY

The relationship between ^{222}Rn in ground water and hydrogeology has been studied throughout the United States (Tanner, 1964a; Brutsaert and others, 1982; Semprini, 1987). This study is the first of its kind in the north-central Tucson Basin, where the city of Tucson is largely dependent on ground water. The aquifer is composed of Cenozoic sediments separated into three main units: the Oligocene Pantano Formation, the Miocene Tinaja beds, and the Quaternary Fort Lowell Formation. The unconsolidated sediments of the Fort Lowell Formation and upper Tinaja beds are the major water-producing formations.

The purpose of this study was to determine the distribution of ^{222}Rn concentrations in the ground water and domestic water of the Tucson area, examine the spatial relationships of ^{222}Rn concentrations in these two water types, and relate the well-water ^{222}Rn concentrations to the hydrogeology of the north-central Tucson Basin. The study area encompassed about 1,114 km^2 (430 mi^2), which included the city of Tucson and areas within 30 km (15 mi) of the city limits.

Water samples from 99 wells and 80 homes were measured for ^{222}Rn through the use of a portable water-degassing instrument and an alpha-scintillation counter. Analyses showed a wide distribution of ^{222}Rn in the ground water, ranging from 83 to 1,404 pCi/l, which is within the range found in other sedimentary aquifers in the United States. Domestic values ranged from 67 to 1,263 pCi/l.

The ^{222}Rn values in domestic water are obviously a direct result of well values; however, the mean and median of the home data were less than those of the well data by 156 and 178 pCi/l, respectively. Apparent spatial trends between well and domestic ^{222}Rn values are not always legitimate. The water-distribution system allows for the delivery of well water with higher ^{222}Rn concentrations to homes 37 km (20 mi) away, whereas some areas receive water from wells only 1 km (0.5 mi) away. In other cases, water produced from a nearby well may travel 10 km (5 mi) through the distribution system before reaching the resident. Understandably, the degradation of ^{222}Rn between wells and homes may vary considerably. Estimates of ^{222}Rn degradation range from 8 to 50% for water distributed directly from a well to a home. For a larger distribution area (e.g., the Santa Cruz well field, which distributes water to the C zone in Tucson), the degradation appears to be about 42%. The semiautomated, dynamic distribution system and the seasonal variation in well operation are responsible for variation in ^{222}Rn concentrations in the domestic water supply.

^{222}Rn concentrations in well water showed a positive correlation with temperature for samples with greater than 500 pCi/l but did not correlate with well discharge or pumping (bowl) depth. ^{222}Rn concentration showed a weak negative correlation with pumping water level and perforation-interval depth. The higher ^{222}Rn levels were associated with ground water between 30 and 122 m (100 and 400 ft) within the Fort Lowell Formation and upper Tinaja beds.

The well field of central Tucson seems to represent background concentrations of ^{222}Rn, ranging from 125 to 483 pCi/l and averaging 254 pCi/l. The ^{222}Rn concentrations in the ground water of this area reflect the ability of the aquifer material to emanate ^{222}Rn. Analyses showed an anomalous trend of ^{222}Rn concentrations (the Santa Cruz ^{222}Rn trend) between 500 and 1,404 pCi/l in well water along the trace of the Santa Cruz River. This trend, defined within the limits of the data, is about 3.5 to 5.5 km (2 to 3 mi) wide in places to the north, and up to about 10 km (5 mi) wide in the southernmost sampled area. In places, the central part of the trend is represented by one well.

The anomalous ^{222}Rn concentrations within the Santa Cruz ^{222}Rn trend may be due to several factors. One hypothesis proposes a fault-related source with deep, high-^{222}Rn waters that move upward along the Santa Cruz Fault. ^{222}Rn emanation in the fault zone is increased because of physically disturbed (crushed) rock. An anomalous amount of ^{226}Ra accumulates in the fault region, deposited by circulating ground water over geologic time. A second hypothesis proposes a lithologic source: (1) high-^{226}Ra, gypsiferous anhydritic deposits within the middle Tinaja beds; (2) sedimentary materials eroded from nearby mountain ranges; (3) the fine-grained facies of the Fort Lowell Formation or upper Tinaja beds; or (4) a "hidden," tectostratigraphic, ^{222}Rn-emanating unit deposited within the Fort Lowell Formation or upper Tinaja beds within the alluvial plain of the fault-controlled, ancestral Santa Cruz River during late Pliocene to Pleistocene time. A third hypothesis proposes that higher ^{222}Rn emanation is associated with aquifer compaction.

One or several of these hypotheses may be responsible for the above-average ^{222}Rn concentrations in the ground water underlying the Santa Cruz River area. Preliminary considerations, however, indicate the probability of certain sources over others.

Crude travel-time calculations support the idea that the ^{222}Rn-emanating source is close to the wells and that ^{222}Rn is not derived from water traveling from great distances or depths. The configuration of the Santa Cruz ^{222}Rn trend indicates that the source is regional. ^{222}Rn's parent, ^{226}Ra, may be associated with any of the following: the fine-grained sediments or sediment compositions characteristic of the area; a unique, uranium- and radium-bearing sedimentary unit deposited specifically in the anomalous region; incoming ground water emanating from the Santa Cruz Fault; or recharge off the Tucson Mountains to the west. The hypothesis that aquifer compaction affects ^{222}Rn emanation is not well supported.

RECOMMENDATIONS

This study was a reconnaissance of ^{222}Rn concentrations in the ground water and domestic water of the Tucson area. To understand more fully the relationship between ^{222}Rn concentrations in wells and those in homes, researchers must make additional measurements and perform more specific experiments. If the EPA sets a maximum contamination level for ^{222}Rn in drinking water, Tucson Water should consider making these additional measurements. An initial step would be to obtain seasonal measurements from representative distribution points throughout the Tucson area. Such points may be storage reservoirs and, of most concern, water mains that carry water directly from a well to a home with little residence time in the distribution system. The average ^{222}Rn concentration could be determined for each zone of the distribution system and adjusted, if necessary, to comply with regulations. Methods to increase degradation or mitigate ^{222}Rn concentrations in public water supplies would include the following: storage to provide time for ^{222}Rn decay; dilution by blending high-^{222}Rn waters with low-^{222}Rn waters; and aeration of water by air stripping towers if necessary. Filtration with granular activated charcoal is effective but is commonly used in separate households, rather than entire well systems. New wells could be targeted for areas of low-^{222}Rn ground water. The first two methods — storage and dilution — would probably be the most practical and cost effective because the means to implement them may already exist.

I recommend the following to determine the specific hydrogeologic correlations with ^{222}Rn concentrations in the ground water of the Tucson area:

(1) Make additional field measurements of ^{222}Rn in well waters, specifically in areas that were not sampled during this study, such as those adjacent to the Santa Cruz ^{222}Rn trend. This would require diligent sampling of private wells and wells of smaller water companies.

(2) Closely examine well cuttings of the anomalous ^{222}Rn-bearing well waters with an instrument sensitive enough to count gamma radiation from small vials of well cuttings.

(3) Sample waters and perform well-packer tests in specific wells. This might clarify which geologic strata are emanating the higher ^{222}Rn concentrations.

(4) Perform laboratory experiments on representative samples of sediments in the Tucson area. Determine ^{222}Rn-emanation rates of different source rocks with varying grain sizes. Perform tests on the effect of compaction and temperature.

(5) Determine uranium and radium concentrations of aquifer materials and ground waters to ascertain the relative equilibrium between these elements.

(6) Carry out soil-gas tests along faults in the Tucson area.

(7) Investigate more thoroughly the hydrogeochemistry of the basin and its relationship to ^{222}Rn concentrations.

REFERENCES

Amirkhanoff, K.I., Brandt, S.B., and Bartnitsky, E.N., 1961, Radiogenic argon in minerals and its migration: Annals of the New York Academy of Science, v. 91, p. 235-275.

Anderson, S.R., 1987a, Cenozoic stratigraphy and geologic history of the Tucson Basin, Pima County, Arizona: U.S. Geological Survey Water-Resources Investigations Report 87-4190, 20 p., 3 sheets, scale 1:250,000.

——— 1987b, Potential for aquifer compaction, land subsidence, and earth fissures in the Tucson Basin, Pima County, Arizona: U.S. Geological Survey Open-File Report 86-482, 3 sheets, scale 1:250,000.

Andrews, J.N., and Wood, D.F., 1972, Mechanism of radon release in rock matrices and entry into groundwaters: Transactions of the Institution of Mining and Metallurgy, v. 81, p. B198-B209.

Asikainen, M., 1981, State of disequilibrium between ^{238}U, ^{234}U, ^{226}Ra, and ^{222}Rn in groundwater from bedrock: Geochimica et Cosmochimica Acta, v. 45, p. 201-206.

Babcock, J.A., Heidenreich, L.K., and Katz, L.T., 1988, Annual static water level basic data report, Tucson Basin and Avra Valley, Pima County, Arizona, 1987: Tucson Water, 137 p., 2 sheets, scale 1:126,720.

Brutsaert, W.F., Norton, S.A., Hess, C.T., and Williams, J.S., 1982, Geologic and hydrologic factors controlling radon-222 in ground water in Maine: Ground Water, v. 19, no. 4, p. 407-417.

Cadigan, R.A., and Felmlee, J.K., 1977, Radioactive springs geochemical data related to uranium exploration: Journal of Geochemical Exploration, v. 8, p. 381-395.

Cech, Irina, Lemma, Mengistu, Prichard, H.M., and Kreitler, C.W., 1987, Radium-226 and radon-222 in domestic water of Houston, Harris County, Texas, *in* Graves, Barbara, ed., Radon, radium, and other radioactivity in ground water: Hydrogeologic impact and application to indoor airborne contamination, NWWA Conference, Somerset, N.J., 1987, Proceedings: Chelsea, Mich., Lewis Publishers, Inc., p. 377-402.

Chen, C.S., and Wilson, J.L., 1987, Radon production in pumping wells, *in* Graves, Barbara, ed., Radon, radium, and other radioactivity in ground water: Hydrogeologic impact and application to indoor airborne contamination, NWWA Conference, Somerset, N.J., 1987, Proceedings: Chelsea, Mich., Lewis Publishers, Inc., p. 423-436.

Cook, G.A., ed., 1961, Argon, helium, and the rare gases: The elements of the helium group: Volume I: History, occurrence, and properties: New York, Interscience Publishers, p. 175.

Cothern, C.R., 1987, Estimating the health risks of radon in drinking water: Journal of the American Water Works Association, v. 79, no. 4, p. 153-158.

Davidson, E.S., 1973, Geohydrology and water resources of the Tucson Basin, Arizona: U.S. Geological Survey Water-Supply Paper 1939-E, 81 p., 7 sheets, various scales.

Dickinson, W.R., 1991, Tectonic setting of faulted Tertiary strata associated with the Catalina core complex in southern Arizona: Geological Society of America Special Paper 264, 106 p., 1 sheet, scale 1:125,000.

Dickinson, W.R., and Shafiqullah, M., 1989, K-Ar and F-T ages for syntectonic mid-Tertiary volcanosedimentary sequences associated with the Catalina core complex and San Pedro trough in southern Arizona: Isochron/West, no. 52, p. 15-27.

Dixon, K.L., and Lee, R.G., 1987, Radon survey of the American water works system, *in* Graves, Barbara, ed., Radon, radium, and other radioactivity in ground water: Hydrogeologic impact and application to indoor airborne contamination, NWWA Conference, Somerset, N.J., 1987, Proceedings: Chelsea, Mich., Lewis Publishers, Inc., p. 311-346.

Eberly, L.D., and Stanley, T.B., Jr., 1978, Cenozoic stratigraphy and geologic history of southwestern Arizona: Geological Society of America Bulletin, v. 89, p. 921-940.

EDA Instruments, 1988, Operation manual, RDA-200 Radon/radon daughter detector: Toronto, Canada, EDA Instruments, Inc.

Gilkeson, R.H., and Cowart, J.B., 1987, Radium, radon, and uranium isotopes in groundwater from Cambrian-Ordovician sandstone aquifers in Illinois, *in* Graves, Barbara, ed., Radon, radium, and other radioactivity in ground water: Hydrogeologic impact and application to indoor airborne contamination, NWWA Conference, Somerset, N.J., 1987, Proceedings: Chelsea, Mich., Lewis Publishers, Inc., p. 403-422.

Hall, F., 1988, Geologic controls on radon gas in ground water, *in* Makofske, W.J., and Edelstein, M.R., eds., Radon and the environment: Park Ridge, N.J., Noyes Publications, p. 48-55.

Hall, F.R., Boudette, E.L., and Olszewski, W.J., Jr., 1987, Geologic controls and radon occurrence in New England, *in* Graves, Barbara, ed., Radon, radium, and other radioactivity in ground water: Hydrogeologic impact and application to indoor airborne contamination, NWWA Conference, Somerset, N.J., 1987, Proceedings: Chelsea, Mich., Lewis Publishers, Inc., p. 15-30.

Harvey, J.P., 1981, Groundwater extraction and radon anomalies in the Picacho area, south-central Arizona: Tucson, University of Arizona, M.S. thesis, 120 p.

Hess, C.T., Casparius, R.E., Norton, S.A., and Brutsaert, W.F., 1978, Investigation of natural levels of ^{222}Rn in groundwater in Maine for assessment of related health effects, *in* Natural radiation environment III: Houston, Texas.

Humphreys, C.L., 1987, Factors controlling uranium and radium isotopic distributions in groundwaters of the west-central Florida phosphate district, *in* Graves, Barbara, ed., Radon, radium, and other radioactivity in ground water: Hydrogeologic impact and application to indoor airborne contamination, NWWA Conference, Somerset, N.J., 1987, Proceedings: Chelsea, Mich., Lewis Publishers, Inc., p. 171-189.

King, C., 1978, Radon emanation on the San Andreas fault: Nature, v. 271, no. 9, p. 516-519.

King, P.T., Michel, J., and Moore, W.S., 1982, Ground water geochemistry of ^{228}Ra, ^{226}Ra, and ^{222}Rn: Geochimica et Cosmochimica Acta, v. 46, p. 1173-1182.

Kruger, P., Stoker, A., and Umana, A., 1977, Radon in geothermal reservoir engineering: Geothermics, v. 5, p. 13-19.

Lee, R.W., and Hollyday, E.F., 1987, Radon measurement in streams to determine location and magnitude of ground-water seepage, *in* Graves, Barbara, ed., Radon, radium, and other radioactivity in ground water: Hydrogeologic impact and application to indoor airborne contamination, NWWA Conference, Somerset, N.J., 1987, Proceedings: Chelsea, Mich., Lewis Publishers, Inc., p. 241-249.

Longtin, J.P., 1988, Occurrence of radon, radium, and uranium in groundwater: Journal of the American Water Works Association, v. 80, no. 7, p. 84-93.

Lorenz, P.J., Rodenberg, O.D., Shadle, L.G., Antes, A.C., and Hess, W.D., 1961, Background radioactivity in the Decorah fault region: Iowa Academy of Science, v. 68, p. 397-403.

Lowry, J.D., and Lowry, S.B., 1988, Radionuclides in drinking water: Journal of the American Water Works Association, v. 80, no. 7, p. 50-64.

Megumi, K., and Mamuro, T., 1977, Concentration of uranium series nuclides in soil particles in relation to their size: Journal of Geophysical Research, v. 82, no. 2, p. 353-356.

Mielke, J.E., 1965, Trace element investigation of the Turkey Track porphyry, southeastern Arizona: Tucson, University of Arizona, M.S. thesis, 76 p.

Nicolaysen, L.O., 1957, Solid diffusion in radioactive minerals and the measurement of absolute age: Geochimica et Cosmochimica Acta, v. 11, p. 41-59.

Prichard, H.M., 1987, The transfer of radon from domestic water to indoor air: Journal of the American Water Works Association, v. 79, no. 4, p. 159-161.

Rama, and Moore, W.S., 1984, Mechanism of transport of U-Th series radioisotopes from solids into groundwater: Geochimica et Cosmochimica Acta, v. 48, p. 395-399.

Reynolds, S.J., Keith, S.B., and Dubois, J.F., 1980, Locations, lithologic descriptions, petrographic information, and analytical data for geochemical samples, *in* Coney, P.J., and Reynolds, S.J., eds., Cordilleran metamorphic core complexes and their uranium favorability: U.S. Department of Energy Open-File Report GJBX-258(80), p. 286-310, 578-585.

Rogers, A.S., 1958, Physical behavior and geologic control of radon in mountain streams: U.S. Geological Survey Bulletin 1052-E, 187 p.

Sellers, W.D., and Hill, R.H., eds., 1974, Arizona climate, 1931-1972: Tucson, University of Arizona Press, 616 p.

Semprini, Lewis, 1987, Radon-222 concentration of groundwater from a test zone of a shallow alluvial aquifer in the Santa Clara Valley, California, *in* Graves, Barbara, ed., Radon, radium, and other radioactivity in ground water: Hydrogeologic impact and application to indoor airborne contamination, NWWA Conference, Somerset, N.J., 1987, Proceedings: Chelsea, Mich., Lewis Publishers, Inc., p. 205-218.

Smith, A.R., Bowman, H.R., Mosier, D.F., Asaro, F., Wollenberg, H.A., and King, C.Y., 1976, ^{222}Rn in subsurface waters as an earthquake predictor: IEEE Transactions on Nuclear Science, v. 23, no. 1, p. 694-698.

Smith, A.R., Wollenberg, H.A., and Mosier, D.F., 1980, Roles of radon-222 and other natural radionuclides in earthquake prediction, *in* The natural radiation environment III: Springfield, Va., National Technical Information Service, p. 154-174.

Spencer, J.E., and Reynolds, S.J., 1989, Middle Tertiary tectonics of Arizona and adjacent areas, *in* Jenney, J.P., and Reynolds, S.J., eds., Geologic evolution of Arizona: Arizona Geological Society Digest 17, p. 539-574.

Starik, I.Y., and Melikova, O.S., 1957, Emanating power of minerals: Radiyevyy Institut Imeni V.G. Khlopina Trudy, v. 5, p. 184-202 (English translation U.S. Atomic Energy Commission Report AEC-tr-4498, p. 206-226).

Szabo, Zoltan, and Zapecza, O.S., 1987, Relation between natural radionuclide activities and chemical constituents in ground water in the Newark Basin, New Jersey, *in* Graves, Barbara, ed., Radon, radium, and other radioactivity in ground water: Hydrogeologic impact and application to indoor airborne contamination, NWWA Conference, Somerset, N.J., 1987, Proceedings: Chelsea, Mich., Lewis Publishers, Inc., p. 283-308.

Tanner, A.B., 1964a, Physical and chemical controls on distribution of radium-226 and radon-222 in ground water near Great Salt Lake, Utah, *in* Adams, J.A.S., and Lowder, W.M., eds., The natural radiation environment: Chicago, University of Chicago Press, p. 253-278.

_____ 1964b, Radon migration in the ground — A review, *in* Adams, J.A.S., and Lowder, W.M., eds., The natural radiation environment: Chicago, University of Chicago Press, p. 161-190.

_____ 1980, Radon migration in the ground — A supplementary review, *in* The natural radiation environment III: Springfield, Va., National Technical Information Service, p. 5-56.

Todd, D.K., 1980, Groundwater hydrology: New York, John Wiley and Sons, 336 p.

United Nations Scientific Committee on the Effects of Atomic Radiation (UNSCEAR), 1982, Ionizing radiation — Sources and biological effects; Annex D, exposures to radon and thoron and their decay products: 1982 Report to the General Assembly, p. 141-210.

Weast, R.C., and Astle, M.J., eds., 1980, Handbook of chemistry and physics: Cleveland, Ohio, CRC Press, Inc., p. B134, B138.

Wei, C., and Yi-Yao, L., 1984, Preliminary study of the application of hydrogeochemistry to earthquake prediction, *in* International Symposium on Earthquake Prediction, Paris, 1979, Proceedings: Terra Science Publishing Co., p. 539-552.

Whitehead, N.E., 1980, Radon measurements at three New Zealand geothermal areas: Geothermics, v. 9, p. 279-286.

Williams, W.J., and Lorenz, P.J., 1957, Detecting subsurface faults by radioactive measurements: World Oil, v. 144, no. 5, p. 126-128.

Wollenberg, H.A., 1974, Radioactivity of Nevada hot-spring systems: Geophysical Research Letters, v. 1, no. 8, p. 359-362.

Yang, I.C., 1987, Sampling and analysis of dissolved radon-222 in surface and ground water, *in* Graves, Barbara, ed., Radon, radium, and other radioactivity in ground water: Hydrogeologic impact and application to indoor airborne contamination, NWWA Conference, Somerset, N.J., 1987, Proceedings: Chelsea, Mich., Lewis Publishers, Inc., p. 193-203.

Uranium and radon in southeastern Arizona[1]

JOHN T. DUNCAN
JON E. SPENCER
Arizona Geological Survey, 845 N. Park Ave., #100, Tucson, Arizona 85719

INTRODUCTION

Several areas in southeastern Arizona are underlain by rock types that are known to contain anomalous concentrations of uranium (>6 parts per million [ppm], as defined in Duncan and Spencer, this volume, p. 93-96). These rock types include Cenozoic closed-basin lacustrine deposits, granitic rocks, and hydrothermally mineralized rocks associated with uranium and copper mineral districts. The only area known to be associated with elevated indoor-radon concentrations is in southwestern Tucson (Spencer and others, this volume, p. 10-16). Other areas with anomalously high uranium concentrations probably do not represent significant radon risk because they are unpopulated or thinly populated. Most of the larger towns in southeastern Arizona are built on Tertiary or Quaternary alluvial materials that contain low concentrations of uranium.

GAMMA-RAY SPECTROMETER SURVEY

A gamma-ray spectrometer survey of southeastern Arizona was completed in the winter of 1992 as part of a statewide investigation of potential indoor-radon hazards caused by high uranium concentrations in geologic materials. The communities of Nogales, Patagonia, Sierra Vista, Benson, St. David, Tombstone, Bisbee, Douglas, Willcox, Safford, Duncan, and Clifton were surveyed. No anomalous uranium concentrations were measured in these towns, which is not surprising because all except Bisbee are built mostly or entirely on upper Tertiary to Quaternary alluvial sediments. Emer and others (1988) reported mildly anomalous uranium concentrations in outcrops of Bisbee Group shales near Tombstone. (See Fig. 4 in Spencer, this volume, p. 8.) The outcrops, however, were not surveyed during this study.

[1]This study was supported by the Arizona Radiation Regulatory Agency, with funds provided by the U.S. Environmental Protection Agency, Arizona State Indoor Radon Grant Program K1-009544-01-0.

in Spencer, J.E., ed., 1993, Radon in Arizona: Arizona Geological Survey Bulletin 199, p. 40-42.

URANIUM-RICH ROCKS IN SOUTHEASTERN ARIZONA

Tertiary-Quaternary Lacustrine Sediments

The uranium anomaly at Cardinal Avenue and Valencia Road in Tucson has been thoroughly investigated and described by Spencer and others (this volume, p. 10-16). Other Tertiary-Quaternary lakebed deposits known to contain high uranium concentrations include the Quiburis Formation in the San Pedro Valley near Mammoth, Willcox Playa, and deposits in the San Simon Valley southeast of Safford (Fig. 1).

The Quiburis Formation lacustrine sediments include red siltstone and associated evaporite, as well as white to gray-green marl, diatomite, and chert. Radiometrically dated tuff beds within the Quiburis Formation range from 5.35 to 6.43 m.y. old (Scarborough, 1975; Reynolds and others, 1986). An areally limited, gamma-ray spectrometer survey indicated uranium concentrations up to 20 ppm in white marl and green chert at the White Cliffs diatomite mine near Mammoth and up to 42 ppm in similar, probably correlative (Lindsay and others, 1984) white marl north of Redington.

Willcox Playa, a closed-basin, ephemeral lake, is associated with Quaternary uranium deposits (Willcox District of Keith and others, 1983). No anomalous uranium concentrations, however, were revealed by NURE-sponsored airborne radiometric surveys of the area (Plate 1) or by portable gamma-ray spectrometer surveys conducted for this study. Descriptions of these uranium deposits are not available. The deposits are probably buried beneath younger playa sediments or are so young that the uranium is far from secular equilibrium with its largely absent daughter products and is therefore difficult to distinguish from non-anomalous strata via a gamma-ray spectrometer. For the same reasons, these deposits probably do not represent a radon hazard.

Pliocene lacustrine and paludal sediments resembling those in the San Pedro Valley are exposed in the 111-Ranch prospects (Scarborough, 1981) in the San Simon Valley near the base of the Whitlock Hills, 17 miles southeast of Safford. Light-colored mudstone, marl, chert, and diatomite contain strongly anomalous uranium concentra-

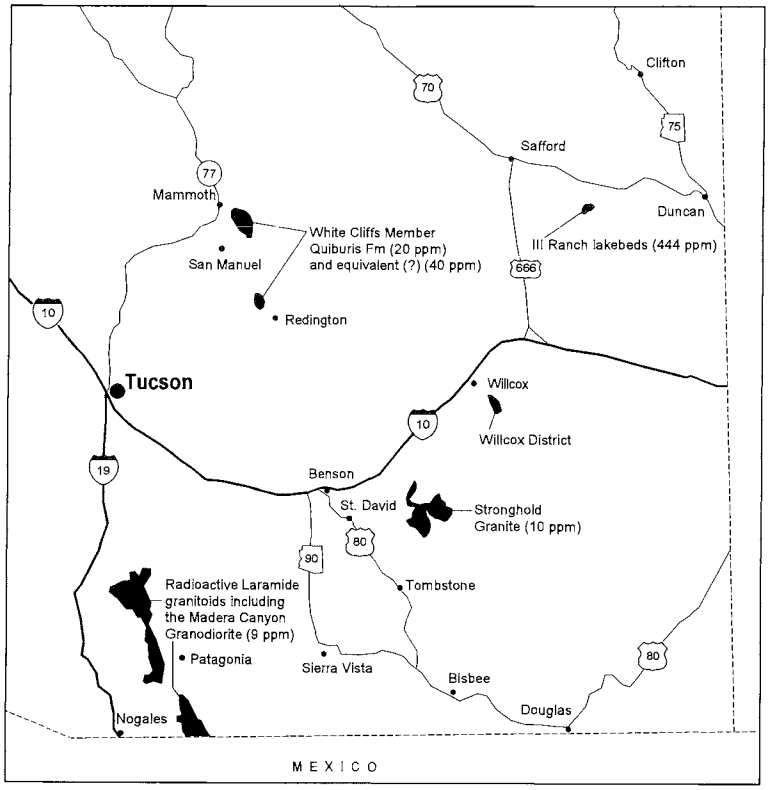

Figure 1. Areas of anomalous uranium content in southeastern Arizona.

tions, as indicated by gamma-ray spectrometer measurements. One commercially analyzed sample of white marl contained 444 ppm uranium. Similar lakebeds near Duncan were not anomalous as measured by the gamma-ray spectrometer in this study but were described as weakly anomalous by Scarborough (1981).

Igneous Rocks

Airborne radiometric data (Plate 1) indicate that several large areas in southeastern Arizona, which are centered on outcrops of felsic igneous rock, contain uranium concentrations greater than 5 ppm. Two of these anomalies were surveyed as part of this study. A swath of Laramide intrusive rocks that trends northwestward from the Mexican border in the Patagonia Mountains to Madera Canyon in the Santa Rita Mountains corresponds very closely to the large, greater than 5-ppm uranium anomaly shown on Plate 1. Handheld-spectrometer measurements of the Madera Canyon Granodiorite (Drewes, 1971) indicate uranium concentrations of up to 9 ppm near the Santa Rita Lodge in Madera Canyon (Fig. 1). The Tertiary Stronghold Granite (Gilluly, 1956; Drewes, 1987) in the Dragoon Mountains contains up to 10 ppm uranium as well as high concentrations of thorium, but no anomalous uranium concentrations were recognized in alluvial-fan material downslope from the granite outcrops.

Hydrothermally Mineralized Areas

Anomalous concentrations of uranium are associated with some of the large copper deposits in southeastern Arizona, notably the Silverbell district northwest of Tucson and the deposits on the flanks of the Sierrita Mountains southwest of Tucson. In addition, numerous prospects and small mines with minor uranium production are scattered throughout the region (Plate 1). These are generally in unpopulated areas or are avoided as residential areas for reasons other than their uranium content. No systematic investigation of these deposits was made for this study. One slightly anomalous (7 ppm uranium) gamma-ray spectrometer reading was taken on pyritic mine-dump material southeast of Bisbee. Other readings on similar material were not anomalous.

CONCLUSION

Most of the population centers in southeastern Arizona lie on Tertiary or Quaternary alluvial materials that have generally low potential for radon production. Uranium-rich granitic rocks are generally confined to sparsely populated or unpopulated mountainous areas and therefore do not currently present serious radon risk. The residential area in Madera Canyon and other minor population centers in the Santa Rita and Patagonia Mountains may, however, be more likely to contain anomalously high concentrations of radon than most homes in southeastern Arizona.

Tertiary and Quaternary lacustrine deposits throughout the State are commonly enriched in uranium (e.g., Scarborough, 1981; Plate 1). Several areas in southeastern Arizona are known to have anomalous uranium concentrations. The Cardinal Avenue locality in Tucson is associated with high radon concentrations in homes, but other uranium anomalies are too remote to cause significant radon problems. Increased population and future development in southeastern Arizona may encroach on known anomalies or expose presently unrecognized, uranium-rich lacustrine deposits. Even if they are not exposed at the surface, these deposits could contribute significant amounts of radon to well water.

REFERENCES

Drewes, Harald, 1971, Geologic map of the Mount Wrightson quadrangle, southeast of Tucson, Santa Cruz and Pima Counties, Arizona: U.S. Geological Survey Miscellaneous Geologic Investigations Map I-614, scale 1:48,000.

_____ 1987, Geologic map and cross sections of the Dragoon Mountains, southeastern Arizona: U.S. Geological Survey Miscellaneous Investigations Series Map I-1662, scale 1:24,000.

Emer, D.F., Shenk, J.D., and Spencer, J.E., 1988, Reconnaissance gamma-ray spectrometer survey of radon-decay products in selected populated areas of Arizona: Arizona Bureau of Geology and Mineral Technology Open-File Report 88-12, 88 p.

Gilluly, James, 1956, General geology of central Cochise County, Arizona: U.S. Geological Survey Professional Paper 281, 169 p., 9 sheets, various scales.

Keith, S.B., Gest, D.E., and DeWitt, Ed, 1983, Metallic mineral districts of Arizona: Arizona Bureau of Geology and Mineral Technology Map 18, scale 1:1,000,000.

Lindsay, E.H., Opdyke, N.D., and Johnson, N.M., 1984, Blancan-Hemphillian land mammal ages and late Cenozoic mammal dispersal events: Annual Review of Earth and Planetary Sciences, v. 12, p. 445-448.

Reynolds, S.J., Florence, F.P., Welty, J.W., Roddy, M.S., Currier, D.A., Anderson, A.V., and Keith, S.B., 1986, Compilation of radiometric age determinations in Arizona: Arizona Bureau of Geology and Mineral Technology Bulletin 197, 258 p., 2 sheets, scale 1:1,000,000.

Scarborough, R.B., 1975, Chemistry of late Cenozoic air-fall ashes in southeastern Arizona: Tucson, University of Arizona, M.S. thesis, 107 p.

_____ 1981, Radioactive occurrences and uranium production in Arizona: Arizona Bureau of Geology and Mineral Technology Open-File Report 81-1, 297 p., 21 sheets, scale 1:250,000.

Investigations of uranium and radon in the Phoenix metropolitan area[1]

JOHN T. DUNCAN
JON E. SPENCER

Arizona Geological Survey, 845 N. Park Ave., #100, Tucson, Arizona 85719

INTRODUCTION

The U.S. Environmental Protection Agency (EPA) considers radon gas to be a potential health hazard when it accumulates in indoor air in concentrations above a specified level. Because radon gas is produced by the radioactive decay of uranium, concentrations of uranium in soil and rock reflect the potential for unacceptably high levels of indoor radon. Uranium concentrations in rock and soil may be measured by portable radiation-detection instruments. Certain rock types commonly contain elevated uranium concentrations. Knowledge of the distribution of these rock types is useful to government agencies, home buyers, and builders who are interested in reducing radon exposure to humans.

Previous geologic and uranium surveys in Arizona have revealed that typical rock and soil contain about 2 parts per million (ppm) uranium. Rock and soil with more than 6 ppm uranium are considered anomalous (Duncan and Spencer, this volume, p. 93-96). Anomalous uranium levels are rare in the Phoenix metropolitan area, but several small anomalous areas were the focus of this study. All known uranium anomalies in the Phoenix area are discussed in this report.

Rocks described in this report that have anomalous uranium concentrations include some Tertiary volcanic rocks in the Phoenix Mountains and several exposures of middle to late Tertiary, tuffaceous, lacustrine carbonate rocks that crop out discontinuously near the northern margin of the Phoenix Basin (Fig. 1). We surveyed these areas with a portable gamma-ray spectrometer and determined uranium concentrations using the methods described in Duncan and Spencer (this volume, p. 93-96). In addition, Chemex Labs in Vancouver, B.C., analyzed representative samples of the more anomalous rocks using neutron-activation analysis. Minor geologic mapping, petrographic study, and

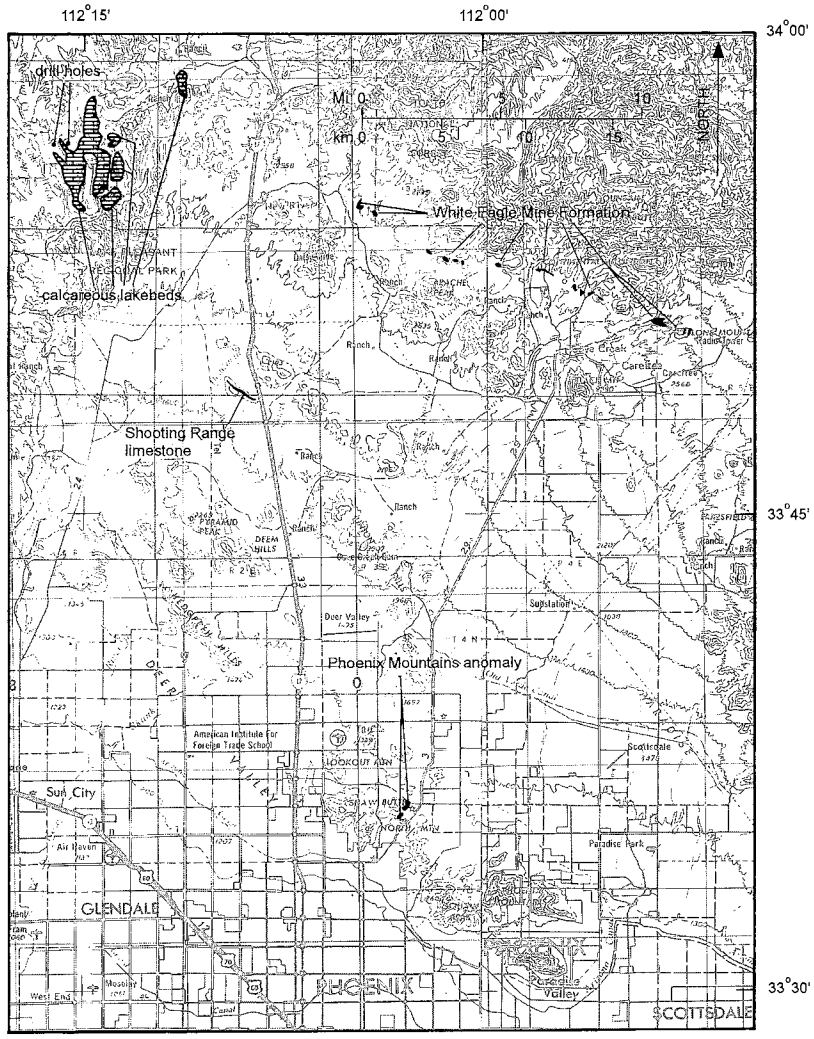

Figure 1. Location map of outcrops that contain anomalous uranium concentrations investigated in this study.

[1]This article supersedes the following report: Duncan, J.T., and Spencer, J.E., 1991, Investigations of uranium and radon in the greater Phoenix metropolitan area, Arizona: Arizona Geological Survey Open-File Report 91-9, 12 p.

in Spencer, J.E., ed., 1993, Radon in Arizona: Arizona Geological Survey Bulletin 199, p. 43-50.

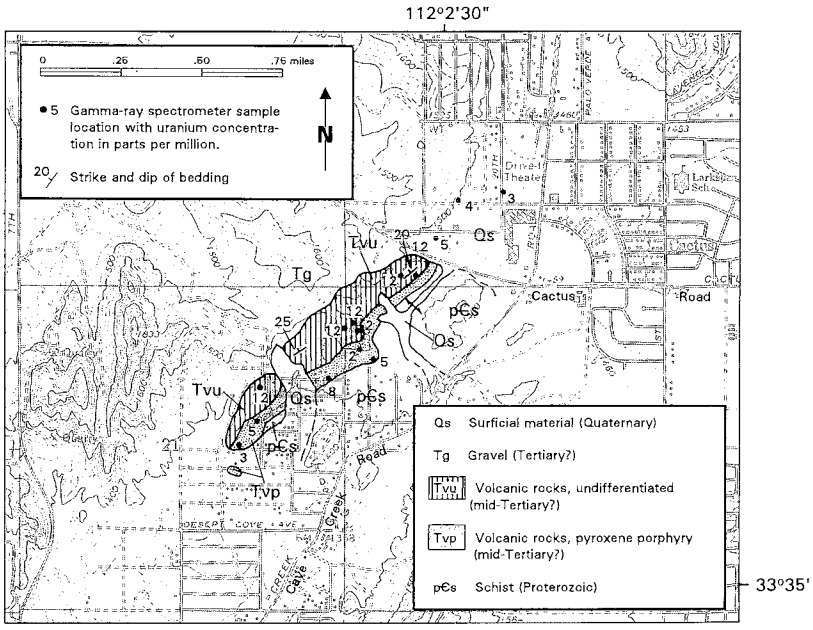

Figure 2. Geologic map of area of Phoenix Mountains uranium anomaly. Anomalous uranium values are confined to the Tertiary volcanic rocks.

whole-rock geochemical analyses were also included in the study of the volcanic rocks.

Radon is not limited to air and rock; it is also a potential health hazard in well water used for domestic purposes. At present, little is known about radon levels in Arizona well water. This report includes an analysis of the relationship between aquifer geology and radon in ground water in the Cave Creek-Carefree area, based on recent studies (Barnett, 1990; Doorn and Péwé, 1991).

PHOENIX MOUNTAINS ANOMALY

Anomalous uranium concentrations were noted (Emer and others, 1988) in Tertiary volcanic rocks exposed southwest of the intersection of Cave Creek Road and Cactus Road in the Phoenix Mountains. The present study, which includes a more detailed survey of the area, indicates that slightly elevated to anomalous uranium concentrations are common in these rocks.

The elevated urani-um concentrations are apparently restricted to a nearly continuous outcrop of mafic to intermediate volcanic rocks that strike northeast and dip northwest (Fig. 2). A lower mafic volcanic unit disconformably overlies Proterozoic schist. This unit contains abundant fresh, prismatic, green pyroxene phenocrysts and blebs of iron oxides, possibly representing altered olivine, in an aphanitic mafic groundmass. The lower unit, where tested, contains mildly elevated but generally nonanomalous uranium concentrations (up to 8 ppm; mean of seven assays = 4.6 ppm). This unit is overlain by an undifferentiated succession of brown-to-gray, intermediate-to-mafic flows with smooth to vesicular texture and variably developed flow foliation. These rocks contain sparse dunite inclusions and are consistently enriched in uranium. A spectrometer survey indicated uranium values up to 12 ppm with a mean of 9.2 ppm (14 samples); commercial analysis of one sample indicated 14.1 ppm uranium. The volcanic rocks are overlain by a thick succession of coarse, heterolithic, unconsolidated gravels.

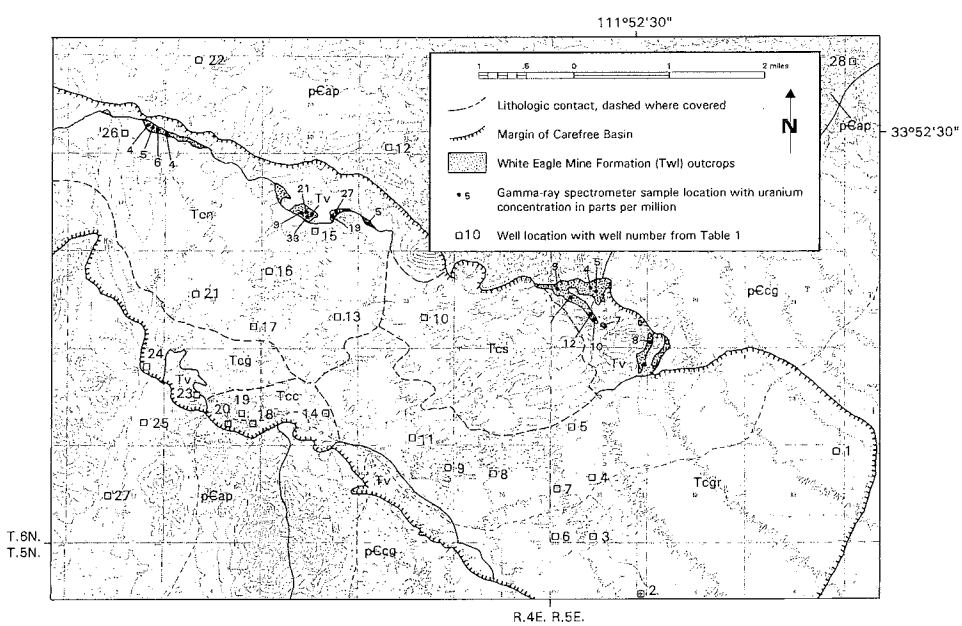

Figure 3. Map of pre-Quaternary geology and primary aquifers of Cave Creek-Carefree area, modified from Doorn and Péwé (1991, Plate 5). See Table 1 for unit identifications.

Table 1. Names, ages, and descriptions of rock units shown in Figure 3. Uranium concentrations (in parts per million) are given for commercially analyzed samples of selected aquifer units.

Unit Name (Symbol)	Age	Description	U
Carefree Fm.	Miocene-Pliocene	alluvial fan deposits	
Grapevine Member (Tcgr)		75% pCcg clasts	2.7
Sombrero Member (Tcs)		42% pCap and 31% undif. metamorphic clasts	NA
Naked Girl Canyon Member (Tcn)		80% Tertiary volcanic clasts	NA
Galloway Member (Tcg)		52% pCap, 21% basalt, 20% undif. meta. clasts	NA
Church Member (Tcc)		96% pCap clasts	3.7
White Eagle Mine Fm. (Twl)	mid- to late Miocene	light-colored, tuffaceous, cherty carbonates	NA
Tertiary volcanic rocks (Tv)	mid-Miocene	mafic to felsic flows and tuffs	NA
Camelback Granite (pCcg)	Middle Proterozoic	coarse-grained, k-feldspar porph. granite	<0.2
Meta-argillite (pCap)	Early Proterozoic	variably foliated metasediments	1.9

The outcrop of uranium-rich volcanic rocks is about 1 mi in length, less than 1,000 ft in average width, and largely contained within the Phoenix Mountains Preserve. The homes built on these outcrops are more likely to have elevated indoor-radon concentrations than homes in surrounding areas, which are built on nonanomalous geologic materials. The outcrop belt is covered on both ends by younger sediments and presumably continues for some distance in the subsurface. The authors discovered no anomalous uranium concentrations in a survey of these outlying areas. Surveys of other Tertiary volcanic rocks in the Phoenix Mountains (Lookout Mountain, Moon Hill, and Shaw Butte) revealed consistently low uranium values. No evidence was found that the area of high radioactivity extends beyond the exposures of Tertiary volcanic rocks (Fig. 2).

WHITE EAGLE MINE FORMATION AND EQUIVALENT(?) ROCKS

White Eagle Mine Formation

Thin, variably tuffaceous, variably cherty, white carbonate rocks are discontinuously exposed in a belt from Carefree to east of New River (Fig. 1). These rocks are part of the older, basin-filling sequence of the Carefree Basin (Doorn and Péwé, 1991) and generally dip moderately to steeply southwestward (into the basin). This unit has been called the White Eagle Mine Formation where it is exposed in the Carefree Basin (Doorn and Péwé, 1991).

Anomalous radioactivity has been reported for the White Eagle Mine Formation in the Cave Creek area (Emer and others, 1988; Doorn, 1989) and near New River (Scarborough and Wilt, 1981). A gamma-ray spectrometer survey of the White Eagle Mine Formation indicated that the formation contains highly variable uranium concentrations that range from 2 to 33 ppm over short distances. Within the Carefree Basin, the spectrometer indicated a mean uranium concentration of 8.4 ppm. The most uranium-rich parts of the formation in the Carefree Basin are soft, chalky, fine-grained carbonate rocks similar to the uraniferous rocks in the Verde Formation (Duncan and Spencer, this volume, p. 51-56). The highest concentrations encountered in the Cave Creek-Carefree area are in exposures in T. 6 N., R. 4 E., sec. 15 (Fig. 3).

Earlier studies (Scarborough and Wilt, 1979; Scarborough, 1981) reported radiation up to 25 times the background level in a small exposure of light-colored dolomite in a wash in the SE¼ of T. 7 N., R. 3 E., sec. 32 (Fig. 4). An investigation of the area for the present study confirmed the anomalous uranium concentrations (up to 247 ppm) in these rocks and found a thick (approximately 200 ft), gently folded, and generally northeast-dipping section of light-colored dolomite interbedded with calcareous mudstone and tuff exposed over a relatively large area in the western part of sec. 32

Figure 4. Geologic map of White Eagle Mine Formation exposed east of New River.

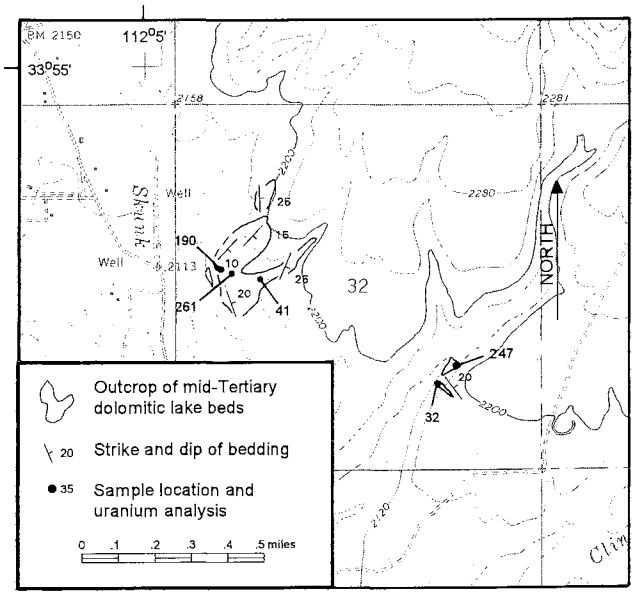

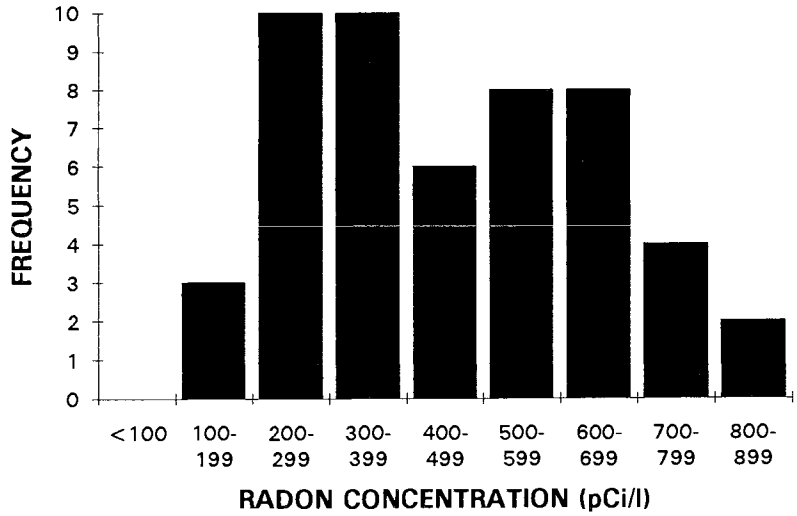

Figure 5. Histogram of radon concentrations in well water from 53 wells sampled by the City of Phoenix Water and Wastewater Department. Duplicate analyses from the same well were averaged so that each well is represented by only one data point.

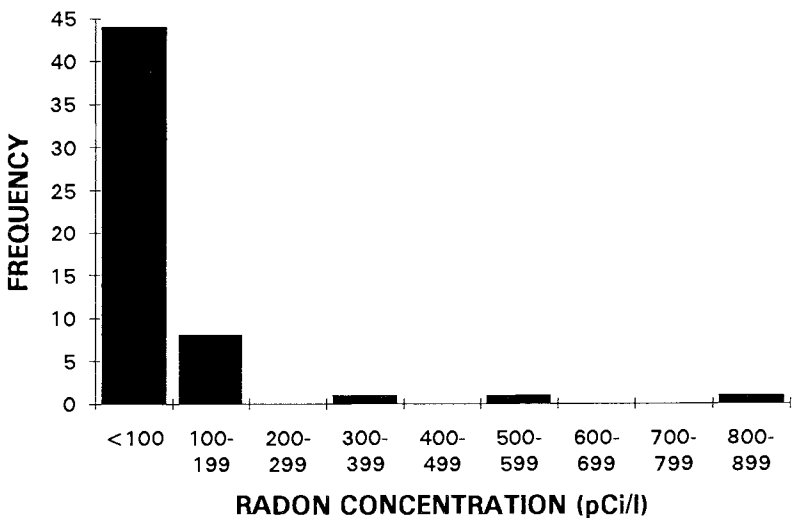

Figure 6. Histogram of radon concentrations in Phoenix tap water sampled by the City of Phoenix Water and Wastewater Department.

(Fig. 4). In the intervening area, the unit is apparently covered by a thin veneer of younger gravel. The dolomite is consistently uranium rich; many gamma-ray spectrometer readings indicated between 30 and 300 ppm, and commercial analyses indicated up to 261 ppm uranium. This unit is herein correlated with and considered part of the White Eagle Mine Formation.

The discontinuous but linear trend of outcrops of the White Eagle Mine Formation (Fig. 1) indicates that the unit is continuous in the subsurface but is variably concealed by younger Tertiary and Quaternary deposits. Where it is exposed in the towns of Cave Creek and Carefree, the unit may cause elevated indoor-radon concentrations in homes built on it. Because the total area of outcrop in Cave Creek and Carefree is relatively small, the unit probably does not pose a major radon problem for these communities. The highest uranium concentrations encountered in this study and one of the largest exposures of the White Eagle Mine Formation are in the northwestern extension of the unit near New River (Fig. 4). This area is not densely populated, but some homes are built near the radioactive exposures. If homes are built on these rocks in the future, very high indoor-radon concentrations could become a problem.

Rifle Range Anomaly

An isolated exposure of white, cherty, lacustrine carbonate rocks similar to the White Eagle Mine Formation is exposed in T. 5 N., R. 2 E., secs. 3 and 4, and T. 6 N., R. 2 E., secs. 33 and 34, on the southern face of the hill behind the Black Canyon shooting range on State Highway 74 (Fig. 1). This unit is either a fault-offset continuation of the White Eagle Mine Formation or a similar but uncorrelated unit of about the same age and depositional setting. Notably cherty and silicified, the exposure overlies a section of light-colored sandstone and is overlain by basalt. A gamma-ray spectrometer survey of the unit indicated elevated to anomalous uranium concentrations up to 17 ppm. Radon hazards at this locality are considered minimal because of the small area of exposure and the low probability of human habitation in the immediate future. (The hill forms the backstop for the rifle range.)

Lake Pleasant Area

Light-colored lacustrine mudstone and limestone with interbedded tuff and chert are exposed around the margins of Lake Pleasant and in canyons tributary to the Agua Fria River in the

northwestern corner of the study area (Fig. 1). Scarborough and Wilt (1979) inferred from stratigraphic relationships that these rocks are younger than the White Eagle Mine Formation and estimated that they are mid-Miocene or younger. The generally un-deformed nature of the rocks and their association with a modern river system suggest that they may be similar in age to the Miocene-Pliocene Verde Formation (see Duncan and Spencer, this volume, p. 51-56). Scarborough and Wilt (1979) report visible carnotite and radioactivity up to 3 times background in some of these beds. Exploration drilling in the late 1970's indicated uranium concentrations up to more than 50 ppm in green mudstone and interbedded limestone (Arizona Geological Survey files). The Lake Pleasant beds, remote from any human population centers and almost entirely within the Lake Pleasant Regional Park, present no significant radon problem.

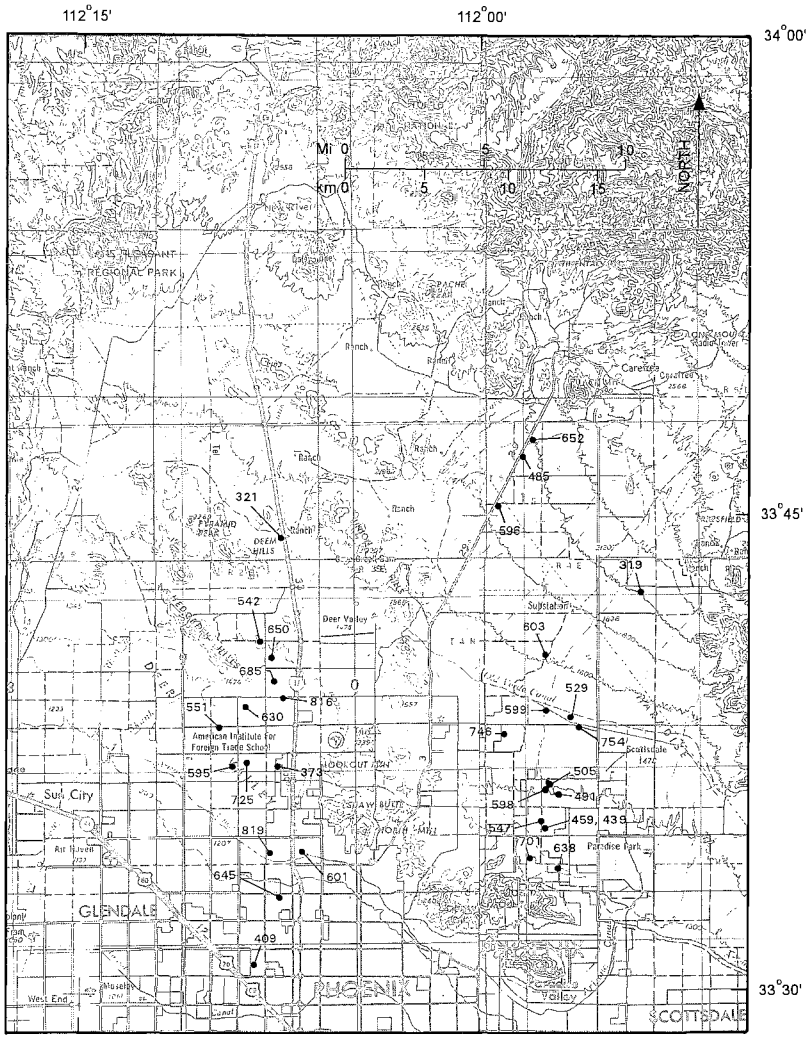

Figure 7. Map showing radon concentrations greater than 300 pCi/l in Phoenix well water.

RADON IN GROUND WATER

Phoenix

The City of Phoenix Water and Wastewater Department tested 53 water wells in Phoenix and found 38 that contain more than 300 pCi/l of radon (Fig. 5). Water from storage tanks and other taps away from the wellhead, however, generally contained less than 100 pCi/l radon (Fig. 6). The wells with the highest radon concentrations (up to 819 pCi/l) are all in the northern part of Phoenix, clustered mainly in two areas: west of I-17 near Bell Road, and between Bell Road and Shea Boulevard east of Tatum Boulevard (Fig. 7). The geologic influences on radon in Phoenix ground water have not been investigated.

Carefree Basin

Introduction. The Carefree Basin (Fig. 3) was the subject of a recent study of radon in ground water. Radon concentrations in ground water from the basin range from 260 to 5,110 pCi/l, and concentrations reach 8,150 pCi/l in wells outside but near the basin (Barnett, 1990). These concentrations are significant for two reasons: (1) they average much higher than the recommended maximum contaminant level of 300 pCi/l that the EPA recently proposed for radon in drinking water (Conference of Radiation Control Program Directors, Inc., 1991); and (2) domestic water is known to contribute, sometimes significantly, to radon concentrations in indoor air (Kearfott, 1989; Barnett, 1990). Radon levels in the Carefree Basin suggest that ground water in other areas of Arizona may contain radon concentrations greater than 1,000 pCi/l. At present, however, data from other areas are scarce.

Recent studies of the Carefree Basin include excellent data on radon in ground water and a detailed description of the geology and hydrology of the basin. For this report, we correlated radon data from Barnett (1990) with the geologic and hydrologic information from Doorn and Péwé (1991) and new uranium analyses of aquifer materials.

Geology. The geology of the Carefree Basin has been described in detail by Doorn and Péwé (1991); the following summary is drawn entirely from that source. The Carefree Basin is a small (approximately 25 sq mi), northwest-trending, struc-

tural and hydrologic basin located about 25 mi north-northeast of downtown Phoenix. The basin formed in mid-Miocene to Pliocene time, largely as a result of Basin and Range normal faulting. The basin is filled with a lower sequence of volcanic rocks and interbedded sediments (13 to 22 m.y. old) and an overlying succession of fanglomerates. The fanglomerates are largely derived from the Proterozoic crystalline rocks that surround and floor the basin; additional material was derived from Tertiary volcanic rocks. The fanglomerates, which were deposited during Basin and Range faulting 13 to 6 m.y. ago, compose the Carefree Formation. This unit includes five members distinguished by clast composition. The Carefree Formation is the most voluminous of the basin-filling units and the primary aquifer in the area. It is overlain in most places by a thin veneer of Quaternary alluvium. A simplified version of Doorn and Péwé's (1991) geologic map of the area is presented in Figure 3; rock units and descriptions are provided in Table 1.

Radon Data. Barnett (1990) analyzed water from 28 wells in the Cave Creek-Carefree area for radon-222 (^{222}Rn) using liquid scintillation methods (see Fig. 3 for well locations and Table 2 for well data). The wells were considered to be representative of the area's water supply; the sample set includes 26 wells that provide water for general domestic purposes and 2 wells used only for irrigation. Of the 26 used for domestic purposes, 16 are public (owned by water companies) and 10

Table 2. Well locations, producing capacities, primary producing aquifers, and concentrations of radon in water for wells analyzed by Barnett (1990). Radon concentrations are mean values for wells sampled more than once. Producing capacity and aquifer formation are mostly from Doorn and Péwé (1991). Capacity numbers marked with an asterisk (*) are midpoints of ranges given by Doorn and Péwé (1991); those marked "est." are J.T. Duncan's estimates based on comparisons to nearby wells producing from the same aquifer. Formation symbols marked with question marks (?) are J.T. Duncan's tentative determinations based on producing aquifers in surrounding wells.

Well #	Location	Capacity (gpm)	Producing Fm.	^{222}Rn
1	A(6-5) 33aaa	87	Tcgr	1,660
2	A(5-5) 6daa	33	Tcgr	690
3	A(6-5) 31cdd	165	Tcgr	1,080
4	A(6-5) 31bda	1,450*	Tcgr	1,290
5	A(6-5) 30cca	160	Tcgr	1,900
6	A(6-5) 31ccc	1,278	Tcgr	770
7	A(6-5) 31bcc	750	Tcgr	1,400
8	A(6-4) 36bda	515	Tcgr	1,830
9	A(6-4) 35aad	220	Tcgr	940
10	A(6-4) 23dbd	25	Tcs	980
11	A(6-4) 26dcc	210	Tcgr	2,100
12	A(6-4) 11cdc	10 (est.)	pCap	2,990
13	A(6-4) 22dac	0	Tcnc	980
14	A(6-4) 27dbd	600*	pCcg	4,590
15	A(6-4) 15dcb	10	Twl	280
16	A(6-4) 22bbc	10	Tcn	430
17	A(6-4) 21dda	135*	Tcn/Tv	1,070
18	A(6-4) 28dda	100	Tcc/pCap	3,930
19	A(6-4) 28dac	80	Tcc/pCap	5,110
20	A(6-4) 28dca	30	Tcc/pCap	2,840
21	A(6-4) 21bdc	15 (est.)	Tcn (?)	1,530
22	A(6-4) 9bab	25	pCap	2,970
23	A(6-4) 28bdc	10 (est.)	Tcg/Tv/pCap (?)	260
24	A(6-4) 29aac	NA	Tcg/Tv (?)	390
25	A(6-4) 29ddb	15 (est.)	Qs/pCap (?)	260
26	A(6-4) 8dcb	100*	Tcn (?)	527
27	A(6-4) 32caa	500	Qs	380
28	A(6-5) 10bbb	NA	pCap	8,150

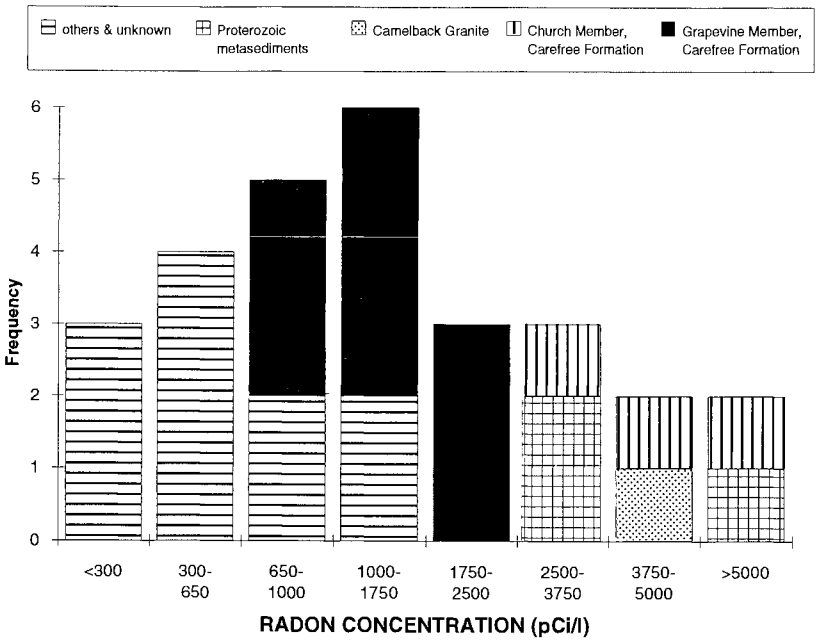

Figure 8. Histogram of concentrations of radon in well water in the Cave Creek-Carefree area, measured by Barnett (1990). Important aquifer units are indicated.

are private. Samples from 27 wells were collected and analyzed in August 1989. This sampling yielded radon concentrations ranging from 260 pCi/l to 5,800 pCi/l, with an average (unweighted arithmetic mean) of 1,740 pCi/l. To verify these results, Barnett resampled monthly (from January through June 1990) 11 of the 12 wells that contained the highest radon concentrations. This long-term sampling program also included a 12th well, which had not been included in the first round but was known to produce unusually radioactive water. The second sampling largely confirmed the results of the first, and the additional well produced the highest average radon content in the study: 8,150 pCi/l. In all, 25 of the 28 wells examined (89%) exceed the EPA's proposed maximum ^{222}Rn level of 300 pCi/l.

The data indicate a correlation between aquifer lithology and radon concentration in ground water (Table 2; Fig. 8). The aquifers associated with the highest radon in ground water are the Proterozoic meta-argillite (schist; pCap) and Camelback Granite (pCcg), as well as the members of the Tertiary Carefree Formation composed primarily of fragments of the Proterozoic schist and granite: the Church Member (Tcc) and the Grapevine Member (Tcgr), respectively.

Discussion. Commercial uranium analyses of samples from the different aquifer materials (Table 1) indicate neither anomalous uranium concentrations nor a clear correlation between uranium concentration and high-radon aquifers. If the samples are representative of the aquifer units, then characteristics other than bulk uranium content are the primary controls on the amount of radon that these rocks contribute to the ground water.

The short half-life of ^{222}Rn (3.8 days) and normal rates of groundwater flow indicate that radon in ground water probably could not migrate more than a few tens of feet to the well site before being destroyed by radioactive decay. A radon source outside the local aquifer is therefore precluded. The immediate radon parent, radium-226 (^{226}Ra), must be present near the well to produce the radon detected in well-water samples. Aquifers that do not contain high overall uranium concentrations could contribute anomalous radon to ground water if the parent radium has greater-than-normal emanation power. (Emanation power is a measure of the efficiency with which radon produced by a geologic material is released from that material and transmitted to surrounding pore spaces that may contain water.) Such conditions would exist if uranium or radium minerals coated fracture or grain surfaces in the aquifer. Radon produced from grain or fracture coatings would presumably have much easier access to the pore water than radon produced in the interiors of clasts or unbroken rock. (Such radon would be trapped in the rock.) It is possible that ground water has mobilized uranium from a source rock, such as the Proterozoic granite, transported the uranium to the Carefree Basin, and then precipitated the uranium on fracture or clast surfaces due to a chemical change in the ground water such as development of less oxidizing and more reducing conditions. Uranium mobility is suggested by analyses of samples of the fanglomerate materials that contain more uranium than the parent rocks from which they were derived (compare the uranium content of Church Creek Member and meta-argillite in Table 1).

The high radon levels in well water near the center of Cave Creek might be explained by the wells' location within or near sediments derived from meta-argillite that are down gradient from a large area of (leached?) Proterozoic granite and granite-derived Tertiary sediments. The change in aquifer lithology could have affected redox or other chemical conditions so that uranium (or radium) was precipitated from migrating ground waters. The Proterozoic metasediments are generally reduced (greenstones) and could be effective

in reducing and precipitating small quantities of oxidized uranium from solution in ground water. Alternatively, reduced iron-rich waters associated with the greenstones could precipitate radium along with iron hydroxides if these waters are mixed with oxidizing ground waters from a different source (Tanner, 1964). Although neither of these mechanisms is supported or may be tested by available data, reasonable assumptions about ground-water conditions make either reaction plausible.

Mechanisms that depend on ground-water chemistry and water-rock reactions are assumed to be responsible for precipitating radon parent elements in minerals or mineral coatings with high emanation power in the aquifer beneath central Cave Creek. The generally high concentrations of radon in the local ground water suggest that the proper conditions for these mechanisms to operate were widespread in the Carefree Basin; similar conditions and processes might also explain the high radon concentrations in water from wells in Proterozoic schist near the margins of the basin. Such conditions should not be entirely unexpected because similar processes were probably responsible for the uranium enrichment of the White Eagle Mine Formation during an earlier stage of basin filling. The uranium was probably deposited contemporaneously with, and locked within, the fine-grained, low-permeability chemical sediments, which would explain the apparent low radon-emanation power of the White Eagle Mine Formation.

Conclusion. The high concentrations of radon in ground water in the Cave Creek-Carefree area do not correlate with unusually high uranium concentrations in aquifer rocks. This is well illustrated by (1) low radon concentrations in water from the only well producing from the uranium-enriched White Eagle Mine Formation; and (2) high radon concentrations in water from wells in the Proterozoic metaargillite, which typically contains low uranium concentrations. Although the data presented here are insufficient to support any detailed model to explain radon concentrations in ground water, the explanation probably lies in the emanation power of the radon parent elements (determined by their physical location in geologic materials), rather than the bulk concentration of these elements in the rocks. The most likely mechanisms for creating conditions favorable to high radon emanation are water-rock reactions involving mobilization of uranium or radium and subsequent precipitation on surfaces exposed to ground water. Such reactions are quite possible and, to some extent, expected (Tanner, 1964; Smith, this volume, p. 17-39), but the specifics of these reactions and systems are beyond the scope of this report.

Overall, the relationships between geology and radon in ground water are not generally understood or even recognized. If the Carefree Basin is any indicator, high radon levels in ground water may be common in many areas of Arizona. Further studies are certainly warranted. In addition to increasing the understanding of radon in ground water, such studies may clarify the relationships between uranium in rocks (and soil) and radon in the air. The systematics of radon emanation from rocks and soil should be similar whether the pore spaces are occupied by water or air.

REFERENCES

Barnett, J.M., 1990, Radon-222 in drinking water: Liquid scintillation detection methods and estimated doses to the lungs: Tempe, Arizona State University, M.S. thesis, 94 p.

Conference of Radiation Control Program Directors, Inc., 1991, Radon in drinking water: Frankfort, Ky., Radon Bulletin, v. 1, no. 4, p. 7.

Doorn, P.L., 1989, Geologic and gravimetric investigations of the Carefree Basin, Maricopa County, Arizona: Tempe, Arizona State University, M.S. thesis, 306 p., 10 sheets, scales 1:24,000 and 1:48,000.

Doorn, P.L., and Péwé, T.L., 1991, Geologic and gravimetric investigations of the Carefree Basin, Maricopa County, Arizona: Arizona Geological Survey Special Paper 8, 187 p., 10 sheets, scales 1:24,000 and 1:48,000.

Emer, D.F., Shenk, J.D., and Spencer, J.E., 1988, Reconnaissance gamma-ray spectrometer survey of radon-decay products in selected populated areas of Arizona: Arizona Bureau of Geology and Mineral Technology Open-File Report 88-12, 88 p.

Kearfott, K.J., 1989, Preliminary experiences with ^{222}Rn gas in homes: Health Physics, vol. 56, no. 2, p. 169-179.

Scarborough, R.B., 1981, Radioactive occurrences and uranium production in Arizona: Arizona Bureau of Geology and Mineral Technology Open-File Report 81-1, 297 p.

Scarborough, R.B., and Wilt, J.C., 1979, A study of uranium favorability of Cenozoic sedimentary rocks, Basin and Range Province, Arizona; part 1, general geology and chronology of pre-late Miocene Cenozoic sedimentary rocks: Arizona Bureau of Geology and Mineral Technology Open-File Report 79-1, 101 p.

Tanner, A.B., 1964, Radon migration in the ground; a review, *in* Adams, J.A.S., and Lowder, W.M., eds., The natural radiation environment: Chicago, University of Chicago Press, p. 161-190.

Uranium-bearing rocks in Verde Valley, Yavapai County, and implications for indoor-radon gas[1]

JOHN T. DUNCAN
JON E. SPENCER
Arizona Geological Survey, 845 N. Park Ave., #100, Tucson, Arizona 85719

INTRODUCTION

Radon gas, which is produced by the radioactive decay of uranium, can accumulate in homes to levels that are considered hazardous by the U.S. Environmental Protection Agency (EPA). Hazardous indoor-radon levels are most common in areas where underlying rock and soil contain unusually high concentrations of uranium. Typical uranium levels in geologic materials in Arizona are about 2 parts per million (ppm). Levels greater than 6 ppm are considered anomalous (Duncan and Spencer, this volume, p. 93-96). Anomalous uranium levels (up to almost 50 ppm) are common in the lower member of the Verde Formation, which is widely exposed in southern and central Verde Valley. A survey of indoor-radon levels in Arizona revealed a significantly greater-than-average proportion of high radon concentrations in the Camp Verde area, which is consistent with evidence of elevated uranium levels in that area.

This study represents part of an evaluation of potential radon hazards in Arizona conducted by the Arizona Geological Survey and Arizona Radiation Regulatory Agency (ARRA). An earlier reconnaissance survey (Emer and others, 1988) discovered anomalous concentrations of uranium in the rocks beneath the town of Camp Verde. The following report confirms this discovery, identifies anomalous uranium concentrations over much of Verde Valley, and associates the anomalies with a specific rock type.

Uranium levels were determined with a portable gamma-ray spectrometer, supplemented by laboratory chemical analyses. The methods used in the spectrometer survey, both for this study and for studies of other parts of Arizona, are described in detail elsewhere (Duncan and Spencer, this volume, p. 93-96). Indoor-radon levels were determined during a statewide survey conducted by the ARRA from 1987 to 1989.

LOCATION

Verde Valley is near the geographic center of Arizona, approximately 60 mi south-southwest of Flagstaff and 100 mi north-northeast of Phoenix. It is a broad valley watered by the Verde River and its major tributaries, as well as numerous springs and abundant ground water. The valley was inhabited by humans even before Europeans settled there, as evidenced by cliff dwellings and other ruins. Verde Valley encompasses the modern communities of Clarkdale, Cottonwood, Cornville, Bridgeport, McGuireville, Middle Verde, Page Springs, Lake Montezuma, and Camp Verde, as well as unincorporated agricultural and residential areas.

GEOLOGY

Verde Valley is a structural depression bounded on the northeast by the Mogollon Rim (the southern edge of the Colorado Plateau) and on the southwest by the Black Hills. The valley was largely formed by normal displacement of up to 6,000 ft along the Verde Fault, which created an asymmetrical basin with a gently southwest-dipping floor and a steep, fault-controlled southwestern margin (Nations and Ranney, 1989). Verde Valley was filled between 8 m.y. and 2 m.y. ago (contemporaneously with Verde Fault movement) with a sequence of interbedded limestones, mudstones, sandstones, conglomerates, evaporites, and volcanic rocks that make up the Verde Formation of Jenkins (1923).

The Verde Formation generally consists of flat-lying lacustrine and fluvial deposits composed of fine-grained clastic and chemical sedimentary rocks along its central axis, which coincides approximately with the present Verde River, and variable amounts of coarser clastic rocks closer to the basin margins. Except where it is covered by Quaternary alluvial deposits, the Verde Formation is exposed over the entire Verde Valley, from well south of

[1] This article and Plate 2 supersede the following report: Duncan, J.T., and Spencer, J.E., 1991, Uranium-bearing rocks in Verde Valley, Yavapai County, Arizona, and implications for indoor-radon gas: Arizona Geological Survey Open-File Report 91-3, 11 p., 2 sheets, scale 1:32,000.

in Spencer, J.E., ed., 1993, Radon in Arizona: Arizona Geological Survey Bulletin 199, p. 51-56.

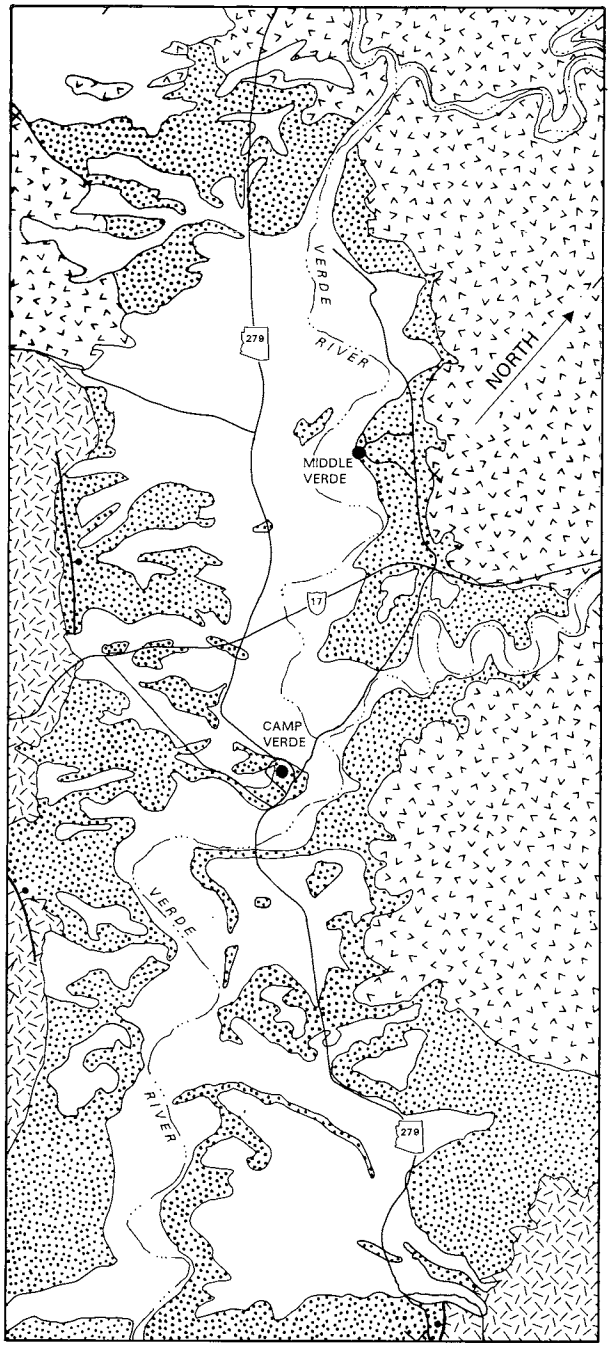

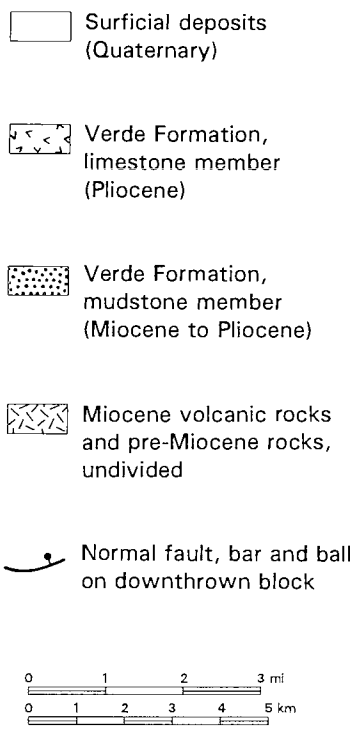

Figure 1. Simplified geologic map of Verde Valley.

Camp Verde to north of Clarkdale and from Page Springs nearly to Jerome. The formation has an outcrop area of more than 300 sq mi (Figs. 1 and 2; Plate 2).

In previous studies, the Verde Formation has been divided into two major units. Nations and Ranney (1989) located the Miocene-Pliocene boundary at an elevation of approximately 3,800 ft, where it separated a lower (Miocene) mudstone- and evaporite-rich unit from an upper (Pliocene) unit dominated by carbonate rocks. Wadell (1972) also mapped a lower mudstone unit and upper limestone unit. He did not locate the contact between the two members at a specific elevation, but did map the contact at approximately 3,400 ft in the cliffs northeast of Camp Verde and Middle Verde.

Reconnaissance mapping during this study generally confirmed the nature and distribution of the two units as previously recognized. The lower unit is characterized by distinctive, soft, gray to olive-green, carbonate-rich (predominantly dolomite and magnesite) mudstones and abundant evaporites (gypsum, halite, and sodium sulfate minerals), but includes lenses and intercalated beds of coarser clastic rocks, tuffs, and tuffaceous sedimentary rocks near the margins of the formation. Soft or chalky, white to yellowish, carbonate mudstone and marl and hard white carbonates are also common, especially near the contact with the upper limestone unit. The mudstone unit is exposed mainly in the southern part of the study area at elevations below 3,400 ft. It generally forms slopes. Good outcrops are visible only in washes or road cuts. The upper limestone unit is exposed over most of the valley at elevations above 3,400 ft. It is characterized by resistant, white, variably cherty and dolomitic limestone, but also includes soft or chalky white marl and carbonate mudstone, as well as sandstone, conglomerate, and minor amounts of volcanic rocks distal to the valley axis.

The carbonates and carbonate-rich muds of the central part of the formation were deposited in a shallow lacustrine environment, as indicated by abundant root and stem casts in parts of the upper limestone unit (Wadell, 1972). The complex facies relationships among limestone, mudstone, and coarser clastic material suggest that water levels and the amount of clastic material from the margins varied considerably during deposition of the formation. The presence of evaporites indicates that the basin was at least intermittently closed and underwent partial or complete desiccation.

Figure 2. Simplified geologic map of the Cottonwood area. Numbered dots indicate uranium level in parts per million as measured with a gamma-ray spectrometer (see Duncan and Spencer, this volume, p. 93-96).

This study involved only minor reconnaissance mapping. Most of the geologic information presented in Figures 1 and 2 and Plate 2 was drawn from other sources. The locations of contacts between the Verde Formation and the older bedrock and Quaternary surficial materials are based on U.S. Geological Survey 1:100,000-scale maps (Billingsley and others, 1988; Weir and others, 1989), except for the southernmost corner of the map, which is based on Wadell (1972). Wadell's general designation of upper and lower units has been accepted, but the locations of his contacts have been modified considerably, based on observations made during this study. The mapping in the present study, however, does not accurately depict the complex facies relationships within the Verde Formation, but only roughly divides the formation into the two major units (upper limestone and lower mudstone) that are relevant to this investigation.

GAMMA-RAY SPECTROMETER SURVEY

Methods

Data consist of 100-second counts of the diagnostic uranium gamma rays (bismuth-214 [^{214}Bi]) that were obtained on accessible outcrops and soils in Verde Valley. The counts were recorded by a geoMetrics model GR-310 gamma-ray spectrometer equipped with an external detector containing a 347-cm^3, thallium-doped, sodium-iodide crystal. The raw data were converted to equivalent uranium concentrations in parts per million by methods that are described elsewhere (Duncan and Spencer, this volume, p. 93-96). All major rock types were sampled. Geographic coverage includes most of the outcrop area of the Verde Formation.

Results

A histogram of calculated uranium concentrations from Verde Valley and from other (nonanomalous) areas in Arizona (Fig. 3) reveals that the mean for the nonanomalous rocks is 1.6 ppm, approximately the average for crustal rocks. All samples with uranium concentrations greater than 6 ppm (more than 2 standard deviations greater than the mean for nonanomalous rocks) are thus considered anomalous. The mean uranium concentrations of the mudstone and limestone units (excluding the Rocking Chair Road anomaly) of the Verde Formation, derived from the nonrandom sampling in this survey, are 11.5 ppm and 4.6 ppm, respectively.

The broad modal peak that extends into the negative range (Fig. 3) is largely due to errors introduced by counting statistics, machine-background correction, and thorium estimates, which are significant only in the samples with the lowest uranium concentrations. Although the correlation between gamma-ray spectrometer assays and commercial uranium analyses for Verde Formation samples is very strong (Fig. 4), atmospheric conditions and soil moisture may produce additional,

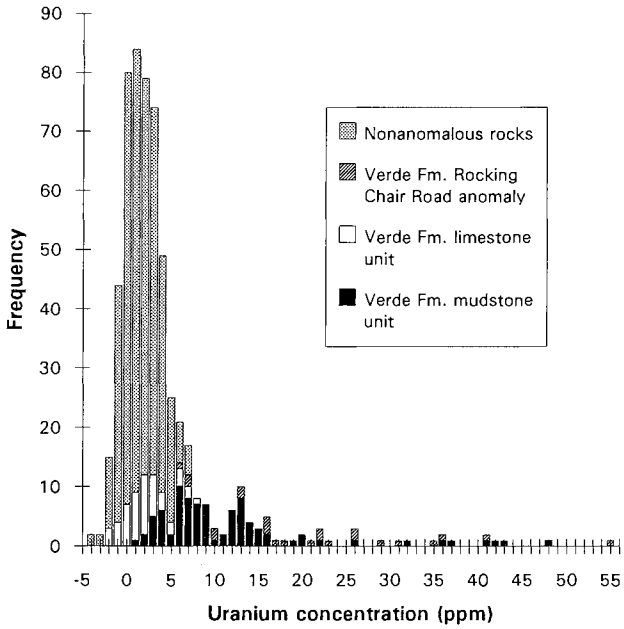

Figure 3. Histogram of uranium concentrations in the rocks of the Verde Formation, with non-anomalous rocks shown for comparison. Concentrations greater than 6 ppm are considered anomalous.

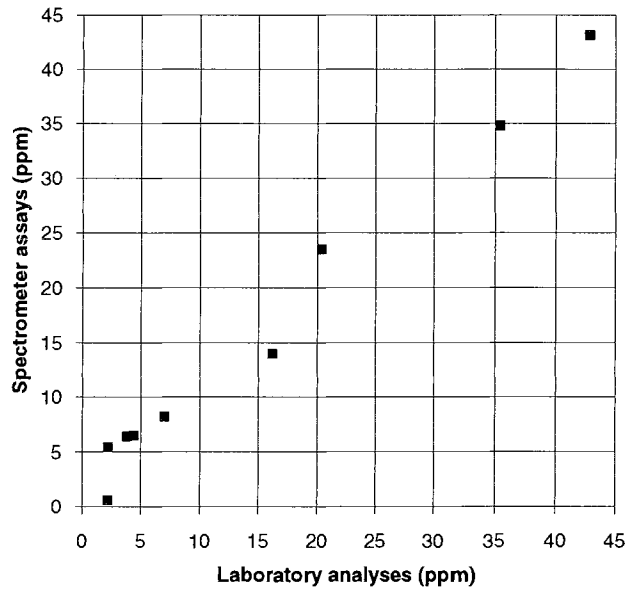

Figure 4. Plot of gamma-ray-spectrometer uranium assays against commercial analyses of Verde Formation samples. Correlation coefficient (r) = 0.99.

more important errors (up to 20%) in gamma-ray spectrometer assays (geoMetrics, undated). All uranium numbers generated in this study should, therefore, be considered estimates and indicators of relative concentrations rather than precise analyses.

We used a gamma-ray spectrometer to determine uranium concentrations (in parts per million) for numerous samples and plotted their locations and concentrations (Fig. 2; Plate 2). Most of the higher uranium values are concentrated in the southern part of the valley from the area south of Camp Verde to the area north of Middle Verde (Plate 2). Another significant cluster of high values is located north of Bridgeport and east of Cottonwood on the eastern side of the Verde River (Fig. 2). All anomalous uranium readings are in the carbonate-rich rocks of the Verde Formation; no elevated levels are in the Quaternary alluvium overlying the Verde Formation or in the coarse clastic materials within the formation. The older bedrock was not surveyed.

URANIUM GEOLOGY

Rock-Type Associations

Most of the anomalous samples are in the lower mudstone unit of the Verde Formation; however, mudstones within this unit that contain a significant sandy, volcanic, or evaporite component are not known to contain anomalous uranium. The widespread, gray to olive-green mudstone commonly contains mildly elevated to slightly anomalous uranium concentrations (approximately 5 to 10 ppm), but is not known to contain the highest concentrations. The most highly uraniferous rocks are soft, chalky, white to gray to yellow-green, carbonate mudstones or marls. These are interbedded with the gray mudstones that are common in the lower unit and with the hard, white, cliff-forming carbonates that characterize the upper limestone unit, and may be a transitional facies between the two. In some localities with the highest uranium concentrations, the rocks are stained yellow (carnotite?) and black (uraninite or organic carbon?). Other outcrops with high uranium concentrations, however, are pure white and contain no evidence of mineralization. All the uraniferous rocks that were studied are unoxidized (white, gray, or yellow-green in color rather than the red, pink, or tan tones of oxidized rocks), and none contain an obvious organic component or exude a fetid odor.

The hard, white, cliff-forming carbonates in the upper limestone unit or interbedded with the mudstones generally do not contain anomalous concentrations of uranium. In fact, the carbonates in the upper unit contain lower-than-average uranium concentrations, as do the interbedded, pink to tan silts and sands in the eastern part of the valley. The upper limestone unit does, however, contain locally anomalous uranium concentrations.

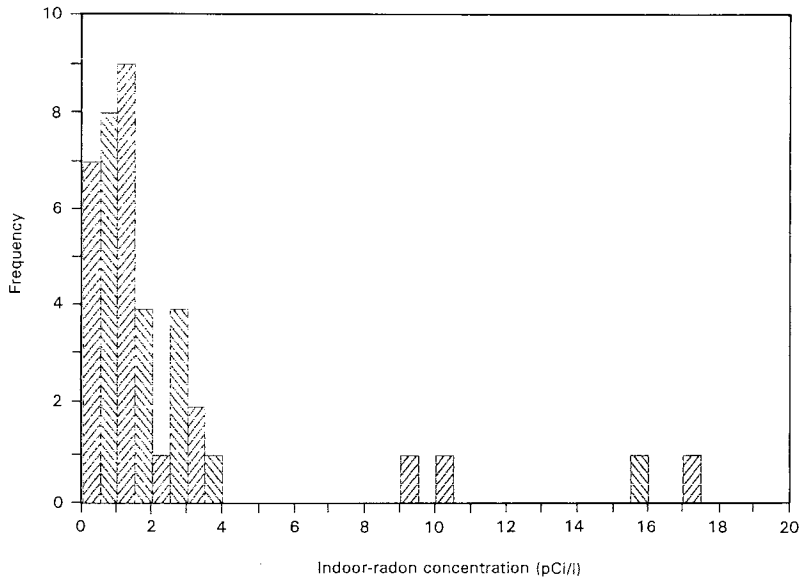

Figure 5. Histogram of indoor-radon levels in the Camp Verde area. Data are from a carbon-canister survey conducted by the ARRA.

One significant example is an area across the Verde River from Cottonwood (Fig. 2), where a set of soft, white, carbonate-rich marl lenses with anomalous uranium is interbedded with red sandy siltstone. This area is at an elevation of approximately 3,400 ft and could represent the transitional facies between (concealed) mudstone below and limestone above. Another possible indicator of anomalous uranium in the upper limestone unit is in the hills northeast of Clarkdale. Very sparse sampling of the area as part of this study did not reveal anomalous uranium in outcrop, but soft white marl and carbonate mudstone are common. A block of land in that area was leased and drilled by a uranium exploration company in the late 1970's, and numerous prospect pits are presumably the result of earlier uranium exploration. These indications of anomalous uranium concentrations are well above the elevation of the mudstone-limestone contact and apparently are not associated with the lower mudstone unit.

Genesis and Implications of Uranium Anomalies

Uranium in the Verde Formation is clearly associated with specific rock types. Although carnotite(?) locally stains the fractures in uranium-bearing rocks, most anomalous rocks show no evidence of mineralization. Anomalous uranium concentrations are nowhere associated with faults, veins, reaction fronts, or other alteration that would suggest an epigenetic origin for the uranium. These facts suggest that the uranium was deposited syngenetically with the enclosing chemical sediments or as a part of early diagenesis by reactions with ground water or aqueous fluids similar to those from which the sediments were deposited.

The Verde Formation was at least partly deposited from a concentrated brine in a completely or intermittently closed basin, which received water from streams that drained areas in which Paleozoic sedimentary rocks, Tertiary volcanic rocks, and Proterozoic granitic rocks were exposed. Weathering of these source rocks may have mobilized the uranium, which was then transported by surface and ground waters in the soluble oxidized (U^{+6}) state until it reached the Verde Basin. Evaporation may have concentrated the uranium, and organic material may have reduced it to the less soluble U^{+4} state, thus causing precipitation of disseminated microscopic uraninite or other uranium-bearing materials. Similar processes are depositing uranium in calcareous organic muds in closed-basin lakes and marshes in Nevada (Macke and others, 1990). Concentrations of uranium similar to those in the Verde Formation also characterize calcareous, lacustrine sedimentary rocks in the Cave Creek-Carefree area and in the San Pedro Valley in Arizona. This type of uranium enrichment, therefore, is not confined to a particular region or to rocks of a particular age.

Correlation with Indoor-Radon Levels

Between 1987 and 1989, the ARRA sampled 40 homes in the Camp Verde area for indoor radon using charcoal canisters. The EPA recommends that occupants of homes with indoor-radon levels above 4 picocuries per liter (pCi/l) take action to reduce these levels. The median indoor-radon level for tested homes in Camp Verde was 1.4 pCi/l, compared with 1.0 pCi/l for all of Arizona. Four homes (10%) in Camp Verde were above 4 pCi/l; three homes (7.5%) were above 10 pCi/l (Fig. 5). In comparison, 5.4% of homes statewide had indoor-radon levels above 4 pCi/l, and only 0.3% had levels above 10 pCi/l (Spencer, this volume, p. 1-9). A greater percentage of homes in the Camp Verde area, relative to homes statewide, contain high (>4 pCi/l) levels of indoor radon, probably because of the anomalous uranium concentrations in the underlying Verde Formation.

CONCLUSION

Portions of the Verde Formation contain elevated uranium concentrations, and a survey of 40 homes suggests that a greater-than-average percentage of homes built on the Verde Formation has indoor-radon levels above the EPA's recommended level of 4 pCi/l. Uranium anomalies in southwestern Tucson (Spencer and others, this volume, p. 10-16) and the Dells Granite near Prescott (Kearfott, 1989) have also been associated with elevated radon levels in overlying homes. The Verde Formation is more widespread than either of these formations and is in an area of population growth. It should, therefore, be considered a potentially significant source of indoor radon.

The mudstone unit of the Verde Formation commonly contains elevated uranium concentrations, but the soft white marls and carbonate mudstones within this unit have the greatest potential to produce elevated levels of indoor radon gas. These rocks are best exposed in and around Camp Verde and below the limestone bluffs on the eastern side of the Verde River from about 4 mi southeast of Camp Verde to about 2 mi north of Middle Verde.

The upper limestone unit apparently does not contain elevated uranium concentrations over most of its extent. Some soft white marls and carbonate mudstones are, however, intercalated with the nonanomalous rocks of the limestone unit and may be uraniferous. The most notable example of anomalous strata within the limestone unit is an area just east of Cottonwood (Fig. 2). Scattered and isolated uranium anomalies were detected in parts of the Verde Formation that are remote from the lower mudstone unit. Residents of homes built on the limestone unit should not ignore the possibility that their homes may contain elevated radon levels.

REFERENCES

Billingsley, G.H., Conway, C.M., and Beard, L.S., 1988, Geologic map of the Prescott 30- x 60- minute quadrangle, Arizona: U.S. Geological Survey Open-File Report 88-372, 8 p., scale 1:100,000.

Emer, D.F., Shenk, J.D., and Spencer, J.E., 1988, Reconnaissance gamma-ray spectrometer survey of radon-decay products in selected populated areas of Arizona: Arizona Geological Survey Open-File Report 88-12, 88 p.

geoMetrics, undated, Operating manual, model GR-310 gamma-ray spectrometer: Sunnyvale, Calif., 51 p.

Jenkins, O.P., 1923, Verde River lake beds near Clarkdale, Arizona: American Journal of Science, v. 5, p. 65-81.

Kearfott, K.J., 1989, Preliminary experiences with ^{222}Rn gas in Arizona homes: Health Physics, v. 56, no. 2, p. 169-179.

Macke, D.L., Schumann, R.R., and Otton, J.K., 1990, Uranium distribution and geology in the Fish Lake surficial uranium deposit, Esmeralda County, Nevada: U.S. Geological Survey Bulletin 1910, 22 p.

Nations, J.D., and Ranney, W.D.R., 1989, Geologic model of a Cenozoic basin in Arizona, *in* Tooker, E.W., ed., Arizona's industrial rock and mineral resources—Workshop proceedings: U.S. Geological Survey Bulletin 1905, p. 44-53.

Wadell, J.S., 1972, Sedimentation and stratigraphy of the Verde Formation (Pliocene), Yavapai County, Arizona: Tempe, Arizona State University, M.S. thesis, 110 p., 2 plates, scale 1:62,500.

Weir, G.W., Ulrich, G.E., and Nealey, L.D., 1989, Geologic map of the Sedona 30' x 60' quadrangle, Yavapai and Coconino Counties, Arizona: U.S. Geological Survey Miscellaneous Investigations Series Map I-1896, scale 1:100,000.

Uranium and radon in the Prescott area, Yavapai County[1]

JOHN T. DUNCAN
JON E. SPENCER
Arizona Geological Survey, 845 N. Park Ave., #100, Tucson, Arizona 85719

INTRODUCTION

Prescott and Chino Valley are populated areas that contain uranium-rich rocks. The climate in these areas (i.e., seasonally cold weather that requires indoor heat and closed doors and windows) increases the probability that indoor-radon hazards are greater there than in lower elevation, desert areas in Arizona. This report is the product of an investigation of the concentration, distribution, and geologic affinities of uranium in the Prescott area. The data are used to assess the potential for anomalously high indoor-radon levels in this area.

The study area is in central Arizona, about 80 miles north-northwest of Phoenix. It extends from south of Prescott to north of Paulden and includes parts of Prescott and Chino Valleys and the surrounding hills (Fig. 1). In the southern part, the bedrock is mostly Proterozoic crystalline rock; in the northern part, the bedrock is mostly Tertiary sedimentary and volcanic rock but includes relatively minor amounts of Paleozoic sedimentary rock. The large valleys contain late Tertiary and Quaternary alluvium and lacustrine sediments.

The populated sections of the study area were surveyed with a geoMetrics GR-310 gamma-ray spectrometer to detect bismuth-214, a uranium-238 decay product. Most of these sections, including granitic rocks in the Prescott area and lacustrine sediments near Prescott Valley, did not contain anomalous concentrations of uranium (>6 parts per million [ppm], as defined in Duncan and Spencer [this volume, p. 93-96]). Three rock units, however, were recognized as uranium enriched and, thus, as potential radon hazards: the Dells Granite northeast of Prescott; a small, unnamed, mafic, alkalic volcanic-flow unit in Prescott; and the Sullivan Buttes Latite near Paulden. This study included field observations; gamma-ray surveys; petrographic studies; and commercial, whole-rock, geochemical, and uranium analyses.

DELLS GRANITE

The Dells Granite, which is named for the community of Granite Dells, about 5 mi northeast of Prescott on U.S. Highway 89 (Fig. 1), is an undeformed alkalic granite dated at 1,400 ± 15 m.y. (Silver and others, 1980). The Dells Granite has been studied by several researchers and is known to contain elevated uranium concentrations (Proctor and others, this volume, p. 61-81). The association of the Dells Granite with high levels of indoor radon has been documented by Kearfott (1989). Although we did not examine the Dells Granite closely for this study, we did try to determine if weathering of the granite has contributed anomalous amounts of uranium to surrounding geologic materials.

Uranium concentrations of up to 6 ppm have been measured in stream sediments immediately downstream from the Dells Granite (Clark, 1979). This suggests that minor secondary concentrations of uranium may also be present in the sediments of Chino and Lonesome Valleys. This study, however, revealed no evidence of a plume of uranium-enriched sediments downslope or downstream from outcrops of the Dells Granite. Weathered surface exposures of the Dells Granite are typically depleted in uranium compared to fresh samples (see also Proctor and others, this volume, p. 61-81). Leaching of uranium during chemical weathering implies mobility in ground or surface waters and suggests that significant amounts of uranium may have been redeposited in rocks in which conditions were conducive to uranium precipitation (Proctor and others, this volume, p. 61-81). No such secondary concentrations, however, were noted in this study. Uranium mobility in ground water is verified by a uranium concentration of 58.7 parts per billion (ppb) — compared to a median background concentration of 2.5 ppb — in well water immediately downgradient from outcrops of the Dells Granite (Clark, 1979).

[1]This study was supported by the Arizona Radiation Regulatory Agency, with funds provided by the U.S. Environmental Protection Agency, Arizona State Indoor Radon Grant Program K1-009544-01-0.

in Spencer, J.E., ed., 1993, Radon in Arizona: Arizona Geological Survey Bulletin 199, p. 57-60.

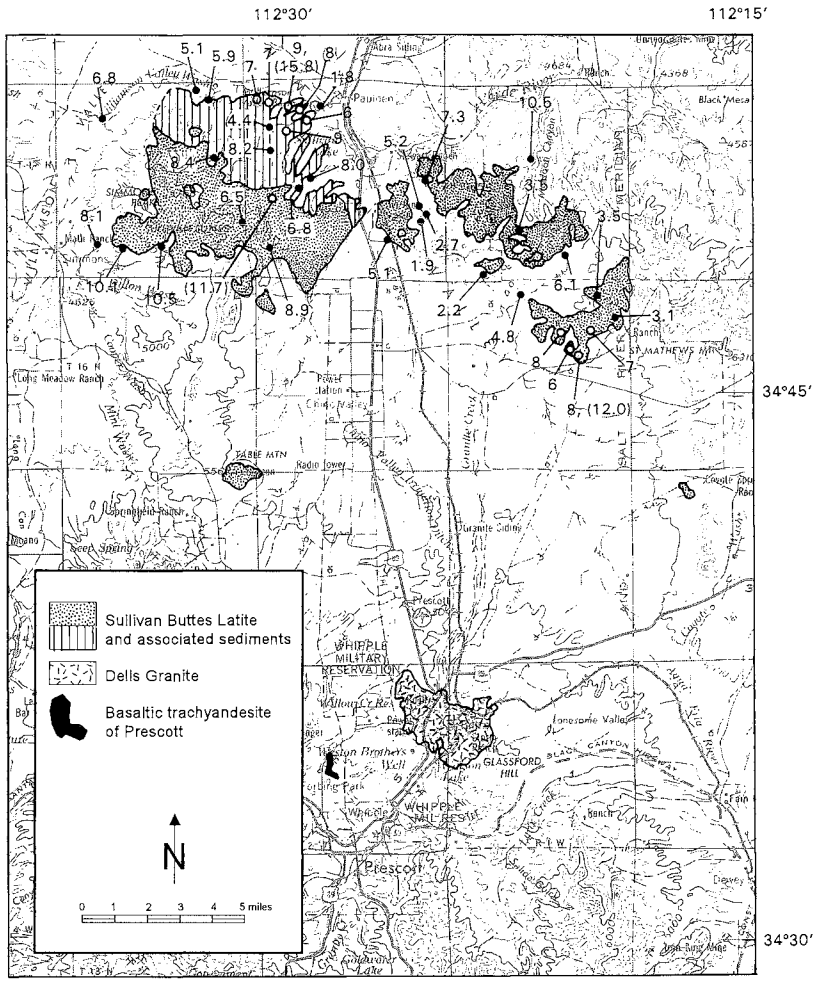

Figure 1. Study area and outcrops of known uranium-rich rocks in the Prescott area. Solid dots and numbers represent stream-sediment sample locations and uranium concentrations from Clark (1979). Open circles represent sample locations and gamma-ray-spectrometer uranium assays made during this study. Numbers in parentheses are commercial uranium analyses. All uranium values are in parts per million.

MAFIC VOLCANIC ROCKS IN PRESCOTT

In their reconnaissance study, Emer and others (1988) reported a basalt exposed within the city of Prescott that contains relatively high concentrations of uranium. The unit was revisited for this study and found to contain up to 11 ppm uranium, as well as relatively high thorium concentrations. Although the outcrop is not extensive (Fig. 2), it is located in a densely populated residential area. The rock is dark brown to black, is slightly vesicular, and contains no phenocrysts discernible in hand samples. Small (<1 mm) blebs of reddish iron oxides possibly represent oxidized olivine. Silica and total alkali content (Table 1, sample PRB), as plotted on the classification diagram of LeBas and others (1986), indicates that the unit is basaltic trachyandesite. The unit shows no evidence of mineralization. It is one of many mesoscopically similar flows in a sequence of Tertiary volcanic and sedimentary rocks that is widely exposed in the study area. This unit directly overlies Proterozoic granite and, as the oldest unit in the volcanic pile, may be more closely related to the older Sullivan Buttes Latite (discussed below) than to the overlying basaltic rocks. Although we identified no other uranium-enriched volcanic rocks in the town of Prescott, we may have missed some small areas.

SULLIVAN BUTTES LATITE AND ASSOCIATED SEDIMENTS

A large area of Tertiary intermediate volcanic rocks and associated sediments is exposed in the Sullivan Buttes southwest of Paulden (Fig. 1). These rocks were described in detail by Krieger (1965) and later by Tyner (1979, 1984) and Tyner and Smith (1986). They were mapped as andesite (Krieger, 1965, 1967) but were named Sullivan Buttes Latite on the basis of geochemical analysis and dated as late Oligocene to early Miocene (Krieger and others, 1971). They are gray to brown, intermediate volcanic rocks that are distinctive in the field because they typically contain abundant ultramafic to mafic inclusions. The inclusions are angular to well rounded and variable in composition. Inclusions commonly consist of unaltered garnet-amphibolite; abundant, partially altered, clinopyroxene-magnetite rock; and highly altered peridotite represented by epidote, iron oxide, talc(?), and other unidentified alteration products. In some outcrops, the inclusions make up 15 to 20% of the total rock volume. The host volcanic rocks typically contain a combination of mafic phenocrysts (amphibole, biotite, or pyroxene) in a fine-grained to aphanitic or glassy matrix in which feldspar microlites are the only identifiable minerals. Quartz and feldspar are rare or absent as phenocrysts.

Whole-rock geochemistry (Table 1, samples SB-1, SB-2, and SB-3) indicates that these rocks are enriched in potassium and, although of intermediate composition based on silica content, are also relatively enriched in magnesium and titanium.

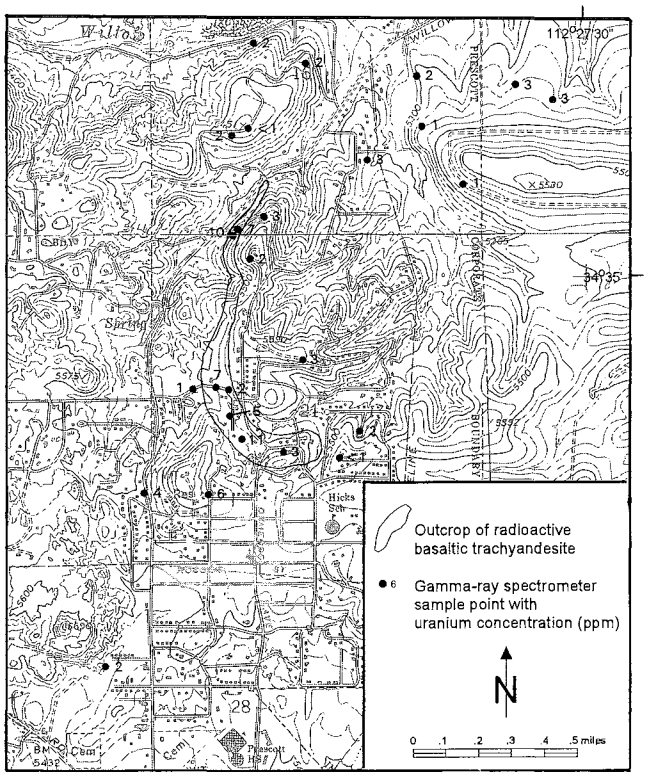

Figure 2. Outcrop of uranium-rich basaltic trachyandesite in Prescott. Numbered dots represent gamma-ray-spectrometer sample locations and uranium assays in parts per million.

Previously classified as latites or potassic latites (Krieger and others, 1971; Tyner and Smith, 1986), the Sullivan Buttes Latite plots as trachyandesite and trachydacite on the classification diagram of LeBas and others (1986). The unusual composition of these latites (rich in both alkalies and mafic elements) and their phenocryst content also allow classification as calc-alkaline lamprophyres (Rock and others, 1989).

The Sullivan Buttes Latite is strongly enriched in uranium and thorium. Outcrops are identifiable by airborne radiometry as a large area that contains greater than 5-ppm-equivalent uranium (Plate 1). A stream-sediment survey also revealed consistently anomalous uranium values (Fig. 1) and elevated thorium concentrations in and around outcrops of Sullivan Buttes Latite (Clark, 1979). A gamma-ray spectrometer survey conducted as part of this study indicated up to 9 ppm uranium in the rocks. Similar values were recorded in latite-derived coarse gravels that are widespread on the northern flanks of the Sullivan Buttes and in latite-derived sediments southwest of Paulden (Fig. 1). These gamma-ray spectrometer assays are somewhat low because of uncertainty in corrections for thorium content, which is also anomalous. Four samples of Sullivan Buttes Latite analyzed commercially by delayed-neutron counting averaged 11.4 ppm uranium and contained up to 15.8 ppm uranium. Commercial analyses indicate that the two samples of latite-derived sediments averaged 9.8 ppm uranium.

High potassium and thorium contents are characteristic of alkalic volcanic rocks (Turner and Verhoogen, 1960). The uranium enrichment in the Sullivan Buttes Latite probably resulted from magmatic processes similar to those that concentrated the potassium and thorium. Felsic, alkalic intrusive rocks, such as the Proterozoic Dells Granite, are well recognized in Arizona as being uranium enriched. Intermediate-composition, alkalic volcanic rocks, such as the Sullivan Buttes Latite and similar rocks surveyed in this study, should also be recognized as potential concentrators of uranium and thorium, based on the results of this study.

Table 1. Major-element-oxide and uranium geochemistry for six mid-Tertiary volcanic rocks from central Arizona. Samples SB-1, SB-2, and SB-3 are Sullivan Buttes Latite; sample PRB is a mafic volcanic rock exposed in Prescott (see Fig. 2); samples NR and PM are inclusion-rich volcanic rocks exposed near New River and in the Phoenix Mountains, respectively. LOI is loss on ignition.

Sample	SB-1	SB-2	SB-3	PRB	NR	PM
SiO_2	59.68	62.32	60.15	53.42	59.99	59.62
Al_2O_3	14.92	14.13	13.74	12.38	14.74	13.76
Fe_2O_3	5.86	5.01	5.19	7.39	5.31	5.22
MnO	0.08	0.08	0.06	0.10	0.08	0.06
MgO	3.08	3.59	4.51	8.29	2.35	4.38
TiO_2	0.91	5.01	0.89	1.52	1.00	1.03
CaO	6.08	5.01	4.62	6.63	5.27	5.40
Na_2O	3.11	2.85	2.57	2.39	2.74	2.38
K_2O	3.48	4.99	5.23	4.94	5.17	6.40
P_2O_5	0.17	0.16	0.17	0.39	0.16	0.34
BaO	0.15	0.17	0.17	0.19	0.14	0.19
LOI	2.75	2.43	3.26	3.24	1.81	3.11
TOTAL	100.25	101.50	100.55	100.90	98.77	101.90
U (ppm)	15.8	11.7	12.0	10.8	8.4	14.1

OTHER SIMILAR ROCKS

The high uranium and thorium contents and similar bulk-rock chemistry suggest that the small exposure of basaltic trachyandesite in Prescott may be genetically related to the Sullivan Buttes Latite. Other Tertiary volcanic rocks with enriched uranium and thorium are also chemically similar to the Sullivan Buttes Latite, including volcanic rocks in the Phoenix Mountains (Table 1, sample PM) and west of New River (Table 1, sample NR). The New River volcanic rocks are nearly identical to the Sullivan Buttes Latite in field and petrographic characteristics. Although not analyzed for uranium, similar rocks have also been identified near Camp Creek, Arizona (Esperanca, 1984). These observations suggest that there is a suite of genetically related, chemically anomalous, alkalic rocks in central Arizona that are commonly uranium enriched.

POTENTIAL RADON HAZARDS

Radon hazards are associated with uranium-enriched rocks. The study area covered in this report contains one rock type, the Dells Granite, that has been documented as being highly enriched in uranium (up to 40 ppm) and is a known source of elevated indoor radon (Kearfott, 1989). The other, less well known, uranium-enriched rocks in the area are mid-Tertiary volcanic rocks and associated sedimentary rocks. Although not as enriched as the Dells Granite, these rocks are distinctly anomalous, and some contain more than 15 ppm uranium. Outcrops are not extensive in the most densely populated areas; however, these rocks are widespread in areas of growing population and, thus, could become significant sources of indoor radon. Where present in the subsurface, these uranium-rich rocks could also contribute radon to ground water.

REFERENCES

Clark, R.J., 1979, Hydrogeochemical and stream sediment reconnaissance basic data report for the Prescott NTMS quadrangle, Arizona: U.S. Department of Energy Open-File Report GJBX-122, 92 p., 6 sheets, scale 1:250,000.

Emer, D.F., Shenk, J.D., and Spencer, J.E., 1988, Reconnaissance gamma-ray spectrometer survey of radon-decay products in selected populated areas of Arizona: Arizona Bureau of Geology and Mineral Technology Open-File Report 88-12, 88 p.

Esperanca, Sonia, 1984, An experimental and geochemical study of the high-K latites and associated nodules from Camp Creek, Arizona: Tempe, Arizona State University, Ph.D. dissertation, 204 p.

Kearfott, K.J., 1989, Preliminary experiences with ^{222}Rn gas in homes: Health Physics, v. 56, no. 2, p. 169-179.

Krieger, M.H., 1965, Geology of the Prescott and Paulden quadrangles, Arizona: U.S. Geological Survey Professional Paper 467, 127 p., 4 sheets, scale 1:48,000.

_____ 1967, Reconnaissance geology of the Simmons quadrangle, Yavapai County, Arizona: U.S. Geological Survey Map I-503, scale 1:62,500.

Krieger, M.H., Creasey, S.C., and Marvin, R.F., 1971, Ages of some Tertiary andesitic and latitic volcanic rocks in the Prescott-Jerome area, north-central Arizona, *in* Geological Survey research 1971: U.S. Geological Survey Professional Paper 750-B, p. B157-B160.

LeBas, M.J., LeMaitre, R.W., Streckeisen, Albert, and Zamettin, Bruno, 1986, A chemical classification of volcanic rocks based on the total alkali-silica diagram: Journal of Petrology, v. 27, p. 745-750.

Rock, N.M.S., Groves, D.I., Perring, C.S., and Golding, S.D., 1989, Gold, lamprophyres, and porphyries: What does their association mean?, *in* Keays, R.R., Ramsay, W.R.H., and Groves, D.I., eds., The geology of gold deposits: The perspective in 1988: Economic Geology Monograph 6, p. 609-625.

Silver, L.T., Williams, I.S., and Woodhead, J.A., 1980, Uranium in granites from the western United States; actinide parent-daughter systems, sites, and mobilization: U.S. Department of Energy Open-File Report GJBX-345(81), 380 p.

Turner, F.J., and Verhoogen, John, 1960, Igneous and metamorphic petrology: New York, McGraw-Hill Book Co., Inc., 694 p.

Tyner, G.N., 1979, Field geology, petrology, and trace element geochemistry of the Sullivan Buttes Latite, Yavapai County, Arizona: Austin, University of Texas, M.S. thesis, 136 p.

_____ 1984, Geology and petrogenesis of the Sullivan Buttes Latite, Yavapai County, Arizona: Field and geochemical evidence: Austin, University of Texas, Ph.D. dissertation, 248 p.

Tyner, G.N., and Smith, Douglas, 1986, Peridotite xenoliths in silica-rich, potassic latite from the Transition Zone of the Colorado Plateau in north-central Arizona: Contributions to Mineralogy and Petrology, v. 94, p. 63-71.

Radiometric and petrochemical characteristics of the Dells Granite, Yavapai County[1]

PAUL D. PROCTOR[2]
KENNETH S. FLECK[3]
AHMED N. SHAHIN[4]

Department of Geology and Geophysics, University of Missouri, Rolla, Missouri 65401

INTRODUCTION

This study was done to fulfill three objectives concerning granites, which, among igneous rocks, contain the highest concentrations of uranium (U) and thorium (Th): (1) to identify the distribution patterns of U, Th, and potassium (K) within an anomalously radioactive granitic pluton, in this case the Dells Granite in central Arizona; (2) to relate these patterns, where possible, to the major-element petrochemistry, mineralogy, and physical characteristics of the rock; and (3) to determine the possibility of solution of U and its downward migration into the granite and surrounding sediments, as well as its possible deposition and enrichment in these geologic environments.

Fieldwork included geologic mapping of the Dells Granite and surrounding rocks, as well as a detailed, gridded radiometric (RM) survey with a portable gamma-ray spectrometer. Laboratory studies included X-ray fluorescence (XRF) analyses of 65 rock samples for 10 major-element oxides and petrographic examination of 48 thin sections. Autoradiographs permitted site identification of U and Th.

Data from this study provide an understanding of the highly radioactive character of the granite and the distribution patterns of radioactive elements within the pluton. The following are of special interest: (1) the granite's mineralogy, chemical composition, and alteration and structural features and the relationship between these and mobilized U; and (2) the possible development of enriched radioactive deposits within the granite and adjacent sediments. Increased knowledge may be useful in the study of other radioactive granites and in the exploration for U ore deposits in these environments.

LOCATION

The Dells Granite is named after Granite Dells, a small town in Yavapai County, Arizona (Fig. 1), approximately 8 km (5 mi) northeast of Prescott. U.S. Highway 89 cuts across the center of the pluton, which is exposed at the western edge of Chino Valley. The pluton lies between the northern end of the Bradshaw Mountains on the west and the Black Hills on the east. It covers about 7.25 sq km (4.5 sq mi) and is within T. 14 N., R. 1 W., secs. 7, 8, 17, 18, and 19 and T. 14 N., R. 2 W., secs. 1, 2, 11, 12, 13, 14, and 24.

Younger rocks and alluvial sediments cover the igneous body on all sides, effectively masking contacts with the host rocks. Tertiary basalts and the Glassford Hill volcanic cone cover the southeastern side of the pluton. Tertiary conglomerates, overlain by younger Tertiary basalts, cover it on the southwest, whereas Tertiary fanglomerates and Quaternary pediment, terrace gravels, and alluvium overlie it on the northeast. Krieger (1965) showed the pluton within Precambrian schists and gneisses.

Willow Creek Reservoir covers part of the western side of the igneous body; Watson Lake covers a portion on the southwest. These reservoirs supply water to Prescott.

SURFACE FORM

The Dells Granite crops out at elevations between 1,547 and 1,759 m (5,100 and 5,800 ft). Most of the pluton is bare rock. The topography is rugged, of high relief, and strictly joint controlled. Weathering and erosion along the joints have produced an unusual set of blocky prominences, straight vertical-walled valleys with local relief up to 91 m (300 ft), and a rectangular drainage system. Several areas of the pluton consist of rounded to flattened exposures that are

---

[1]This report supersedes the following report: Proctor, P.D., Fleck, K.S., and Shahin, A.N., 1987, Radiometric and petrochemical characteristics of the Dells Granite, Yavapai County, Arizona: Arizona Bureau of Geology and Mineral Technology Open-File Report 87-8, 67 p.

[2]Present address: Dept. of Geology, Brigham Young University, Provo, UT 84602.

[3]Present address: Energy West Mining Co., P.O. Box 310, Huntington, UT 84528.

[4]Present address: Gulf of Suez Petroleum Co. (GUPCO), P.O. Box 2400, Cairo, Egypt.

in Spencer, J.E., ed., 1993, Radon in Arizona: Arizona Geological Survey Bulletin 199, p. 61-81.

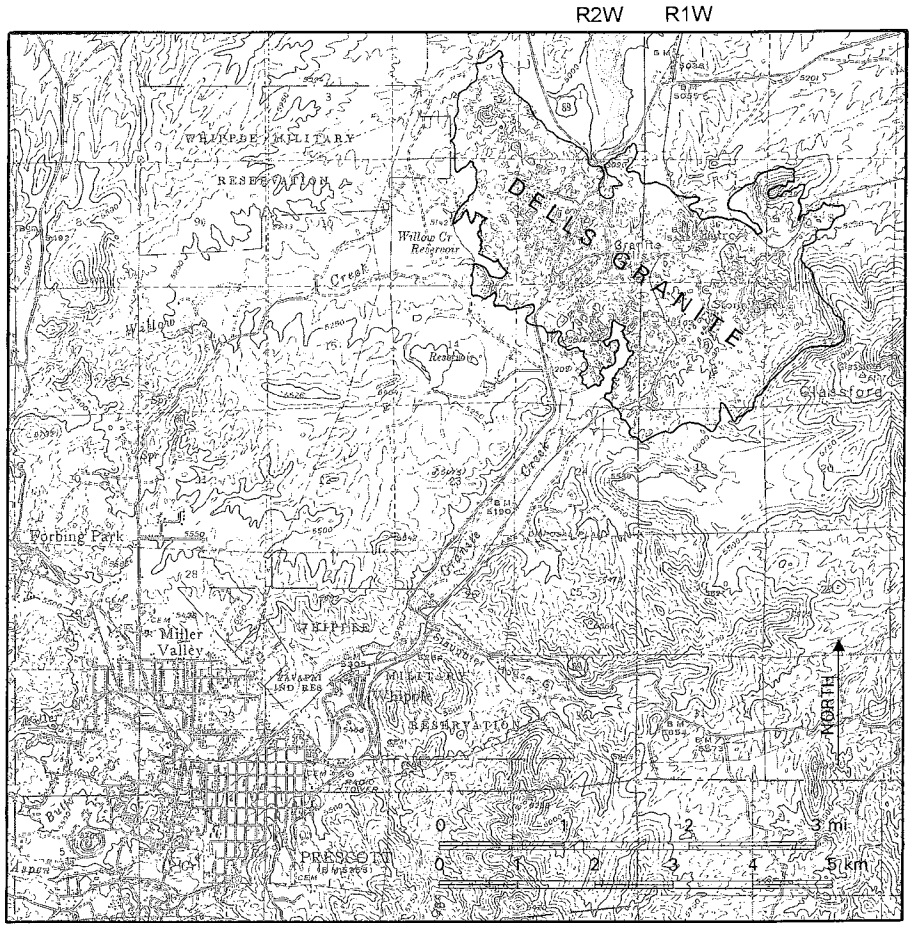

Figure 1. Index map showing the location of the Dells Granite.

relatively less jointed and more weathered than the rest of the igneous body. These areas are covered with soil that supports ponderosa pine and juniper, which are uncommon in this region at such low elevations.

The Dells Granite is light pinkish gray to orange. On fresh surfaces, it is usually light gray to white. Surface exposures are very rough because of weathering and erosion along the numerous joints. Distinctive concentric bands resembling bull's-eyes consist of brown to black iron oxides and stain the rock parallel to the joint surface.

PREVIOUS WORK

Evans and Goodman (1941), Keevil and others (1944), Larsen and Phair (1954), Whitfield and others (1959), Larsen and Gottfried (1960), and Rogers and Ragland (1961), among others, measured U and Th contents in various igneous rocks. Their results showed that U, Th, and K, which follow similar paths during magmatic differentiation, tend to be concentrated in late differentiates such as granites, alkali granites, and pegmatites.

Larsen and others (1956), Adams and others (1959), Vinogradov (1963), and Ragland and others (1967) described the geochemistry of U, Th, and K. Heier and Adams (1965) and Lambert and Heier (1967) concluded that mobile U and Th tend to migrate upward and away from areas of prograde metamorphism deep within the Earth's crust.

Chentsov (1961) measured concentrations of U and Th in rock-forming minerals. He found the highest concentrations in accessory zircon, allanite, and monazite and the lowest concentrations in major rock-forming minerals. U and Th isomorphically or endocryptically substitute for calcium (Ca), iron (Fe), and magnesium (Mg) in the crystal lattices of these accessory minerals.

Numerous studies described the U, Th, and K concentrations of granite bodies in various locations worldwide. Particularly related to this study are reports on the Conway Granite of New Hampshire, which is enriched in U and Th (Adams and others, 1962; Rogers and Adams, 1963), and on the U-Th province of the Colorado Front Range (Phair and Gottfried, 1964). Heier and Rhodes (1966) noted the high levels of U, Th, and K in a leucocratic granite in the Rum Jungle igneous complex of Australia. This body is similar to the Dells Granite of Arizona. Stuckless and Nkomo (1978) and Stuckless and others (1981) discussed the possible leaching of U from the granite of Granite Mountains, Wyoming. Malan and Sterling (1969) and Malan (1972) described the results of extensive studies of U and Th in Precambrian rocks of the western United States and Missouri. O'Brien (1978) and Proctor and O'Brien (1980) conducted a detailed study of the U, Th, and K distributions in the Graniteville Granite of Missouri, one of the most radioactive granites in the United States. Fleck and others (1981) compared the U, Th, and K characteristics of the Graniteville Granite with those of the Dells Granite of Arizona; Proctor and others (1981) compared the Graniteville Granite with the Bokan Mountain Granite of Alaska. Silver and others (1980, 1984) investigated U and Th distributions in radioactive granites of central Arizona, including the Dells Granite, and described elevated U in accessory zircon. Krieger

(1965) studied the Dells Granite as part of a regional study of sulfide ore deposits at Jerome and Humboldt, Arizona, but did not note the high radioactivity of the granite or its U and Th concentrations.

Malan and Sterling's (1969) study of Precambrian rocks of California, Nevada, Arizona, and New Mexico included an analysis of a sample of the Dells Granite but did not note that it was anomalously radioactive. In a later paper, Malan (1972) summarized the distribution of U, Th, and K in the Precambrian rocks of the western United States and included a geochronology of western Precambrian igneous plutons. He concluded that granites contain the highest concentrations of U, Th, and K (4.7 parts per million [ppm], 37.8 ppm, and 4.1%, respectively) of all rock types studied. He also noted that U and Th concentrations are highest in granites formed during the Mazatzal Revolution, about 1,400 m.y. ago. P.D. Proctor, A.N. Shahin, and P. Doraibabu sampled and performed a reconnaissance gamma-ray spectrometer survey of the Dells Granite in 1978; they reported anomalous U and Th concentrations and RM response for the pluton. A.N. Shahin described mineralogical and petrographic characteristics, major-element analyses by XRF, and modal classification of the Dells Granite.

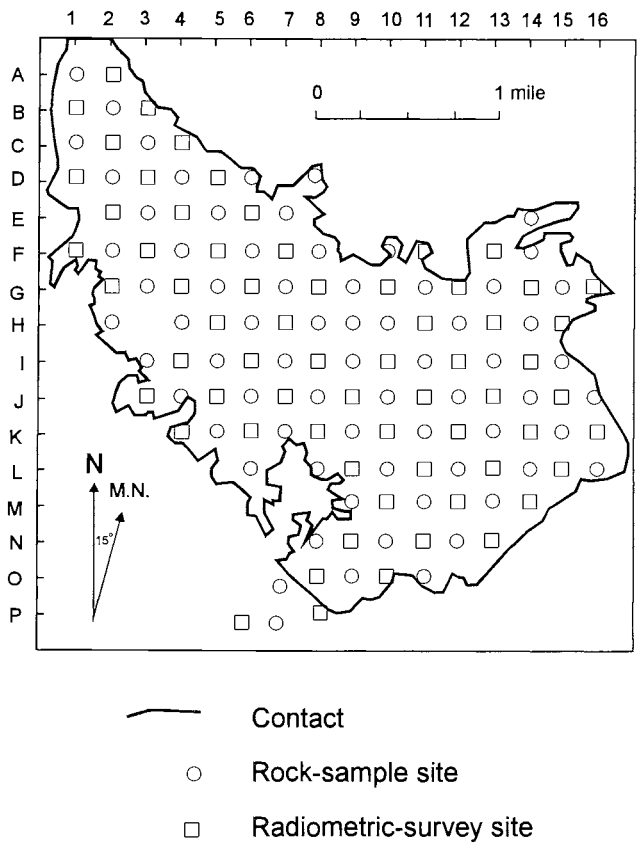

Figure 2. Rock-sample and RM-survey sites for the Dells Granite.

Aero Service (1979) described "Anomaly 23" from the Dells Granite as "an excellent U, U/K, and U/Th anomaly" and the pluton as one of the most radioactive granites in Arizona. Based partially on the results of this aerial RM survey, Silver and others (1980, 1984) studied one sample of the Dells Granite that weighed approximately 50 kg (110 lb). They discovered new information on major- and trace-element mineralogy and geochemistry and on U-Th-lead [Pb] systematics. They also radiometrically dated the granite at 1,400 ± 15 m.y. The sample yielded 39.6 ppm U and 35.6 ppm Th.

FIELD STUDY

The contacts of the granite body were outlined from aerial photographs of the Granite Dells region. A north-south, east-west grid of 303-m (1,000-ft) spacing was plotted on topographic maps and aerial photos, and sample sites were located at the grid intersections. These sites are identified in Figure 2 by letters on the y (north-south) axis and by numbers on the x (east-west) axis.

The field study of the Dells Granite included (1) an RM survey for each of the elements U, Th, and K, as well as a total RM response; (2) rock-sampling; and (3) geologic mapping. RM readings, rock samples, and geologic data were obtained at about 140 evenly spaced field stations across the igneous body. Rugged terrain made it necessary to relocate some stations, but these were no more than 15 m (50 ft) from the original locations.

RM Survey

A portable Scintrex GAM-1 gamma-ray spectrometer was used to determine U, Th, and K concentrations in the pluton. The instrument identifies gamma-ray energies associated with the U daughter product bismuth-214 (^{214}Bi; 1.76 mega electron volts [MeV]), the Th daughter product thallium-208 (^{208}Tl; 2.615 MeV), and the K isotope ^{40}K; (1.46 MeV), as well as total RM response. The energy responses of the daughter products are read separately from a meter, which registers from 1 to 10,000 counts per second (cps). Readings are converted into equivalent percentage for K and equivalent parts per million for U and Th through a series of equations (Baird and Nargolowalla, 1975).

Field procedures followed a consistent routine to minimize instrument and personal bias. This daily routine included a half-hour warmup of the instrument, calibration at a set location over low-RM-response alluvium, and background readings

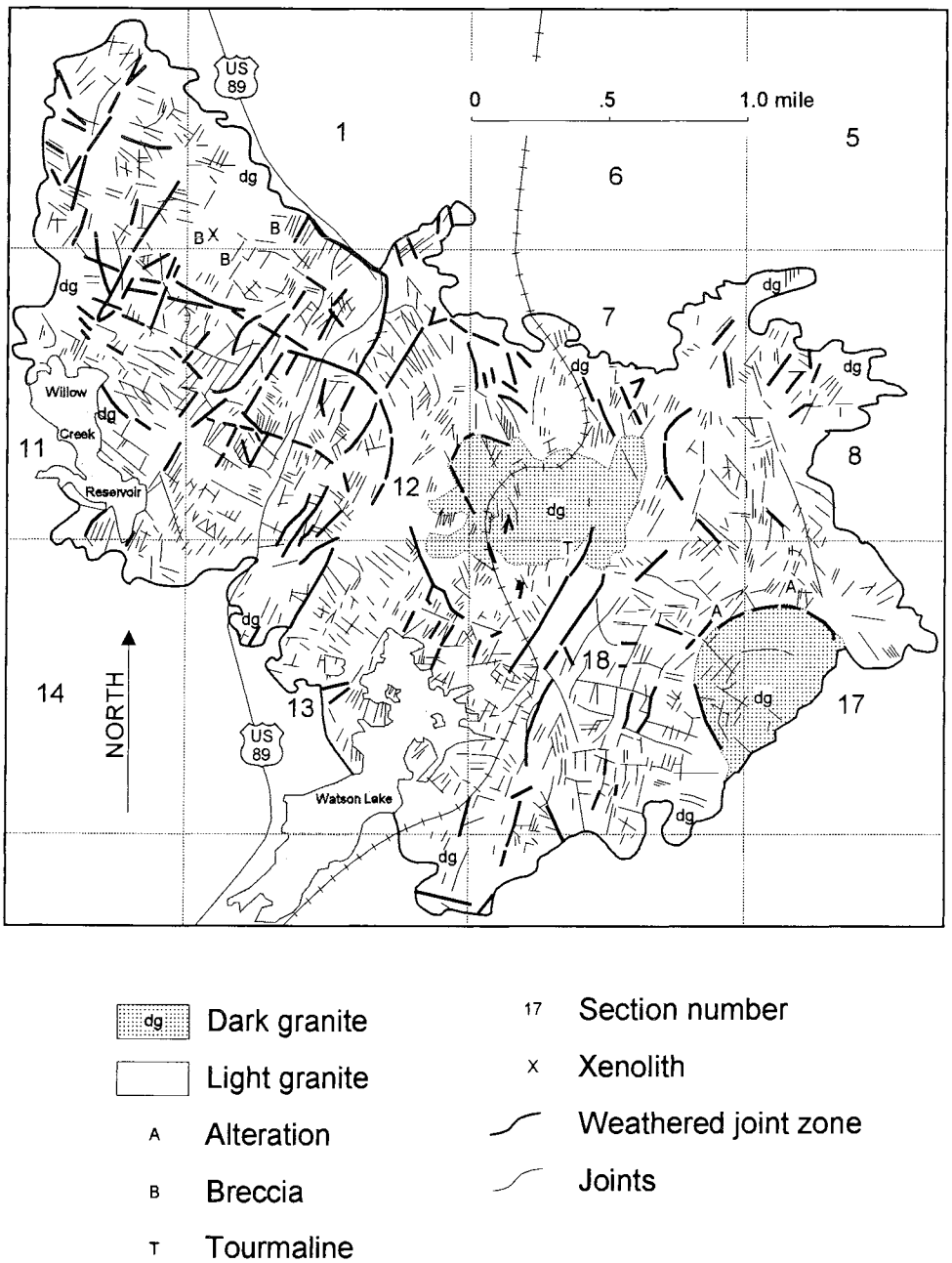

Figure 3. Geologic map of the Dells Granite.

on all four channels. The RM survey followed, with recalibration each hour.

RM response was measured on all four channels at five separate locations at each station to obtain the optimum rock-detector geometry for readings. Readings were commonly taken with the spectrometer held directly against flat rock surfaces. Twenty readings were made at each station: five for each element plus five for total RM response.

Sampling and Mapping

Rock samples weighing 0.23 kg (0.5 lb) were collected at each of the 140 stations (Fig. 2). Most samples were weathered granite. Samples from pegmatite and quartz-tourmaline veins, rhyolite dikes, and xenoliths were also collected for laboratory study. Weathering characteristics, rock alteration, lithologic characteristics, and joint orientations were identified at each of the stations and are shown on a geologic map (Fig. 3).

LABORATORY INVESTIGATIONS

XRF Analysis

Sixty-five evenly distributed rock samples from the original 140 were selected for XRF analysis. Samples were broken, pulverized to -200 mesh or smaller in a Spex model shatterbox, and pressed into 4.1-cm (1.6-in.)-diameter pellets, with boric acid as a substrate, for direct use in the sample holders of a Phillips 1410-1140 XRF spectrometer. The failure rate of sample pellets was greatly reduced when they were heated to 275°C (527°F) on a heating plate before XRF analysis. (This procedure eliminates water absorbed in clay minerals in the weathered granite. The water normally vaporizes rapidly as vacuum is applied and causes the compressed rock powder to break out of the boric acid substrate.)

The XRF spectrometer measured the responses of 10 major-element oxides in the 65 samples, as well as the U content in 20 samples. The oxides included Fe, Mg, Ca, K, silicon (Si), aluminum (Al), sodium (Na), titanium (Ti), phosphorus (P), and manganese (Mn). Samples were analyzed in groups of three. Before and after the analysis of each element in the sample group, a standard rock slab

was analyzed for that element to correct for background noise and instrument drift.

Raw spectrometer analytical data were entered into a Tektronix 31 desk calculator using software developed by Dr. Sheldon K. Grant of the Geology and Geophysics Department of the University of Missouri at Rolla. The program permits direct computation of the percentages of the 10 major-element oxides in each sample, normalizes them to 100%, calculates the percentages of normative mineral molecules by the C.I.P.W. system (Johannsen, 1931), and calculates ratios of orthoclase, albite, and anorthite for each sample.

Petrographic Study

Forty-eight thin sections were studied to determine the petrography and petrology of the Dells Granite and associated rocks. Seventeen were of the Dells Granite, 18 of associated granites (10 darker granites, 8 altered granites), 4 of veins, 4 of dikes, and 5 of xenoliths and other inclusions.

A major objective was to verify reported petrographic details (Krieger, 1965; A.N. Shahin, personal commun., 1980) and to understand better the general petrography and petrology of this unique granite. A second objective was to identify possible U-bearing accessory minerals and characteristics of the darker phases of the granite, pegmatites, quartz-tourmaline veins, intrusive dikes and pipes, xenoliths, and breccia fragments that were not detailed in earlier reports.

Autoradiography

An autoradiograph of a rock is taken by placing X-ray film in direct contact with a radioactive rock slab or thin section. The plate is exposed by the natural radioactivity of the minerals in the rock.

Twenty Dells Granite rock samples, cut into slabs and ground as flat as possible, were placed directly on individual sheets of standard DuPont X-ray film. Exposed for 3.5 weeks, the film gave acceptable results. The most radioactive minerals showed as dark spots and patches on the developed film. The least radioactive and nonradioactive minerals, together with unexposed portions of the film, remained essentially transparent.

REGIONAL GEOLOGY AND GEOLOGIC HISTORY

The Dells Granite is exposed at the western edge of Chino-Lonesome Valley, within the Transition Zone between the Colorado Plateau Province to the northeast and the Basin and Range Province to the southwest. Tertiary block faulting has affected the Transition Zone, but Paleozoic strata that were not removed by erosion still lie essentially flat (Wilson, 1962).

Older Precambrian rocks in the area consist of intensely metamorphosed basaltic, andesitic, and rhyolitic flows and belong to the Big Bug Group (formerly Alder Formation) of the Yavapai Series (Anderson and others, 1971). About 1,400 m.y. ago, these rocks were intruded by large granitic to gabbroic plutons during an anorogenic intrusive episode (Silver and others, 1977). One such pluton was the Dells Granite.

A long period of uplift and erosion occurred after the Mazatzal Revolution. During the Paleozoic Era, what is now the Dells Granite was at the northern edge of the emergent "Mazatzal Land" (Wilson, 1962). Any Paleozoic sediments deposited near the Dells Granite were stripped away. Krieger (1965) suggested that Mesozoic rocks were not deposited in this area. Paleozoic and Cenozoic rocks near the Dells Granite are all nearly horizontal and lie unconformably on the Precambrian Big Bug Group and plutons within it.

Exposed Tertiary rocks consist of flat-lying basalt and andesite flows, partially eroded cinder cones, and some sedimentary rocks in the Chino-Lonesome Basin. Gravels, sands, silts, clays, and scarce freshwater limestones cover the older rocks.

GEOLOGY OF THE DELLS GRANITE

Mineralogy and Petrography

The Dells Granite is medium to coarse grained and fairly equigranular, with a granitic and slightly porphyritic texture. It is light gray to white on fresh surfaces and pinkish orange to brown on weathered outcrops. The primary minerals are white feldspars, clear-gray to light-blue smoky quartz, and green to black biotite. Accessory minerals include tourmaline, fluorite, hematite, and magnetite. The mineralogy of the Dells Granite is summarized in Table 1.

Microcline composes about 27% of the rock and forms anhedral and interstitial grains up to 5 mm (0.2 in.) in length. Rare phenocrysts range up to 5 cm (2 in.) in length. Albitic plagioclase, An_7 (Krieger, 1965) to An_{10} (Silver and others, 1980), composes up to 35% of the granite and forms large rare phenocrysts (Krieger, 1965) and subhedral to euhedral crystals up to 4 mm (0.16 in.) in length in perthitic intergrowths in microcline. Faint zoning is present in some albite crystals.

Anhedral grains of quartz, somewhat circular in form and up to 5 mm (0.2 in.) in diameter, make up 30 to 35% of the rock. In thin section, the quartz is clear and contains accessory zircon and apatite. In hand specimens, the quartz appears cloudy or smoky. Undulatory extinction of quartz suggests

Table 1. Mineralogy of the Dells Granite.

Primary Minerals	
Microcline	27%
Plagioclase	35%
Phenocrysts	
Perthitic intergrowths in microcline	
Quartz	30-35%
Smoky	
Strained	
Biotite[1] (varying amounts with inclusions of magnetite, specular hematite, ilmenite, and leucoxene with haloes)	
Muscovite	
Hornblende	1%
(inclusions of sphene, apatite, and magnetite)	
Chlorite (alteration of hornblende)	
Accessory Minerals	
Fluorite[1]	Most abundant (in fractures and as inclusions)
Tourmaline[1]	
Magnetite[2]	
Ilmenite[1]	
Hematite[1]	
Leucoxene[1]	
Garnet	
Almandine	
Spessartite	
Andradite	
Grossularite	
Zircon[1] (common intergrowths with thorite)	
Apatite[1]	
Sphene	
Epidote	
Clinozoisite	
Allanite[1] (rare)	
Thorite[1] (often as contemporary inclusions in biotite)	
Xenotime[1]	
Monazite[1]	
Coffinite[1] (rare)	
Niobates[1] (metamict)	
Titanates[1]	
Rutile (rare)	
Several unidentified metamict phases[1]	

[1]Associated with radioactive phase
[2]Radioactive
Source: Present study and Silver and others (1984)

that some strain occurred.

Green to black biotite appears in varying amounts throughout the granite. Krieger (1965) reported the presence of dark-green biotite books up to 4 mm (0.16 in.) in diameter in the northeastern part of the pluton but noted that most of the biotite is bleached to a pale-olive color. The 2V angle of the bleached pale mica is too large for muscovite. Silver and others (1980), however, reported that the granite contained both muscovite and biotite.

Dark pleochroic haloes are visible around included zircons in some biotite grains. Pleochroism ranges from light to dark brown in the green biotite. The bleached biotite is colorless to pale olive and only weakly pleochroic. In some of the biotite grains, alternating platelike grains of magnetite, specular hematite, ilmenite, and leucoxene parallel the (001) cleavage planes. Very dark pleochroic haloes surround some of these alternating platelike or lens-shaped grains. Bleached biotite appears to be associated with deuteric or hydrothermal fluorite (Krieger, 1965), with the latter mainly near biotite grains. Up to 1% hornblende in the rock, which forms green subhedral crystals up to 4 mm (0.16 in.) in length, is associated with biotite. It is locally altered to chlorite and contains sphene, apatite, and magnetite inclusions. Accessory minerals include magnetite, ilmenite, hematite, leucoxene, fluorite, tourmaline, red garnet (Krieger, 1965), zircon, apatite, sphene (this study), epidote, clinozoisite, allanite, thorite, xenotime, and several unidentified metamict phases (Silver and others, 1980).

Tourmaline and fluorite are the most abundant minerals. Tourmaline is present in pegmatitic pods, lenses, and alteration zones and is also disseminated throughout the body. Individual crystals range from less than 1 mm (0.04 in.) to more than 25 cm (10 in.) in length. Some single crystals are triangular in cross section and up to 2 cm (0.8 in.) in diameter. Tourmaline forms large radiating aggregates of fine needlelike crystals up to 30 cm (12 in.) in diameter within quartz or quartz-feldspar pegmatites. In some areas, pipe- or pod-shaped outcrops up to 9.1 m (30 ft) in diameter consist of almost solid, fine-grained tourmaline that composes up to 90% of the total rock mass. The largest of these outcrops grades irregularly outward to tourmaline-quartz rock, then tourmaline-feldspar rock, and finally normal granite within a distance of 1.5 to 15.2 m (5 to 50 ft).

Fluorite appears as small, clear to purple veinlets and granular masses in thin section and in some hand specimens (Krieger, 1965). Colors range from pale green to pink (Silver and others, 1980).

Chemical and Modal Classification

Percentages of the 10 major-element oxides and normative mineral values (Johannsen, 1931) were calculated from XRF analyses of 65 samples of Dells Granite. Normative feldspar values for albite, orthoclase, and anorthite were plotted on the albite-orthoclase-anorthite face of the albite-ortho-

clase-anorthite-quartz tetrahedron, according to the classification proposed by O'Connor (1965) for quartz-rich, igneous rocks (Fig. 4). The feldspar face of the tetrahedron is permitted in this system when the quartz content of the rock is greater than 10%. This classification is particularly applicable to the Dells Granite, in which the quartz content generally exceeds 30%.

Plots of the 65 analyzed samples fall within the granite field (Fig. 4). Feldspars are almost exclusively orthoclase (microcline) and albite, indicating a granite high in K_2O and Na_2O. Anorthite is practically absent; consequently, the CaO content is very low.

Krieger (1965) and A.N. Shahin plotted modal analyses of the minerals within thin sections of the Dells Granite based on quartz-plagioclase-orthoclase ternary diagrams. A.N. Shahin classified these data by the systems described by Johannsen (1931), Bateman and others (1963), and Streckeisen (1967). The Johannsen and Bateman classifications place the Dells Granite entirely within the granite field. The Streckeisen classification, however, categorizes the Dells Granite as a syenogranite.

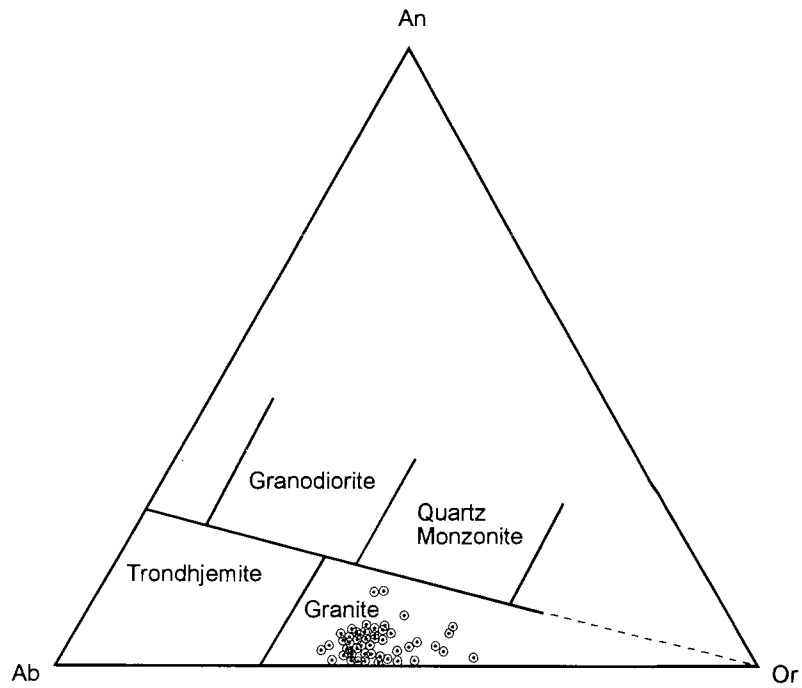

Figure 4. Normative feldspar ratios from the Dells Granite. Sixty-five partial molecular norms are plotted on an albite-orthoclase-anorthite ternary diagam modified from O'Connor (1965).

Structural Characteristics

The Dells Granite varies in texture and mineralogy. Locally the rock grades into pinkish-orange pegmatitic masses, which range from small pockets 15 cm (6 in.) or less in diameter to dikes and lenses several meters (tens of feet) long and up to 60 cm (2 ft) wide. Their composition is simple and includes mostly quartz and feldspar. Quartz is massive, gray to white, and milky or smoky. The principal feldspar is white to pink microcline in crystals up to 25 cm (10 in.) in length (Krieger, 1965). Graphic intergrowths of microcline and quartz are present in several pegmatites, and tourmaline is common as large single crystals in quartz or as radiating masses of fine needlelike crystals. Albite, biotite, and muscovite are also present (Krieger, 1965). Alternating layers of pegmatite and fine-grained aplite, similar to a layered pegmatite structure, appear in some of the larger pods and lenses. The aplitic texture varies from finely crystalline to almost microcrystalline.

Dark Granite. A large area of the southeastern portion of the pluton near station L-14 (Figs. 2 and 3) and three other areas — two small ones at stations M-6 and K-15 and a larger, but less apparent, darkened area around station I-10 — are distinctly different in color, texture, and mineralogy from the main granite. Here the outcrops are much less weathered, have smoother surface textures, and are dark grayish pink to dark bluish gray. They are also finer grained and porphyritic and contain up to 15% biotite and other mafic minerals, which are sparse in the main granite. Quartz is much less abundant than in the main granite, whereas biotite, hornblende, and magnetite are much more abundant. Pegmatites are absent. Abundant xenoliths of similar color and texture are present here but are rare in the surrounding granite. The dark granite may represent a less differentiated or more basic portion of the crystallized magma, or zones of partial assimilation of more basic xenolithic masses.

Altered Zones. Two large altered zones are present in the northeastern portion of the granite at stations K-15 and L-13. These zones consist of a central core of pegmatitic and aplitic rocks surrounded by a halo of intensely altered granite. The altered granite grades laterally into unaltered granite.

The K-15 zone is an altered irregular zone about 210 m (700 ft) long to 90 m (300 ft) wide that strikes N45°W. It consists of intensely bleached and corroded, sugary-white granite, with a central core of bleached pegmatite and aplite.

The outer alteration halo in the granite in-

cludes early altered feldspars that become increasingly corroded, fragmented, and finer grained toward the center of the zone. Quartz is less metamorphosed. The altered granite has a sugary-white appearance and contains fine- to medium-grained quartz suspended in a fine-grained, crumbly, feldspar-mica matrix, as well as small quantities of epidote and small reddish garnets. The center of the altered zone consists of alternating layers of aplite and pegmatite that are white, crumbly, and bleached.

Three large masses of tourmaline-quartz-feldspar rock also crop out at station K-15. Solid tourmaline-quartz grades outward into tourmaline-feldspar, and finally to normal granite.

Near station M-6, fine-grained silicified granite, less than 0.93 sq m (10 sq ft) in area, is intensely veined by epidote. The numerous veinlets of fine-grained epidote range from 0.1 to 10 mm (up to 0.4 in.) in thickness. This zone is unique in the Dells Granite. Numerous epidote-rich rocks, however, appear as clasts in Tertiary sediments and fanglomerates that overlie the granite. Krieger (1965) identified several silicified zones in the granite north and west of Storm Ranch.

Xenoliths. Xenoliths of probable basement rocks of black biotite schist and quartz-feldspar-biotite gneiss are fairly abundant in the Dells Granite. These increase in size and frequency in the northwestern portion of the body. Near stations C-2, D-3, D-4, and D-5, numerous, generally tabular xenoliths up to 91 cm (3 ft) long and 15 cm (6 in.) wide parallel the N40°E vertical foliation of the original metamorphic rocks. In several zones, the rock mass may consist of up to 75% xenoliths. Other xenoliths appear in breccialike bodies. In contrast, a single xenolith of fine-grained granitic schist and gneiss about 18 m (60 ft) in length is exposed at station D-4. This xenolith is cut by dikelets of granite up to 30 cm (1 ft) in width. Unoriented xenolithic clusters and numerous single xenoliths also crop out near station D-3. The size and number of xenoliths in this area of the Dells Granite indicate that it was near the host rocks.

Dikes. Two light-bluish-gray dikes with aphanitic porphyritic texture are in the south-central area of the granite. These are subparallel to a prominent joint set and trend N20°E at the southern end of the southern dike and N40°E at the northern end of the northern dike over a distance of 1,219 m (4,000 ft). The dikes average 4.6 m (15 ft) in width, are poorly resistant to weathering, and are visible in stream beds.

The light-bluish-gray dikes consist of 50% aphanitic groundmass, as well as phenocrysts of white, locally zoned, K-feldspar up to 3 mm (0.1 in.) in length; abundant, euhedral black biotite grains; and rare magnetite and hornblende. The phenocrysts rarely exceed 1 mm (0.04 in.) in size. The aphanitic groundmass consists of quartz and feldspar. The dikes contain very fine grained chill zones 30 to 60 cm (1 to 2 ft) thick, adjacent to the host granite. The dikes are rhyolitic (Wilson, 1962; Krieger, 1965) and are strictly joint controlled.

Figure 5. Rose diagram of 337 joints in the Dells Granite.

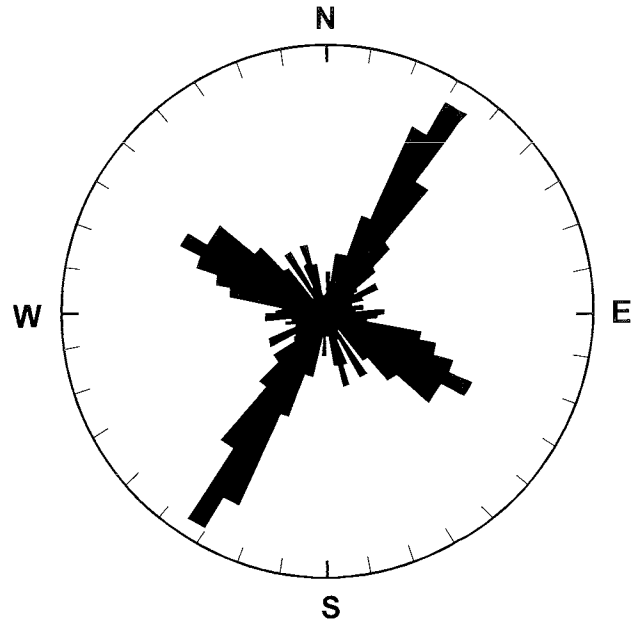

A Tertiary basalt intrusion, less than 3 m (10 ft) thick, appears to have locally brecciated the granite near station J-9. Fragments of granite, several centimeters (inches) in diameter, are included within the black, somewhat vesicular basalt. This rock mass is probably related to basaltic flows of the Glassford Hill volcanic cone just east of the Dells Granite pluton.

Secondary Structures. The well-developed joint system of the Dells Granite has played a major role in the weathering and morphology of the pluton, as well as the movement of ground water within it. To study these relationships, we used the methods of Dennison (1968) to plot 337 joints on an equal-area circular histogram (rose diagram; Fig. 5). The major joint sets trend N30°E and N60°W. Both sets are nearly vertical. A subordinate third set of approximately horizontal attitude is also present. These three joint sets have strongly influenced the shape of the weathered outcrops, resulting in a series of columnar, cuboidal, and spheroidal forms.

Faint arcuate lineaments around the darker granite are visible on aerial photographs. These lineaments suggest that this segregated zone is the center of a domal structure.

The joint-pattern map derived from a photogeological study and field checks (Fig. 3) supple-

Table 2. Compositional and statistical data for the Dells Granite.

MAJOR-ELEMENT OXIDES[1]					
Oxide	Mean in %	Standard Deviation	Range	Variance	Coefficient of Variation
SiO_2	75.3	0.90	72.86 - 77.75	0.81	1.7
Al_2O_3	13.97	0.46	12.87 - 77.75	0.21	3.3
Fe_2O_3	0.94	0.35	0.35 - 2.73	0.12	37.2
MgO	0.055	0.15	0.00 - 1.11	0.02	272.7
CaO	0.49	0.28	0.12 - 1.62	0.08	57.1
Na_2O	4.32	0.44	2.67 - 4.98	0.19	10.2
K_2O	4.78	0.52	4.04 - 7.02	0.27	10.9
TiO_2	0.047	0.037	0.0068 - 0.249	0.001	78.7
P_2O_5	0.026	0.030	0.0042 - 0.178	0.001	115.4
MnO	0.056	0.030	0.0071 - 0.143	0.001	53.6
RADIOACTIVE ELEMENTS[1]					
Element	Mean	Standard Deviation	Range	Variance	Coefficient of Variation
U (ppm)	8.83	8.30	0.0 - 39.7	68.88	94.0
Th (ppm)	26.8	5.80	8.9 - 47.4	33.36	22.0
K (%)	5.9	1.07	3.8 - 8.3	1.15	18.0
Total Response (cps)	340.1	80.8	185 - 568	6,526.17	23.8

[1]Analyses by gamma-ray spectrometry and XRF. Statistics based on 65 samples.

ments the joint pattern derived from field observations (Fig. 5). The two main, nearly vertical joint sets are clearly visible. Conspicuous, erosion-accented joint zones are also present. Mainly occupied by stream valleys and commonly overgrown with vegetation, these joint zones are shown as darker lines on the map. The distinctive arcuate joint set is superimposed on the other sets. One of the arcuate structures lies in the southeastern quarter of the area, where it essentially bounds the darker granite. A less developed joint set is subparallel to this arcuate structure. The northeast-northwest sets that are prominent elsewhere either disappear in this area or bend around the structure.

Two other parabolic, erosion-accented joint sets that open to the southeast and southwest are 1 to 2 km (1 to 1.5 mi) to the northwest and lie just northwest of the second dark granite zone. Joint sets are not well developed in the dark granite.

Another distinctive, arcuate fracture zone is almost directly west of the dark granite (E½ sec. 12). This zone is approximately 0.8 km (0.5 mi) in diameter and opens to the west. It encloses a large area of block-jointed granite, but conspicuous joints are subparallel to the main fracture zone, which appears to be younger than the other joint sets.

Several modes of origin are possible for the joint patterns in the Dells Granite: (1) they may have formed in response to thermal stresses as the pluton cooled; (2) they may be related to regional stresses on the pluton; (3) they may be related to forceful magmatic emplacement; or (4) any combination of the above.

Krieger's (1965) map of the Prescott quadrangle shows numerous joint sets in various rock types, including granite. In general, however, the joint sets do not match the conspicuously developed sets in the Dells Granite. Krieger did record that two sets in two Paleozoic formations in the region trend about the same as those in the granite. If regional stresses were the cause, however, one would expect a greater commonality of fracture patterns.

Weathering. Surface exposures of the granite body are very rough, crumbly, rounded, and intensely weathered. The granite breaks down easily and yields a coarse grus that is abundant in low areas and stream beds. The grus consists of coarse individual grains of quartz and feldspar.

A singular weathering characteristic of the granitic outcrop is a persistent Liesegang banding of iron oxides. The banding is joint controlled and consists of concentric spheres and ovals of iron oxide within cuboidal joint blocks. On the exposed face of a joint block, they appear as concentric rings, 0.6 to 5 cm (0.25 to 2 in.) thick. Elsewhere in the granite the banding is somewhat irregular, although joint control is evident. In some cases, xenoliths within the granite are surrounded by iron oxide haloes.

The degree of development, density, and width of bands vary in the exposed pluton. At station K-6, up to 15 or 20 concentric bands appear within a single joint block. In other areas, only one or two bands may be present. The bands vary in color from yellow orange in fresh granite to dark brown or black in the more intensely weathered areas.

Krieger (1965) suggested that the Liesegang

banding was caused by the inward movement of iron-bearing, oxidized ground water from joint surfaces toward the center of the cuboidal joint blocks. Iron was apparently leached from the granite face at the joint surfaces, carried inward, and redeposited within the rock to the depth of penetration of the water. Significantly, RM responses across the individual joint blocks showed that the interiors of the concentrically banded zones have a higher total response than the edges at or near the joint surfaces. This suggests that outside joint surfaces have been leached of some of their radioactive components.

RM SURVEY RESULTS AND ROCK ANALYSES

Statistical results of the RM survey of the pluton and the XRF analyses for the 10 major-element oxides in 65 large samples were compared to determine the existence and significance of correlations between (1) the distribution of U, Th, K, and total RM responses, and (2) SiO_2, Al_2O_3, Fe_2O_3, MgO, CaO, Na_2O, K_2O, TiO_2, P_2O_5, and MnO concentrations in the granite.

Statistical data for each element were generated with Statistical Analysis System (SAS) software (SAS Institute, 1979), using the UNIVARIATE option, which calculates a complete set of univariate statistics for each element, including the mean, standard deviation, range, variance, and coefficient of variation. These statistical measurements are summarized in Table 2.

The same data were used to produce computer-generated contour maps of the concentration of each element and the total RM response in the Dells Granite. The contour intervals were based on the standard deviation from the mean for each element; each contour represented 1 or more standard deviations above or below that mean. Fourteen contour maps were constructed: 1 each for U and Th (in parts per million), 1 each for ^{40}K and total RM response (in counts per second; Fig. 6), and 10 for the major-element oxides (by percentage; Fig. 7).

RM Survey Results

RM data were corrected for background radiation and interference by subtracting background counts from each channel and applying stripping equations applicable to the Scintrex GAM-1 instrument (Baird and Nargolowalla, 1974). This technique can eliminate the effects of interference of Th in the U channel and of U and Th in the K channel. There is no natural interference in the Th channel. Stripping factors, which vary according to the instrument and assay conditions, are determined by carefully measuring the count rates produced in all channels by a pure, series equilibrium U source and a pure, series equilibrium Th source (Baird and Nargolowalla, 1974). The following equations were derived for this survey:

equivalent uranium (eU; ppm) = 16.4 (cps U - 0.9 [cps Th]) - 9.27
equivalent thorium (eTh; ppm) = 19.26 (cps Th) - 0.7421
equivalent potassium (eK; %) = k (cps K - cps U - 0.9 [cps Th] - 0.88 [cps Th])

The constants were determined by comparing the stripped RM values to a set of known chemical U-Th assays of Dells Granite samples. Because no chemical assay data for ^{40}K were available, the $e^{40}K$ values remain in counts per second (constant k in equation for eK was not determined) and show only the relative high- and low-content areas of $e^{40}K$ for the granite mass.

U Distribution. U distribution within the Dells Granite was determined by XRF, which measures chemical U content, and by gamma-ray spectrometry, which measures the abundance of the nuclide ^{214}Bi, one of the daughter products from the decay of uranium-238 (^{238}U). When ^{214}Bi is in series equilibrium with ^{238}U and other daughter products, gamma-ray spectrometry is a reliable indicator of the eU content.

Twenty-one rock samples were analyzed for chemical U content by XRF. The results were compared by linear regression to the corrected and stripped RM response in the U channel for the same samples. An equation (see previous section) was developed from which the chemical U content for each station could be calculated directly from the corrected eU reading in the U channel.

A contour plot of U distribution in the Dells Granite was generated (Fig. 6a). Specific U content ranges from below the detection limit of the XRF unit at several stations to 39.7 ppm at station G-6. Contour values are 8.8 ppm, 17.13 ppm (1 standard deviation above the mean), and 25.43 ppm (2 standard deviations above the mean).

Two areas have eU contents that are 2 standard deviations or more above the mean. These are shown as shaded areas (Fig. 6a) and are at the center of larger areas with increased U content and a general northeast or(?) northwest trend. Three larger areas and one small area exceed 1 standard deviation or more above the mean. Two of these trend northwest and are closely related in the western half of the pluton. The third large area and the smaller area near the southern extremity of the pluton (station O-8 in Fig. 6a) trend northeast.

The mean U content of the Dells Granite (8.83 ppm) is more than double that of the average granite (Malan, 1972; Nishimori and others, 1977). The highest U content (39.7 ppm) is almost 10

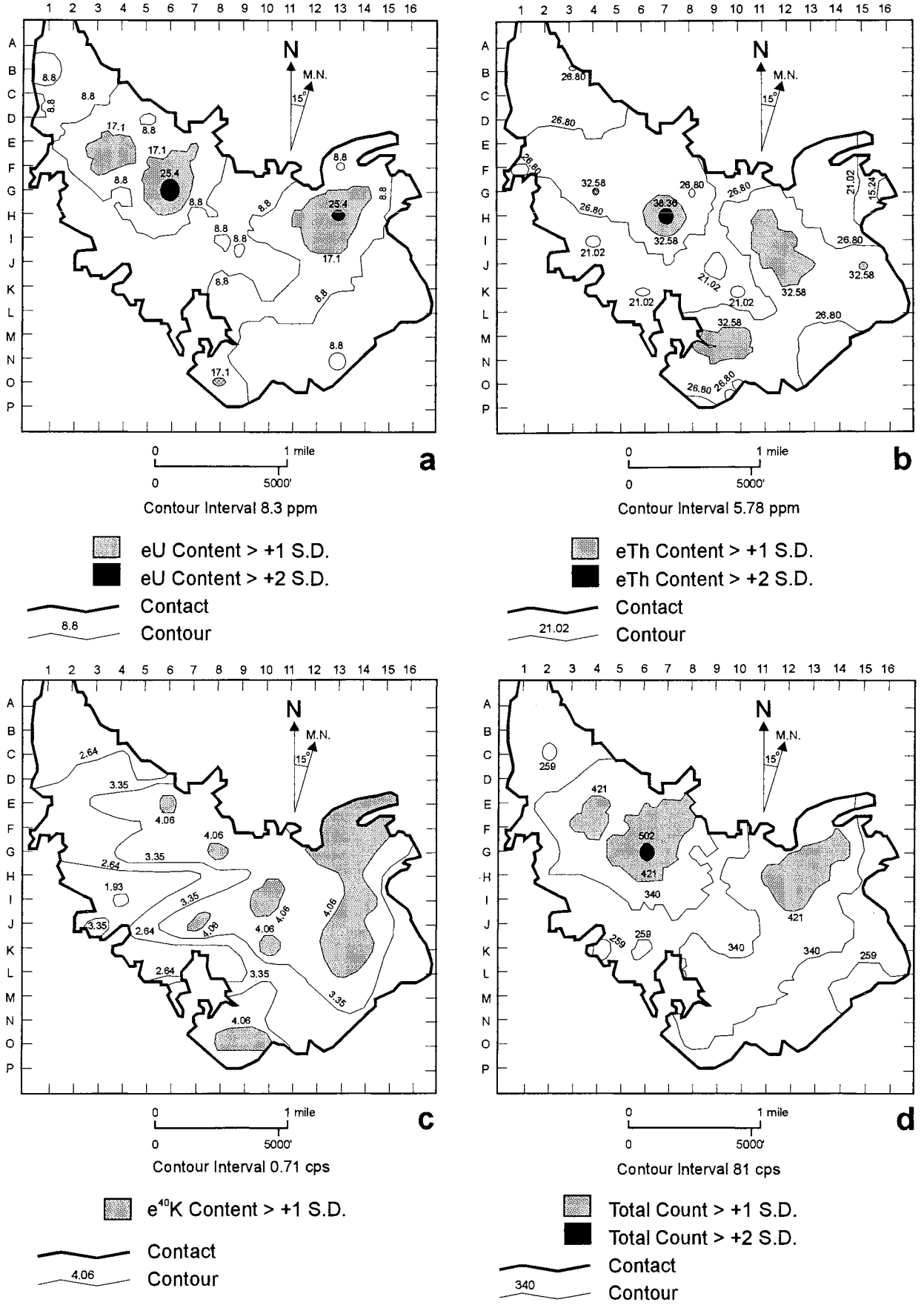

Figure 6 (a-d). Equivalent U, Th, and ^{40}K content and distribution and total-RM-response distribution in the Dells Granite. Analyses by gamma-ray spectrometry.

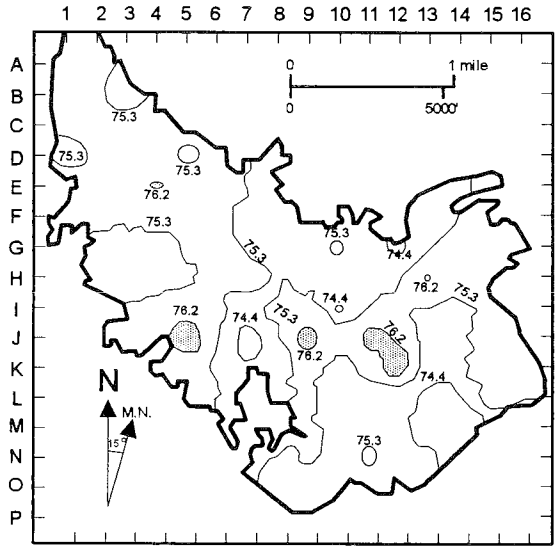

SiO_2 mean=75.3% **a**

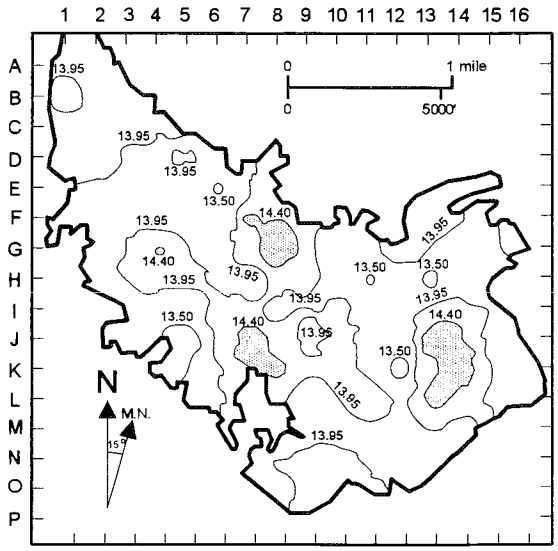

Al_2O_3 mean=13.97% **b**

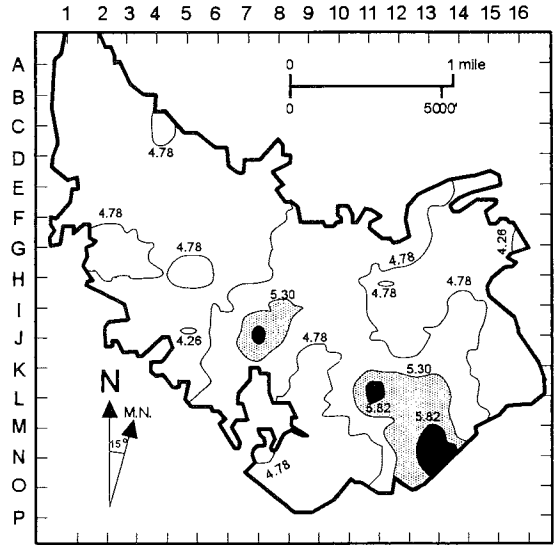

K_2O mean=4.78% **c**

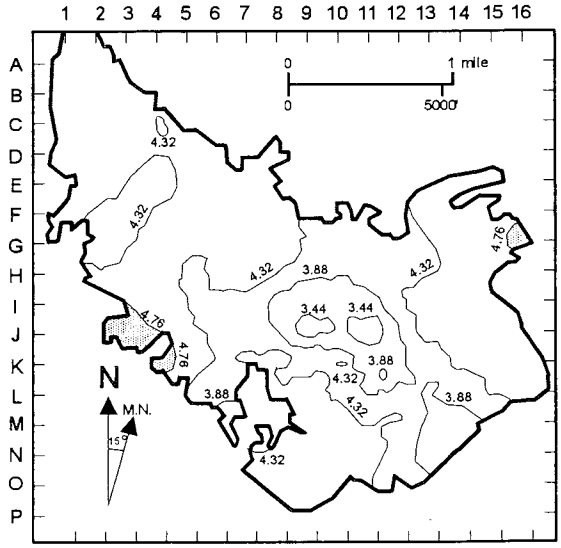

Na_2O mean=4.32% **d**

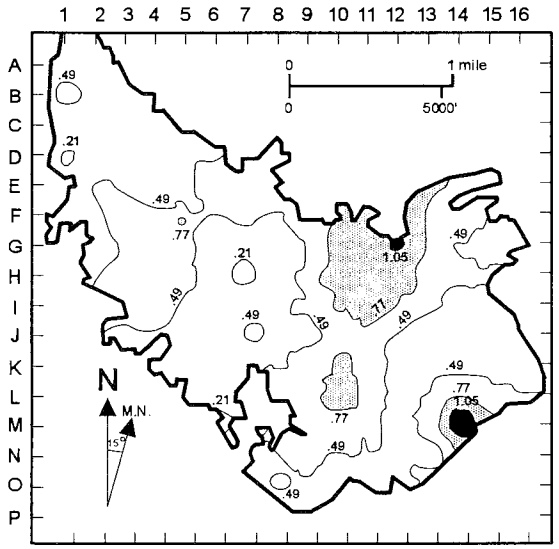

CaO mean=0.49% **e**

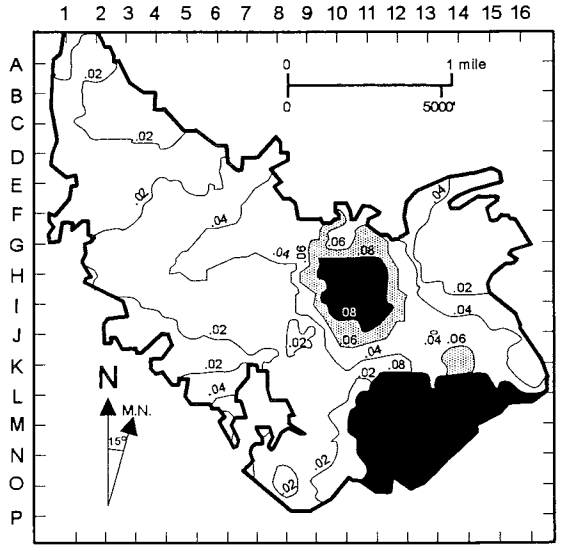

MgO mean=0.055% **f**

Figure 7 (a-j; opposite and below). Major-element-oxide content patterns in the Dells Granite. The contour interval is 1 standard deviation from the mean. Dark areas are anomalous, and gray areas are threshold, content (ATC) zones.

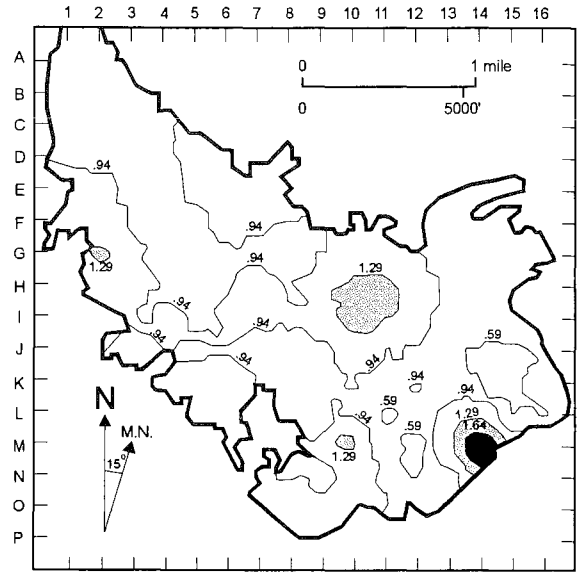

Fe_2O_3 mean=0.94% **g**

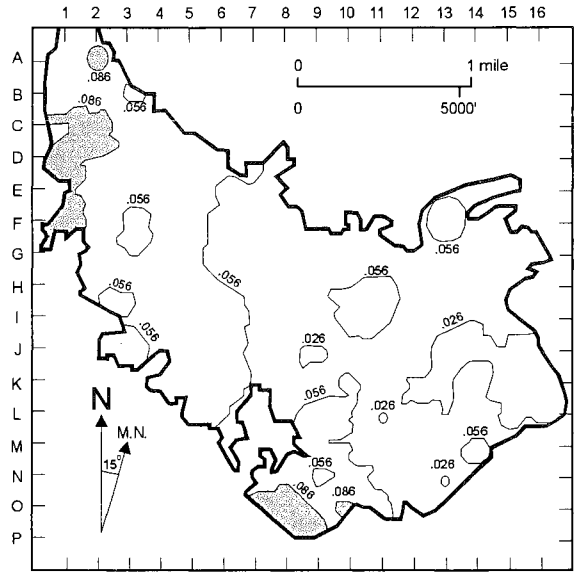

MnO mean=0.056% **h**

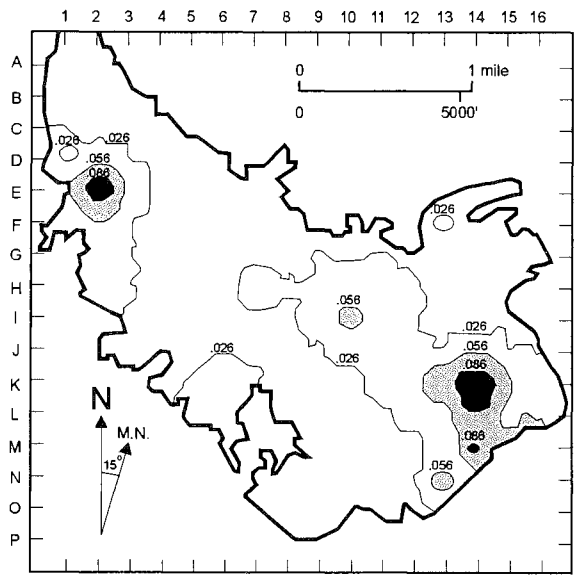

P_2O_5 mean=0.026% **i**

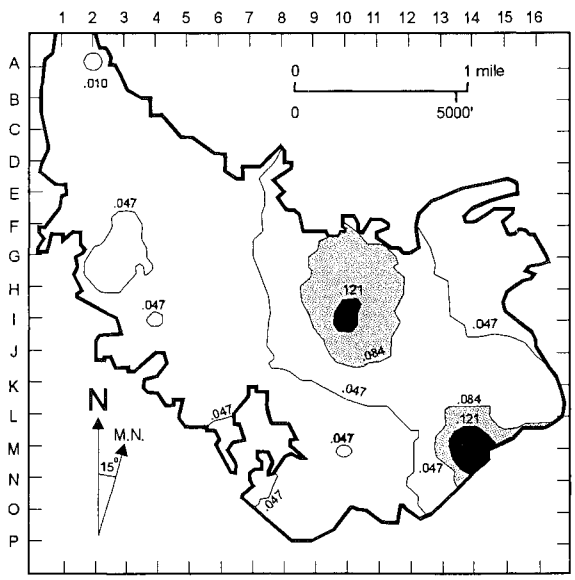

TiO_2 mean=0.047% **j**

times that of the average granite. Approximately 40% of the exposed granite exceeds 8.83 ppm (the mean), 10% exceeds 17.1 ppm (>1 standard deviation above the mean), and about 2% exceeds 25.4 ppm (>2 standard deviations above the mean).

Th Distribution. Equivalent Th content of the Dells Granite was determined by gamma-ray spectrometry and equated to the chemical assay values that P.D. Proctor determined in 1978. The gamma-ray spectrometer actually measures levels of ^{208}Tl, a daughter isotope of Th. The equation for converting raw count values into parts-per-million eTh was presented in a previous section (p. 70).

Equivalent Th values range from 8.9 ppm at station G-16 to 47.4 ppm at station H-7. The mean content is 26.8 ppm, and the standard deviation is 5.8 ppm. A contour interval of 5.78 ppm is used in Figure 6b. Three large and two small areas have eTh values greater than 1 standard deviation above the mean. One area at station H-7 exceeds 2 standard deviations above the mean.

The mean Th content of the Dells Granite is

somewhat less than the 37.8 ppm that Malan (1972) suggested as the average Th content of Precambrian granites in the western United States. The Th content of the Dells Granite more closely approaches the 28.2 ppm cited for quartz monzonites and the 25.8 ppm mean Th content of the continental crust.

K Distribution. K distribution in the Dells Granite was determined by XRF and gamma-ray spectrometry. XRF measures K content, whereas gamma-ray spectrometry measures the isotope ^{40}K, the major radioactive isotope of K, which constitutes 0.012% by weight of naturally occurring K. With a half-life of 1.3×10^9 years, ^{40}K emits gamma radiation at 1.46 MeV, which is detected in the K window of the gamma-ray spectrometer.

Conversion of counts per second to eK requires a set of standard K samples to correlate with count values obtained in the field. Such a set of previously analyzed samples for K, however, was unavailable. Raw data were therefore corrected for background radiation and interference, and plotted in counts per second. The results (Fig. 6c) are not absolute, but they show the relative distribution of ^{40}K within the pluton. The contour interval is 0.71 cps, or 1 standard deviation from the mean value of 3.35 cps. The range of count values is from 1.9 cps at station I-4 to 4.75 cps at station I-10.

Seven areas within the pluton show ^{40}K values greater than 1 standard deviation above the mean. These include six small areas in the central and southern parts of the granite body and a more extensive area that trends north in the northeastern corner of the pluton. Values exceeding the mean are mainly in the northeastern and central parts of the granite. Values that are 1 standard deviation below the mean mainly fall in an east trend in the western half of the body; the lowest values are clustered in the extreme northwestern corner of the pluton. In general, iso-element contours trend east in the western half and north in the eastern half of the pluton.

K_2O content, calculated from K content as determined by XRF, is shown as a percentage of the whole rock in Figure 7c. The contour interval is 0.52%, or 1 standard deviation from the mean content of 4.78%, and therefore represents percentages of the whole-rock composition. Three small, isolated areas show K_2O contents greater than 2 standard deviations above the mean. These areas form a rough zone that trends northwest from the southeastern corner of the pluton to its center. Areas with values greater than 1 standard deviation above the mean roughly parallel this trend. Areas containing less than the mean K content fall in the northwestern third, southern extremity, and northeastern corner of the pluton. The K content ranges from 4.04% at station G-16 to 7.02% at station N-13.

Total RM Response. The total RM response, which is the total of all gamma-radiation counts above 0.15 MeV, is measured in counts per second and corrected for background radiation (Fig. 6d). Total RM response in the Dells Granite ranges from 185 cps at station G-16 to 568 cps at station G-6. The mean value is 340.1 cps, and the standard deviation is 80.8 cps. Contour intervals are 81 cps.

Three areas in the northern half of the granite exceed 1 standard deviation above the mean. A small portion of the central area has an RM response greater than 2 standard deviations above the mean.

Comparison of U, Th, and K Contents and Total RM Response. ***U and Total RM Response.*** The contours of the U content in the pluton are very similar to those of the total RM response (Figs. 6a and 6d). The areas that are greater than 1 standard deviation — two in the western half and one in the eastern half — essentially coincide on both maps, as does the small area that is greater than 2 standard deviations at station G-6. Four other areas of high total RM response, one at the northwestern tip and three across the center and along the southeastern edge of the pluton, also roughly coincide with areas of high U content. An exception is the high-U-content area at station O-8, which has no corresponding high on the total-RM-response map. These overall coincidences of eU patterns and total RM response suggest a linear relationship between U content in the pluton and total RM response of the granite.

U and Th. The U and Th distributions in the granite correspond closely (Figs. 6a and 6b). The area that is greater than 2 standard deviations in U content at station G-6 relates closely to an area with high Th content at H-7. Similarly, the area near station I-12 shows both high U and high Th content. This area overlaps an area with high U content in the southwestern portion of the pluton. Areas with lower U concentrations in the northwestern and central parts closely match those with lower Th concentrations. The similarities in U and Th contour maps suggest a close genetic relationship between these elements in the granite.

U, Total RM Response, and K. The eU, U, and total RM response show an antipathy to K_2O content (Figs. 6a, 6d, and 7c). Areas of high eU concentration and correspondingly high total RM response do not correspond with those of high K_2O content. Areas of high eU concentration do, however, correspond with the relative ^{40}K content of the body (Figs. 6a and 6c).

Areas with high eU and total-RM-response values at stations I-12 and O-8 correspond fairly well with high ^{40}K areas at or near the same localities. An area of high eU content around

station G-6 overlaps one of relatively high ^{40}K content. Areas of low-content eU and ^{40}K correspond well. An exception is the N40°E zone, which trends across the center of the body and is low in eU content and high in ^{40}K.

Th and K. As expected, Th shows the same type of antipathy with K_2O as do eU and total RM response (Figs. 6b and 7c). The high eTh contents at stations H-7, I-12, and N-9 are in areas of very low K_2O content. Yet, high eTh areas do not relate as well to high ^{40}K areas as do the high eU and total-RM-response areas (Figs. 6b and 6c). The high eTh and ^{40}K areas are concentrated in the central and northern parts of the granite.

Variance of eU and eTh Values. The eTh content of the pluton has a smaller range and variance than does the eU content. This suggests a more uniform distribution pattern for Th within the granite than for U. The coefficient of variation for eTh is 21.6%, whereas the coefficient of variation for eU is 94%, which is 4.5 times greater (Table 2). If the U and Th contents were originally fairly uniform in the newly formed pluton, then U has been mobilized and possibly redeposited as a result of exogenous processes. These might include weathering and supergene leaching, which would account for the large coefficient of variation in eU values. U is more susceptible to mobilization in the natural environment because it is easily oxidized from the +4 to the much more mobile +6 valence state. Additional evidence of such chemical mobilization is the ubiquitous banding of the granite, which is caused by leaching and redeposition of iron oxides adjacent to joints in the granite. RM response of the granite decreases from the center of joint blocks to their edges. This indicates that radioactive elements, such as the mobile U, were removed from the granite adjacent to the joints, which served as conduits for oxidizing ground water.

Th/U Ratios. Th/U ratios for each of the 65 sample stations were calculated from gamma-ray spectrometry and XRF (Fig. 8). Because of the irregular patterns of the Th/U ratios, the map is not contoured. Each station, however, is represented by a circle that indicates the Th/U ratio and follows the system that O'Brien (1978) developed for the Graniteville Granite of southeastern Missouri.

The Th/U ratios for the Dells Granite are unusual. Three distinct population groups are present (Fig. 9). The main group has a mean value of 2.2, the second group a mean of 6.27, and the third group a mean of 10.18. The low-ratio group has the greatest frequency and is considered the most representative of the granite.

Malan (1972) reported a Th/U ratio of 6.8 for Precambrian igneous rocks in the western United States and a ratio of 8.8 specifically for western Precambrian granites. If a 2.3 ratio is representative of the Dells Granite, then it is quite anomalous, being more than three times smaller than the mean ratio for Precambrian granites in the western United States.

One explanation for this low Th/U ratio in the Dells Granite is the low mean Th content of 26.8 ppm, which is 32% lower than the 39.5 ppm cited for western Precambrian granites. Another explanation is the high mean U content of 8.83 ppm, which is almost twice the 4.5 ppm mean for similar granites (Malan, 1972). Silver and others' (1980) analysis of a single bulk sample of Dells Granite resulted in a Th/U ratio of 0.8, which they describe as "unusually low."

Typical Th/U ratios for crustal igneous rocks are between 2.5 and 4.0 (Nishimori and others, 1977). Igneous rocks in this range are believed to be derived from mantle rocks or from sediments that form continental-margin, eugeosynclinal belts. Nishimori and others (1977) stated that "deposits with low Th/U ratios may have undergone some type of surficial reprocessing, in which uranium could have been concentrated by surface waters, or may have undergone sedimentary recycling, resulting in extreme concentrations of uranium."

Nishimori and others (1977) described the high-U-content Rossing deposit in Southwest Africa (Namibia), where the G-4 granite intrudes a suite of metasedimentary rocks. The high U content is reported to be the result of continued recycling of the rocks. The youngest granite, the anatectic G-4 granite, contains more than 30 ppm U and is the final repository for U concentrated by the recycling process. The researchers suggested that the U could have been concentrated by supergene processes in the hot arid climate of the desert. The unusually high U content of the Dells Granite and its low Th/U ratio may be the result of either or both of these enrichment processes.

The two subordinate groups of Th/U ratios, with mean values of 6.27 and 10.18, have a relatively low U content. These areas were most likely formed from leaching and removal of U by surface weathering, but the distinct break between them is somewhat enigmatic. The irregular distribution patterns of Th/U values probably resulted from variations in weathering intensity over the granite. Krieger's (1965) suggestion that the present outcrop of the Dells Granite is close to an ancient erosional surface supports this hypothesis.

Patterns of Major-Element Oxides

Concentration patterns of the 10 major-element oxides of the Dells Granite are shown in Figure 7. The contour interval used for each map is the standard deviation from the mean for the individual major-element oxides (Table 2), except for

MgO, which is contoured on an interval of 0.02%. All oxide concentration values are in weight percent of the whole rock. The similarities and differences in the distribution patterns of radioactive elements, major-element oxides, and total RM response are summarized in Table 3.

All members of the Fe-Mg-Ca-P-Ti group of elements have very similar distribution patterns. A main area of pattern similarity is in the southeastern part of the pluton, which corresponds with the area of dark granite in Figure 3. Another major area is in the north-central part of the pluton, also an area of dark granite. Fe, Mg, Ca, and Ti are generally in higher concentrations in the more mafic rocks than in the more felsic rocks.

No strong statistical or visual correlations exist among Si, K, and the radioactive elements in the Dells Granite. Si and K, however, generally show strong correlations with U and Th in alkali igneous rocks (Nishimori and others, 1977). Fe and U also lack similar distribution patterns in the Dells Granite. O'Brien (1978), Proctor and O'Brien (1980), and Fleck and others (1981), however, showed that Fe and U correlate well in the Graniteville Granite in Missouri, a granite similar to the Dells Granite. U is associated with Fe-bearing minerals, such as biotite, in the Dells Granite. The biotite contains inclusions of hematite, magnetite, and ilmenite, as well as other minerals (Silver and others, 1980, 1984). These researchers suggested that immiscible fluids in the late magmatic stage permitted significant amounts of the radioactive accessory minerals to crystallize (see Table 1). The lack of strong correlation between Fe and U in the Dells Granite may also relate to the intense weathering of the granite and to the extensive redistribution of both Fe and U within the granite. Evidence of these processes includes the Liesegang banding of iron oxides throughout the pluton and the depletion of U in the banded areas.

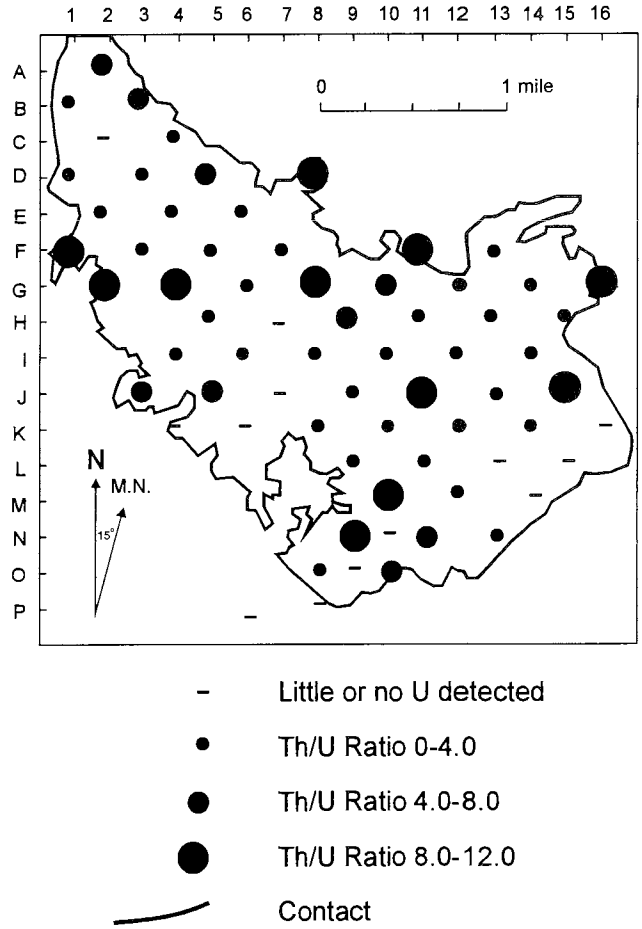

Figure 8. Th/U ratio distribution in the Dells Granite. Analyses by gamma-ray spectrometry and XRF.

Table 3. Element and oxide correlations of the Dells Granite.

Element or Oxide[1]	Positive Correlation	Negative Correlation
U	Th, Total RM Response	
Th	U, Total RM Response	
K		
SiO_2		Al_2O_3, Fe_2O_3, CaO, K_2O
Al_2O_3	K_2O	SiO_2
Fe_2O_3	CaO, TiO_2, MnO	SiO_2
MgO		
CaO	Fe_2O_3	SiO_2
Na_2O		K_2O,TiO_2
K_2O	Al_2O_3	SiO_2, Na_2O
TiO_2	Fe_2O_3, CaO, P_2O_5	Na_2O
P_2O_5	TiO_2	
MnO	Fe_2O_3	

[1]Major-element-oxide correlations are based on computer-generated correlation coefficients; radioelement correlations are estimated from maps.

Radioelement Distribution and Autoradiographs

Autoradiographs clearly show the distribution of radioactivity among the minerals of the Dells Granite. The most intensely exposed spots due to radioactivity were produced by biotite. Feldspars gave an intermediate response, which appeared as a faint gray on the

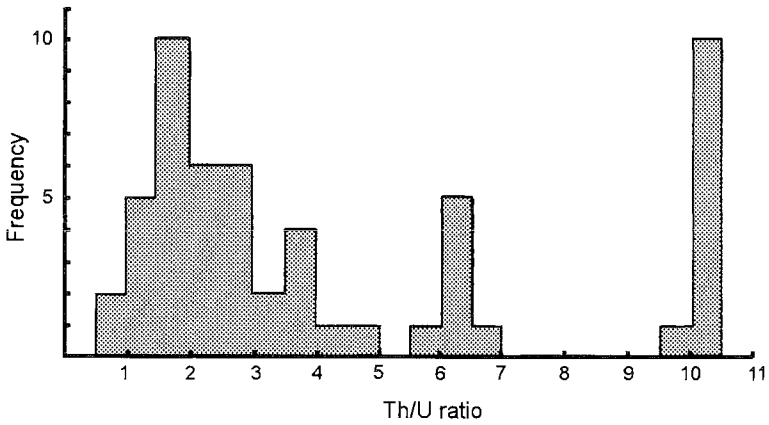

Figure 9. Histogram of Th/U ratio values for the Dells Granite. Analyses by gamma-ray spectrometry and XRF.

autoradiographs. Quartz gave little or no response and did not expose the film. A quartz-mica-muscovite-pegmatite sample from station I-13 gave a response that was less than that of feldspars in other samples.

The intensity of the mottled pattern for radioactive feldspar was fairly consistent in samples taken throughout the granite. Autoradiographs of biotite, on the other hand, varied widely in the number and intensity of darker spots produced by radioactivity. Zones in the pluton that contain abundant biotite grains correspond well with those of high RM response in the spectrometer survey (Table 4).

Rocks from pegmatites and altered zones produced weak-intensity autoradiographs. Individual biotite grains in pegmatites yielded little or no response, yet biotite, because of its mineral inclusions, is the most radioactive mineral in the granite. This suggests that U was localized in the granite and was not concentrated in the residual magma that formed the pegmatites.

Because of its high RM response, biotite is the apparent source of the anomalous concentrations of U in the Dells Granite. Conspicuous pleochroic haloes are visible around zircon, hematite, magnetite, ilmenite, and other minerals within the biotite grains. Though much less radioactive, the feldspars contribute to the total radioactivity of the granite. Their contribution is more constant throughout the rock than that of biotite.

THE DELLS GRANITE AS A POSSIBLE SOURCE OF ECONOMIC URANIUM DEPOSITS

Malan (1972) cited four important aspects of the relationship between Precambrian igneous rocks and stratiform U deposits in Mesozoic and Cenozoic sedimentary rocks in the western United States:

1. "Significant radioelement enrichment in Precambrian rocks correlates regionally with the distribution of major stratiform uranium deposits in sandstones.

2. "Most major stratiform uranium deposits in the western United States are on the foreland of the Cordilleran ... fold [and thrust] belt, on the cratonic platform where Precambrian rocks are at shallow crustal levels. Detritus from the erosion of these Precambrian rocks usually forms part of the host rocks, particularly those of Tertiary age, of the uranium deposits.

3. "The uranium in the major stratiform deposits in sandstone is generally assumed to have been de-rived from granitic rocks in the provenance.... The granitic rocks are largely Precambrian.... Thus the original source of the uranium would be in the Precambrian rocks.

4. "The regional relationship of the distribution of anomalous amounts of uranium in Precambrian rocks to the distribution of known major uranium deposits in Mesozoic and Cenozoic sediments indicates favorability of undiscovered deposits in ... basins within that portion of the Mesozoic Cordilleran fold [and thrust] belt in western Arizona and adjacent southern Nevada and southern California where Precambrian rocks are enriched in uranium."

The Dells Granite contains anomalous amounts of U. The pluton has been near the surface of the Earth since the end of the Precambrian and has undergone prolonged erosion, weathering, and leaching. Furthermore, the body is in the western United States, an area that Malan (1972) concluded is favorable to the formation of stratiform U deposits.

Based on Malan's conclusions and the known radioelement distribution in the Dells Granite, the pluton is a likely source for mobile U. The leached, mobilized U could have been transported by ground-water processes and redeposited into possible economic U deposits, either in adjacent Tertiary sediments or possibly within the granite itself.

Likely host rocks for stratiform U deposits are in the Chino-Lonesome Basin north of the Dells

Most Intense	Least Intense
E-4	B-2
E-6	I-6
F-7	J-3
G-3	J-5
G-6	J-9
G-11	K-16
H-9	L-13-1
K-12	L-13-2
	M-10
	M-13
	P-7

Table 4. Autoradiograph intensities at map stations.

Granite. Upper Tertiary sediments and interbedded basalt flows in this basin were probably more than 600 m (2,000 ft) thick before erosion removed the uppermost sediments. Today, the sediments are probably no more than 300 m (1,000 ft) thick in the deepest parts of the basin. The sediments consist of fanglomerates; mud flows; interbedded, rhyolitic and basaltic, tuffaceous material and basalt flows along the margins of the basin; and channel gravel, sand, silt, and clay in the interior of the basin (Krieger, 1965).

The surface and ground waters that flow over or through the Dells Granite continue northward into the Chino-Lonesome Basin. In a hydrogeochemical reconnaissance survey of the Prescott 1° by 2° NTMS quadrangle, Clark (1979) identified 50 to 100 parts per billion U in a stream-water sample downstream from the Dells Granite. A reconnaissance RM traverse across Granite Creek, about 9.7 km (6 mi) north of the present study area, gave readings up to 2 times the background level over gravel bars that are similar to the Dells Granite in composition and color. This suggests that surface waters transport radioactive material, in both solid and solute form, considerable distances north of the Dells Granite.

U may have been concentrated into economically recoverable deposits in or around the Dells Granite as follows:

1. Oxidized and mobile U, leached from the Dells Granite, may have been transported down the hydraulic gradient into the Chino-Lonesome Basin. The U may have been deposited and concentrated along an oxidation-reduction boundary, as were the roll-front deposits of Wyoming.

2. Malan (1972) stated that "anomalous U and Th in outcrops of iron-stained Precambrian granitic masses in several areas result from oxidizing syngenetic or hypogene epigenetic concentrations of iron minerals and radioelements. Supergene remobilization of mobile uranium in such an environment might result in economic deposits being formed at depth near the oxidation-reduction boundary." This explanation suggests that an economic deposit of U may have been formed deep within the granite body if the necessary reducing conditions were present at or near the present water or paleowater table.

Both types of deposits are of major interest in U exploration. Using data obtained during this study, an estimate was made of the amount of U that has been leached from the high-U-content areas of the granite body. This mobile U may have been carried outward from the granite body by ground or surface waters, to be redeposited elsewhere, or it may have been redeposited within the granite body itself at an oxidation-reduction boundary.

To make this estimate, several basic assumptions were made:

1. Only the areas containing U contents greater than +1 standard deviation were considered.

2. The depth of leaching was assumed to be 30 m (100 ft) because of the severely weathered and jointed nature of the granite.

3. Because the amount of weathering and jointing of the granite varies considerably, one-half of the granite, by volume, was considered to have been leached; of this half, one-half of the total U content was also considered to have been leached. This resulted in an estimate of 25% as the net removal of U by leaching.

4. The U content of the +1-standard-deviation zones was assumed to be 21.3 ppm, halfway between +1 standard deviation (17.1 ppm) and +2 standard deviations (25.4 ppm). U content of the +2-standard-deviation zones was assumed to be 29.6 ppm, halfway between +2 standard deviations (25.4 ppm) and +3 standard deviations (34.2 ppm).

The total amount of U contained in the +1-standard-deviation zones of the granite (1.14 sq km; 0.44 sq mi), if one assumes a grade of 0.00213% (21.3 ppm) and a leaching depth of 30 m (100 ft), is approximately 24 million kg (53 million lb). The total amount of U in the +2-standard-deviation zones (0.067 sq km; 0.026 sq mi), if one assumes a grade of 0.00296% (29.6 ppm) and a leaching depth of 30 m (100 ft), is approximately 163,000 kg (360,000 lb). The total U content of the +1- and +2-standard-deviation zones to a depth of 30 m (100 ft) is 24.2 million kg (53.4 million lb). Of this, 25%, or 6.05 million kg (13.4 million lb), is assumed to have been removed by leaching. This is a significantly large amount.

CONCLUSION

The principal objective of this study was to identify the concentrations and distributions of 10 major-element oxides, U, Th, and K in the highly radioactive Dells Granite. A secondary objective was to evaluate the possibility of economic concentrations of U within or near the pluton. The following conclusions are a result of this study.

1. The mean eU content of the granite is 8.8 ppm, which is double the U content of average granites in the western United States (Malan, 1972). The eU ranges from below detection limits to 39.7 ppm. The higher limit is approximately 10 times the mean eU for granites in the West. The highest eU content, greater than 2 standard deviations above the mean, is restricted to two small areas in the northern half of the pluton.

High alkali granites, similar to the Dells Granite, contain the highest concentrations of U. In

these bodies, U and Th tend to concentrate in the late magmatic fluids because of their large ionic radii and are thus excluded from the crystal structures of the common rock-forming minerals. Igneous rocks formed at the last stages of magmatic differentiation, such as alkali granites, therefore contain higher concentrations of U and Th, as well as late-stage minerals formed from volatiles such as fluorine.

2. The mean eTh content of the granite is 26.8 ppm, which is somewhat lower than the 37.8 ppm mean eTh content that Malan (1972) reported for Precambrian granites in the West. The eTh content ranges from 8.9 ppm to 47.4 ppm. The Th distribution in the granite generally follows that of U.

3. The mean K_2O content of the granite is 4.8%, with a range of 4 to 7%. The mean is slightly higher than that reported for Precambrian western granites. Only relative counts-per-second values were obtained for the content of ^{40}K, the main radioactive isotope of K. K appears to have an antipathy for U. This is somewhat unusual because U should follow K as the magma differentiates and crystallizes into granite.

4. Total RM response of the granite ranges from 185 cps to 568 cps, with a mean of 340 cps. The pattern of total RM response correlates closely with that of eU.

5. Th/U ratios of the Dells Granite are highly variable. Three distinct population groups have been recognized: a main group comprising about half of the sampled areas, with a mean Th/U ratio of 2.2; and two subordinate groups, with mean Th/U ratios of 6.27 and 10.18. The low Th/U ratio of the main group is explained by the relatively low mean eTh of 26.8 ppm and the high mean eU of 8.8 ppm. Dells Granite samples with low Th/U ratios have not been significantly leached of their U content. The two Th/U groups with high values have probably been significantly depleted of U by leaching and weathering processes. The granite is intensely weathered over much of its surface and is conspicuously stained with iron oxides. Less U is present in the iron-stained bands than in the less weathered or stained zones.

6. Petrographic examination of the Dells Granite indicates that the U content is closely related to magnetite, hematite, ilmenite, and leucoxene, which are in and around biotite, and in the radioactive trace minerals zircon, allanite, thorite, xenotime, and metamict phases (Silver and others, 1980, 1984). Dark pleochroic haloes, indicative of radioactivity, are visible around these mineral inclusions in the biotite. No late, interstitial, U-bearing minerals were evident, although the internal weathering of the granite could have modified the original patterns.

7. Autoradiographs of Dells Granite samples show that radioactivity is concentrated in the biotite grains and accessory minerals. Feldspars (mostly microcline) also exhibit faint radioactivity, possibly because of the presence of the ^{40}K isotope.

8. High U concentrations of a small fraction of the Dells Granite (>25 ppm eU for about 2% of the granite) probably reflect the original concentration (Silver and others, 1984). Most of the granite, however, has exhibited open-system behavior, and U has been leached from the granite. Therefore, the present overall U content is only 8.83 ppm. U concentration varies greatly within the pluton because of the varying effectiveness of leaching.

Several models for U deposition in the area are possible:

1. Oxidized and mobile U, leached from the granite by weathering processes and carried down the hydraulic gradient, could be precipitated and concentrated at an oxidation-reduction boundary in the Tertiary sediments of the Chino-Lonesome Basin. Such a deposit would resemble the roll-front deposits of Wyoming. Organic debris in channel deposits of the basin could also act as a reductant and form deposits similar to those on the Colorado Plateau.

2. Supergene enrichment of near-surface mobilized U at an oxidation-reduction boundary deep within the pluton could form a U deposit. Supergene enrichment requires reducing conditions at depth and stabilization of the U ion to the U^{+4} state at or near the level of the present water table or paleowater table.

3. The local areas of greater-than-25-ppm eU content, which compose about 2% of the exposed pluton, make up large, low-grade zones of disseminated U within the body. These zones are not high enough in U content to constitute an orebody, but they do represent another possible ore model.

If one assumes certain parameters for the amount of U leached from selected areas of the granite and a leaching depth of 30 m (100 ft), approximately 6 million kg (13 million lb) of U may have been leached from the main pluton, circulated in ground and surface waters, and redeposited according to the proposed models.

ACKNOWLEDGMENTS

We thank Dr. S.K. Grant of the University of Missouri-Rolla, who assisted with the XRF analysis and computer programs. The technical assistance of Mike Roberson is gratefully acknowledged. We also thank the residents of Granite Dells, the late Mrs. V.H. McNutt, the V.H. McNutt Memorial Foundation, and Phillips Petroleum Company for financial support.

REFERENCES

Adams, J.A.S., Kline, M.C., Richardson, K.A., and Rogers, J.J.W., 1962, The Conway Granite of New Hampshire as a major low-grade thorium resource: Proceedings of the National Academy of Sciences, v. 48, p. 1,898-1,905.

Adams, J.A.S., Osmond, J.K., and Rogers, J.J.W., 1959, The geochemistry of thorium and uranium, *in* Ahrens, L.H., Press, Frank, Rankama, Kalewa, and Runcorn, S.K., eds., Physics and chemistry of the Earth, v. 3: London, Pergamon Press, p. 298-348.

Aero Service, 1979, Airborne gamma-ray spectrometer and magnetometer survey, Las Vegas, Williams, Prescott, and Kingman quadrangles, Arizona: U.S. Department of Energy Report GJBX-59 (79), p. 1-34, 49-62.

Anderson, C.A., Blacet, P.M., Silver, L.T., and Stern, T.W., 1971, Revision of Precambrian stratigraphy in the Prescott-Jerome area, Yavapai County, Arizona: U.S. Geological Survey Bulletin 1324-C, 16 p.

Baird, J.G., and Nargolowalla, S., 1974, Instruction manual for Scintrex GAM-1 Differential Single Channel Gamma Analyzer: Scintrex Co., 31 p.

_____ 1975, Nuclear exploration brief: Scintrex Co., Application Brief 75-1, p. 4-5.

Bateman, P.C., Clark, L.D., Huber, N.K., Moore, J.G., and Rinehart, C.D., 1963, The Sierra Nevada batholith — A synthesis of recent work across the central part: U.S. Geological Survey Professional Paper 414-D, 46 p.

Chentsov, I.G., 1961, The entry of uranium into some of the rock-forming minerals: International Geology Review, v. 3, no. 1, p. 5.

Clark, R.J., 1979, Hydrogeochemical and stream sediment reconnaissance basic data report for the Prescott NTMS quadrangle, Arizona: U.S. Department of Energy Report GJBX-122 (79), 15 p.

Dennison, J.M., 1968, Analysis of geological structures: New York, W.W. Norton and Company, Inc., p. 129-130.

Evans, R.D., and Goodman, Clark, 1941, Radioactivity of rocks: Geological Society of America Bulletin, v. 52, p. 459-490.

Fleck, K.S., Shahin, A.N., and Proctor, P.D., 1981, Petrographic and chemical characteristics of two radioactive granites — Missouri and Arizona [abs.]: Missouri Academy of Sciences Transactions, v. 15, p. 244.

Heier, K.S., and Adams, J.A.S., 1965, Concentration of radioactive elements in deep crustal material: Geochimica et Cosmochimica Acta, v. 29, p. 53-62.

Heier, K.S., and Rhodes, J.M., 1966, Thorium, uranium, and potassium concentrations in granites and gneisses of the Rum Jungle Complex, Northern Territory, Australia: Economic Geology, v. 61, p. 563-571.

Johannsen, A., 1931, A descriptive petrology of igneous rocks (2d ed.): Chicago, University of Chicago Press, v. 1, p. 140-161.

Keevil, N.B., Larsen, E.S., Jr., and Wank, F.J., 1944, The Ayer granite-migmatite at Chelmsford, Massachusetts, pt. 6 — The distribution of helium and radioactivity in rocks: American Journal of Science, v. 242, no. 7, p. 345-353.

Krieger, M.H., 1965, Geology of the Prescott and Paulden quadrangles, Arizona: U.S. Geological Survey Professional Paper 467, 127 p.

Lambert, I.B., and Heier, K.S., 1967, The vertical distribution of uranium, thorium, and potassium in the continental crust: Geochimica et Cosmochimica Acta, v. 31, p. 377-390.

Larsen, E.S., and Gottfried, D., 1960, Uranium and thorium in selected suites of igneous rocks: American Journal of Science, v. 258-A, p. 151-169.

Larsen, E.S., and Phair, G., 1954, The distribution of uranium and thorium in igneous rocks, *in* Faul, H., ed., Nuclear geology: New York, John Wiley and Sons, Inc., p. 763-772.

Larsen, E.S., Phair, G., Gottfried, D., and Smith, W.L., 1956, Uranium in magmatic differentiations: U.S. Geological Survey Professional Paper 800, p. 65-74.

Malan, R.C., 1972, Summary report — Distribution of uranium and thorium in the Precambrian igneous rocks of the western United States: U.S. Atomic Energy Commission Report AEC-RD-12.

Malan, R.C., and Sterling, D.A., 1969, An introduction to the distribution of uranium and thorium in Precambrian rocks including the results of preliminary studies in the southwestern United States: U.S. Atomic Energy Commission Report AEC-RD-9, 54 p.

Nishimori, R.K., Ragland, P.C., Rogers, J.J.W., and Greenberg, J.K., 1977, Uranium deposits in granitic rocks: U.S. Department of Energy Report GJBX-13 (77), 93 p.

O'Brien, W.P., 1978, Petrochemistry and K, U, and Th distribution in the Graniteville Granite, Iron County, Missouri: Rolla, University of Missouri, M.S. thesis, 118 p.

O'Connor, J.T., 1965, A classification for quartz-rich igneous rocks based on feldspar ratios, *in* Geological Survey research 1965, chapter B: U.S. Geological Survey Professional Paper 525-B, p. B79-B84.

Phair, G., and Gottfried, D., 1964, The Colorado Front Range as a uranium and thorium province, *in* Adams, J.A.S., and Lowder, W.M., eds., The natural radiation environment: Chicago, University of Chicago Press, p. 7-38.

Proctor, P.D., and O'Brien, W.P., 1980, Radiometric signature and petrochemistry of the Graniteville Granite of the St. Francois Mountains of southeast Missouri [abs.]: Geological Society of America Abstracts with Programs, v. 12, no. 5, p. 254.

Proctor, P.D., O'Brien, W.P., and Grant, S.K., 1981, Graniteville Granite, Missouri: A possible Bokan Mountain, Alaska, analog? [abs.]: Geological Society of America Abstracts with Programs, v. 13, no. 7, p. 333.

Ragland, P.C., Billings, G.K., and Adams, J.A.S., 1967, Chemical fractionation and its relationship to the distribution of thorium and uranium in a zoned granite batholith: Geochimica et Cosmochimica Acta, v. 31, p. 17.

Rogers, J.J.W., and Adams, J.A.S., 1963, Log normality of thorium concentrations in the Conway Granite: Geochimica et Cosmochimica Acta, v. 27, p. 775-783.

Rogers, J.J.W., and Ragland, P.C., 1961, Variations of thorium and uranium in selected granitic rocks: Geochimica et Cosmochimica Acta, v. 25, p. 99-109.

SAS Institute, 1979, User's guide to the Statistical Analysis System: Cary, N.C.

Silver, L.T., Bickford, M.E., Van Schmus, W.R., Anderson, J.L., Anderson, T.H., and Medaris, L.G., 1977, The 1.4-1.5 b.y. transcontinental anorogenic plutonic perforation of North America [abs.]: Geological Society of America Abstracts with Programs, v. 9, no. 7, p. 1,176-1,177.

Silver, L.T., Williams, I.S., and Woodhead, J.A., 1980, Uranium in granites from the southwestern United States: Actinide parent-daughter systems, sites and mobilization: First-year report: U.S. Department of Energy Report GJBX-45(81), 380 p.

Silver, L.T., Woodhead, J.A., Williams, I.S., and Chappell, B.W., 1984, Uranium in granites from the southwestern United States: Actinide parent-daughter systems, sites and mobilization: U.S. Department of Energy Report GJBX-7(84), 431 p.

Streckeisen, A.L., 1967, Classification and nomenclature of igneous rocks (final report of an inquiry): Neues Jahrbuch fur Mineralogie Abhandlungen, v. 107, p. 144-240.

Stuckless, J.S., and Nkomo, I.T., 1978, Uranium-lead isotopic systematics in uraniferous alkali-rich granites from the Granite Mountains, Wyoming: Implications for uranium source rocks: Economic Geology, v. 73, p. 427-441.

Stuckless, J.S., Nkomo, I.T., and Doe, B.R., 1981, U-Th-Pb systematics in hydrothermally altered granites from Granite Mountains, Wyoming: Geochimica et Cosmochimica Acta, v. 45, p. 635-645.

Vinogradov, A.P., ed., 1963, The essential features of the geochemistry of uranium, a symposium: Moscow, U.S.S.R. Academy of Sciences Publishing Office, 609 p.

Whitfield, J.M., Rogers, J.J.W., and Adams, J.A.S., 1959, The relationship between the petrology and the thorium and uranium contents of some granitic rocks: Geochimica et Cosmochimica Acta, v. 17, p. 248-271.

Wilson, E.D., 1962, A resume of the geology of Arizona: Arizona Bureau of Mines Bulletin, v. 171, 140 p.

Radon on the Navajo Nation Indian Reservation, Arizona, New Mexico, and Utah

MICHAEL A. TAYLOR — *Navajo Area Indian Health Service, P.O. Box G, Window Rock, Arizona 86515*
JOHN T. DUNCAN — *Arizona Geological Survey, 845 N. Park Ave., #100, Tucson, Arizona 85719*

INTRODUCTION

During the first quarter of 1990, the Navajo Area Indian Health Service (NAIHS) surveyed Navajo homes across the contiguous Navajo Nation in Arizona, New Mexico, and Utah (Fig. 1). The survey was designed to produce a statistically valid characterization of indoor-radon concentrations. Only private homes that are normally occupied year-round were selected for the survey; no federally managed or non-Navajo homes were included. The Navajo Nation Chapters of Ramah, Alamo, and Canoncito were not included in this survey because of their geographic isolation. The survey design resulted from a cooperative effort of the NAIHS, Navajo Environmental Protection Agency (NEPA), U.S. Environmental Protection Agency (EPA), and Research Triangle Institute (RTI), an EPA contractor for radon survey projects. The EPA provided testing equipment and radon analyses, and RTI analyzed the data statistically.

Figure 1. Location of Navajo Nation.

SURVEY DESIGN AND PROCEDURES

The radon survey was designed using 1980 U.S. census information to obtain a statistically valid data set of approximately 1,000 homes, or 3% of the homes on the Navajo Nation. To achieve a representative sample, each Census Enumeration District (CED, the smallest unit defined by the U.S. Census Bureau) within the Navajo Nation was statistically weighted according to the number of homes reported in that district. A CED containing 50 homes would, therefore, be 10 times as likely to be selected as one with 5 homes. From this population, 160 CED's (10 groups of 16) were randomly selected. Each selected CED was then assigned a "measure of size" (MOS) representing the number (with rounding) of 10-home groups within the CED. For example, a CED containing 48 homes would receive an MOS of 5, whereas one containing 14 homes would receive an MOS of 1. After the actual number and location of occupied homes in each of these CED's were verified (and, where necessary, corrected) by field inspection, the homes in each selected CED were grouped geographically into segments, with the number of segments equal to the MOS number. To the extent possible, all of the segments in each CED contained the same number of homes. Finally, one segment from each selected CED was randomly chosen to represent the CED in the charcoal-canister radon-testing program.

Although the intention was to sample all homes selected by the process described above, NAIHS personnel recognized that the entire program might not be completed. To prevent statistical bias resulting from the sequence in which CED's were tested if the program were not completed, each of the 10 groups of 16 CED's was randomly assigned a number from 1 through 10. Technicians then tried to test all the homes in CED's assigned the number 1 before testing the homes in CED's assigned the number 2,

in Spencer, J.E., ed., 1993, Radon in Arizona: Arizona Geological Survey Bulletin 199, p. 82-85.

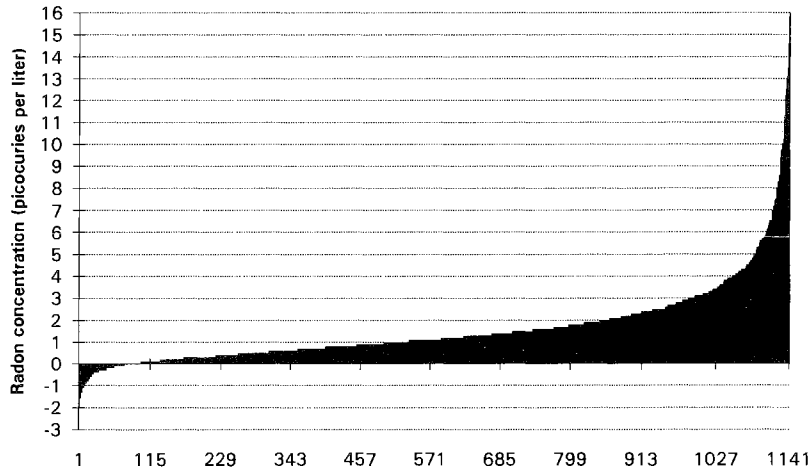

Figure 2. Plot of 1,142 raw charcoal-canister radon measurements from the Navajo Nation, sorted by radon concentration. Individual measurements range from -2.4 to 16.0 pCi/l. The tick marks and numbers are located at intervals of approximately 10% of the total data set.

and so on. Each number was tested sequentially, resulting in 10 potential sampling "waves."

Charcoal-canister testing for radon was done during the winter heating season under closed-house conditions to determine the highest seasonal radon levels in the homes. In the first quarter of 1990, following the procedures described above, NAIHS personnel placed a total of 1,166 charcoal radon-testing canisters in 1,050 individual homes. Two canisters were placed in approximately 10% of the homes to provide duplicate measurements for data quality control. The canisters were left open for a minimum of 48 hours and were subsequently collected by NAIHS personnel and analyzed at the EPA laboratory in Montgomery, Alabama.

NAIHS personnel also placed long-term, alpha-track detectors in 102 of the homes selected in the first wave (approximately 10% of the tested homes). These devices (two per home) were left in the homes for 1 year to determine annual average indoor-radon concentrations.

SURVEY RESULTS

Charcoal-Canister Data

RTI statistically analyzed the charcoal-canister data. Of the 1,166 canisters placed, the results from 24 were lost or discarded because of handling errors. The remaining 1,142 were considered valid radon measurements, but 370 were deemed statistically invalid because they were part of incomplete sampling waves. Data from the remaining 772 canisters were considered statistically valid and were used by RTI to calculate statistics (Tables 1 and 2). Of these 772 measurements, 413 are from Arizona, 332 are from New Mexico, and 27 are from Utah.

The mean and mode of the sample population used by RTI do not differ significantly from the larger sample population made up of all valid charcoal-canister radon measurements. Because the purpose of this paper is not to calculate risks but to disseminate information, we have used the larger population to generate Figures 2 and 3.

The larger data set includes radon measurements that are smoothly distributed between -2.4 and 16.0 picocuries per liter (pCi/l; Figs. 2 and 3). The negative values reflect the imprecision of the measurements, presumably due to counting statistics. RTI replaced values of zero or less with a constant (0.05 pCi/l) before calculating statistical parameters.

Table 1. Statistical parameters calculated by RTI for 772 charcoal-canister radon measurements.

Arithmetic mean (pCi/l)	1.7
Geometric mean (pCi/l)	0.9
Median (pCi/l)	1.1
75th percentile (pCi/l)	2.0
90th percentile (pCi/l)	3.6
Percentage of houses with radon concentration >4 pCi/l	8.3
Percentage of houses with radon concentration >20 pCi/l	0.0

Alpha-Track-Detector Data

Of the 204 alpha-track devices placed in homes, 153 (75%) resulted in valid measurements. This data set includes at least one valid measurement for 84 (82%) of the tested homes. RTI's statistical analysis indicated that the average annual radon concentration in the tested homes was 1.2 pCi/l and that 81 of the 84 homes (96.4%)

Table 2. List of the 10 highest indoor-radon concentrations measured on the Navajo Nation.

Radon (pCi/l)	County
16.0	Apache (AZ)
15.8	Navajo (AZ)
14.6	McKinley (NM)
13.0	Apache (AZ)
12.5	McKinley (NM)
10.9	McKinley (NM)
10.1	Apache (AZ)
10.0	Apache (AZ)
9.8	Apache (AZ)
9.7	Apache (AZ)

Figure 3. Histogram of charcoal-canister radon data. Raw data are rounded to integer values.

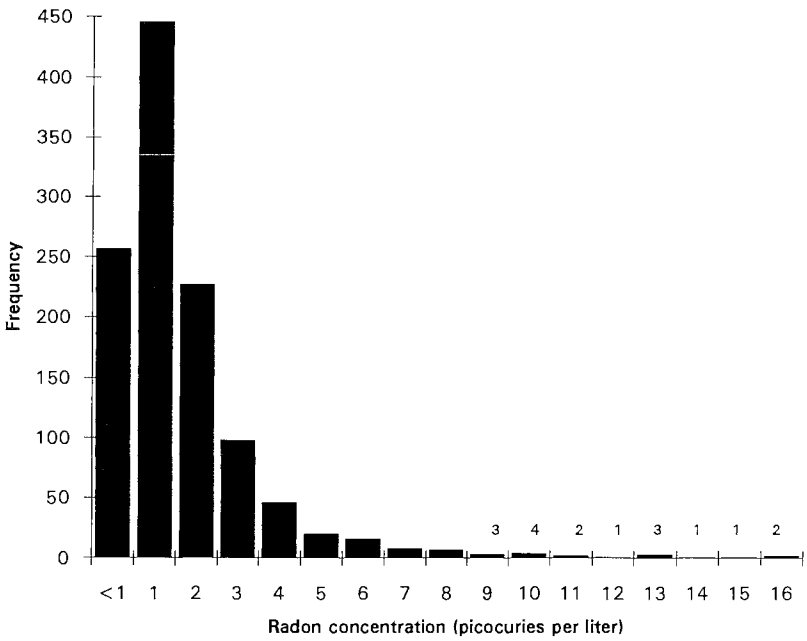

had average annual indoor-radon concentrations of less than 4 pCi/l. The highest level measured was 8.4 pCi/l (Fig. 4).

DISCUSSION

The distribution of indoor-radon levels revealed by charcoal-canister and alpha-track-detector testing indicates that mean indoor-radon concentrations on the Navajo Nation are not significantly different from the 1.3-pCi/l national average estimated by the EPA (Conference of Radiation Control Program Directors, Inc., 1991). Statistical analysis by RTI indicates that 8.3% of homes tested by charcoal canister and 3.6% of homes tested by alpha-track detector exceed the 4-pCi/l radon concentration above which remediation is recommended. These numbers are slightly higher than those found in Arizona outside the Navajo Nation, where 5.4% and 1.6% of homes were determined by charcoal canister and alpha-track detector, respectively, to have indoor-radon concentrations greater than 4 pCi/l (Spencer, 1992).

The correlation between the results of short-term, charcoal-canister tests and long-term, alpha-track-detector tests is reasonably strong. Of the 26 houses with long-term, indoor-radon levels greater than the mean of 1.2 pCi/l, 17 (65.4%) also had short-term, indoor-radon levels greater than the short-term average of 1.7 pCi/l. A correlation coefficient (r) of 0.77 was calculated between the 84 successful alpha-track-detector measurements and the corresponding charcoal-canister measurements. A plot of the data (Fig. 5) shows that the canister data are scattered around the alpha-track-detector data, but most high alpha-track-detector measurements (>2 pCi/l) correlate with high charcoal-canister measurements. A similar correlation (r = 0.74) exists if the larger set of 153 valid alpha-track detector measurements is compared with the corresponding canister test results. These relationships indicate that relatively inexpensive, charcoal-canister radon surveys are likely to identify homes with high average indoor-radon concentrations.

In an effort to recognize any regional groupings or trends that might exist in indoor-radon concentrations, we divided the Navajo Nation into 39 regional map areas and calculated the mean indoor-radon concentration for each area for which data were available (27 areas; Fig. 6). At this resolution, no significant "hot spots" or regional trends are apparent. The only area with an average radon level higher than 2.2 pCi/l is in the westernmost part of the Navajo Nation northwest of the town of Moenkopi.

At the resolution of individual CED's, however, geology appears to influence average indoor-

Figure 4. Histogram of alpha-track-detector radon data. Raw data are rounded to integer values.

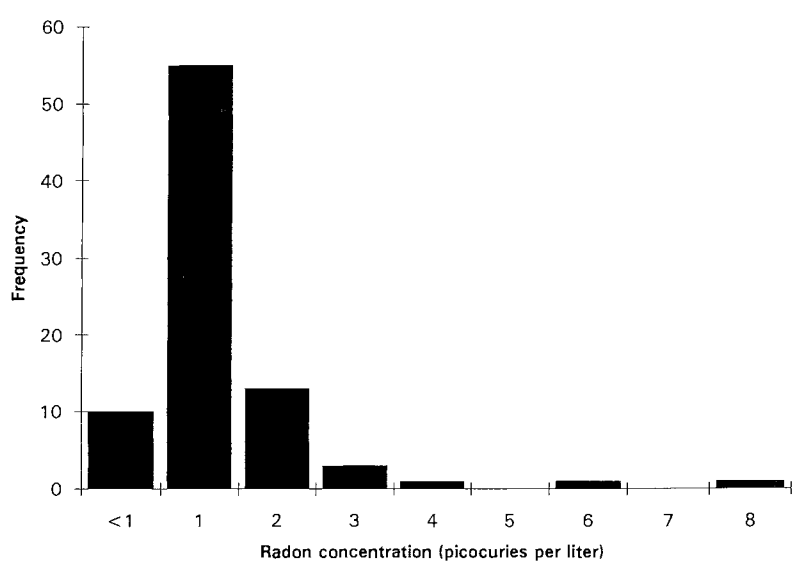

radon concentrations. The Triassic Chinle and Jurassic Morrison Formations host most of the known uranium deposits within the Navajo Nation and commonly contain above-average uranium concentrations, even in areas where they do not host ore. Of the 22 CED's that have mean radon concentrations greater than or equal to 2.5 pCi/l, 18 (82%) are located, at least in part, on outcrops of the Chinle or Morrison Formations or within known uranium districts. These areas constitute less than 25% of the total area of the Navajo Nation. Although population and sample density in these areas may be somewhat higher than the average for the study area as a whole, sampling density does not appear to explain the association of high indoor-radon levels with uranium deposits and the Chinle and Morrison Formations.

Figure 5. Plot of long-term, alpha-track-detector radon measurements and corresponding short-term, charcoal-canister radon measurements for the 84 homes that were successfully tested. Correlation coefficient (r) = 0.77.

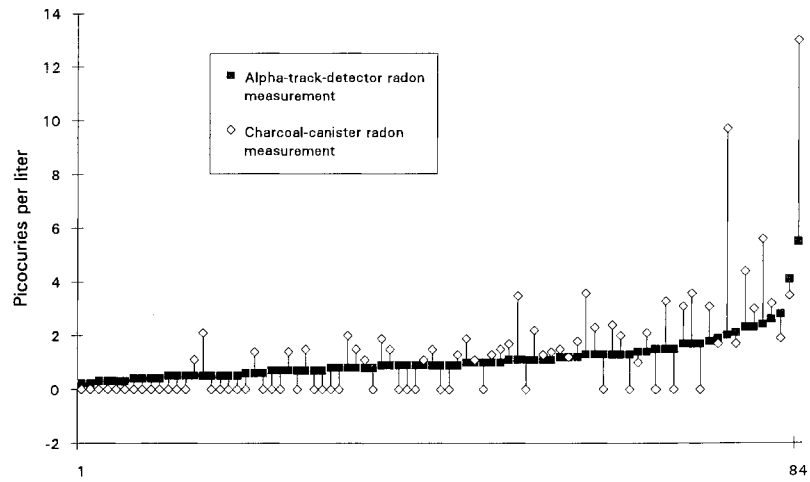

CONCLUSION

This study shows that most homes on the Navajo Nation do not have high indoor-radon concentrations. The Navajo Nation has average indoor-radon levels that are comparable to the estimated national average and to the average for the State of Arizona. Fewer than 10% of homes are likely to contain radon concentrations greater than 4 pCi/l, the level at which remediation is recommended. This is not significantly different from the national average. This study also confirms that short-term, charcoal-canister testing of radon levels can effectively identify homes with high average indoor-radon concentrations.

Although a "first-pass" analysis of the data shows no obvious patterns in the distribution of indoor-radon concentrations across the Navajo Nation, a more detailed analysis suggests that geology exerts significant control over the distribution of high radon levels. Most high (2.5 pCi/l) average indoor-radon levels are in CED's that overlie, at least in part, either the uranium-enriched Chinle or Morrison Formations or known uranium-producing areas.

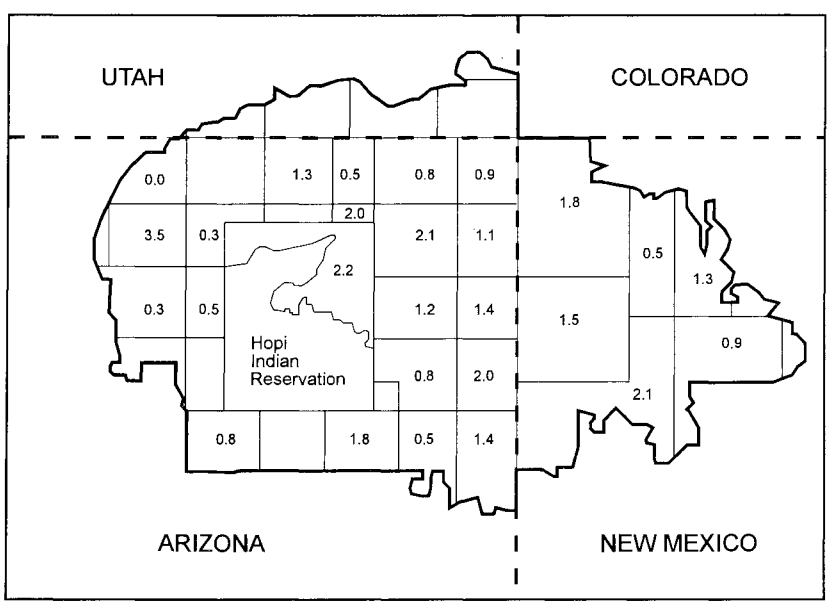

Figure 6. Average indoor-radon concentrations for 27 regional map areas in the Navajo Nation. Data are from the charcoal-canister survey.

REFERENCES

Conference of Radiation Control Program Directors, Inc., 1991, National residential radon survey: Frankfort, Ky., Radon Bulletin, v. 2, no. 1, p. 4.

Spencer, J.E., 1992, Radon gas: A geologic hazard in Arizona: Arizona Geological Survey Down-to-Earth Series 2, 17 p.

A reconnaissance study of radon and other radionuclides in Arizona well water[1]

JOHN T. DUNCAN
JON E. SPENCER
Arizona Geological Survey, 845 N. Park Ave., #100, Tucson, Arizona 85719

PEJMAN ESHRAGHI
Radiation Measurements Facility, Arizona State University, Tempe, Arizona 85287-5706

STEVEN M. EMRICK
Arizona Department of Environmental Quality, 3033 N. Central Ave., Phoenix, Arizona 85012

INTRODUCTION

Much attention has been paid in recent years to the health hazards associated with radon gas in indoor air. The source of most indoor radon is underlying rock and soil, but radon in domestic water contributes an estimated 5% of the radon gas in homes served by ground water (Conference of Radiation Control Program Directors, Inc., 1991). Although no standard has yet been established for radon gas in domestic water, the U.S. Environmental Protection Agency (EPA) is considering a maximum contaminant level of 300 picocuries per liter (pCi/l). Surface water contains very low concentrations of radon gas because dissolved radon is rapidly degassed and dissipated when water is exposed to air. Ground water is therefore the only domestic water source likely to contain significant concentrations of radon.

The Arizona Department of Environmental Quality and the Arizona Geological Survey (AZGS) jointly conceived and funded this study for two purposes: (1) to generate baseline data on radon in Arizona ground water, and (2) to determine if radon concentrations in ground water can be predicted from the geologic or geochemical characteristics of aquifer rocks or surrounding bedrock.

METHODS AND DATA

We selected eight populated areas of Arizona for ground-water sampling on the basis of geographical distribution and local geology. The sampled areas are in or near Kingman, New River, Paulden, Payson, Safford, Sierra Vista, Verde Valley, and Yuma. The New River and Paulden areas and Verde Valley are underlain by rocks that contain anomalous uranium concentrations (Duncan and Spencer, this volume, p. 43-50, p. 51-56, and p. 57-60). Payson is underlain by granite that contains nonanomalous uranium concentrations in surface exposures. Kingman, Safford, and Yuma are underlain by sedimentary rocks that are not known to contain high uranium concentrations, but owing to nearby uraniferous rocks or other geologic criteria, may contain uranium-rich rocks in the subsurface. The rocks underlying Sierra Vista were not known or suspected to contain high concentrations of uranium or other radioactive elements when the study was planned.

We collected 39 ground-water samples from 32 water wells (7 duplicate samples were included for quality control) from the 8 areas and analyzed them for radon-222 (^{222}Rn), radium-226 (^{226}Ra), uranium-234 (^{234}U), uranium-238 (^{238}U), and gross alpha and beta activity. We collected these samples from spigots at or as near as possible to the wellheads and purged the wells to ensure that the sampled water came directly from the aquifer. Each sample consisted of one filled 4-l plastic container and two 40-ml glass vials that we filled, with minimal aeration, to a high meniscus and sealed with flexible Teflon-lined caps to allow no head space.

Water from the 40-ml vials was analyzed for radon by liquid scintillation, and water from the larger containers was analyzed for the other nuclides by alpha spectroscopy and for gross alpha and beta activity by gas-flow proportional counting. All analyses were performed at the Radiation Measurements Facility at Arizona State University in 1992. The results of the analyses are presented in Table 1.

DISCUSSION

To calculate statistics and chart data, we averaged duplicate samples together and treated

[1]This research was conducted under the terms of Arizona Department of Environmental Quality Contract No. 2217-000000-2-7-EK-2067.

in Spencer, J.E., ed., 1993, Radon in Arizona: Arizona Geological Survey Bulletin 199, p. 86-92.

Table 1. Radiochemical data generated by this study. All data are listed in picocuries per liter. A "d" after the well number indicates a duplicate sample. α = alpha activity; β = beta activity.

Area	Well	^{222}Rn	Gross α	Gross β	^{238}U	^{234}U	^{226}Ra
Payson	1	4,220±170	3.80±0.60	2.30±0.60	0.45±0.07	2.90±0.20	<0.10
	2	1,750±80	3.80±0.60	2.10±0.70	0.87±0.12	3.40±0.30	0.16±0.05
	3	2,070±90	1.40±0.40	5.90±0.80	0.20±0.05	0.98±0.11	0.21±0.06
	4	6,310±250	3.20±0.60	4.00±0.70	0.33±0.07	2.30±0.02	0.15±0.05
	5	4,030±170	<0.90	2.20±0.60	0.03±0.04	0.55±0.06	<0.10
	5d	3,710±150	<0.90	1.10±0.60	0.07±0.04	0.81±0.10	<0.10
Sierra Vista	1	1,220±65	1.40±0.50	<1.9	0.47±0.06	1.20±0.10	0.14±0.05
	2	886±51	1.60±0.50	2.40±0.60	0.41±0.06	1.300.10	<0.10
	3	777±46	4.10±0.70	2.10±0.70	0.46±0.07	1.20±0.10	<0.10
	4	1,120±61	2.10±0.50	<1.8	0.39±0.06	1.40±0.10	0.15±0.05
	4d	930±53	3.80±0.70	2.80±0.60	0.40±0.06	1.10±0.10	0.11±0.04
Paulden	1	937±52	4.60±0.70	5.60±0.80	0.70±0.08	2.30±0.20	0.13±0.05
	2	885±50	3.30±0.60	3.50±0.70	0.45±0.06	1.50±0.10	<0.10
	3	252±23	2.60±0.50	4.60±0.70	0.39±0.06	1.60±0.20	<0.10
	3d	271±23	3.50±0.60	3.40±0.70	0.41±0.06	1.90±0.20	<0.10
Kingman	1	729±42	3.20±0.60	5.30±0.80	1.00±0.10	2.10±0.20	<0.10
	1d	657±39	3.80±0.70	5.30±0.80	0.77±0.10	2.00±0.20	<0.10
	2	628±38	4.20±0.70	7.00±0.08	0.88±0.10	2.70±0.20	0.10±0.04
	3	945±51	7.00±0.90	5.10±0.70	0.39±0.05	0.98±0.12	<0.10
	4	434±30	7.50±0.90	7.30±0.90	0.69±0.09	2.50±0.20	0.13±0.05
Yuma	1	380±29	7.30±0.90	7.80±1.00	2.50±0.20	3.50±0.30	<0.10
	1d	415±30	6.20±0.80	7.80±1.00	2.60±0.20	3.60±0.20	<0.10
	2	497±34	3.90±0.70	5.10±0.80	1.60±0.20	2.20±0.20	0.23±0.05
	3	300±26	2.60±0.50	6.00±0.90	0.16±0.03	0.18±0.04	0.25±0.06
	4	1,450±70	3.20±0.60	8.70±1.00	0.50±0.07	0.73±0.09	0.99±0.12
Verde Valley	1	277±26	10.5±1.10	12.9±1.10	6.60±0.50	7.00±0.40	<0.10
	1d	301±26	12.2±1.20	9.00±1.00	6.80±0.60	6.20±0.50	<0.10
	2	158±19	3.00±0.60	2.40±0.70	0.50±0.06	1.50±0.10	<0.10
	3	2,560±120	5.00±0.70	5.40±0.80	1.70±0.20	2.30±0.20	0.69±0.09

(continued on page 88)

Table 1 (continued).

Area	Well	^{222}Rn	Gross α	Gross β	^{238}U	^{234}U	^{226}Ra
Verde Valley	4	99±17	3.40±0.60	<1.9	0.24±0.04	1.60±0.10	0.14±0.04
	5	<45	2.20±0.50	1.70±0.70	0.45±0.07	1.20±0.10	<0.10
New River	1	1,340±70	4.80±0.70	5.90±0.80	1.70±0.10	4.00±0.30	0.63±0.10
	1d	1,350±70	5.20±0.80	3.90±0.80	1.90±0.20	3.80±0.03	1.40±0.10
	2	252±21	1.40±0.40	2.70±0.70	0.39±0.06	1.20±0.10	<0.10
	3	195±19	1.60±0.50	2.00±0.70	0.43±0.06	1.10±0.10	<0.10
Safford	1	279±26	<1.2	3.30±0.70	0.22±0.04	0.29±0.04	<0.10
	2	461±28	9.60±1.0	7.70±1.00	1.80±0.20	3.40±0.20	<0.10
	3	476±28	3.70±0.60	3.80±0.80	0.80±0.09	1.70±0.10	<0.10
	4	1,020±50	11.0±1.10	5.50±1.00	1.90±0.20	2.30±0.20	0.59±0.08

Table 2. Correlation coefficients between radon concentration and the other analyzed radiochemical parameters. α = alpha activity; β = beta activity.

	^{222}Rn vs. Gross α Activity	^{222}Rn vs. Gross β Activity	^{222}Rn vs. ^{238}U Concentration	^{222}Rn vs. ^{234}U Concentration	^{222}Rn vs ^{226}Ra Concentration
Correlation Coefficient	- 0.149	- 0.148	- 0.178	+ 0.029	+ 0.127

them as one sample. We substituted the value of the lower limit of detection for analytical values that were below detection.

The mean radon content of the 32 samples was 1,148 pCi/l, and the median value was between 693 and 777 pCi/l. Twenty-three (72%) of the samples had radon concentrations greater than 300 pCi/l. These levels are higher than the average concentrations in Tucson and Phoenix, the only areas in the State where large studies have been done (Smith, this volume, p. 17-39; City of Phoenix, unpublished data). The high average radon concentrations measured in this study might be explained because areas containing rocks with high uranium concentrations were specifically targeted. The high-uranium areas targeted in this study, however, have on average no more radon in ground water than other areas examined in this study. In fact, New River, Paulden, and Verde Valley, which contain rocks with anomalous uranium levels, had the seven lowest radon values in the study. Ground-water samples from these areas also have lower average radon levels than samples from Sierra Vista, which were expected to contain low radon concentrations (Fig. 1).

The gross alpha and beta activity and the ^{238}U, ^{234}U, and ^{226}Ra concentrations of the samples (Figs. 2 through 6) comply with EPA standards for drinking water. The data show no significant correlations between radon levels and other radio-

Figure 1. ^{222}Rn concentrations in well water, grouped by area. Each vertical bar represents one well.

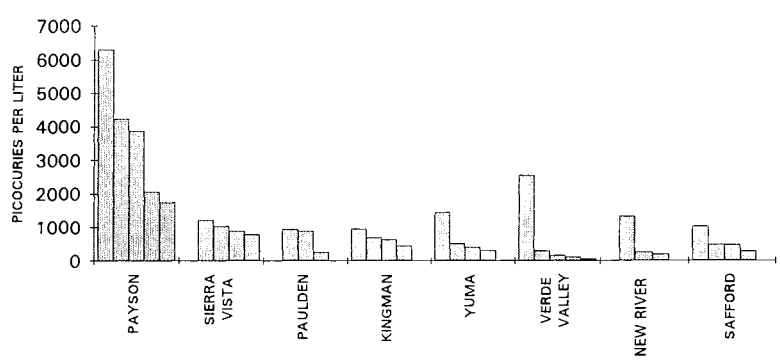

Figure 2. Gross alpha activity of well water, grouped by area. Each vertical bar represents one well.

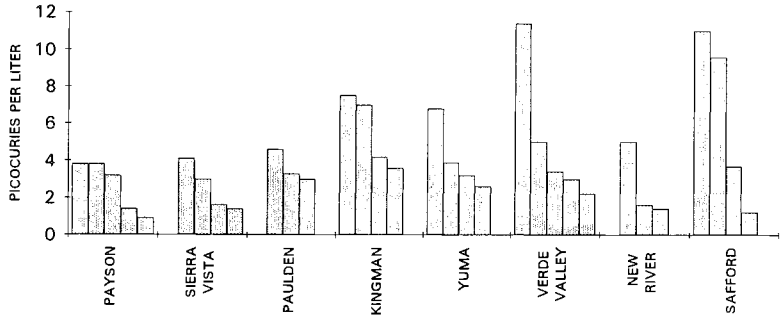

Figure 3. Gross beta activity of well water, grouped by area. Each vertical bar represents one well.

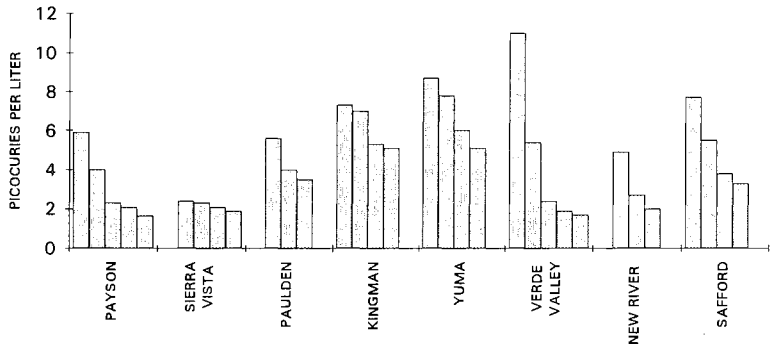

Figure 4. ^{238}U concentrations in well water, grouped by area. Each vertical bar represents one well.

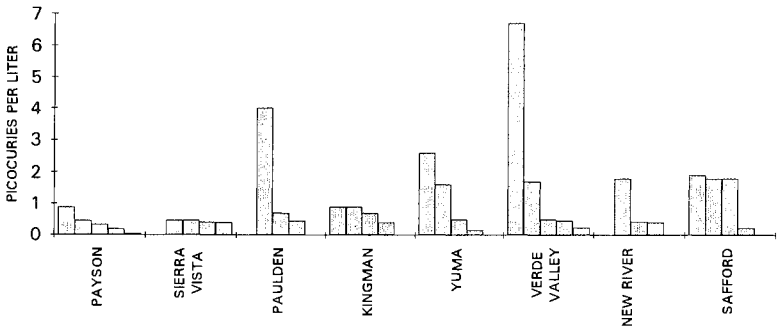

chemical parameters and no clear patterns of nuclide concentrations within specific areas or geologic environments (Fig. 7; Table 2). Geologic interpretations of the radon data from each area are discussed individually below.

Payson

The highest ground-water radon concentrations (mean of 3,644 pCi/l) measured in this study are from Payson, which is mainly underlain by Proterozoic granitic rocks that do not contain anomalous uranium concentrations, as indicated by gamma-ray spectrometry (Plate 1; AZGS, unpublished data). All five wells sampled in Payson produce water from the granite.

The high radon concentrations in water may be explained in two ways: (1) These granitic rocks have a greater capacity to emit radon to the ground water than most rocks with similar uranium content; and (2) The concentration of uranium (or uranium daughter elements) in surface exposures is not a good indicator of uranium concentration at aquifer depths. Although both explanations are valid, it seems unlikely that differences in emissivity are sufficient to account for the high radon levels in the Payson samples (approximately five times the median concentration measured in this study).

Evidence from studies of the Dells Granite near Prescott (Duncan and Spencer, this volume, p. 57-60; Proctor and others, this volume, p. 61-81) and other uranium-rich granites (AZGS, unpublished data) indicates that uranium is commonly leached by meteoric water from the near-surface parts of the rock. In at least some cases, the leached uranium is apparently precipitated at or near the water table to form a layer of supergene enrichment. Even if supergene enrichment has not occurred in the granitic rocks underlying Payson, it is still likely that leaching near the surface has caused lower uranium concentrations in these rocks in outcrop than at the depth of the water table. High uranium concentrations in aquifer rocks probably account for the unexpectedly high radon concentrations in ground water.

Sierra Vista

The area with the second highest, mean radon concentration in ground water (978 pCi/l) is Sierra Vista, an area that was not expected to have high radon levels. All sampled wells are in Tertiary fanglomerate at the surface, and it was assumed when this study was planned that the fanglomerate was the primary aquifer. This may not be true. A drill log was available for only one of the four

wells sampled in the Sierra Vista area, but the log for this 1,000-ft well indicates that it penetrated (unspecified) bedrock at a depth of 543 ft below the surface, less than 80 ft beneath the static water level at 465 ft. This information shows that the primary aquifer may lie within or directly over the bedrock.

The consistency of radon concentrations in the four samples indicates that the aquifer is fairly uniform in its radon emissivity and that no highly enriched point source is present. Proterozoic granite is exposed in the lower parts of the Huachuca Mountains west of Sierra Vista. It probably constitutes a significant fraction of the fanglomerate material and is the most likely bedrock below the sedimentary cover. The granite is not abnormally uranium rich, as indicated by gamma-ray spectrometry (Plate 1); however, the value of spectrometry as a predictor of uranium concentrations at depths of hundreds of feet, as discussed above, is unclear. The granite is the only obvious candidate for a radon source.

Figure 5. ^{234}U concentrations in well water, grouped by area. Each vertical bar represents one well.

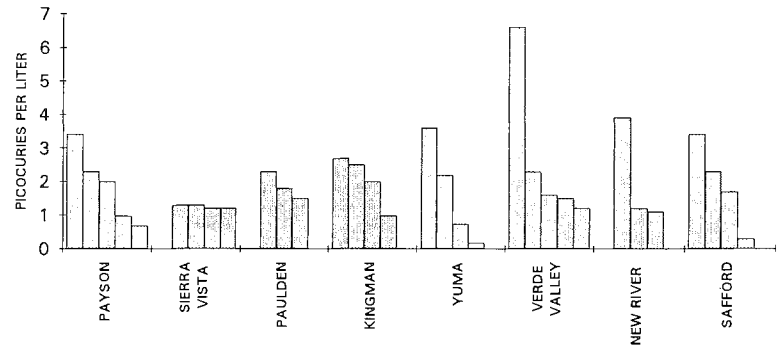

Figure 6. ^{226}Ra concentrations in well water, grouped by area. Each vertical bar represents one well.

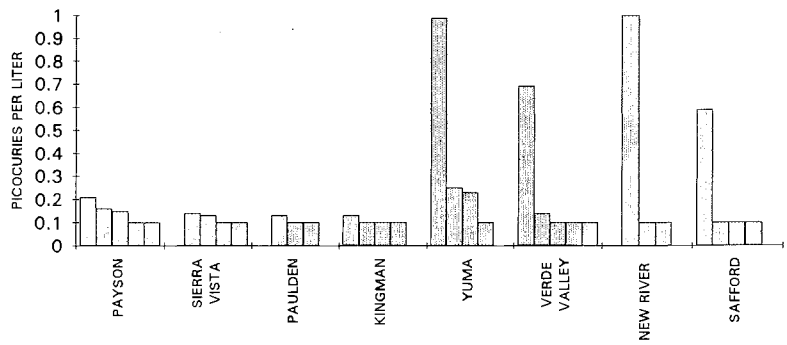

Figure 7. Average values of all radiochemical parameters, grouped by area. Each vertical bar represents the arithmetic mean of the values of one parameter from all the wells sampled in the area.

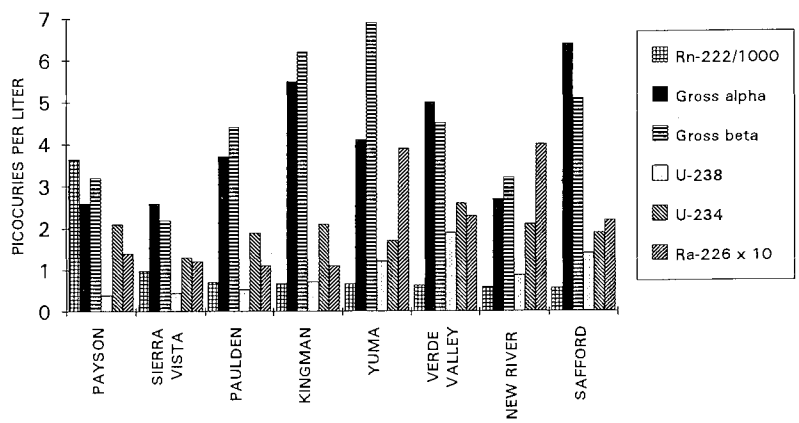

Paulden Area

The three wells sampled in the Paulden area (mean radon concentration of 695 pCi/l) were all in Sullivan Buttes Latite, which is known to contain anomalous uranium concentrations (Duncan and Spencer, this volume, p. 57-60), or in sediments derived from this latite. Although two samples contained radon concentrations higher than the median value in this study, neither was exceptionally high, and the third was less than 300 pCi/l.

Kingman

Ground-water samples from Kingman contained a mean of 675 pCi/l of radon. All four wells produced from Tertiary basin fill. Rocks with higher-than-average uranium content, such as felsic tuffs exposed in and around Kingman and Proterozoic granite in the Cerbat and Hualapai Mountains to the north and south, probably make up a large component of the basin fill and account for the moderate radon concentrations in the ground water.

Yuma

The four wells sampled in Yuma are drainage wells operated by the U.S. Interior Department. They produce water from a gravel bed in Quaternary Colorado River sediments. The source of the

water is recharge from ditch irrigation. Although the mean radon content was 661 pCi/l, only one of the four samples, at 1,450 pCi/l, contained more than 500 pCi/l of radon. The one high value might be explained by the well's proximity to granitic bedrock in the subsurface, but there are no nearby outcrops to substantiate this speculation.

Verde Valley

Of the five samples taken from wells in the Verde Valley, four contained less than 300 pCi/l of radon; the fifth contained 2,560 pCi/l, resulting in a mean of 630 pCi/l. Three samples were taken from wells known or believed to produce from hard, porous, white, Verde Formation limestone. These rocks, where exposed at the surface, do not contain anomalous uranium concentrations (Duncan and Spencer, this volume, p. 51-56). The other two wells produce from Quaternary river gravels and from Tertiary tuffs and tuffaceous sediments that were apparently deposited at the same time as the Verde Formation lakebeds.

The one high radon value is from a well within the town of Camp Verde. The well produces from Verde Formation limestone and is near outcrops of Verde Formation marl that contain strongly anomalous uranium concentrations. The producing aquifer in this well is probably near, and possibly directly underlain by, uranium-rich marl or mudstone. Similar aquifer rocks in the wells in Cottonwood and Montezuma's Castle National Monument are presumably not as close to uranium-rich marl or mudstone.

New River Area

Three wells sampled in an area east of New River contain a mean of 596 pCi/l of radon. The area was chosen because of high uranium concentrations in the locally exposed, White Eagle Mine Formation. It is unlikely that any of the sampled wells produce water from this formation because the uranium-rich rocks are dense, fine-grained dolomite and dolomitic mud that are almost certainly poor aquifers. Houses built on the outcrops or projected subcrops of the White Eagle Mine Formation are served by a small, private water company with wells outside the area. Poor aquifer conditions in the White Eagle Mine Formation probably make private wells on those properties unproductive. The one sampled well on the projected subcrop of the White Eagle Mine Formation is shallow (60 ft) and apparently produces from Quaternary stream gravels, but may penetrate the underlying(?) uranium-rich rocks. This well contained 1,340 pCi/l of radon. The other two wells, which are near, but not on, the outcrop or projected subcrop of the targeted rocks, contained less than 300 pCi/l of radon.

Safford

The four wells sampled in the Safford area contained a mean of 559 pCi/l of radon. A well at the Federal prison on the flanks of the Pinaleño Mountains produces from Tertiary fanglomerate that is mainly composed of Proterozoic crystalline rocks, including granite; water from this well contained less than 300 pCi/l of radon. Two wells along the Gila River that produce from Quaternary river gravels and possibly Tertiary fanglomerate contained radon concentrations of 461 and 476 pCi/l. The fourth well, which produces from late Tertiary lacustrine sediments similar to the Verde and White Eagle Mine Formations, contained 1,020 pCi/l of radon.

CONCLUSION

The data reported here indicate that radon concentrations greater than 300 pCi/l are normal for ground water from a variety of aquifer rocks in widely scattered parts of Arizona. Although average radon levels reported here are higher than those reported from studies of the Phoenix and Tucson areas (Smith, this volume, p. 17-39; City of Phoenix, unpublished data), they are much lower than those in the Carefree-Cave Creek area, the only other area in Arizona that has been carefully studied (Barnett, 1990).

Radon concentrations in ground water could not be predicted from the uranium content of surface rocks, as determined by gamma-ray spectrometry. This lack of success is partly due to two factors: (1) Many of the uranium-enriched rocks that were targeted are not aquifers and, thus, were not successfully tested; and (2) Some surface exposures have apparently been leached of their original uranium content, leaving little evidence of higher, possibly supergene-enriched, uranium concentrations at depth. The other radiochemical parameters that we tested — gross alpha and beta activity and ^{238}U, ^{234}U, and ^{226}Ra concentrations — were also poor predictors of radon concentrations in ground water.

Characteristics other than uranium (or radium) content also play a part in determining how much radon the rocks contribute to ground water. Radon emissivity, which is basically a measure of a rock's permeability to radon at a submicroscopic scale, is probably the single most important complicating factor. Emissivity is dependent on several specific rock characteristics.

The high radon concentrations in samples from the granitic aquifer in Payson are a significant

finding. These data indicate that granites, regardless of uranium content in surface exposures, are likely to be associated with high radon concentrations in ground water. The data from Sierra Vista, if we are correct in interpreting that the main aquifer is within or immediately above the granitic bedrock, also support the association between granite and radon.

RECOMMENDATIONS

The high radon concentrations in the ground water in Payson indicate that granitic rocks, even those with low uranium concentrations in surface exposures, should be targeted for further sampling. The relatively few communities in Arizona that depend on water from aquifers in granitic rocks are concentrated in the Transition Zone, or Mountain Province, of the State and include the areas near and between the cities of Prescott and Payson, as well as scattered outlying communities. A few communities in the mountains of southeastern Arizona, such as Oracle, also probably use ground water from granitic aquifers. Communities that depend on ground water from granitic aquifers should be located and their water tested for radon.

Lack of specific information prevents us from correlating the radon content of well water with the uranium or radium concentration or other characteristics of the aquifer materials at depth in the wells, but presumably some correlations exist. Detailed geologic and geochemical studies of cores or cuttings from water wells, combined with radon data from the water in the same wells, may provide more information on these correlations and lead to reliable predictors of radon concentrations in ground water.

REFERENCES

Barnett, J.M., 1990, Radon-222 in drinking water: Liquid scintillation detection methods and estimated doses to the lungs: Tempe, Arizona State University, M.S. thesis, 94 p.

Conference of Radiation Control Program Directors, Inc., 1991, Radon in drinking water: Frankfort, Ky., Radon Bulletin, v. 1, no. 4, p. 7.

A survey of uranium concentrations in rocks and soils in populated areas of Arizona: Methods[1]

JOHN T. DUNCAN
JON E. SPENCER
Arizona Geological Survey, 845 N. Park Ave., #100, Tucson, Arizona 85719

INTRODUCTION

Recent studies by the Arizona Geological Survey (AZGS) and the Arizona Radiation Regulatory Agency (ARRA) have revealed that anomalously high uranium levels are present in rocks in and near populated areas in Arizona (Scarborough and Wilt, 1979; Emer and others, 1988). Other studies have shown that uranium concentrations in geologic materials correlate positively with radon concentrations in homes built on those materials (Duncan and Spencer, this volume, p. 51-56; Spencer and others, this volume, p. 10-16). In 1990, the ARRA received a grant from the U.S. Environmental Protection Agency to evaluate potential radon hazards in Arizona. The AZGS carried out geologic aspects of this evaluation under contract with the ARRA to determine the extent and character of known and undiscovered uranium anomalies within or near populated areas. A portable gamma-ray spectrometer was used to measure uranium levels and to identify and delineate areas of anomalous uranium concentrations. This report outlines the methods used in the spectrometer survey, details of data reduction, and results of a study to determine the typical range of uranium levels in geologic materials that underlie most of the populated areas in Arizona.

DATA ACQUISITION

AZGS geologists carried out the survey using an EG&G geoMetrics model GR-310 gamma-ray spectrometer equipped with an external detector containing a 347-cm^3, thallium-doped, sodium iodide crystal. The instrument provides independent measurements of the diagnostic gamma radiation for uranium (bismuth-214 [^{214}Bi], 1.76 million electric volts [MeV]) and thorium (thallium-208, 2.62 MeV), which are needed for uranium assays, as well as for potassium and total gamma radiation. Gamma-ray bandwidths for measuring peaks are 0.2 MeV for uranium and potassium and 0.4 MeV for thorium. Counting time may be set to 1, 10, 100, or 1,000 seconds.

The survey was confined to populated areas and areas likely to be populated in the near future. The early stages of the survey were directed at areas where anomalous uranium concentrations are known or suspected to exist based on previous studies or geologic considerations. Most sample locations are near roads and on relatively flat surfaces. Readings were taken with the detector held about 1 ft above the ground surface and oriented perpendicular to it.

Most uranium-level determinations represent count times of 100 seconds. Because radioactive decay is a random process, longer count times (more individual gamma rays counted) lead to greater statistical precision in gamma-ray-spectrometer uranium assays. The 100-second count time is a compromise between precision and economy of time. In this study, gamma rays generated by uranium in geologic materials were detected at count rates ranging from less than 1 to more than 100 counts per second. At the high end of this range, statistical error should be less than 1%, but at the low end, error could be greater than 15%. These errors were not a major problem for the survey because they are significant only in rocks with the lowest concentrations of uranium. In samples of the most interest — those with higher uranium concentrations — these errors are insignificant.

Other, potentially more important, sources of error in the raw data exist. First, variations in atmospheric conditions and soil moisture could combine to produce errors of more than 20% (geoMetrics, undated). Second, equilibrium conditions may not exist. Gamma-ray-spectrometer uranium assays are calculated from the measurement of gamma rays resulting from the radioactive decay of ^{214}Bi, a radioactive decay product of uranium. The calculation incorporates two assumptions: (1) that equilibrium exists between uranium and its decay products; and (2) that decay

[1]This article supersedes the following report: Duncan, J.T., and Spencer, J.E., 1991, A survey of uranium concentrations in rocks and soils in populated areas of Arizona: Methods: Arizona Geological Survey Open-File Report 91-2, 9 p.

in Spencer, J.E., ed., 1993, Radon in Arizona: Arizona Geological Survey Bulletin 199, p. 93-96.

Figure 1. Machine background (gamma radiation from nongeologic sources) is mainly caused by cosmic rays and is strongly correlated with elevation. Cosmic rays, which originate from space, are stopped by air molecules and thus are less abundant at lower elevations. The elevation effect was corrected in this study by fitting exponential curves ($y = ab^x$) to plots of elevation vs. raw uranium and thorium gamma counts (from nonanomalous rocks). The curves were then shifted downward by subtracting a constant, so that they intersect machine-background readings measured over a swimming pool in Tucson, where geologic sources of radiation are negligible. The results of this adjustment are curves that approximately trace the lower edges of the plots of raw uranium and thorium gamma counts and approximate the elevation-dependent machine background. For gamma-ray-spectrometer uranium assays, the value of the correction curve at the sample elevation is subtracted from each raw gamma reading to produce the corrected values used in the assay equation, U (ppm) = 4.7 (U_c - 0.682 Th_c).

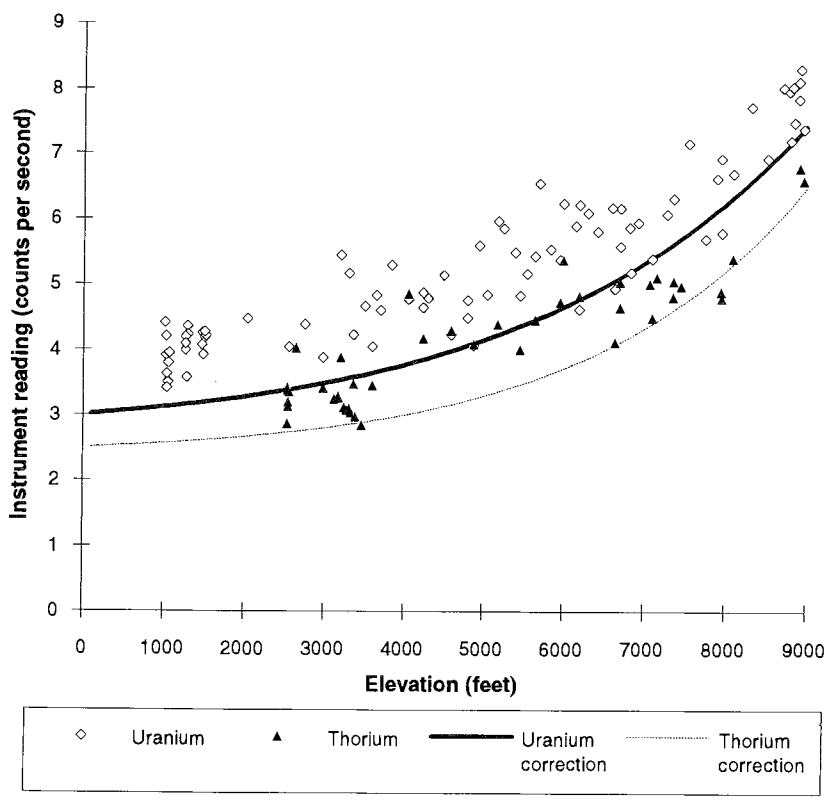

products have not been removed from or added to the rock. If equilibrium conditions do not exist, the numbers given are inaccurate with respect to uranium; however, because radon gas (radon-222) is an intermediate product of the same decay process and is a parent isotope of ^{214}Bi, the uranium assays are still likely to reflect relative radon concentrations. Third, because gamma rays can travel only a short distance through geologic materials, the gamma-ray spectrometer can effectively sample only the upper 20 to 45 cm of rock or soil (Ward, 1981).

DATA REDUCTION

The manufacturer of the GR-310 gamma-ray spectrometer provided an equation for estimating uranium concentration from gamma-ray readings: uranium (parts per million [ppm]) = 3.55 (U_c - 0.682 Th_c). U_c and Th_c represent uranium and thorium gamma-ray spectrometer readings (in counts per second) that have been corrected for machine background. This correction is made by subtracting from the spectrometer reading the amount of gamma radiation derived from nongeologic sources.

Uncorrected spectrometer readings correlate positively with elevation because cosmic rays are the major source of radiation from nongeologic sources and are filtered out by the atmosphere so that fewer reach low elevations. The amount of gamma radiation from cosmic rays was determined, as a function of elevation, by taking numerous measurements at different elevations over rock types with fairly low and consistent radioactivity. This nongeologic gamma radiation is approximated by the two curves shown in Figure 1. Corrected counts were determined by subtracting the value of the correction curves at the sample elevation from the raw gamma-ray spectrometer readings. Through this method, the raw data were largely corrected for elevation in the statewide database. Although this method introduced some error into the assays, it obviated the time-consuming job of establishing machine background in every area investigated.

Because thorium readings vary only slightly within a specific rock type and thorium generally contributes little to the calculated uranium concentrations in most rocks, thorium gamma rays were counted for only a few samples. For the other samples, average thorium values or estimates for particular rock types were used in the assay equation. Errors introduced by estimated thorium readings are significant only in rocks with the lowest uranium concentrations.

To check the accuracy of gamma-ray spectrometer assays, several samples were measured with

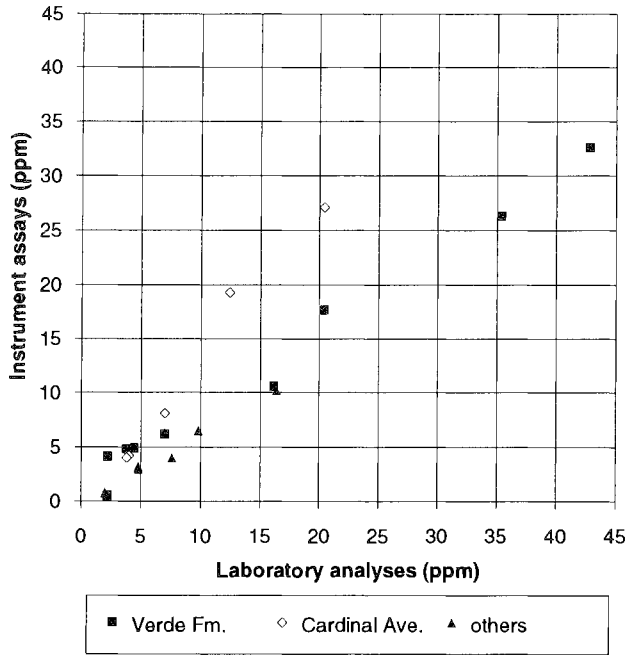

Figure 2. Plot of gamma-ray-spectrometer uranium assays (using the assay equation supplied by the manufacturer of the instrument) against commercial laboratory analyses of the same samples. Correlation coefficient = 0.93.

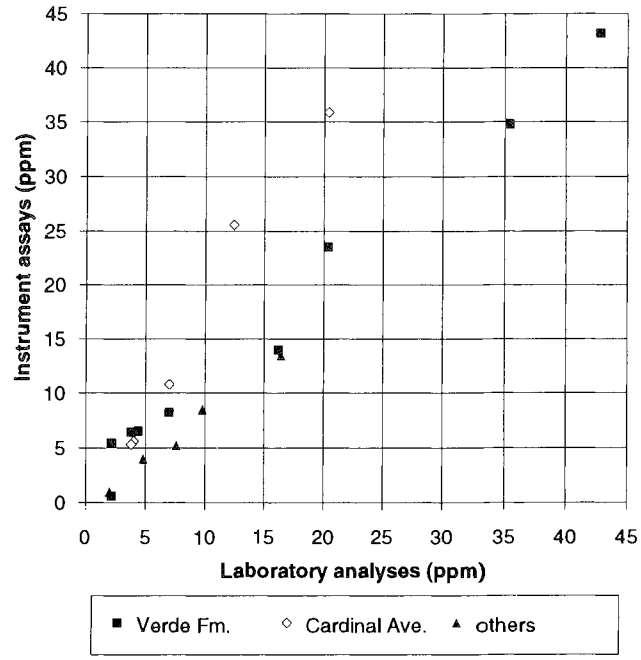

Figure 3. Plot of gamma-ray-spectrometer uranium assays (using the modified assay equation developed for this study) against commercial laboratory analyses of the same samples. Correlation coefficient (r) = 0.93 (r = 0.99 if the two Cardinal Avenue samples are excluded).

long count times in the field and then analyzed for uranium by delayed-neutron counting at a commercial lab. The correlation between gamma-ray spectrometer assays and commercial analyses is crude but clear (Fig. 2). Most of the scatter in the assay correlation is the result of two samples from the area near Cardinal Avenue and Valencia Road in southwestern Tucson. These samples contain significantly less uranium as measured by commercial analysis than by gamma-ray spectrometer and, thus, may have lower uranium concentrations than the much larger volume of rock measured by the spectrometer. This possibility is supported by the observation that uraniferous limestone in this area contains veinlets of yellow carnotite, which indicates that the distribution of uranium in the limestone is heterogeneous on a scale of centimeters. Another possible explanation for the discrepancy is that the gamma-ray spectrometer measurements were taken under abnormal conditions (atmospheric pressure, soil moisture, or instrument calibration). Deleting these two samples from the data set produces a more linear array.

Although the lack of a 1:1 correlation between the two types of analysis is inexplicable, it may be corrected by slightly adjusting the assay formula's scaling factor, from 3.55 to 4.7. This produces a higher correlation (Fig. 3). The modified formula, U (ppm) = 4.7 (U_c - 0.682 Th_c), was used in this study to calculate uranium concentrations from gamma-ray spectrometer readings.

DATA ANALYSIS AND RESULTS

Several hundred spectrometer measurements were taken in areas in Arizona where underlying geologic materials are not known to contain unusually high concentrations of uranium (Fig. 4). Most of these measurements were made over young, unconsolidated to weakly consolidated surficial deposits within modern topographic basins that underlie most of Arizona's population centers (including most of Phoenix, Mesa, Scottsdale, and Tucson). These data reveal the typical, or non-anomalous, range of uranium concentrations in most populated areas of Arizona. Errors from counting statistics and estimates of machine background largely account for the relatively broad distribution that extends into the negative range (Fig. 4), which indicates that gamma-ray spectrometer assays are precise only to within ±4 ppm. The mean at 1.6 ppm, however, is a fairly accurate representation of "average" or "background" uranium concentration and is consistent with the 1.8-ppm crustal abundance of uranium (Klein and Hurlbut, 1985, p. 151). The data (Fig. 4) show an approximately normal distribution about the mean,

with a standard deviation of 2.0 ppm. In a normal distribution, approximately 95% of the data fall within 2 standard deviations of the mean, and any points falling outside that range may be considered anomalous. Based on this analysis, any geologic materials that contain uranium in concentrations higher than 2 standard deviations above the mean (>6 ppm) are considered anomalous.

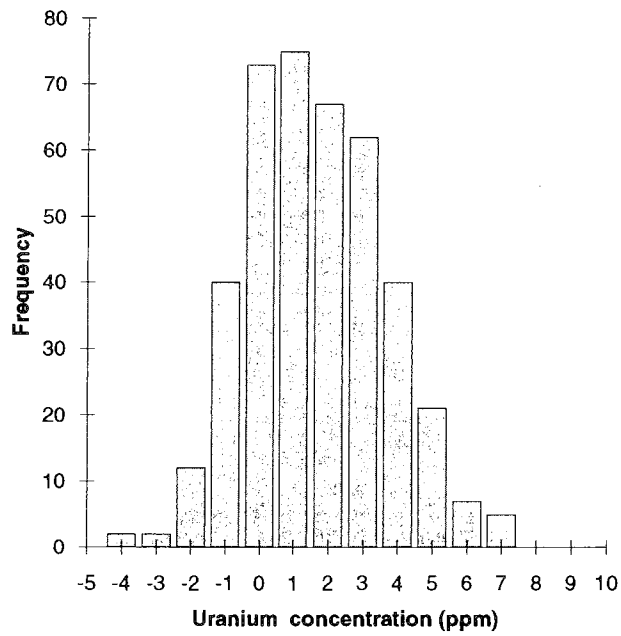

Figure 4. Histogram of gamma-ray-spectrometer uranium assays of nonanomalous rocks in Arizona. The mean and mode are near the average uranium content of the crust; the broad peak extending into the negative range is largely the result of errors introduced by counting statistics, thorium estimation, and elevation correction, which are significant only at low uranium concentrations. The distribution (standard deviation = 2 ppm) suggests that the assays are precise to within ±4 ppm (2 standard deviations).

CONCLUSION

Measurements of uranium concentrations in geologic materials by gamma-ray spectrometry correlate with those by commercial chemical (neutron-activation) analysis, which indicates that the portable gamma-ray spectrometer is sufficiently accurate to delineate areas of anomalous uranium concentrations that may be radon-hazard areas. The correlation is improved by correcting for elevation and thorium concentration. Based on several hundred spectrometer measurements in areas with typical uranium concentrations, the mean concentration in geologic materials in Arizona is 1.6 ppm, and the standard deviation is 2.0 ppm. Anomalous uranium concentrations, therefore, are those higher than 6 ppm (i.e., more than 2 standard deviations above the mean).

REFERENCES

Emer, D.F., Shenk, J.D., and Spencer, J.E., 1988, Reconnaissance gamma-ray spectrometer survey of radon-decay products in selected populated areas of Arizona: Arizona Bureau of Geology and Mineral Technology Open-File Report 88-12, 88 p.

geoMetrics, undated, Operating manual, model GR-310 gamma ray spectrometer: Sunnyvale, Calif., 51 p.

Klein, Cornelis, and Hurlbut, C.S., 1985, Manual of mineralogy (20th ed.): New York, John Wiley and Sons, 596 p.

Scarborough, R.B., and Wilt, J.C., 1979, A study of uranium favorability of Cenozoic sedimentary rocks, Basin and Range Province, Arizona; part 1, general geology and chronology of pre-late Miocene Cenozoic sedimentary rocks: Arizona Bureau of Geology and Mineral Technology Open-File Report 79-1, 101 p.

Ward, S.H., 1981, Gamma-ray spectrometry in geologic mapping and uranium exploration, *in* Skinner, B.J., ed., Economic geology seventy-fifth anniversary volume: El Paso, Economic Geology Publishing Co., p. 840-849.

ARIZONA GEOLOGICAL SURVEY

The Arizona Geological Survey (AZGS) became a stand-alone State agency on July 1, 1988, in accordance with Senate Bill 1102, which was enacted in 1987. The purpose of the AZGS is to encourage and assist stewardship of lands and mineral resources in Arizona by conducting scientific and investigative research and providing geologic information. Responsibility for regulating the drilling and production of oil, gas, geothermal resources, and helium was assigned to the AZGS on July 1, 1991.

The Office of the Territorial Geologist was established by the Territorial Legislature in 1881. Its primary duties were to collect and provide information about mineral resources. From 1893 until statehood in 1912, Territorial Geologists were affiliated with the University of Arizona and its mineral-testing laboratory, known informally as the "Bureau of Mines." A 1915 statute created the Arizona Bureau of Mines as a State agency administered by the University of Arizona, continuing, essentially unchanged, the functions of the Territorial Geologist and "Bureau of Mines." Data collection and research activities continued to be concentrated on mineral resources. In 1977, the agency's enabling legislation was modernized and its name was changed to the Arizona Bureau of Geology and Mineral Technology. It continued to be administered by the University of Arizona. The agency was charged with investigating geologic hazards and limitations, as well as the geologic framework and mineral resources of Arizona, in anticipation of population growth and increased competition for and conflict over land, water, mineral, and energy resources.

AZGS geologists prepare geologic maps of Arizona; investigate the State's geologic framework; conduct research on Arizona's geologic hazards and limitations, as well as its mineral and energy resources; compile data; and maintain a geologic library and a repository of rock cuttings and cores. AZGS geologists regularly conduct cooperative projects with Federal, State, and local agencies and work closely with university faculty and graduate students on projects within Arizona. Advisory committees for environmental and engineering geology, mineral resources, and earth science education provide program guidance.

The Arizona Geologic Information System (AGIS) includes several databases: AZGS library holdings; AZMIN, which contains mining production data, mine names, and mineral-related references; AZAGE, a compilation of radiometric age determinations; and AZGEOBIB, a comprehensive bibliography of more than 11,000 references on Arizona geology. The AZGS publishes maps, reports, and *Arizona Geology*, a quarterly newsletter. A list of available publications may be obtained from the AZGS at the address listed below. The AZGS library is open to the public during normal working hours.

To obtain copies of this publication, contact the Arizona Geological Survey,
845 N. Park Ave., Suite 100, Tucson, AZ 85719-4816; phone: (602) 882-4795.